COPPER MANGANESE BASED MIXED OXIDES FOR AMBIENT TEMPERATURE CO OXIDATION AND HIGHER TEMPERATURE OXIDATION REACTIONS

Thesis submitted in accordance with the requirement of
Cardiff University for the degree of Doctor of Philosophy

Kieran John Cole

2008

CARDIFF
UNIVERSITY

PRIFYSGOL
CAERDYD

UMI Number: U585078

UMI

Dissertation Publishing

ProQuest

Abstract

The catalytic oxidation of carbon monoxide is an important reaction in heterogeneous catalysis. Copper manganese mixed oxides in the form of Hopcalite, $CuMn_2O_4$, is used as a catalyst for the oxidation at ambient temperature and is important in respiratory protection, particularly in mining industries. These types of catalysts are prepared by a co-precipitation method; variables in this preparation procedure are known to control catalytic activity. Previous work has shown that the addition of a cobalt dopant metal to the catalyst structure can have a positive effect on activity towards CO oxidation.

This thesis furthers the work of dopant addition by studying the effects of zinc on the copper manganese catalyst. Catalyst testing for CO oxidation showed that the addition of the zinc dopant metal increases the stability of catalytic activity. Temperature Programmed Reduction studies show that the addition of zinc has an effect on the redox properties of the catalyst.

Prepared copper manganese oxide catalysts were used as supports for gold catalysts. Gold supported CuMnOx was prepared by a deposition precipitation method. The addition of gold to these active materials leads to a marked increase in the catalytic activity. Scanning Electron Microscopy (SEM) showed that the morphology of the support used, played an important role in producing a highly active catalyst. Also, the ageing time of the catalyst precursor was shown to influence catalytic activity. The most effective catalyst for CO oxidation was found to be a 1 wt% Au supported catalyst. The presence of moisture in the gas feed is known to be detrimental to a Hopcalite catalyst for ambient temperature CO oxidation. The effect of moisture on the copper manganese mixed oxide catalysts highlighted the improvement in moisture tolerance with the addition of gold. The method of depositing gold onto an oxide support was shown to be applicable to a commercially available catalyst.

The gold supported CuMnOx catalysts prepared were tested for oxidation reactions at higher temperatures. The reactions investigated were ethylene oxide oxidation and preferential oxidation (PROX) of carbon monoxide. Studies showed the addition of gold to the CuMnOx catalysts, improves activity compared to an undoped catalyst.

Acknowledgments

I would like to take this opportunity to thank the people who have helped and supported me over the past three years.

I would like to thank my supervisors Graham Hutchings and Stuart Taylor for their input, advice and support during my project. The Post Docs past and present, who helped with problems in the lab that I encountered along the way – many thanks.

My thesis would not have been possible without funding from the EPSRC and from my industrial sponsors, Molecular Products. I would like to thank Mandy Crudace and Michael Clarke for their support. Their advice and suggestions have helped me focus on aspects of my research.

I would like to thank the following people: Ferg, Matt D, Pete L, Uma, Nishlan, Edwin and to members of the group past and present. I also thank friends in the department who I have met over past three years. Thanks go to Chris Jones who helped me during the early stages of my project. Members of staff must get a special mention, both technical and administrative. They have always been welcoming and always willing to help whenever I would come to see them. They are a credit to the department of chemistry.

I thank my friends and family who have been supportive to me, keeping my feet on the ground and making sure I didn't lose the plot! Laura, thank you for being there for me, I don't know what I would have done without you. A special mention goes to Grandma and my late Grandfather, who put in place funds for me to go to university. I am truly grateful.

Finally, I would like to thank my Mum and Dad. I dedicate this thesis to them. They have always been supportive to me, given me advice and made sure that I made the right choices for myself in life. Thank you so much.

Contents

Introduction

1

1.1 Aims of the thesis

The aim of this research is to investigate the catalytic activity of copper manganese based mixed oxides for ambient temperature carbon monoxide oxidation. The aim was to develop previous preparation methods to produce a series of catalysts that are reproducible and robust. The effect of ageing times on catalyst precursors will be studied; especially the incorporation of other elements into the Hopcalite system. The addition of dopant metals and the effect on catalytic activity will be investigated. Previous work has reported that the addition of small amounts of dopant metal to the Hopcalite catalyst can have a promotional effect on activity towards CO oxidation.

The aim of the work is to compare and contrast the activities of the copper manganese mixed oxide catalyst with a commercially available catalyst. Many issues have been reported concerning the deactivation of Hopcalite catalysts in the presence of moisture. The aim is develop the Hopcalite catalyst to become more robust towards CO oxidation in the presence of moisture. The effect of moisture and possible reaction pathways will be discussed. Copper manganese mixed oxide catalysts have been extensively researched for CO oxidation reactions. The possibility of other catalytic

reactions will be explored to investigate the versatility of the prepared catalyst. A variety of preparation methods and characterisation techniques will be used to further understand the properties of the Hopcalite catalyst.

The aim of this chapter is to review the work taken place that has made copper manganese based mixed oxides an integral part of heterogeneous catalysis.

1.2 Carbon monoxide

Carbon monoxide is a colourless, odourless and tasteless gas. CO gas can cause severe and even fatal asphyxiation, i.e. impairing the lung ventilation by reducing the oxygen transport capacity of the blood [1-2]. The toxicity of CO is due primarily to its affinity for haemoglobin, the oxygen carrier of blood, forming carboxy haemoglobin.

Carbon monoxide is formed by the combustion of carbon in oxygen at high temperatures when there is an excess of carbon. In an oven, air is passed through a bed of coke. The initially produced CO_2 equilibrates with the remaining hot carbon to give CO. Motor vehicles, various appliances that use carbon-based fuels, and fireplaces used for heating homes are the main sources of CO.

1.3 Catalytic oxidation of Carbon Monoxide

Catalytic oxidation is the most effective means for its removal from air. CO oxidation is a relatively simple reaction, irreversible at low temperatures without parallel or secondary reactions. CO oxidation is one of the basic model reactions reported upon in thousands of publications in surface science [3]. It is well documented that in

catalytic combustion processes for hydrocarbons and oxygenates, partial oxidation reactions must be avoided, CO_2 and water being possibly the only products [4].

In automotive emission control, due to increasingly strict environmental regulations, the complete oxidation of carbon monoxide is highly important. The catalytic oxidation of CO at ambient temperature and atmospheric pressure is a key process for a number of applications.

1.4 Copper manganese based mixed oxides

Mixed oxides composed of manganese and copper have been frequently used as catalysts for CO oxidation. Transition metal oxide or mixed oxides have been established as inexpensive alternatives to precious metals and noble metal containing catalysts. Noble metal catalysts are known for low temperature applications but are expensive and prone to poisoning and deactivation. Copper manganese oxides have long been established as a catalyst of choice for many applications; they are powerful oxidation catalysts which can catalyse near room temperature the oxidation of CO to CO_2. Copper manganese mixed oxides for CO oxidation is an important process for respiratory protection, including mining industries and deep sea diving. Low levels of harmful carbon monoxide are oxidised to harmless carbon dioxide in personal protective masks and respirators. Catalysts are used in CO_2 lasers for weather monitoring and other remote sensing applications. Closed cycle CO_2 lasers produce CO and O_2 in the laser discharge resulting in a rapid loss of power output. Catalysts are required to convert CO and O_2 back to CO_2 [5-6]. Other uses have arisen in strictly modern applications such as CO sensors, which provide invaluable early warning signals of a build up of potentially lethal CO gas [7]. Recent developments

have examined the use of transition metal oxides as catalysts within fuel cells. Maintaining long and stable operations, reducing the CO concentration effectively from the reformer and enhancing CO tolerance of the fuel cell have become significant topics [8].

1.5 Development of CO oxidation catalyst

1.5.1 Copper Manganese oxide – Hopcalite

Copper manganese mixed oxides as catalysts for CO oxidation have been extensively researched since the beginning of the 20th century. The commercial copper manganese mixed oxide is given the name Hopcalite. This name was derived from the Johns Hopkins University ("Hop") and the University of California ("Cal"), in which the process from fundamental investigations of carbon monoxide oxidation during the First World War was discovered [9]. The development of the Hopcalite catalyst was supported by funding from the US Navy department for the manufacture of a carbon monoxide mask for naval use. It was decided that it was important to discover a catalyst that would rapidly oxidize carbon monoxide at low temperatures, have considerable capacity, be hard and firm enough to retain a porous structure with rough handling and be chemically stable.

1.5.2 Palladium as a catalyst

The first investigation to give positive results of carbon monoxide oxidation at room temperature was a palladium catalyst. This was investigated by Stieglitz and co-workers at the University of Chicago [9]. While it was recognized that the limited supply and high cost of the metal was a handicap, it was hoped that a method might be developed for using this substance in minute quantities. Palladium oxide and

mixtures of the oxide with the metal (palladium black) were tested. Air containing 0.5 to 3% CO dried over soda lime and calcium chloride was passed though the catalyst. Carbon monoxide was completely removed but the catalysts experienced high deactivation

However, the activation of certain metal oxides with small amounts of palladium was also considered by many other researchers. Copper oxide granules were impregnated with a dilute solution of palladium nitrate [9]. Copper oxide alone removed 20 to 50% CO from a 1% CO mixture with air. Copper oxide doped with 0.25 and 0.4% Pd was tested for CO removal. Initially, 95 to 100% CO was removed at room temperature and 80 to 85% after 3 hours use. However, due to the sensitiveness of palladium to impurities and the cost of the work, the work was not continued.

1.5.3 Silver oxide

In 1918, the activity of silver oxide towards carbon monoxide was recognised by Stieglitz. He reported that CO in air was rapidly oxidised, at room temperature, by silver oxide and sodium peroxide arranged in alternate layers in a glass tube [9]. At room temperature neither of the two components alone rapidly oxidise CO at a low concentration in air. It was discussed why the mixture operates so much better than the silver oxide alone. Stieglitz suggested that the probable function of the sodium peroxide was to remove the carbon dioxide formed, and thus prevent the formation of silver carbonate on the surface of the silver oxide.

1.5.4 Metallic oxide mixtures

Research at the University of California in 1917 discovered that a precipitated copper oxide activated with 1% silver oxide was an efficient catalyst for the oxidation of arsine [9]. Following this discovery, Bray and co-workers found that the mixtures that were effective for arsine oxidation, were also reactive towards carbon monoxide/air mixtures. However, only 50% of CO was removed and the lifetime of the catalyst was very short. A mixture of 60% active copper oxide and 40% cobalt oxide was prepared from intimate mixture of moist hydroxides and was tested at the University of Berkeley in March 1918. The test analysis showed that the mixture was highly efficient and displayed a longer life time (ca. 2hours). A similar development of oxide absorbents had also been carried out by Frazer and co-workers at Johns Hopkins University. They discovered that a mixture of manganese dioxide and silver oxide showed encouraging results for oxidation of carbon monoxide. At first sodium hydroxide was added as a component in the mixtures and it was found that the reactivity increased. The presence of small amounts of fused granular calcium chloride in layers in the absorption tube increased the life of the absorbent. The investigators found that the efficiency of the material varied greatly with the physical character of the manganese dioxide.

1.5.5 Development of Hopcalite catalyst

In 1918, investigations at the Johns Hopkins laboratory soon discovered that much more active varieties of manganese dioxide could be prepared and that the omission of sodium hydroxide from the mixture of silver oxide and manganese dioxide increased the lifetime of the material. The most active manganese oxide was prepared by Fremy [10], where potassium permanganate was treated with a cool mixture of concentrated

sulphuric acid. It was discovered that with dry gas the action of a mixture of equal parts of manganese dioxide and silver oxide became *catalytic* – the carbon monoxide was oxidised continuously "by the oxygen of the air".

A four component mixture containing 50% MnO_2, 30% CuO, 15% Co_2O_3 and 5% Ag_2O was chosen in August of 1918, as a standard catalyst to be tested on a larger scale. This mixture was given the name Hopcalite I. Whilst Hopcalite I was in production, a cheaper catalyst was investigated consisting of a two component mixture of MnO_2 (60%) and CuO (40%). It was prepared from active manganese dioxide and copper carbonate. The latter was transformed into the oxide in the drying process. However, as this material was still in the development stage, when it was decided which mixture would be used in large scale production; the four component mixture was chosen. However, the lack of basic understanding of the catalysis left the so-called "mixture effect" unanswered.

1.5.6 Renewed Interest

Towards the end of the 1960's, the application of the Hopcalite catalyst in catalytic conversion of automotive exhausts led to a renewed interest of this mixed oxide material. Emphasis of research was to develop contaminant resistant base metal oxides to replace part of the precious metals used in catalytic converters [11], and to develop oxide catalysts with extremely high thermal stability for catalytic combustion [12].

1.6 Structure of Copper Manganese oxide system

Metal oxides and mixed metal oxide systems with spinel-like structure have received considerable attention because of their considerable electrical and magnetic properties. It has been reported that these properties are influenced by the nature of the metal ions and their distribution in the crystal lattice. In oxide spinels containing more than one transition metal ion per formula unit, the distribution and valence sites of the cations among both the tetrahedral (A sites) and octahedral (B sites) sub-lattices of the spinel structure, continue to be a problem.

Structural investigations of $CuMn_2O_4$ by X-ray diffraction were carried out by Sinha and co-workers [13]. A *priori* was thought that $CuMn_2O_4$, in analogy with $CuFe_2O_4$, $CuCr_2O_4$ and other cupric compounds, should have a tetragonal pseudo-spinel structure with inverse arrangement of cations. It was expected Cu^{2+} had displaced Mn^{3+} from the octahedral sites in the spinel. However, the authors found the compound to be a normal cubic structure. They also discussed that both Cu^{2+} and Mn^{3+} have substantial Jahn-Teller stabilisation energies, considerable distortion from the cubic symmetry would be expected. These inconsistencies were resolved by Sinha and co-workers [13] who proposed the occurrence of an electron transfer, giving rise to the resonance system:

$$Cu^{2+} + Mn^{3+} \leftrightarrow Cu^{+} + Mn^{4+} \qquad (Eq.1)$$

Zaslavskii and co-workers [14] reported that $CuMn_2O_4$ is an inverse, cubic spinel, but were unable to decide whether the inversion was complete or whether the cation distribution was statistical. Miyahara [15] believed that the absence of distortion

might be due to a compensation effect of Cu^{2+} and Mn^{3+}. Dollimore and Tonge reported similar observation supporting the ideas of Sinha and co-workers, regarding the presence of Mn^{4+} and Cu^+ [16]. It is unlikely that only Mn^{3+} and Cu^{2+} should be present because the high electric conductivity, in $CuMn_2O_4$ [17,18], requires that the same metal ions should be present in mixed valence states enabling electron hopping at either the tetrahedral or the octahedral sites. There were many reports on the structure and oxidation states of the components of $CuMn_2O_4$. However, little was known about the active sites in this catalyst, the role of Cu as a 'promoter', the mechanism of oxidation, or the mechanisms of deactivation.

1.7 Active sites

There has been much debate as to the nature of the active sites present in the $CuMn_2O_4$ catalyst. The catalyst is reported to be active at temperatures above water loss. The effect of water has suggested that Mn^{3+} (as MnOOH) is transformed to Mn^{4+} which is assumed to be the active site for O_2 adsorption [19,20]. This assumption from Kanungo did not agree conceptually with either the acid-base properties of the reactants (CO and O_2) or the relative basicity of hydrated Cu and Mn oxide surface. Veprek and co-workers [21] envisioned a coupled dehydration reaction between hydrated Cu and Mn oxides. The acid-base properties of the reactants were used to support the discussion. CO is basic [22,23] and O_2 is acidic [22]. It was expected that hydrated Cu oxide will dehydroxylate and hydrated Mn oxide will protonate to form water. This process would form a comparatively unstable Cu^{3+} cation but the Mn^{3+} would remain unchanged [24]. The excess electron on MnOO⁻ would be transferred to Cu^{3+} generating Cu^{2+}. This idea brought about a schematic to follow the redox couples and their adsorption properties.

$$CO \rightarrow Cu^{2+} - Mn^{3+} \leftarrow O_2 \qquad\qquad (Eq.2)$$

$$O_2 \rightarrow Cu^{3+} - Mn^{4+} \leftarrow CO$$
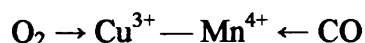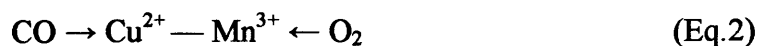
This model was supported with the fact that Cu_2O and MnO_2 are active catalysts for

CO oxidation [25]. This idea was supported by Kanungo's findings [19,20] in that the

maximum activity occurs for Cu mole fraction of 0.5 coincidental with the maximum

H_2O content and the maximum Mn^{3+}/Mn^{4+} ratio. Schwab and Kunungo [26] have the

attributed the oxidation activity of $CuMn_2O_4$ to Mn^{4+} where:

$$CO + Mn^{4+} \rightarrow CO^+_{ads} + Mn^{3+} \qquad\qquad (Eq.3)$$
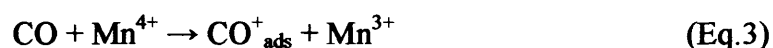
The promotion of Cu has further been linked to the reduction of O_2:

$$\tfrac{1}{2} O_2 + Cu^{1+} \rightarrow Cu^{2+} + O^-_{ads} \qquad\qquad (Eq.4)$$

The oxidation occurs by the process:

$$O^-_{ads} + CO^+_{ads} \rightarrow CO_2 \qquad\qquad (Eq.5)$$

The resonance reaction system brings the catalyst back to the active state

$$Cu^{2+} + Mn^{3+} \leftrightarrow Cu^{1+} + Mn^{4+} \qquad\qquad (Eq.1)$$
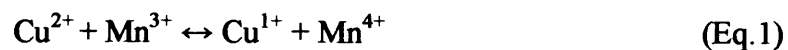
Veprek and co-workers [21] stated that if Equations 1,3 and 5 applied, the

deactivation of this catalyst system cannot be linked to the oxidation state of Cu or

Mn as long as the redox couple remains active.

1.8 Activity of the Hopcalite catalyst

The methods of X-ray diffraction (XRD), thermal analysis, surface area determination and activity measurements were used to characterise the Hopcalite catalyst. However, at that time, no surface analysis techniques were used to further explain the properties of the catalyst. Since heterogeneous catalysis occurs on the very outer surface of solids, previous studies correlated with bulk composition [19,20] and structural changes were in doubt. This led to Veprek and co-workers [21] to consider the effect of electronic and structural promoters on the activity of the Hopcalite catalyst.

1.8.1 Oxidation States

Veprek and co-workers [21] used a surface sensitive tool, X-ray photoelectron spectroscopy, to study the deactivation of a commercial Hopcalite catalyst and the importance of the oxidation states present. Experimental evidence from the chemical shifts of the Cu 2p line and the multiplet splitting of the Mn 3s clearly demonstrated the existence of the redox couple in the Hopcalite catalyst. The redox couple apparently operates in both the amorphous state and crystalline spinel but is shifted predominately towards the more stable Cu^{1+}/Mn^{4+} state on crystallisation as predicted by Vanderberghe [27].

The activity of mixed copper manganese oxide for CO oxidation showed two maxima at ca. 0.1 and 0.5 CuO mole fraction [19,20]. The minimum activity occurred in the middle of the composition range. Dollimore and Tonge [16] attribute this behaviour to the amount of Cu^{1+} in the surface. Their understanding being Cu^{1+} forms stable complexes with CO. A high Cu^{1+} surface concentration would give strongly adsorbed CO and block the surface causing lower activity. The highest Cu^{1+} concentration was

predicted to be in the middle of the concentration range. The catalyst in their study did not reactivate at the oxidising conditions used for the amorphous samples. Also, plasma-induced re-oxidation to Cu^{2+} did not re-establish activity. However, because of potassium segregation, which is irreversible and causes catalyst deactivation, it was not possible to link redox couple directly to catalytic activity.

Porta and co-workers [28] reported studies on the preparation conditions that could possibly influence the catalytic activity of the material. Cu-Mn hydroxycarbonate-carbonate precursors were prepared by co-precipitation of nitrates. The Cu-Mn mixed oxides were obtained by heating the precursors at 450°C for 24h in N_2 and in Air. Cu-Mn precursors heated in N_2 at 450°C, depending on the Cu/Mn atomic ratio gave CuO, $CuMn_2O_4$ [$Cu(II)Mn(III)_2O_4$], $CuMnO_2$, Mn_3O_4 and MnO. The precursors heated in air at 450°C, depending on the Cu/Mn atomic ratios, gave CuO, Mn_5O_8, α-Mn_2O_3 and $CuMn_2O_4$ [$Cu(I)_xCu(II)_{1-x}Mn(III)_{2-x}Mn(IV)xO_4$]. The data from XPS and XRD analysis is in agreement with Veprek and co-workers [21], that the electronic configuration of Cu (I) occupies in the $CuMn_2O_4$ spinel structure, the octahedral sites where they are subjected to larger extra-atomic relaxation energy.

A series of copper manganese oxide catalysts of approximate composition $Cu_{1+x}Mn_{2-x}O_4$ (x = 0.54 ± 0.04), which were aged for various times and at different pH values, was studied by XPS [29]. The results shown by Mirzaei and co-workers [29] showed that $CuMn_2O_4$ was a predominately Cu^{2+} species. This was represented by a Cu $2p_{3/2}$ peak at a value of 933.6 eV and a separation of 20.2 between the Cu $2p_{3/2}$ and $Cu_{1/2}$ peaks. The Mn oxidation states were difficult to distinguish due to the narrow binding energy range between the oxides. Manganese exhibited oxidation between Mn^{3+} and Mn^{4+}. These results were in agreement with previous reports [21, 30,31]

1.8.2 Oxidation Reaction

Further work has looked at the synergistic effects in the Hopcalite catalyst. Buciuman and co-workers [32] have reported a possible oxidation reaction taking place over the Hopcalite catalyst. Different samples of 'copper manganite' calcined at 550°C or deactivated by calcination at 1000°C in air were tested. The reaction rates of H_2 and CO oxidation over copper and manganese oxides showed that the single-phase catalysts CuO, Mn_2O_3 and the spinel $CuMn_2O_4$ calcined at 1000°C showed similar activities at low temperature. However, at higher temperatures, the reaction rate over CuO increased strongly. The activity of the $CuMn_2O_4$ catalyst calcined at 550°C was much higher than the single phase catalysts for low temperature CO oxidation. Buciuman and co-workers [32] believed that this was an indication that there was a synergy between physically mixed copper and manganese oxide phases.

Copper oxide and manganese oxide display opposite characteristics that could be assigned to different mechanisms. Boreskov [33] has reported that oxidation reactions can proceed through an associative or a redox mechanism: the former takes place by using adsorbed oxygen species and the latter involves oxygen from the catalyst lattice and displays high activation energies.

Jernigan and Somorjai [34] have demonstrated by experiment that stoichiometric CuO can hardly adsorb gas-phase oxygen, due to its insulator character; this process took place only on a pre-reduced surface. TPR experiments showed that a low reduction temperature confirmed the availability of lattice oxygen for CuO. In comparison, Mn_2O_3 displayed the kinetic characteristics of an associative mechanism, likely to occur owing to the oxygen adsorption capacity and poor reducibility in the temperature range of the kinetic runs. For the $CuMn_2O_4$ spinel, both its reducibility

and oxygen adsorption capability place it between CuO and Mn_2O_3. The oxidation reaction taking place could be a combination of the associative and redox mechanism.

1.9 Preparation conditions of copper manganese mixed oxides

Veprek and co-workers [21] have claimed that an 'amorphous' copper manganite as active phase in Hopcalite catalysts. The amorphous to crystalline transition of $CuMn_2O_4$, together with segregation of potassium would cause thermal activity decay. It has been well documented that amorphous, $CuMn_2O_4$, Hopcalite is a powerful oxidation catalyst that can catalyse, at higher temperatures, the combustion of several organic compounds [21,35].

The activity of copper manganese oxide is known to depend upon the structure of the catalyst precursor, which is controlled by the preparation route. Porta and co-workers [36] reported that the structure of the hydroxyl-carbonate precursor phase of copper manganese catalysts is crucial in preparation process. This idea that the preparation conditions of copper manganese mixed oxides control catalytic activity towards CO oxidation, led to extensive research by Hutchings and co-workers.

Mixed oxide catalyst precursors containing copper are typically prepared using a co-precipitation procedure in which suitable metal salts, typically nitrates, are premixed and a precursor is precipitated using sodium carbonate. However, the effect of ageing the catalyst precursor had not been reported. This led to Hutchings and co-workers [37] reporting their initial findings on the effect of ageing on catalytic activity. Their results indicated that the ageing time is a parameter of crucial importance in the preparation of active copper manganese mixed oxide catalysts. The unaged precursor

was found to be well crystalline copper hydroxy nitrate together with manganese carbonate. On ageing, the copper hydroxy nitrate re-dissolved and all the aged precursors were comprised of poorly crystalline manganese carbonate.

Hutchings and co-workers [38] investigated the effect of preparation conditions on the catalytic performance of copper manganese oxide catalysts for CO oxidation. They discussed that several variables during the preparation procedure affected the structure and activity of the catalyst. The variables included the precipitate ageing time, pH and temperature of precipitation, the [Cu]/[Mn] ratio of the precipitation solution and the catalyst calcination temperature. The optimum conditions for highest CO conversion were reported to be:

- [Cu]/[Mn] ratio = 1/2

- Precipitation pH = 9.0

- Precipitation temperature = 80°C

- Ageing time = 12h

- Calcination = 500°C for 17h

Powder X-ray diffraction analysis showed similar results to their initial findings in that ageing the precursor, the copper hydroxyl carbonate re-dissolved and only poorly crystalline manganese carbonate was identified. The effect of ageing has been discussed [38], as the ageing time is increased; the formation of mixed CuMnOx oxides becomes more predominant.

Calcination at 500°C produced a relatively amorphous catalyst, which showed the highest CO conversion (ca. 90%) and was composed of the stoichiometric Hopcalite phase $CuMn_2O_4$. Catalysts calcined at 300 and 400°C showed similar diffraction

patterns and comprised of separate $MnCO_3$ and CuO phases, which contributed to lower activity (ca. 60-80% conversion). The most active catalyst was produced with a precipitation pH 9.0, however the most active phase was stoichiometric $CuMn_2O_4$ prepared at pH 8.3. Precipitation at pH at 8.3 caused the solution pH not to influence the Cu/Mn bulk ratio of the prepared catalysts as they were close to the preparation media. The temperature of the ageing solution was varied and the results showed that the bulk phases present were $Cu_{1.4}Mn_{1.6}O_4$ and Mn_2O_3. There was a direct link between increasing ageing time and CO oxidation activity. The optimum practical temperature was considered to be $80^{\circ}C$.

The Cu/Mn ratio of 1/2 was the most active catalyst and this preparation media corresponded to the ratio of the stoichiometric Hopcalite phase $CuMn_2O_4$, which as been identified as the phase with the highest specific activity for CO oxidation from the pH ageing studies [37].

Studies by Mirzaei and co-workers looked into further characterisation of the copper manganese oxide catalysts [39]. The effect of ageing time was investigated using powder X-ray diffraction (XRD), temperature programmed reduction (TPR) and transmission electron microscopy (TEM). X-ray diffraction studies for the unaged precursor showed the crystalline copper hydroxyl nitrate together with manganese carbonate. On ageing, the copper hydroxyl re-dissolved, and poorly crystalline manganese carbonate was identified. The X-ray diffraction patterns for the calcined catalysts showed that the materials were less crystalline than the precursors and the phases present were dependant on ageing time.

The TPR investigation showed that copper oxides could be reduced at lower temperatures compared to manganese oxides. The TPR signals of the mixed compounds could not be attributed to well defined reduction peaks, due to the complexity of the systems due to the large number of possible combinations of different oxidation states of copper and manganese. Transmission electron microscopy showed that ageing the precipitates leads to profound changes in morphology. Amorphous, irregularly shaped aggregates present in the unaged catalyst, transformed to the flat, more regularly shaped aggregates in the 120 minute aged sample.

Hutchings and co-workers also reported that the presence of residual sodium can lead to catalyst poisoning [40]. Sodium carbonate is used to control the pH of the precipitation mixture during preparation of the copper manganese precursor. It was reported that as the ageing time increases, the Cu/Mn surface ratio decreases, which was consistent with previous analysis of the bulk structure [37, 38]. The highest activity was recorded for the sample aged for 12h (ca. 80% conversion). The Na/Mn surface ratio was significantly lower with longer ageing time. The surfaces of the aged catalysts were analysed by X-ray photoelectron spectroscopy (XPS) and it was apparent that ageing at pH 8.3 showed the lowest concentration of Na^+ cation. Veprek at co-workers [6] have shown that the presence of K^+ on the surface of Hopcalite catalysts is also a cause of deactivation.

Jones [41] has also reported that the preparation procedure was important. There were problems due to the lack of reproducibility during the synthesis procedure. The factors affecting the preparation were the lack of pH control, during the precipitation procedure, combined with the poor maintenance of the temperature, thought to have

arisen from heating the reaction vessel in an isothermally maintained water bath. The heating method proved inadequate as temperature differences were observed between the temperature of the water bath and the temperature of the precipitate within the reaction vessel. This temperature fluctuation was identified to be an influencing factor in the preparation of catalyst precursors [38]. The catalyst preparation apparatus was modified and is shown in chapter 2.

Jones also investigated the calcination temperature of the catalyst precursor. The calcination temperature and length of time reported by Hutchings and co-workers [38] was thought to be too high. It has previously been suggested that high temperature treatment might destroy the porous nature of the material [9]. Jones reported that the calcination conditions of heating at 400°C for 2h were the optimum settings for producing a highly active catalyst. This finding was in agreement with Mirzaei's work [42].

It has been well reported that the pure and mixed oxides of copper and manganese have involved the use of nitrate precursors. Nitrates have been used because of their high solubility and the ease of removal of the nitrate anion during calcination [43]. The advantage of nitrates is that no residue is left on the catalyst, whereas the use of chlorides and sulphates has led to the retention of anions on the surface. It was reported that the preparation of alumina supported manganese oxide catalysts, with manganese acetate as a precursor, led to a highly dispersed oxide phase, homogeneously distributed throughout the alumina particles [44,45] The formates of copper and manganese decompose to the corresponding oxides at temperatures ca. 350-400°C. Sol-gel derived binary copper manganese oxides for CO oxidation in dry air at room temperature have been investigated [46]. These types of catalysts are used

in Proton Exchange membrane fuel cells and have high catalytic activity. The high

activity was due to a combination of high surface area, an amorphous state and the

presence of Cu^{2+} and Mn^{3+}.

1.10 Addition of components to the structure

The application of copper manganese mixed oxides as catalysts for CO oxidation has

been well documented. Further research has looked at improving the activity of these

catalysts. The catalytic properties of pure substances are generally well known but the

possibilities for improvement through the use of suitable promoters can also be

considered. A promoter is a substance that can be added to a catalyst during

preparation, which will increase activity, selectivity, and stability for the desired

reaction [47].

Active centres of many oxide catalyst can be strongly linked to the presence of lattice

defects that occur near the surface. A small amount of impurity can largely increase

the number of lattice defects since each interstitial foreign atom may be at the centre

of a lattice defect that extends for 10 Å or more.

Spinels exhibit a variety of applications in electronics, magnetic materials and as

catalysts [48,49]. The catalytic properties of these oxide spinels can suitably be

modified by incorporating different metal ions in the lattice to improve the quality of

the materials.

Salker and Gurav [50] have tried to understand the effect of tetrahedral (A) site

substitution by copper in the lattice of $CoMn_2O_4$. They also investigated the catalytic

activity of manganites with various cationic compositions prepared by co-

precipitation in the oxidation of CO. For $Co_{1-x}Cu_xMn_2O_4$, at $x=0.3$, higher catalytic activity was due to the octahedral Mn^{3+}/Mn^{4+} ratio. They described intermediate compositions exhibiting better catalytic activity than the end compositions which was evidence of synergism. The electrical resistivity of different compounds were found to depend on the ion pair association (Mn^{3+}/Mn^{4+}) occupying the octahedral site of the spinel. Magnetic susceptibilities showed higher value for cubic system $(CuMn_2O_4)$ and lower value for tetragonal system $(CoMnO_4)$.

Jones has reported the addition of small quantities of other elements to the CuMnOx catalyst. The addition of Co, Ag, Ni and Fe as the possibility of a promotion of activity towards CO oxidation was investigated [41]. Doping the Hopcalite catalysts with cations, particularly nickel and cobalt, contributed to increased stability with time on line. Jones discussed that it was likely that the nickel was reacting sacrificially with any water vapour present in the feed gas, thereby protecting the catalyst from water poisoning.

The cobalt doped catalysts showed the highest overall improvement in catalytic activity compared to the other dopants. A 2% Co doped CuMnOx catalyst aged for 6h showed ca. 90% steady state CO conversion. However, the initial activity of the Co doped catalyst was lower than an industrial Hopcalite catalyst. Jones commented that the presence of cobalt may be contributing electronically to the oxidation mechanism or re-oxidation mechanism occurring in the catalyst. Temporal Analysis of Products studies indicated that oxidation using lattice oxygen was longer lasting where the catalyst was cobalt doped. This was evidence that the role of cobalt, in the re-oxidation mechanism of a reduced species came from the fact that the deactivated

cobalt doped catalyst surface, was more responsive to re-oxidation experiments than the undoped CuMnOx surface.

Wright and co-workers [51] have also reported catalytic studies of systems containing copper, cobalt, and manganese. Of all the mixed-metal oxides prepared, the $CuCoMnO_4$ spinel had the highest specific activity towards CO oxidation as well as the highest surface area. .

Yang and co-workers [42] have discussed the effect of surface enrichment in mixed oxides of copper, cobalt, and manganese, and its effect on CO oxidation. Segregation in mixed oxides of transition metals is highly complicated. It has been shown that the segregation is related to the size of the segregating ion, which depends strongly on its oxidation state, the electric charge and the concentration of defects at the surface, the structure of the surface, and the gas atmosphere the surface is exposed to. In many cases the dominant factor determining the segregation is the size of the segregating cation, and the larger the size, the stronger the enrichment at the surface [52]. Yang and co-workers commented that this is not the case for mixed oxides of Mn, Cu, and Co, because the most enriched Mn^{4+} has the smallest size among all the cations present at the surface.

1.11 Copper - zinc oxide catalysts

1.11.1 Copper – Zinc Interaction

Copper zinc oxide catalysts are widely used for hydrogenation and dehydrogenation reactions. They have importance as commercial catalysts for low temperature water gas shift reactions and methanol synthesis [53,54]. The CuO-ZnO system has received

a great deal of fundamental work devoted to clarify the role played by each component and the nature of the active sites. There are several conflicting issues involving the species present.

There is a general agreement of the central role played by the reduced copper in the catalyst [54-57]. In particular, the interaction of copper with ZnO and the oxidation state of copper are supposed to be involved as active sites during catalytic processes. Several authors report that a synergy effect arises, the contact of copper with ZnO being the binary catalyst, which is more active than each component on its own [58-60]. In contrast to this, other authors claim that the active site is placed on a particle of copper metal and that no Cu-ZnO synergy occurs [61,62]. The presence of Cu^+ species in the reduced Cu/ZnO and $CuO/ZnO/Al_2O_3$ catalysts has been reported [55-57,63-65]. There is reported evidence of the formation of monovalent copper upon reduction in hydrogen of Cu/ZnO catalysts and the role of ZnO has been discussed [66-68]. Moretti and co-workers have reported XPS studies that provide evidence that a strong CuO-ZnO interaction exists in both high [68] and low [69] copper content.

Fierro and co-workers [70] have discussed the reduction kinetics of some CuO-ZnO catalysts. They discovered a promoting effect of ZnO on the copper reducibility using temperature programmed reduction (TPR) analysis. The preparation method markedly influenced the catalyst reduction and homogeneity. A Cu:Zn = 50:50 catalyst (ex-hydroxycarbonate precursor) was less reducible than a CuO:ZnO = 50:50 catalyst (ex-hydroxycarbonate precursor) and showed a dual Cu speciation not found in the latter catalyst [71]. The precipitation conditions and type of precursor can influence the nature of the working catalyst [48].

1.11.2 Copper-zinc manganites

Copper-zinc manganites with the general formula $Cu_xZn_{1-x}Mn_2O_4$ have been prepared and reported by Fierro and co-workers [72]. They were prepared by thermal decomposition of carbonate precursors obtained by co-precipitation at constant pH. X-ray diffraction analysis showed that for all samples a single rhodochrosite – like phase, $Cu_xZn_yMn_{1-x-y}CO_3$, with Cu^{2+}, $Mn2^+$ and Zn^{2+} in solid solution was present.

The copper-zinc manganite catalysts have been tested for catalytic activity towards reduction of NO by hydrocarbons. Manganese based mixed oxides such as Mn_3O_4, $ZnMn_2O_4$ and their solid solutions, are known to be efficient catalysts for the selective gas phase reduction of nitrobenzene to nitrosobenzene [73]. Fierro and co-workers reported that $ZnMn_2O_4$ was an active catalyst for NO reduction by C_3H_8. However, the additional presence of copper in zinc manganites remarkably promotes the activity, even at low concentration. According to TPR analysis, copper strongly enhances the reducibility of $Cu_xZn_{1-x}Mn_2O_4$ spinels with respect to pure $ZnMn_2O_4$ [72]. Ferraris and co-workers have investigated further the catalytic behaviour of copper-zinc manganites for the reduction of NO by hydrocarbons [74]. They also reported that the presence of copper in the spinel enhanced the catalytic activity of NO reduction by propane and slightly improved that of N_2O reduction. The difference with the studies here, is that these types of catalysts are used for reducing NO using propane, whereas reducing O_2 using CO would be the target reaction for this thesis. It would be interesting to see, in oxidising conditions, whether zinc has similar effects on a copper manganese mixed oxide catalyst for CO oxidation.

1.11.3 Cobalt-zinc manganites

Fierro and co-workers [75] also reported cobalt-zinc manganites for the reduction of NO by hydrocarbons. They discovered similar results to the copper based catalyst in that the presence of cobalt enhanced catalytic activity. However, the TPR analysis showed that the reducibility in H_2 of the mixed Co-Zn manganites was not influenced by cobalt, whereas copper does in the Cu-Zn manganite system.

1.11.4 Copper zinc oxide catalysts for CO oxidation

Taylor and co-workers [76] reported the first results that copper zinc oxide catalysts, prepared by co-precipitation, can display much higher activity towards CO oxidation than the current commercial Hopcalite catalyst. Hutchings and co-workers [77] extended the initial findings by studying the effect of catalyst ageing on the morphology and activity of copper zinc oxide catalysts.

The catalysts were prepared using a co-precipitation technique, similar to the one they reported to synthesise copper manganese oxide catalysts [16-19]. The samples were analysed by transmission electron microscopy (TEM) and electron dispersive spectroscopy (EDS) in a scanning transmission electron microscope (STEM). The composition and morphology of the non-calcined precursor changed from an initial amorphous state to micro-crystalline aurichalcite and rosaite, which were present as needles and platelets. Microscopy showed that a dispersion of Cu-rich nanoparticles progressively formed as the precipitate age increased. Using STEM-EDS, it was possible to establish that Cu was present in solid solution within the ZnO crystallites and vice-versa. The copper zinc catalysts showed appreciable improvement of CO oxidation compared to the copper manganese oxide (Hopcalite) catalyst.

Powder X-ray diffraction analysis of copper zinc oxide catalysts, with varying time, showed that the unaged precursor was amorphous to X-rays, whilst increasing the ageing time resulted in the observation of crystalline diffracting phases [78].

Copper zinc mixed oxide catalysts were all active for ambient temperature CO oxidation. Increasing the catalyst ageing time up to 165 minutes was accompanied by an increase in CO oxidation, ca. 20% conversion for an unaged catalyst and ca. 50% conversion for a catalyst aged for 165 minutes.

1.12 Alternative reactions

The properties of Hopcalite-type catalysts have shown that they are versatile to other reactions. Amorphous $CuMn_2O_4$ has been stated to catalyse, at temperatures up to 500°C, the combustion of some organic substances, such as hydrocarbons and hydroxyl-, halide and nitrogen containing compounds [79-81].

1.12.1 NO_x reduction with CO

The activity of Cu-Mn spinels, both unsupported [82] and γ-Al_2O_3 supported [83] towards NO-CO and NO-CO-O_2 have been reported. The unsupported spinel $CuMn_2O_4$ exhibited an activity several times higher than that of Ni and Co manganites. Maximum activity of supported Cu-Mn spinels was reported for samples with a Cu/Mn atomic ratio close to that of the stoichiometric $CuMn_2O_4$.

The activity of CuO-MnOx catalysts, for NOx reduction, is dependant on the preparation method [84], similarly for catalysts used for CO oxidation. At ambient temperature both adsorption and interaction of CO and NO become more intense with

increasing atomic fraction of copper content. The most active catalyst, the degree of NO conversion to N_2 attained with a $CO/NO/O_2/Ar$ mixture was almost the same as that obtained with a $CO/NO/Ar$ mixture. A Langmuir-Hinshelwood mechanism was proposed. Increasing temperature under the conditions of a $CO/NO/O_2/Ar$ mixture, reduction of the catalyst surface began. This lead to a depression of the CO-NO reaction at temperatures up to $130°C$, and to progressive acceleration of the CO-NO reaction at temperatures above $130°C$. In the presence of oxygen, CuOx-MnOx catalyst had an even higher activity over a wider temperature range ($75-300°C$).

1.12.2 NOx reduction with NH_3

Cu-Mn mixed oxides prepared by a co-precipitation method were applied for low temperature NO reduction with NH_3 in the presence of excess oxygen [85]. Catalysts were analysed for effects of [Cu]/[Mn] ratio and calcination temperatures. High NOx conversion was obtained over $Cu_{0.01}Mn_{0.50}$ compared with $Cu_{0.01}Mn_{0.25}$ when both catalysts were calcined at $450°C$. Increased calcination temperature, led to NOx conversion decreasing over both catalysts.

1.12.3 Oxidation of toluene

Catalytic combustion at lower temperatures is an alternative route to eliminate volatile organic compounds (VOCs), which can reduce energy costs and formation of harmful by-products such as dioxins from chlorinated compounds and nitrogen oxides in contrast to incineration [86].

Li and co-workers [87] investigated a series of $MnOx/ZrO_2$, $MnOx/Fe_2O_3$, MnOx/CoOx and MnOx/CuOx catalysts for the catalytic oxidation of toluene. The

Cu-Mn catalyst gave the highest activity for complete oxidation of toluene. The molar ratio of Mn:Cu was 2:1 and the total oxidation of toluene was ca. 220°C, which was close to the activity of the widely investigated Pd catalyst for this reaction [87]

1.12.4 Oxidation of ethanol and propane

Ethanol oxidation generates a lot interest with regard to the control of the emissions from ethanol fuelled vehicles. A drawback to this type of function is the formation of partial oxidation products, such as acetaldehyde, which are more harmful than the original organic compound. Stationary applications are favourable because it is easy to control the temperatures and always keep the catalyst temperature high enough to secure complete oxidation to CO_2 and H_2O.

Cu-Mn mixed oxides prepared by a co-precipitation method with varying ageing time of 4, 18 and 24h were prepared for propane and ethanol oxidation [88]. In both reactions, the Cu-Mn catalysts are more active than Mn_2O_3 and CuO pure oxides. In the case of propane oxidation, the total conversion on the Cu-Mn catalyst was achieved at ca. 390°C, which is 70°C lower than on Mn_2O_3 and ca. 50°C less than on CuO. Morales and co-workers reported that catalytic activity of the Cu-Mn catalyst increased with increasing ageing time. The catalytic behaviour was related to the existence of a $Cu_{1.5}Mn_{1.5}O_4$ mixed phase.

Larsson and Andersson have investigated the combustion of ethanol over CuO_x/Al_2O_3, CuO_x-CeO_2/Al_2O_3, $CuMn_2O_4/Al_2O_3$ and Mn_2O_3/Al_2O_3 catalysts [89]. They reported that the $CuMn_2O_4/Al_2O_3$ catalyst was more active than $CuOx-CeO_2/Al_2O_3$ for the combustion of ethyl acetate and ethanol. However, the CuOx-

CeO_2/Al_2O_3 catalyst was more active for the oxidation of CO. They state that different active sites can be involved or the oxidation of the compounds can be affected differently by electronic and synergistic effects between the catalyst constituents.

It was revealed that a synergetic effect between copper and manganese, giving higher activity over the $CuMn_2O_4/Al_2O_3$ catalyst than is obtained over the alumina supported single oxides of copper and manganese. The synergetic effect has also been reported by Dollimore and Tonge [16] and can be due to the formation $CuMn_2O_4$. It was observed by Larsson and Andersson that an addition of 3 vol% water to the feed did not decrease the complete oxidation of ethyl acetate and ethanol with the $Cu_6Mn_{12}Al$ catalyst whereas the Cu_6Ce_6Al catalyst did. This was an interesting observation since that the $CuOx/CeO_2$ catalysts are quite insensitive to humid feeds [90], whereas Hopcalite catalysts are known to be sensitive [91].

1.12.5 Selective ortho-methylation of phenol with methanol

Catalytic alkylation of phenols has received increased attention due to the importance of alkyl phenols as the starting materials for various commercial applications. These include manufacture of dyes, drugs, antioxidants and plastics. Methylation of phenol with methanol as an alkylating agent to produce 2,6-xylenol was reported over copper manganese oxide spinels [92]. The initial activity increased with increasing copper content. Higher copper containing catalysts were reported to be more prone to reduction under reaction conditions, leading to rapid deactivation. The catalysts with low copper content were more active and selective to 2,6-xylenol. A high ortho-selectvity of 100%, with 2,6-xylenol selectivity of 74%, was observed over $Cu_{0.25}Mn_{2.75}O_a$ at 400°C.

1.12.6 Steam reforming of methanol

The increasing demand for energy has caused development of energy conversion processes, such as fuel cells, that are efficient and have minimal environmental impact [93]. Fuel cells are appropriate for automotive applications, solid polymer fuel cells (SPFCs) are considered as suitable candidates for vehicles and small stationary power plants [94]. The primary fuel for these systems is hydrogen, which can be supplied from liquid fuels, such as methanol. Hydrogen production from methanol is possible through several routes: decomposition, steam reforming, partial oxidation and combined reforming [95,96]. Copper manganese mixed oxide catalysts have been studied for steam reforming of methanol [97,98]. These catalysts were prepared by a urea-nitrate combustion method and showed high activity towards H_2 production with high selectivity.

1.13 Catalysis by gold

Gold was not regarded as particularly promising for catalytic purposes until the late 1980's. Its low activity was generally explained by the presence of partially filled d-orbitals, which makes metallic gold unable to chemisorb small molecules [99]. It was in 1987, that Haruta and co-workers [100] reported that supported gold nano-crystals can be highly effective catalysts for CO oxidation at very low temperatures. Hopcalite catalysts, which are used extensively for CO oxidation reactions, are not water tolerant [101]. A number of systems, Pt/SnOx and Pd/SnOx [102-104], are effective for this reaction. However, there are complications with the currently used catalysts such as need for pre-treatment, large induction periods before reaching maximum catalytic efficiency [105].

Haruta and co-workers [100] reported novel gold catalysts prepared by co-precipitation from an aqueous solution of chloroauric acid and the nitrate of transition metals. The highest oxidation activity was achieved using gold combined with α-Fe_2O_3, Co_3O_4, or NiO. These new gold catalysts were not only more active but also much more stable than the conventional Hopcalite catalyst. In particular, the catalyst composed of Au and α-Fe_2O_3 (Au 5: Fe 95 in atom %) was sufficiently stable that it could maintain the initial activity observed at -70°C even after a subsequent continuous run with dried reaction gas at 0°C for 7 days. These findings stimulated extensive research in the last twenty years [106].

The synthesis of highly dispersed small gold particles is highly sensitive towards the preparation method. Haruta and co-workers [107,108] showed that the incipient wetness impregnation is unsuitable to produce highly dispersed gold catalysts, and that in order to obtain high activity gold catalysts, the materials have to be prepared via co-precipitation or deposition-precipitation.

The preparation method which can be applied to the widest range of different support materials is the deposition-precipitation method. Beside the preparation method, also the synthesis conditions, like pH value during precipitation, temperature of calcination and the pre-treatment conditions have a significant effect on the properties of gold catalysts. In such a preparation method, $HAuCl_4$ is used as a metal precursor. The chloroauric anion hydrolyses in solution to form $Au(OH)_xCl_{4-x}^-$. The extent of hydrolysis depends on the pH, and Cl concentrations [109]. It has be been reported that preparation at a pH ranging from 7 to 8 is preferable depending on the support [110]. At this pH, the value of x is close to 3. At lower pH there is less hydrolysis of the Au-Cl bond. Additionally, at pH below the isoelectric point of the support, the

surface is positively charged and is capable of adsorbing more of the negatively charged gold species. This leads to not only a larger gold loading, but also a high concentration of chloride on the surface. The presence of chloride increases the mobility of the support, leading to large gold particles [111]. At pH above the isoelectric point of the oxide, adsorption of the negatively charged gold complex decreases rapidly, resulting in a lower gold loading. However, there will be less chloride at the catalyst surface, leading to smaller gold particles being formed.

Gold deposited on a variety of supports including TiO_2, Al_2O_3, Fe_2O_3, and CeO_2 has been reported [106,112-115]. The most studied catalyst for CO oxidation is gold supported in TiO_2 because it is one of the most active catalysts for this reaction at low temperatures. The optimum gold particle size in these catalysts was found to be 2-3 nm [116,117]. An important requirement is that the support materials should have high specific surface areas, preferably larger than 50 m^2g^{-1} [118].

High activity Au/CuO-ZnO catalysts for the oxidation of carbon monoxide at ambient temperature have been studied [119]. The catalysts were prepared by a co-precipitation method. Au/CuO-ZnO, Au/ZnO and Au/CuO catalysts were found to give sustained activity without deactivation during the 800 minutes experimental test. The undoped CuO-ZnO catalyst prepared using the same co-precipitation method displayed a much lower activity and a general decline in CO conversion.

The extensive research of Au supported oxides and Hopcalite catalysts for CO oxidation have been discussed in many literatures. However, it was interesting that there were very little studies on the addition of Au to Hopcalite catalysts. The only such investigation of the addition of Au to the Hopcalite catalyst was reported by Taylor and co-workers [120]. Au-containing Hopcalite catalysts for low temperature

CO oxidation were prepared by a co-precipitation method. The addition of Au to the CuO-MnO system resulted in a marked improvement in catalytic activity. The most active catalyst was a 3% doped CuMnOx sample, with an increased rate of CO oxidation compared to an undoped CuMnOx catalyst. Furthermore, the addition of Au caused a decrease in the extent of catalyst deactivation.

1.14 Conclusion

The majority of papers reporting the preparation of Hopcalite catalysts use a co-precipitation method. The reported work of particular interest is the papers reported by Hutchings and co-workers, on the preparation of copper manganese mixed oxides. The importance being that the preparation parameters can be controlled to produce mixed oxide species that are highly active for CO oxidation. The catalyst preparation procedure, reported by Hutchings and co-workers, will form the basis of this thesis. The copper zinc oxide catalyst for ambient temperature CO oxidation [76] has highlighted a possibility that zinc could be incorporated into a copper manganese oxide catalyst. Taylor and co-workers have reported that copper zinc mixed oxides are active for CO oxidation at low temperatures. This leads to a plan that a copper zinc manganese mixed oxide catalyst could show improvement in activity compared to a Hopcalite catalyst. Fierro and co-workers discovered a promoting effect of ZnO on the copper reducibility using temperature programmed reduction (TPR) analysis [70]. This would be interesting to see the same effect with a copper zinc manganese mixed oxide, whether that similar promoting effects occur with manganese as they do with copper.

In the last decade, there has been a significant amount of papers published on gold supported oxides for ambient temperature. Where different oxide supports can affect the overall activity of the catalyst. However, there is no work reported on Hopcalite catalysts acting as a support for gold particles. The only reported work on Au doped Hopcalite catalysts is by Taylor and co-workers [120], however this is where gold is pre-mixed with the copper manganese bulk material. This process uses a larger amount of gold starting material compared to gold being deposited onto an oxide support. The plan would be to use a deposition precipitation method to incorporate gold particles with the Hopcalite catalyst making it a more efficient process.

1.15 Chapter 1 References

[1]   P. Chovin, Carbon monoxide: analysis of exhaust gas investigations in Paris. Environ. Res. 1 (1967) 198.

[2]   R.F. Christman, Chemistry of air pollution. In Air Pollution Control: Guidebook for Management, ed. A.T. Rosano. Environment Sciences Services, Wilton, CT, 1969, pp. 87-91.

[3]   J.W. Saalfrank, W.F. Maier, C.R. Chimie 7 (2004) 483.

[4]   M. Baldi, E. Finocchio, F. Milella, G. Busca, Appl. Catal. B: Environment 16 (1998) 43.

[5]   S.D. Gardner, G.B. Hoflund, B.T. Upchurch, D.R. Schryer E.J. Kielin, J. Schryer, J. Catal. 129 (1991) 114.

[6]   S.D. Gardner, G.B. Hoflund, D.R. Schryer, J. Schryer, B.T. Upchurch, E.J. Kielin, Langmuir 7 (1991) 2135.

[7]   N. Yamamoto, S. Tonomura, T. Matsuoka, Jap. J. Appl. Phys 20 (1981) 721.

[8]   D.L. Shawn, T.-Ch. Hsiao, J.-R. Chang, A.S. Lin, J. Phys. Chem. B 97 (1999) 103.

[9]   A. Lamb, W.C. Bray, C.W. Fraser, J. Ind & Chem. Eng. 12 (1920) 213.

[10]   E.F. Fremy, Comp. Rend. 82 (1876) 1231.

[11]   K.C. Taylor, in Catalysis Science and Technology (J.R. Anderson and M. Boudart Eds.), Vol. 5, Chap. 2. Springer-Verlag, Berlin, 1984.

[12]   M. Machida, K. Eguchi, H. Arai, J. Catal. 120 (1989) 377.

[13]   A.P.B. Sinha, N.R. Sanjana, A.B. Biswas, J. Phys. Chem. 62 (1958) 191.

[14]   A.I. Zaslavskii, Z.V. Karachentseva, A.I. Zharinova, Kristallografiya, 7 (1962) 835.

[15]   S. Miyahara, J. Phys. Soc. Japan, 17 (1962) B-1 181.

[16]   D. Dollimore and K.H. Tonge, J. Chem. Soc. A (1970) 1728.

[17]   G. Blasse, J. Phys Chem. Solids 27 (1966) 383

[18]   D.B. Ghare, A.B.P. Sinha, L. Singh, J. Mater. Sci. 3 (1968) 389.

[19]   S.B. Kanungo, " Symposium on Science of Catalysis and Its Application in Industry FPDIL, Sindri, India, 1979."

[20]   S.B Kanungo, J. Catal. 58 (1979) 419.

[21]   S. Veprek, D.L. Cocke, S. Kehl, H.R. Oswald, J. Catal. 100 (1986) 250.

[22]   H. Knözinger, "Advances in Catalysis," Vol. 25, p. 184, Academic Press, New York, 1976.

[23]   H. Knözinger, Catal. Rev. Sci. Eng. 17 (1978) 31.

[24]   K. Wahl, W. Klemm, Z. Anorg. Allg. Chem. 270 (1952) 270.

[25]   F.S. Stone, "Advances in Catalysis," Vol. 13, p.1. Academic Press, New York, 1962.

[26]   G.M. Schwab, S.B. Kanungo, Z. Phys. Chem. N.F. 107 (1997) 109.

[27]   R.E. Vanderberghe, Phys. Status Solidi 50 (1978) K85.

[28]   P. Porta, G. Moretti, M. Musicanti, A. Nardella, Solid State Ionics 63-65 (1993) 257.

[29]   A.A. Mirzaei, H.R. Shaterian, M. Kaykhaii, Appl. Surf. Sci. 239 (2004) 246.

[30]   B.L. Yang, S.F. Chang, W.S. Chang, Y.Z. Chen, J. Catal. 130 (1991) 52.

[31]   E.S. Shipiro, W. Grunert, R. W. Joyner, G.N Baeva, Catal. Lett. 24 (1994) 159.

[32]   F.C. Buciuman, F. Patcas, T. Hahn, Chem. Eng. Proc. 38 (1999) 563.

[33]   G.K. Boreskov, Catalytic Activation of Dioxygen, in: J. Anderson, M. Boudart (Eds.), Catalysis-Science and Technology, vol. 3, Springer Verlag, Ch. 3, Heidelberg, 1982.

[34]   G. Jernigan, G.A. Somorjai, J.Catal. 147 (1994) 567.

[35]   L.S. Puckhaber, H. Cheung, D.L. Cocke, A. Clearfield, Solid State Ionics 32/33 (1989) 206.

[36]   P. Porta, G. Moretti, M. Musicani, A. Nardella, Catal. Today 9 (1991) 211.

[37]   G.J. Hutchings, A.A. Mirzaei, R.W. Joyner, M.R.H. Siddiqui, S.H. Taylor, Catal. Lett. 42 (1996) 21.

[38]   G.J. Hutchings, A.A. Mirzaei, R.W. Joyner, M.R.H. Siddiqui, S.H. Taylor, Appl. Catal. A: Gene. 166 (1998) 143.

[39]   A.A. Mirzaei, H.R. Shaterian, M. Habibi, G.J. Hutchings, S.H. Taylor, Appl. Catal. A: Gen. 253 (2003) 499.

[40]   A.A. Mirzaei, H.R. Shaterian, R.W. Joyner, M. Stockenhuber, S.H. Taylor, G.J. Hutchings, Cat. Comm. 4 (2003) 17.

[41]   C.D. Jones, PhD Thesis, The ambient temperature oxidation of carbon monoxide by copper-manganese oxide based catalysts, Cardiff Univ., Sept 2005.

[42]   A.A. Mirzaei, PhD Thesis, Low temperature carbon monoxide oxidation catalysts, Univ. of Liverpool, June 1998.

[43]   V. Koleva, D. Stoilova, D. Mehandjiev, J. Solid State Chem. 133 (1997) 133.

[44]   F. Kapteijn, A. Dick van Langeveld, J. Moulijn, A. Andreini, M. Vuurman, A. Turek, J. Jehng, I. Wachs, J. Catal. 150 (1994) 94.

[45]   F. Kapteijn, L. Singoredjo, M. van Driel, A. Andreini, J. Moulijn, G. Ramis, G. Busca, J. Catal. 150 (1994) 105.

[46]   M. Krämer, T. Schmidt, K. Stöwe, W.F. Maier, Appl. Catal. A: Gen. 302 (2005) 257.

[47]   Handbook of Heterogeneous Catalysis, Ed. By G. Ertl, H. Knozinger, J. Weitkamp, Wiley-VCH, 1997.

[48]   G.T. Bhandage, H.V. Keer, J. Phys. C. Solid State Phys. 8 (1975) 501.

[49] K.R. Krishnamurthy, B. Vishwanathan, M.V.C. Sastri, Indian J. Chem. A 15 (1977) 205.

[50] A.V. Salker, S.M. Gurav, J. Mater. Sci. 35 (2000) 4713.

[51] P.A. Wright, S. Natarajan, J.M. Thomas, Chem. Mater. 4 (1992) 1053.

[52] W.D. Kingery, Pure Appl. Chem. 56 (1984) 1703.

[53] M.S. Spencer, Catal. Lett. 66 (2000) 255.

[54] M. V. Twigg, Catalyst Handbook, Wolfe, London, 1989.

[55] K. Klier, Adv. Catal. 31 (1982) 243.

[56] G.C. Chinchen, P.J. Denny, J.R. Jennings, M.S. Spencer, K.C. Waugh, Appl. Catal. 36 (1988) 1.

[57] J.C.J Bart, R.P.A. Sneeden, Catal. Today 2 (1987) 1.

[58] K. Klier, Appl. Surf. Sci. 19 (198) 267.

[59] G.E. Parris, K. Klier, J. Catal. 97 (1986) 374.

[60] E.J.M. Dominguez, G.W. Simmons, K. Klier, J. Mol. Catal. 20 (1983) 369.

[61] G.C. Chinchen, K.C. Waugh, D.A. Whan, Appl. Catal. 25 (1986) 101.

[62] G.C. Chinchen, K.C. Waugh, J. Catal. 97 (1986) 280.

[63] J.B. Bulko, R.G. Herman, K. Klier, G.W. Simmons, J. Phys. Chem. 83 (1979) 3118.

[64] T.H. Fleisch, R.L. Mieville, J.Catal. 90 (1984) 165.

[65] G. Sankar, S. Vasudevan, C.N.R. Rao, J. Chem. Phys., 85 (1986) 2291.

[66] S. de Rossi, G. Ferraris, R. Mancini, Appl. Catal. 38 (1988) 359.

[67] P.Porta, R. Dragone, M. Lo Jacono, G. Minelli, G. Moretti, Solid State Ionics 32/33 (1989) 1019.

[68] G. Moretti, G. Fierro, M. Lo Jacono, P. Porta, Surf. Interf. Anal. 14 (1989) 325.

[69] G. Moretti, S. De Rossi, G. Ferraris, Appl. Surf. Sci. 14 (1990) 341.

[70] M.C. Annesini, M. Lo Jacono, M.C. Campa, G. Fierro, R. Lavecchia, L. Marrelli, G. Moretti, P. Porta, Solid State Ionics, 63-65 (1993) 281.

[71] G. Fierro, M. Lo Jacono, M. Inversi, P. Porta, F. Cioci, R. Lavecchia, Appl. Catal. A: Gen. 137 (1996) 327.

[72] G. Fierro, S. Morpurgo, M. Lo Jacono, M. Inversi, I. Pettiti, Appl Catal. A: Gen. 166 (1998) 407.

[73] A. Maltha, H.F. Kist, B. Brunet, J. Ziolkowski, H. Onishi, I, Iwasawa, V. Ponec, J. Catal. 149 (1994) 356.

[74] G. Ferraris, G. Fierro, M. lo Jacono, M. Inversi, R. Dragone, Appl. Catal. B: Environ. 45 (2003) 91.

[75] G. Fierro, M. Lo Jacono, M. Inversi, R. Dragone, G. Ferraris, Appl. Catal. B: Environ. 30 (2001) 173.

[76] S.H. Taylor, G.J. Hutchings, A.A Mirzaei, Chem. Commun. (1999) 1373.

[77] D. M. Whittle, A.A. Mirzaei, J.S. Hargreaves, R.W. Joyner, C.J. Kiely, S.H. Taylor, G.J. Hutchings, Phys. Chem. Chem. Phys. 4 (2002) 5915.

[78] S.H. Taylor, G.J. Hutchings, A.A. Mirzaei, Catal. Today 84 (2003) 113.

[79] J.G. Christian, J.E. Johnson, Int. J. Air wat. Poll. 9 (1965) 1.

[80] J.K. Mušick, F.W. Williams, Ind. Eng. Chem. Prod. Res. Dev. 13 (1974) 175.

[81] R.W. McCabe, P.J. Mitchell, Ind. Eng. Chem. Prod. Res. Dev. 23 (1984) 196.

[82] M. Khristova, D. Panayotov, D. Mehandjiev, in "Prep. 7th International Symposium on Heterogeneous Catalysis," Part 2, p. 1025, Burgas, Bulgaria, 1991.

[83] D. Panayotov, React. Kinet. Catal. Lett. 58 (1996) 73.

[84] L.S. Puckhaber, H. Cheung, D.L. Cocke, A. Clearfield Solid State Ionics 32/33 (1989) 206.

[85] M. Kang, E.D. Park, J.M. Kim, J.Y. Yie, Catal. Today 111 (2006) 236

[86]   J.j. Spivey, Ind. Eng. Chem. Res. 26 (1987) 2165.

[87]   W.B. Li, W.B. Chu, M. Zhuang, J. Hua, Catal. Today 93-95 (2004) 205.

[88]   M.R. Morales, B.O. Barbero, L.E. Cadús, Appl. Catal. B: Environ. 67 (2006)
        229 236.

[89]   P.-O Larsson, A. Andersson, Appl. Catal. B: Environ. 24 (2000) 175.

[90]   W. Liu , M. Flytzani-Stephanopoulos, J. Catal. 153 (1995) 304.

[91]   J.B. Butt, J.J. Spivey, S.K. Agrawal, in: B. Delmon, G.F. Froment (Eds.),
        Catalyst Deactivation 1994, Elsevier, Amsterdam, 1994, p. 19.

[92]   A.S. Ready, C.S. Gopinath, S. Chilukuri, J. Catal. 243 (2006) 278.

[93]   J.J. Spivey, Catal. Today 100 (2005) 171.

[94]   A. Ghencu, Curr. Opin. Solid State Mater. Sci. 6 (2002) 389.

[95]   S. Velu, K. Suzuki, Top. Catal. 22 (2003) 235.

[96]   B. Lindström, J. Agrell, L.J. Pettersson, Chem. Eng. J. 93 (2003) 91.

[97]   J. Papavasiliou, G. Avgouropoulos, T. Ioannides, Catal. Commun. 5 (2004)
231.

[98]   J. Papavasiliou, G. Avgouropoulos, T. Ioannides, J. Catal. 251 (2007) 7.

[99]   J. Schwank, Gold. Bull. 16 (1983) 103.

[100]   M. Haruta, T. Kobayashi, H. Sano, N. Yamada, Chem. Lett. 4 (1987) 405.

[101]   M.I. Brittan, H. Bliss, C.A. Walker, AIChE J., 16 (1970) 305.

[102]   D.S. Stark, A. Crocker, G.J. Steward, J. Phys. E: Sci. Instrum. 16 (1983) 158.

[103]   D.S. Stark, M.R. Harris, J. Phys. E: Sci. Instrum. 16 (1983) 492.

[104]   D.S. Stark, M.R. Harris, J. Phys. E: Sci. Instrum. 21 (1988) 715.

[105]   D.R. Schryer, B.T. Upchurch, J.D. van Norman, K.G. Brown, J. Schryer, J.
        Catal. 122 (1990) 193.

[106]   M. Haruta, Cattech 6 (2002) 102.

[107]   M. Haruta, J. Catal. 36 (1997) 153.

[108] M. Haruta, S. Tsubota, T. Kobayashi, H. Kageyama, M.J. Genet, B. Delmon, J. Catal. 144 (1993) 175.

[109] C.F. Baes Jr., R.E. Mesmer, in: The Hydrolysis of Cations, Wiley, New York, 1976, p. 281.

[110] A. Wolf, F. Schuth, Appl. Catal. A 22 (2002) 1.

[111] H.-S. Oh, J.H. Yang, C.K. Costello, Y. Wang, S.R. Bare, H.H. Kung, M.C. Kung, J. Catal. 210 (2002) 375.

[112] T.V. Choudhary, D.W. Goodman, Top. Catal. 21 (2001) 25.

[113] H.H. Kung, M.C. Kung, C.K. Costelo, J. Catal. 216 (2003) 425.

[114] A.S.K. Hashmi, G.J. Hutchings, Angew. Chem. Int. ed. 45 (2006) 425.

[115] G.C. Bond, C. Louis, D.T. Thompson, Catalysis by Gold, Imperial College Press, London, 2006.

[116] G.R. Bamwenda, S. Tsubota, T. Nakamura, M. Haruta, Catal. Lett. 44 (1997) 83.

[117] M. Valden, X. Lai, D.W. Goodman, Science 281 (1998) 1647.

[118] M. Haruta, Catal. Surv. Jpn 1 (1997) 61.

[119] G.J. Hutchings, M.R.H. Siddiqui, A. Burrows, C.J. Kiely, R. Whyman, J. Chem. Soc., Faraday Trans. 93(1) (1997) 187.

[120] B. Solsona, G.J. Hutchings, T. Garcia, S.H. Taylor, New. J. Chem. 28 (2004) 708.

Experimental Procedure

2

This chapter details the experimental procedures used to synthesise the catalysts that are discussed in later chapters. The characterisation techniques used to analyse the catalysts are described in detail.

2.1 Catalyst Preparation

Copper manganese mixed oxides prepared using the co-precipitation method have been reported to have several critical preparation conditions [1]. They are summarised as follows:

- Temperature of precipitation
- pH of precipitate
- Precipitate ageing time
- [Cu]/[Mn] ratio
- Calcination temperature

The control of these variables is critical in order to obtain a reproducible catalyst. The variables quoted have not changed. This enables to clearly compare the work reported in this thesis with previous work [2].

2.1.1 Preparation of CuMnOx Hopcalite catalyst

Catalysts were prepared using a co-precipitation procedure that is described as follows. Aqueous solutions of $Cu(NO_3)_2.3H_2O$ (0.25 mol l^{-1}) and $Mn(NO_3)_2.3H_2O$ (0.25 mol l^{-1}) were premixed in a 1:2 ratio (Cu:Mn) and the resulting solution (150 ml) was heated to 80°C. Aqueous Na_2CO_3 (2 mol l^{-1}) and the mixed nitrate solution were co-added at a rate of 12ml min^{-1}, within a thermostatted vessel, whilst continuously stirred at 600 rpm. The mixture was maintained at 80°C and the pH was controlled at 8.3 (+/- 0.1 unit). The procedure took approximately 15 minutes to complete. The resulting precipitate was left to stir in this medium for a time described as the ageing time at the required pH and temperature used for precipitation. The precipitate was then filtered, washed several times with warm and cold distilled water until no further Na^+ ions was observed in the washings. Na^+ ions, the presence of excess sodium, have an adverse affect on catalytic activity [3]. The precipitate was dried at 110°C for 16 h to give a material denoted as the catalyst precursor. The final catalyst was produced by calcination of the precursor in static air at 415°C for 2 h. This procedure was repeated three times to verify reproducibility of the preparation procedure. The prepared catalyst was tested within a 24 hour period after calcinations.
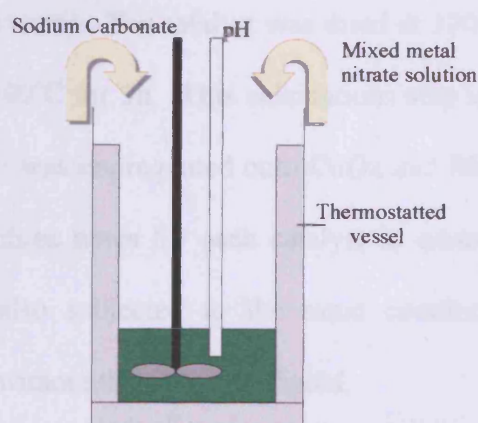
Figure 2.1 Diagram of co-precipitation apparatus

2.1.2 Preparation of co-precipitated doped Hopcalite catalyst

The CuMnOx catalyst was prepared by a co-precipitation method. A modification to this procedure has been reported [2], in which the CuMnOx catalyst can be modified by the addition of a dopant metal. The copper nitrate present in the starting reagent mixture was replaced with another nitrate metal. The ratio of the copper to the dopant metal was controlled so that the overall stoichiometry of the starting reagent was 1:2 (Cu + dopant) : Mn. The ratios quoted are in terms of stoichiometry of the metal not the metal nitrate in the precursor.

2.1.3 Preparation of Au supported Hopcalite by deposition precipitation

Gold supported CuMnOx was prepared by a deposition precipitation procedure [4]. The procedure was used as a method to deposit gold particles onto a support. In this case, the CuMnOx was acting was a support. The CuMnOx catalyst was prepared by the co-precipitation method as described previously. The calcined mixed oxide was mixed with distilled water and stirred at room temperature. To this paste, a solution of $HAuCl_4 \cdot xH_2O$ was added. The mixture was adjusted to pH 9 with an aqueous solution of NaOH, and was then aged for 1 h at this pH with vigorous stirring, filtered and washed with cold and hot water. The catalyst was dried at 120 °C. The Au supported sample was calcined at 400°C for 3h. This calcinations step was reported by Carley and co-workers where Au was impregnated onto CuOx and MnOx supports [4]. This procedure was repeated three times for each catalyst to ensure reproducibility. The CuMnOx catalyst was also subjected to the same conditions as the deposition precipitation method but without the addition of gold.

2.2 Gas Chromatography

Chromatography as a method of instrumental analysis is capable of producing data which may describe the qualitative and quantitative composition of mixtures. Gas chromatography is one of the most extensively used techniques for analytical purposes. It provides a quick and simple way of determining the number of components in a mixture, including the presence of impurities.

The main components of a Gas Chromatograph (GC) are as follows:

- Carrier Gas Supply

- Injection port

- Column

- Detectors

- Data Acquisition System
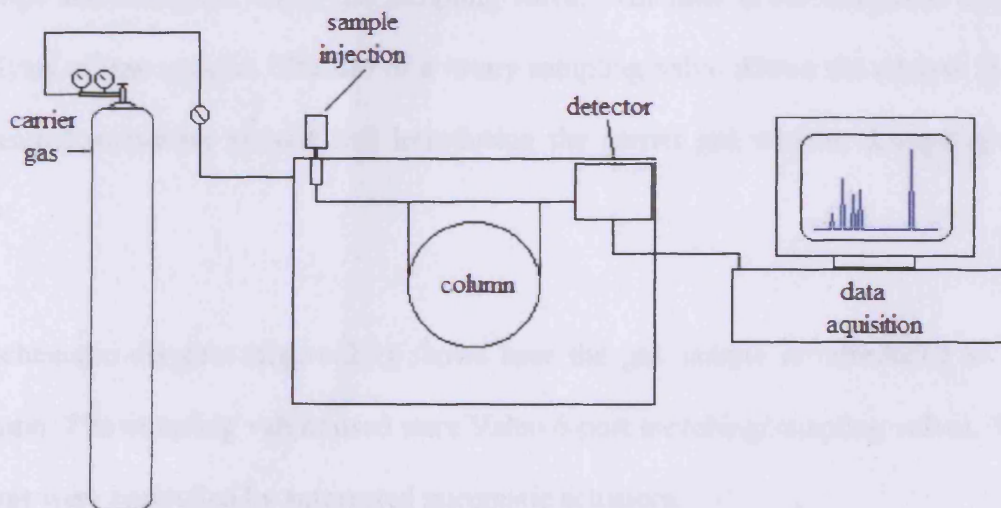
Figure 2.2 Diagram of a gas chromatograph system

2.2.1 Carrier Gas

The carrier gas (mobile phase) is the gas which is passed continuously through the column and whose passage promotes the elution of the components of the sample. The carrier must be chemically inert. The most common gas used is helium. Helium has a larger range of flow rates that are comparable to hydrogen in efficiency, with the added advantage that helium is non-flammable, and works with a greater number of detectors.

2.2.2 Sample Injection

The mixture of components in the sample is introduced into the chromatograph through the injection port. At this point, the analytes are vaporized (if not already in the gas phase) by the high temperature maintained in the injection port. The gas phase analytes are then immediately swept onto the chromatographic column by the mobile phase.

There are two methods for delivering samples to the column, through a gas tight syringe and through a rotary gas sampling valve. The later is the form used during analysis of gas samples. The use of a rotary sampling valve allows the analyte to be measured in precise volume and introducing the carrier gas without disrupting the flow.

A schematic diagram (figure 2.3) shows how the gas sample is introduced to the column. The sampling valves used were Valco 6-port switching/sampling valves. The valves were controlled by automated pneumatic actuators.
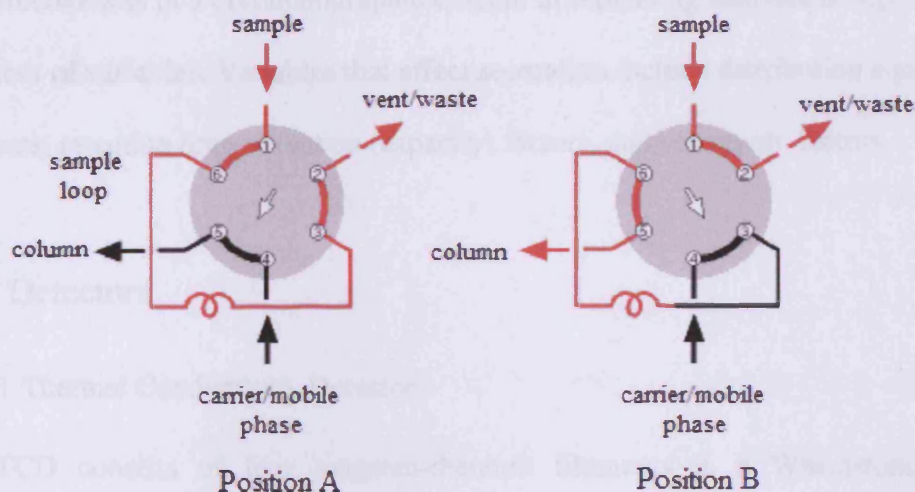
Figure 2.3 Schematic diagram of 6 port-valve

With the valve in Position A, sample flows through the external loop while the carrier flows directly through to the chromatographic column. When the valve is switched to Position B, the sample contained in the sample loop and valve flow passage is injected onto the column.

2.2.3 Columns

There are two types of column used in gas chromatography, packed and capillary. A packed column typically uses a stainless steel or glass tube with a 1/8th inch inner diameter packed with a solid stationary phase.

A capillary column is an open tube made of fused silica with an outer coating of durable plastic and an inner coating of stationary-phase material. However, despite its problems with sample injection, the packed column is seen as the 'state of the art' column and is by far the most popular column system in general use.

The columns used in the GC analysis for this investigation were all packed columns.

The packed columns are detailed with the GC experimental procedure.

46

The effectiveness of a chromatographic column in separating analytes is dependent on a number of variables. Variables that affect separation include distribution equilibrium constants, retention time, retention (capacity) factors, and selectivity factors.

2.2.4 Detectors

2.2.4.1 Thermal Conductivity Detector

The TCD consists of four tungsten-rhenium filaments in a Wheatstone bridge configuration. Electric current flows through the four filaments causing them to heat up. The carrier gas (typically helium which has very high thermal conductivity) flows across the filaments removing heat at a constant rate. When a sample molecule with lower thermal conductivity exits the column and flows across the two sample filaments, the temperature of the filaments increase unbalancing the Wheatstone bridge and generating a peak as the sample molecules transit through the detector. The TCD detector detects all molecules, not just hydrocarbons, so it is commonly used for fixed gas analysis (O_2, N_2, CO, CO_2, H_2S, NO, NO_2) where the target analytes do not respond well on other more sensitive detectors.

2.2.4.2 Flame Ionization Detector (FID)

A flame ionization detector (FID) consists of a stainless steel jet constructed so that carrier gas exiting the column flows through the jet, mixes with hydrogen, and burns at the tip of the jet. Hydrocarbons and other molecules which ionize in the flame are attracted to a metal collector electrode located just to the side of the flame. The resulting electron current is amplified by a special electrometer amplifier which converts very small currents to milli volts.

The FID is sensitive to almost all molecules that contain hydrocarbons. The FID is a destructive detector that can be used in series only after non-destructive detectors.

2.2.5 Data Acquisition

The acquisition and extensive possibilities of the storage of digitalised raw data can be performed flexibly. The raw data can be re-plotted to form analogue chromatograms in variable scales of retention and the response axis. The computer based systems offer extensive tools to analyse the data from data systems.

2.3 Catalyst Testing

Three GC systems have been used to investigate the catalytic performance of samples produced.

1. CO oxidation at ambient temperature

2. Ethylene oxide oxidation

3. Preferential CO oxidation (PROX)

The following procedures briefly explain the conditions used for catalyst testing. The full conditions for the GC systems are found in Appendix 1.

2.3.1 CO oxidation – ambient temperature

Catalysts were tested for CO oxidation using a fixed bed laboratory micro reactor. Samples were tested within a 24 hour time period after calcination. The reactant gases were premixed in a cylinder that was supplied by BOC. The gas line did not contain any moisture filters. Typically, CO (5000ppm CO in synthetic air) was fed to the reactor at a controlled rate (21.3ml/min) using a mass flow controller and passed through the catalyst (100mg) at 25°C. The temperature of the reactor was isothermally controlled by the placement of the reactor in a water bath. The products were analysed using on-line gas chromatography with a 1.5 m packed Carbosieve column. These conditions were equivalent to a total gas hourly space velocity of 12,000 h^{-1}.
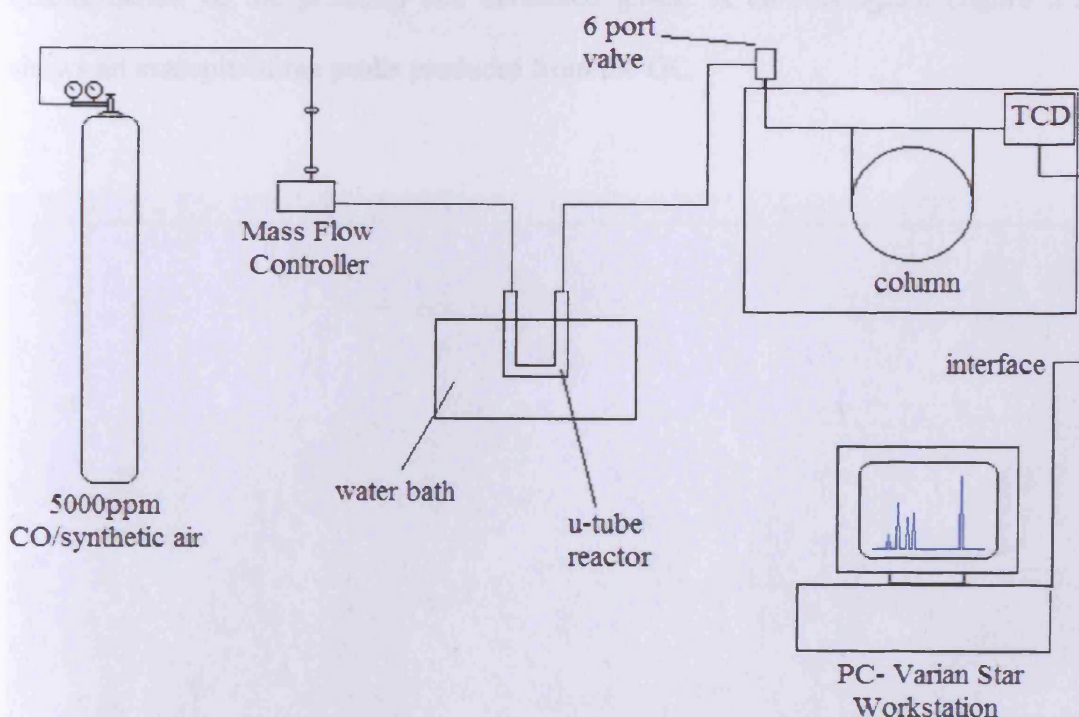
Figure 2.4 Schematic diagram of the micro reactor system

for CO oxidation at ambient conditions

The GC used helium as a carrier gas and one column was used to separate the components of the gas from the reactor.

The GC was programmed to automatically inject the exit gas from the reactor, using an auto injector, in intervals of 4 minutes for a period of 2h. This would enable to analyse the product gas as a function of time. A Carbosieve column was used to separate the components of the sample gas. The temperature of the column oven was maintained at 195°C, which was close to the temperature limit for that column. This allowed good separation of the CO/Air and CO_2 peak. A limitation to the analysis was that the column could not separate CO, O_2. They were eluted as a broad peak at t_r = 0.5 mins. A thermal conductivity detector was used for the detection and quantification of the products and unreacted gases. A chromatogram (figure 2.5) shows an example of the peaks produced from the GC.
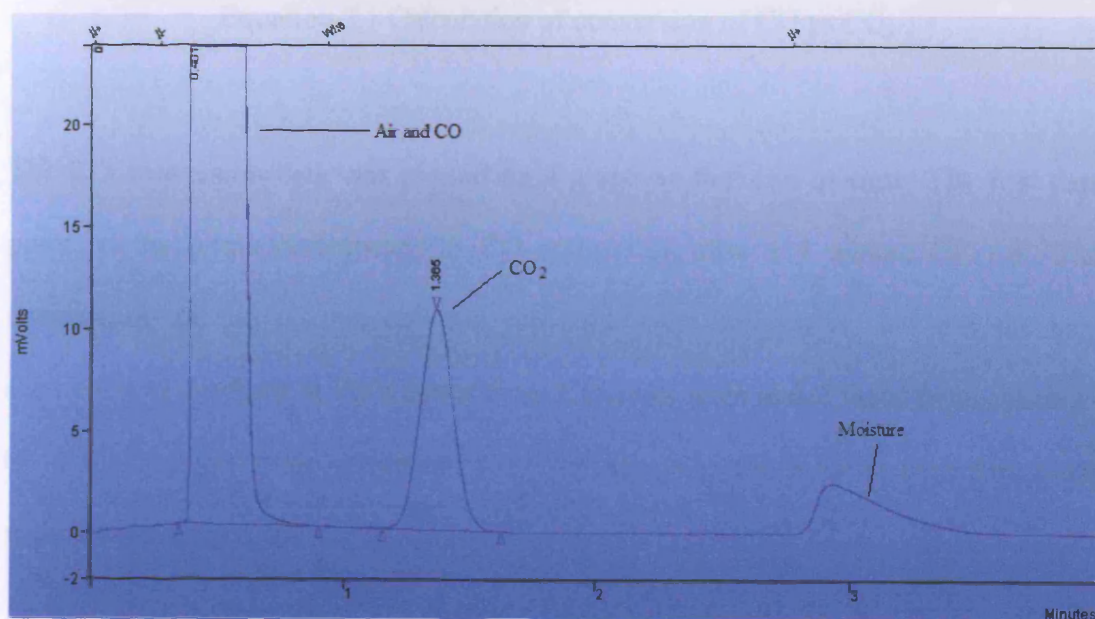
Figure 2.5 Chromatogram of CO oxidation calibration

The retention times for the gases were determined and are shown in table 2.1.

Product	Retention Time (mins)
CO/O$_2$	0.5
CO$_2$	1.5

Table 2.1 Retention times of products for CO oxidation reaction

The GC was calibrated to calculate the conversion of CO to CO$_2$. A known concentration of CO$_2$ was used to determine the maximum peak area that would correspond to total conversion (5000ppm CO would produce 5000ppm CO$_2$). The calculation is shown in equation 2.1.

$$\text{Conversion CO (\%)} = \left(\frac{CO_2 \text{counts}}{\text{total} CO_2 \text{ counts}} \right) \times 100$$

Equation 2.1 Calculation of conversion of CO to CO$_2$

The CO conversion data was plotted on a graph as function of time. The first data point on the graph corresponds to CO conversion after a 4 minute GC run. The temperature of the column and the run time were selected to achieve the best separation of products in the shortest time. Catalysts were tested three times, in order to verify that the testing conditions were reproducible. The error in each data point was shown to be ca. 2%.

2.3.2 Ethylene oxide oxidation

Catalysts were tested for ethylene oxide oxidation using a straight walled fixed bed reactor. A mixture of ethylene oxide (3000ppm EtO in balance N_2, 18ml/min) and O_2 (3ml/min) were fed to the reactor using mass flow controllers. The reactor was placed in a Carbolite furnace and the temperature was controlled by a Carbolite furnace control box. The temperature of reactions ranged from 25°C to 250°C. A thermocouple was placed inside the reactor to monitor the temperature of the catalyst bed. The amount of catalyst tested was ca. 100mg. The outlet of the reactor was heated by means of a heating tape to avoid possible condensation of products.
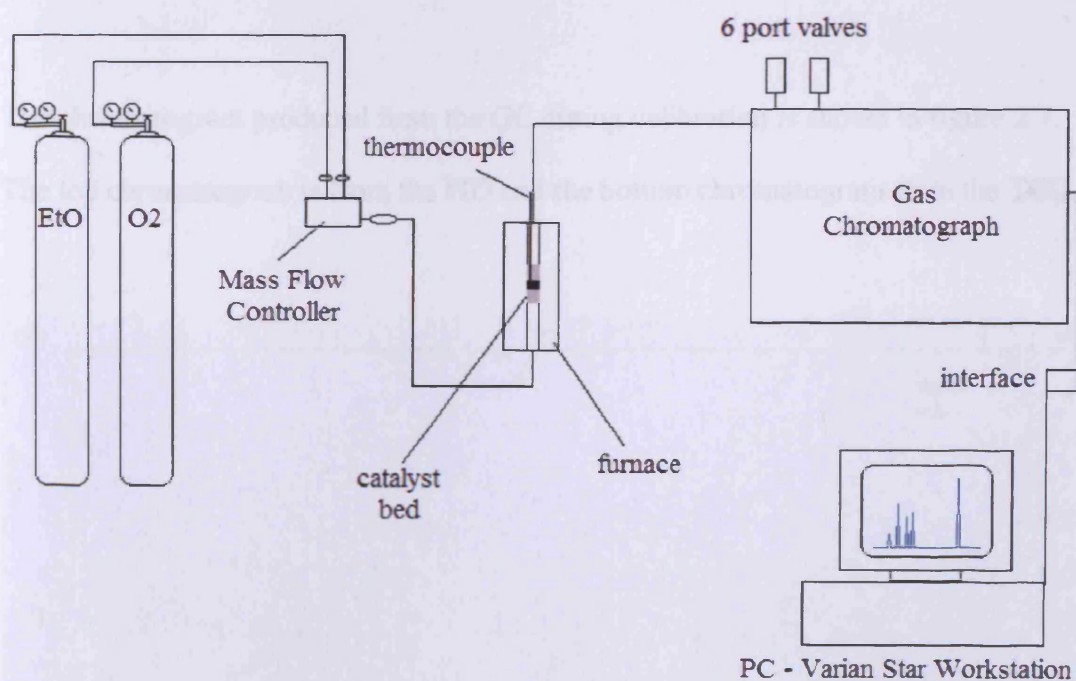
Figure 2.6 Schematic diagram of the reactor for Ethylene oxide oxidation

The components of the sample gas were separated using Poropak Q (PQ, 2m x 2mm i.d) and Molecular Sieve 13X (MS13X, 2m i.d) columns. A thermal conductivity detector (TCD) and flame ionization detector (FID) were used for the detection and quantification of the products and unreacted gases.

The calculation of ethylene oxide oxidation was determined and shown in equation 2.2.

$$\text{Conversion CO (\%)} = \frac{[EtO]_{IN} - [EtO]_{OUT}}{[EtO]_{IN}} \times 100$$

Equation 2.2 Calculation of ethylene oxide oxidation

The chromatogram produced from the GC during calibration is shown in figure 2.7. The top chromatogram is from the FID and the bottom chromatogram from the TCD.
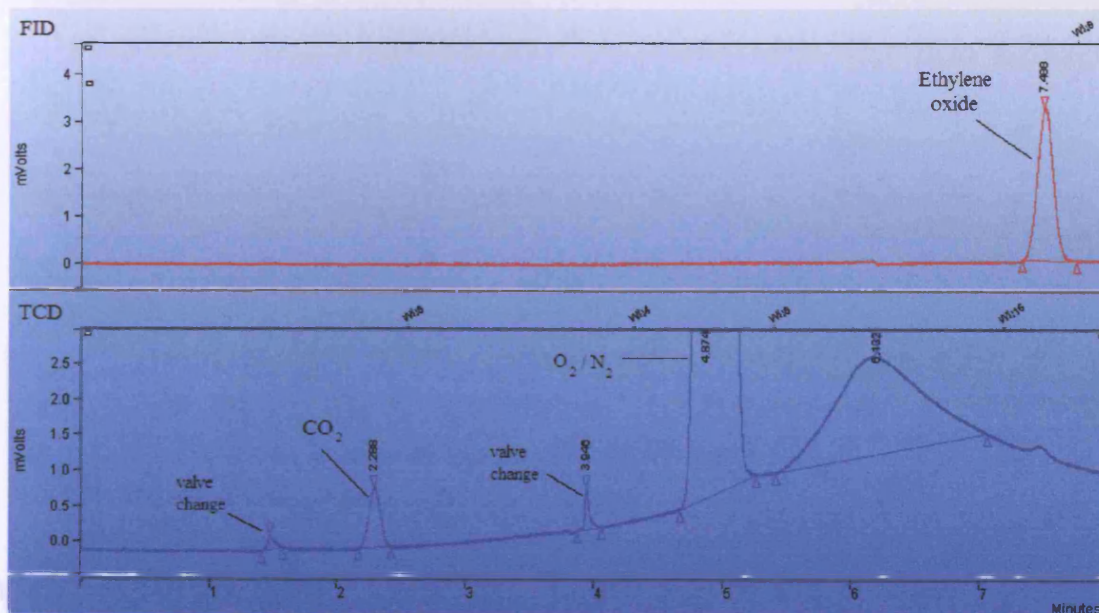
Figure 2.7 Chromatogram of Ethylene oxide calibration

Components of the mixture of gases and retention times were determined and shown

in table 2.2.

Product	Retention Time (mins)	Detector
CO_2	2.5	TCD
O_2/N_2	5	TCD
C_2H_4O	7.5	FID

Table 2.2 Components of the mixture of gases and retention times

The peaks (1.4 mins and 3.9 mins) on the chromatogram in figure 2.7 correspond to

valve changes between the two columns contained with the GC.

2.3.3 Preferential CO oxidation (PROX)

Catalysts were tested for preferential CO oxidation (PROX) using a straight walled fixed bed micro reactor. A mixture of 1% CO/24% CO_2/20% N_2/55% H_2 (18ml/min) and Air (1ml/min) were fed to the reactor using mass flow controllers. The reactor was placed in a furnace and the temperature was controlled by a Eurotherm controller. The amount of catalyst tested was ca. 50mg. The temperature of reactions was set to 100°C. A thermocouple was placed inside the reactor to monitor the temperature of the catalyst bed.
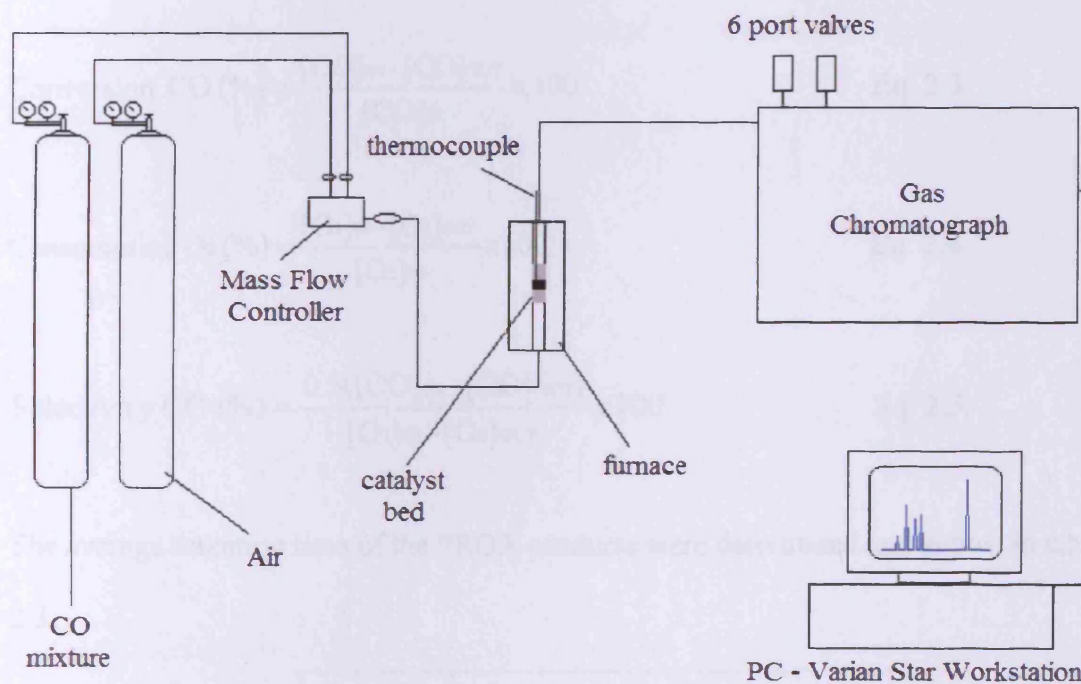
Figure 2.8 Schematic Diagram of the reactor system used for PROX.

The GC was programmed to automatically inject the exit gas from the reactor, using an auto injector, in intervals of 25 minutes for a period of 5h. This would enable the product gas to be analysed as a function of time. The components of the gases were

separated using Molecular Sieve 5A column and a Porapak column. The conditions of the GC enabled the separation of CO, CO_2, O_2, N_2 and H_2. The Molecular Sieve 5A column eluted H_2, CO, O_2 and N_2 whilst the Porapak column eluted CO_2. A thermal conductivity detector was used for the detection and quantification of the products and unreacted gases. The two detected gases CO and O_2 were used to calculate CO oxidation – this method is different to the ambient temperature CO oxidation GC, where the detected CO_2 gas is only used in the conversion calculation. CO conversion (equation 2.3), O_2 consumption (equation 2.4) and selectivity of CO in the presence of excess hydrogen (equation 2.5) are shown.

$$\text{Conversion CO (\%)} = \frac{[CO]_{IN} - [CO]_{OUT}}{[CO]_{IN}} \times 100 \qquad \text{Eq. 2.3.}$$

$$\text{Consumption } O_2 \text{ (\%)} = \frac{[O_2]_{IN} - [O_2]_{OUT}}{[O_2]_{IN}} \times 100 \qquad \text{Eq. 2.4.}$$

$$\text{Selectivity CO (\%)} = \frac{0.5([CO]_{IN} - [CO]_{OUT})}{[O_2]_{IN} - [O_2]_{OUT}} \times 100 \qquad \text{Eq. 2.5.}$$

The average retention time of the PROX products were determined and shown in table 2.3.

Product	Retention time (mins)
H_2	2.1
O_2	3.8
N_2	4.2
CO	5.7
CO_2	17.1

Table 2.3 Retention times for PROX products

2.4 Characterisation Techniques

2.4.1 BET Surface Area measurements

Physisorption measurements are widely used to determine the surface area and pore size distribution of catalysts. Physisorption occurs when a gas (adsorptive) is brought in contact with an outgassed solid (adsorbent). The measurement of surface area by nitrogen adsorption using the BET equation has been employed to characterise catalysts for many years [5]. The theory behind the BET equation is an extension of the Langmuir model for monolayer molecular adsorption. The adsorption in the first layer is assumed to take place in an array of surface sites with uniform energy. Molecules in the first layer act as sites for multilayer adsorption, which in the simplest case approaches infinite thickness as p $\rightarrow$ p$_o$.

$$\frac{p}{n(p_o - p)} = \left(\frac{1}{n_m C}\right) + \left(\frac{C-1}{n_m C}\right)\frac{p}{p_o}$$

Figure 2.7 BET equation

p is the sample pressure, p_o is the saturation vapour pressure, n is the amount of gas adsorbed at the relative pressure p/p$_0$, n_m is the monolayer capacity and C is the BET constant.

$$C = \exp\left(\frac{E_1 - E_2}{RT}\right)$$

E_l is the heat of adsorption for the first layer; E_L is that for the second and higher levels and is equal to the heat of liquefaction.

The range of linearity of the BET plot is severally restricted with all known experimental isotherms. The BET equation is applied to type II and type IV isotherms.

The value obtained for C can indicate the validity of the application of the BET method to a particular adsorbant. If C > 350, the pressure corresponding to a monolayer coverage is low (p/p_o < 0.05), point B is well defined. If C < 20, the monolayer coverage corresponding to the monolayer coverage is high (p/p_o > 0.18), point B is ill defined. The surface area is obtained from the BET monolayer capacity n_m:

$$a_{BET}\,(m^2g^{-1}) = n_{m.}\,L\sigma$$

Figure 2.9 Calculation of surface area.

L= Avagadros constant, σ = average area occupied by adsorbant gas,

$a_{BET(m}$ a_{BET} = surface area measured in m^2g^{-1}.

Figure 2.10 shows an idealised form of the adsorption isotherm for phyisorption on a nonporous solid. At low pressures the surface is only partially occupied by the gas, until at higher pressures (point B on the curve) the monolyer is filled and the isotherm reaches a plateau. This part of the isotherm, from zero pressures to point B, is equivalent to the Langmuir isotherm. At higher pressures a second layer starts to form, followed by restricted multilayer formation. This is a Type II isotherm
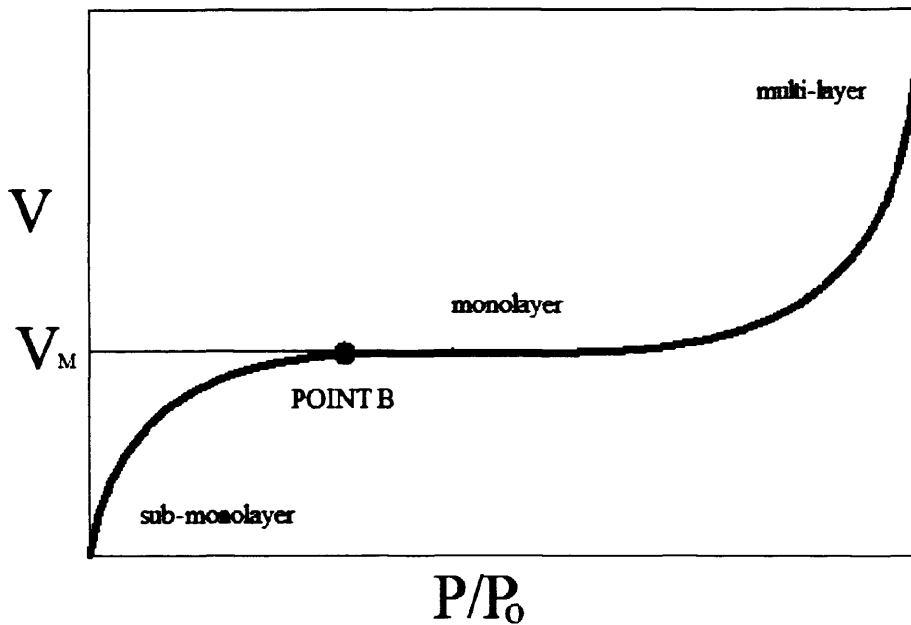
Figure 2.10 Type II isotherm

Surface area analysis was determined using a Micromeritics Gemini 2360 analyser controlled by a PC. The sample was degassed- at least to an extent of removing physisorbed material – before analysing the surface area. A known amount of sample (100mg) was placed in a straight wall tube and degassed in nitrogen at 110°C for 1h. The weight loss associated with degassing was recorded and the sample weight was adjusted accordingly. The surface area was analysed using a single point BET programme, typically analysing at five different pressures ranging from P = 0.05 to 0.3.

2.4.2 Powder X-ray Diffraction

Powder X-ray diffraction (XRD) is a non-destructive bulk technique widely used to characterise crystalline material. The method is normally applied to data to collect in

ambient conditions but *in situ* diffraction can be used to interpret solid state transformations under different temperatures, pressures and atmospheres.

The technique uses a monochromatic X-ray beam incident on a finely powdered sample, comprising of an infinite amount of crystallites arranged randomly in no preferred orientation. Interaction of X-rays with the sample creates secondary diffracted beams of X-rays related to interplanar spacings in the crystalline powder. For any set of planes the diffracted radiation forms a cone where the angle between the diffracted and undiffracted beam is 2θ. This is defined as Bragg's Law:

$$n\lambda = 2d\sin\theta$$

Figure 2.11 Bragg's law

n is an integer, λ is the wavelength of radiation, d is the inter planar lattice spacing, θ is the Bragg angle.

The rays of the incident beam are always in phase and parallel up to the point at which the top beam strikes the top layer at atom z (Figure 2.12). The second beam continues to the next layer where it is scattered by atom B. The second beam must travel the extra distance AB + BC if the two beams are to continue travelling adjacent and parallel. This extra distance must be an integral (n) multiple of the wavelength (λ) for the phases of the two beams to be the same:

$$n\lambda = AB + BC \qquad Eq\ 2.6$$

Substituting Eq. 2.5 in Eq. 2.6 becomes,

Incident
radiation

'reflected'
radiation

θ z θ

A C

B

d

transmitted radiation
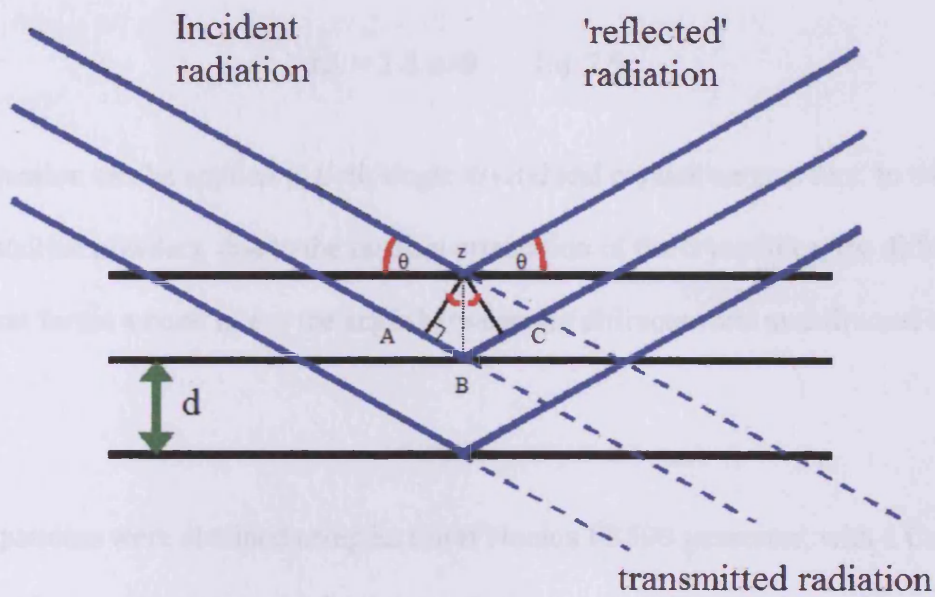
Figure 2.12 Diagram of Bragg's Law

Recognizing d as the hypotenuse of the right triangle ABz (Figure 2.13), trigonometry

can relate d and θ to the distance (AB + BC). The distance AB is opposite θ so,

z

θ

d

A B
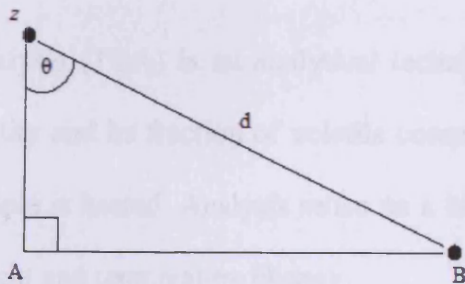
Figure 2.13 Triangle ABz

The distance AB is opposite θ so

$$AB = d \sin\theta \qquad \text{Eq. 2.7}$$

Because AB = BC Eq. 2.6 becomes,

$$n\lambda = 2AB \qquad \text{Eq. 2.8}$$

Substituting Eq. 2.7 in Eq. 2.8 we have,

$$n\lambda = 2\ d\ \sin\theta \qquad \text{Eq. 2.9}$$

The equation can be applied to both single crystal and crystalline powders. In the case of crystalline powders, due to the random orientation of the crystallites, the diffracted radiation forms a cone where the angle between the diffracted and undiffracted beams is 2θ.

X-ray patterns were obtained using an Enraf Nonius FR590 generator, with a $CuK_{\alpha 1}$ source. X-rays were detected using a curved position sensitive scintillater X-ray operated at 1.2kW (40mA and 30kV). The sample was spun to ensure a random arrangement of crystallites. A sample was run for 0.5 h and the diffractogram was compared to known patterns on the JCPDS database.

2.4.3. Thermogravimetric Analysis - TGA

Thermogravimetric Analysis (TGA) is an analytical technique used to determine a material's thermal stability and its fraction of volatile components by monitoring the weight change as a sample is heated. Analysis relies on a high degree of precision in two measurements: weight and temperature change.

The measurement is normally carried out in air or in an inert atmosphere and the weight is recorded as a function of the increasing temperature. Changes in weight are the result of the formation of various physical and chemical bonds at elevated temperatures that lead to the evolution of volatile products or the formation of heavier reaction products [6].

A sample is placed into a tared TGA sample crucible which is attached to a sensitive microbalance assembly. The sample holder portion of the TGA balance assembly is subsequently placed into a high temperature furnace. The balance assembly measures the initial sample weight at room temperature and then continuously monitors changes in sample weight (losses or gains) as heat is applied to the sample. TGA tests may be run in a heating mode at some controlled heating rate, or isothermally. Typical weight loss profiles are analyzed for the amount or percent of weight loss at any given temperature, the amount or percent of non-combusted residue at some final temperature, and the temperatures of various sample degradation processes.

Samples were run on a Labsys TG-DTA/DSC 1600 machine using 30mg sample for each analysis.

2.4.4 Temperature Programmed Reduction – TPR

Temperature programmed reduction (TPR) is a technique for the determination of the reducibility of a material as a function of temperature.

The term TPR was first used in a paper by Robertson *et al.* [7] but the basic idea of characterising catalysts by monitoring their reducibility was first suggested by Holm and Clark [8].

The technique involves the adaptation of the temperature programmed gas chromatograph to the purpose of measuring reduction. The catalyst can be pre-treated in different gas streams prior to the actual TPR experiment. When the sample is ready for TPR experiment the gas is switched to a gas of composition 10% H_2/balance Ar

and this passes through one arm of the thermal conductivity detector then through the reactor and via a series of traps (to remove reduction products) through the other arm of the thermal conductivity detector, where the change in hydrogen concentration of the gas stream brought about by any reduction process, is monitored via the thermal conductivity change. H_2 and Ar have widely different thermal conductivities.

The gas flow is constant meaning that the change in hydrogen concentration is proportional to the rate of catalyst reduction.

Distinct reducible species in the catalyst show up as peaks in the TPR spectrum.

* Analysis was performed using a Thermo TPDRO 1100. The machine is designed to perform several experiments including pulse chemisorption, temperature programmed reduction, desorption and oxidation.

The sample (15mg) was suspended in a plug of silica wool in a straight wall sample tube. The sample tube is loaded into the furnace. The sample is degassed in Ar for 1h prior to analysis. The TPDRO machine is controlled by a PC, which is loaded with reaction conditions that operate during analysis. The sample is heated from ambient temperature to $500°C$ at a rate of $5°C/min$. The reducing gas used was a mixture of 10% H_2 in balance Ar.

2.4.5 Atomic Absorption Spectroscopy - AAS

Atomic absorption spectroscopy is an analytical technique to determine the concentration of a particular element in a sample. The technique makes use of the wavelengths of light specifically absorbed by an element. They correspond to the

energies required to promote electrons from one energy level to another, higher, energy level.

AAS essentially consists of a light source, sample cell, monochromator and a detector.
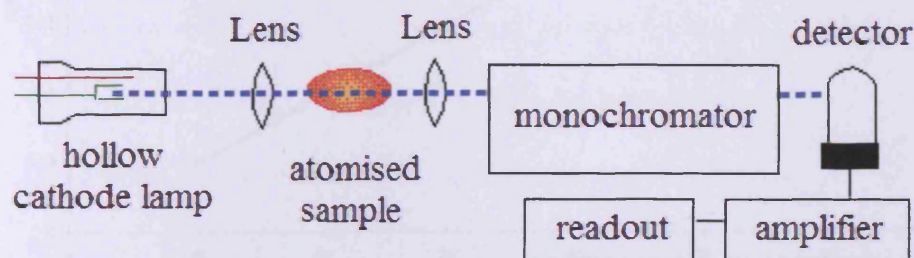
Figure 2.14 Schematic of an atomic absorption spectrometer

AA spectroscopy requires that the analyte atoms be in the gas phase. Ions or atoms in a sample must undergo desolvation and vaporization in a high-temperature source such as a flame. Flame AA can only analyze solutions.

A hollow cathode lamp is used as a source of radiation. The lamp is made of the same metal as the analyte. For example with copper, a lamp containing copper emits light from excited copper atoms that produce the right mix of wavelengths to be absorbed by any copper atoms from the sample. The disadvantage of these narrow-band light sources is that only one element is measurable at a time. The amount of light absorbed is proportional to the number of copper atoms.

A calibration curve is constructed by running several samples of known copper concentration under the same conditions as the unknown. The amount the standard absorbs is compared with the calibration curve and this enables the calculation of the copper concentration in the unknown sample.
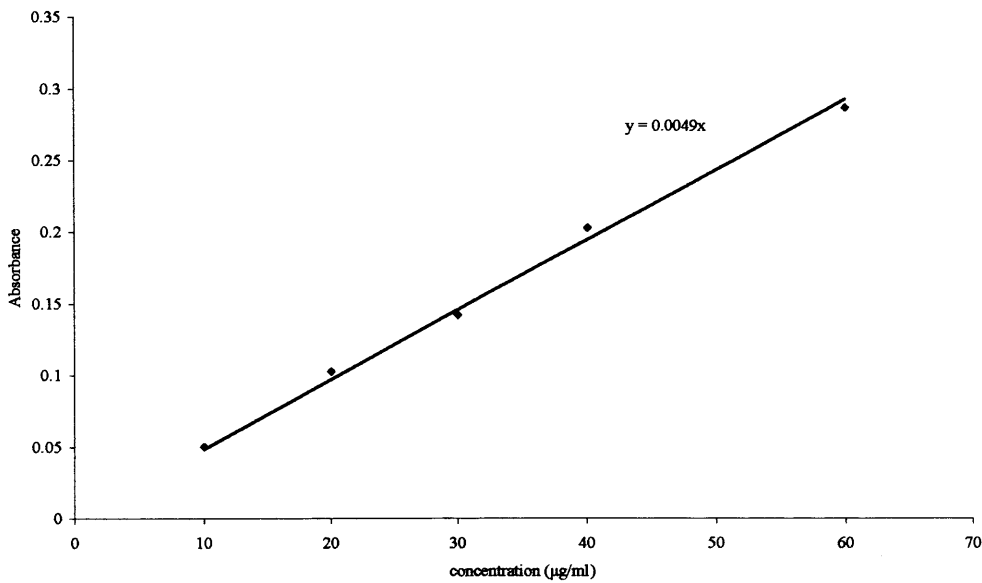
Figure 2.15 Example of calibration curve in AAS for Cu.

Flame AAS uses a slot type burner to increase the path length, and therefore to increase the total absorbance - Beer-Lambert law.

The Beer-Lambert law is the linear relationship between absorbance and concentration of the analyte.

$$-\log\left(\frac{I}{Io}\right) = A = \varepsilon c b$$

Figure 2.16 Beer- Lambert law

Io = Incident radiation power, I = transmitted radiation power, ε = absorption coefficient, c = concentration of absorption atoms, b = length of absorption path

The linearity of the Beer-Lambert law is limited by chemical and instrumental factors. Causes of nonlinearity include:

- deviations in absorptivity coefficients at high concentrations (>0.01M) due to electrostatic interactions between molecules in close proximity

- scattering of light due to particulates in the sample

- fluoresecence or phosphorescence of the sample

- changes in refractive index at high analyte concentration

- shifts in chemical equilibria as a function of concentration

- non-monochromatic radiation, deviations can be minimized by using a relatively flat part of the absorption spectrum such as the maximum of an absorption band

- stray light

Samples were analysed using a Varian SpectrAA 220Z Flame AA Spectrometer.

2.4.6 Scanning Electron Microscopy – SEM

The scanning electron microscope (SEM) is a form of electron microscope with high magnification, large depth of focus, good resolution and ease of sample preparation.

In basic scanning electron microscopy (SEM), a beam of highly energetic (0.1-50 keV) electrons is focused by one or two condenser lenses into a beam with a very fine focal spot (1-5nm). The beam passes through pairs of scanning coils in the objective lens, which deflect the beam horizontally and vertically so that it scans in a raster fashion over a rectangular area of the sample surface. The energy exchange between the electron beam and the sample results in the emission of secondary electrons and electromagnetic radiation, which can be detected to produce an image.
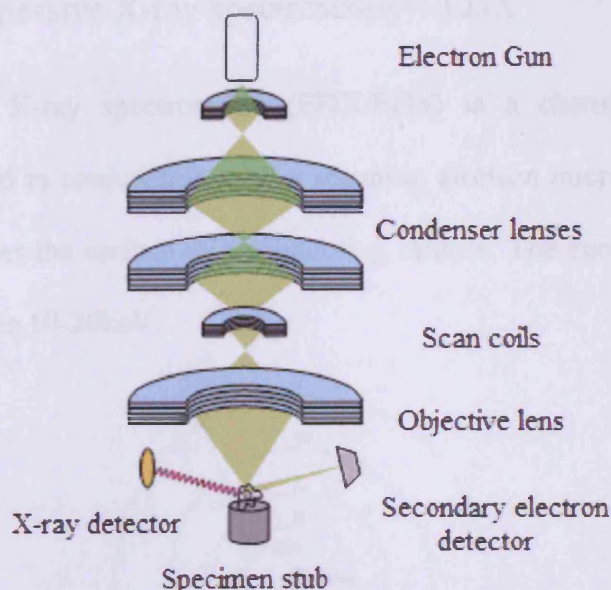
Figure 2.17 Schematic diagram of a scanning electron microscope

The electrons are detected by a type of scintillator-photomultiplier device and the resulting signal is rendered into a two-dimensional intensity distribution that can be viewed and saved as a Digital image. This process relies on a raster-scanned primary beam. The brightness of the signal depends on the number of secondary electrons reaching the detector. If the beam enters the sample perpendicular to the surface, then the activated region is uniform about the axis of the beam and a certain number of electrons "escape" from within the sample. As the angle of incidence increases, the "escape" distance of one side of the beam will decrease, and more secondary electrons will be emitted. Thus steep surfaces and edges tend to be brighter than flat surfaces, which results in images with a well-defined, three-dimensional appearance.

The analysis was performed using a Zeiss Evo-40 Series scanning electron microscope.

2.4.7 Energy Dispersive X-ray spectroscopy – EDX

Energy dispersive X-ray spectroscopy (EDX/EDS) is a chemical microanalysis technique performed in conjunction with a scanning electron microscope (SEM). An electron beam strikes the surface of a conducting sample. The energy of the beam is typically in the range 10-20keV.
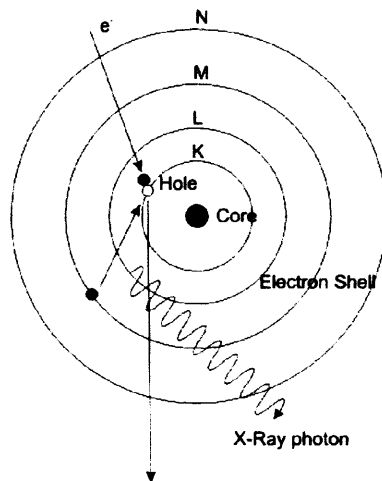
Figure 2.18 Scheme of X-ray interactions

An electron beam is aimed down into the sample to be characterised. At rest, an atom within the sample contains ground state electrons situated in concentric shells around the nucleus. The incident beam, however, excites an electron in an inner shell, prompting its ejection and resulting in the formation of an electron hole within the atom's electronic structure. An electron from an outer, higher-energy shell then fills the hole, and the excess energy of that electron is released in the form of an X-ray.

The EDX detector measures the number of emitted X-rays versus their energy. The energy of the X-ray is characteristic of the element from which the X-ray was emitted. The EDX detector converts the energy of each individual X-ray into a voltage signal of proportional size. This is achieved through a three stage process. Firstly the X-ray

70

is converted into a charge by the ionization of atoms in the semiconductor crystal. Secondly this charge is converted into the voltage signal by the Field Effect Transistor preamplifier. Finally the voltage signal is input into the pulse processor for measurement. The output from the preamplifier is a voltage 'ramp' where each X-ray appears as a voltage step on the ramp. EDX detectors are designed to convert the X-ray energy into the voltage signal as accurately as possible. At the same time electronic noise must be minimized to allow detection of the lowest X-ray energies. In traditional EDX analysis in the SEM, the spatial resolution is limited to around one micron by the interaction volume of the beam within the sample.

The equipment used was a Zeiss Evo-40 series SEM inconjuction with a INCAx-sight EDS detector.

2.5   Chapter 2 References

[1]   G.J. Hutchings, A.A. Mirzaei, R.W. Joyner, M.R.H. Siddiqui, S.H. Taylor, App. Catal. A: Gen. 166 (1998) 143.

[2]   C.D. Jones, PhD Thesis, "The Ambient Temperature Oxidation of Carbon Monoxide by Copper Manganese Oxide based Catalysts", Cardiff (2005).

[3]   A.A. Mirzaei, H.R. Shaterian, R.W. Joyner, M. Stockenhuber, S.H. Taylor, G.J. Hutchings, Catal. Comm. 4 (2003) 17.

[4]   B.E. Solsona, T. Garcia, C. Jones, S.H Taylor, A.F. Carley, G.J. Hutchings, App. Catal. A: Gen. 312 (2006) 67.

[5]   S. Brunauer, P.H. Emmet, E. Teller, Adsorption of Gases in Multimolecular Layers, J. Am. Chem. Soc. 60 (1938) 309.

[6]   Willard, Merrit, Dean, Instrument Methods of Analysis (Fifth Edition), 1974.

[7]   S.D. Robertson, B.D. McNicol, J.H. de Baas, S.C. Kloet, J.W Jenkins, J. Catal. 37 (1975) 424.

[8]   V.C.F. Holm, A. Clark, J. Catal. 11 (1968) 305.

Zinc doped copper manganese mixed oxides

3

3.1 Introduction

Ambient temperature CO oxidation has been widely reported as an important process for respiratory protection. The most widely used commercial catalyst is a copper manganese mixed oxide, $CuMn_2O_4$ (Hopcalite). Hutchings and co-workers [1-2] have reported that the preparation of the Hopcalite catalyst is influenced by many variables; the most important variable for controlling CO oxidation was the ageing time of the catalyst precursor. They reported that the ageing of the precipitate in a co-precipitation preparation method is an important factor influencing the structure and morphology of the precursors and catalysts. The ageing of the precipitates obtained by co-precipitation leads to phase changes towards thermodynamically more stable structures.

Jones [3] reported that altering the original Hopcalite catalyst by doping the materials with metal cations (Co^{3+}, Ni^{2+}, Fe^{3+}, and Ag^+) can improve activity towards CO oxidation. It was reported that a 2% Co/CuMnOx catalyst aged for 6h had shown

significantly improved activity for CO oxidation, compared to an undoped Hopcalite catalyst.

The addition of zinc to the CuMnOx catalyst has yet to be investigated for CO oxidation. The Zn^{2+} anion is similar in size to the Cu^{2+} ion, so it was hoped that it could be incorporated into the Hopcalite catalyst without disrupting the Hopcalite structure (Cu^{2+} has an ionic radii of 87pm and Zn^{2+} has a radii of 88pm). Hem and co-workers [4] published a report where $ZnMn_2O_4$, a spinel-structured analog of hausmannite, Mn_3O_4, was prepared by precipitation. Hem and co-workers stated that zinc can influence manganese oxidation processes.

Fierro and co-workers [5] have investigated Cu-Zn based manganites by a procedure slightly different to the co-precipitation procedure described in chapter 2. Their investigation looked at the reduction of NO by hydrocarbons. They discussed that there was the possibility of replacing cations in both the tetrahedral and octahedral sites available in the spinel crystal lattice.

Catalysts based on CuO/ZnO mixed oxides are of considerable industrial interest due to their activity for low temperature and pressure methanol synthesis and the water gas shift reaction [6,7]. Studies on the mechanism of the water-gas shift reaction [8] and methanol synthesis [9], using Cu/ZnO based catalysts, have indicated that carbon monoxide oxidation can be an integral step in these processes. Taylor and co-workers [10] reported a copper/zinc mixed oxide prepared by a co-precipitation method for CO oxidation. It was shown that all the catalysts prepared exhibited significant CO oxidation activity.

There are several ways a catalyst can be promoted. A structural promoter can be added to increase surface area of the active component. Electronic promoters are dispersed in the active phase and influence the electronic chemical bonding to the adsorbate. Many metals have vacant orbitals that possess a high affinity for additional electrons. Lattice defect promoters are described as the addition of a promoter that encourages the formation of lattice defects and hence the active sites. The action of promoters is explained on the basis that the lattice defects or the irregularities on the surface of a catalyst are the active sites for catalysis.

In this chapter the effect of adding small quantities of another element to the standard Hopcalite preparation was investigated. The element added to the Hopcalite structure was zinc. The catalysts were prepared using a co-precipitation method that is described in chapter 2. The ratio of copper to zinc was varied but the overall reactant stoichiometry remained at 2:1 (Mn : [Cu+Zn]).

The variables investigated were the amount of zinc added to the catalyst and effect of ageing time during preparation. It has been shown that ageing time is an important factor influencing the structure of copper zinc oxide catalysts [11-12].

3.2 Zn doped CuMnOx aged for 0h

A series of zinc doped CuMnOx catalysts were prepared by a co-precipitation method. In each case, an ageing time of 0h was used on the catalyst precursor.

3.2.1 Catalyst activity

The activities of the undoped CuMnOx and Zn doped catalyst, Figure 3.1, show that

the addition of the dopant has a positive effect towards improving CO conversion.
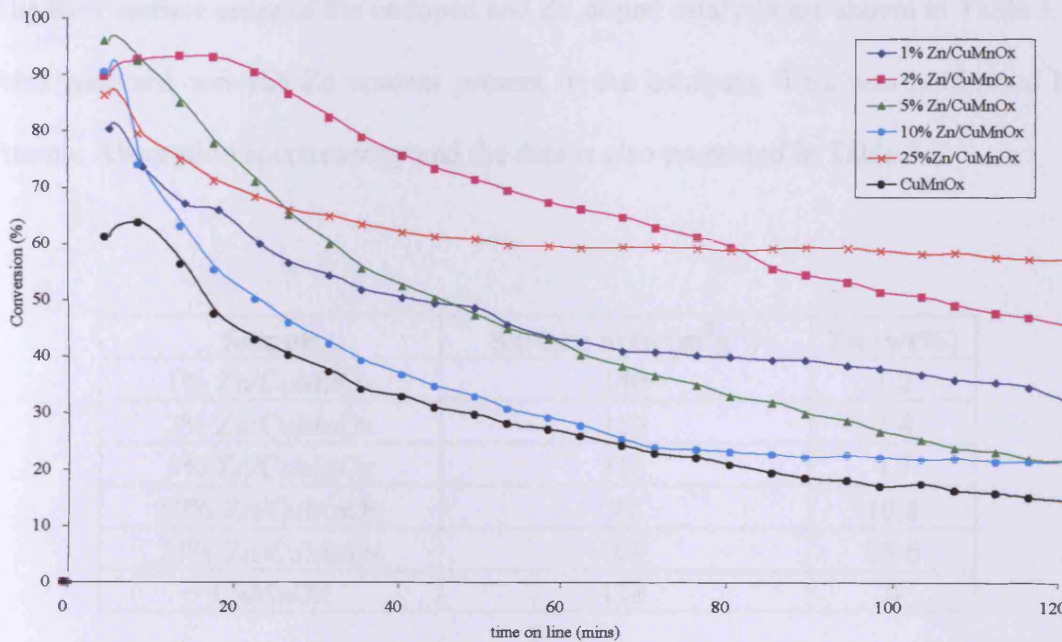
Figure 3.1 CO oxidation - Zn doped CuMnOx catalysts aged for 0h

The Zn doped CuMnOx catalysts all show initial activity improvement. The initial 20

minutes of catalyst testing has shown that the presence of the zinc dopant has

improved activity by ca. 20%. The profiles of activity are similar in that they all

exhibit high activities followed by gradual deactivation, as time on line in increased.

There is no relationship between the amount of zinc added and the catalytic activity.

The 2% Zn doped catalyst shows significantly improved activity, ca. 90% conversion

for the first 30 minutes of testing however this is this followed by a high rate of

deactivation, compared to the 25% Zn doped catalyst. The addition of 25 wt% Zn to

the CuMnOx catalyst shows steady state activity compared to the other catalysts. The

start up activities of the 2% and 5% doped catalysts are higher but show greater deactivation compared to the 25% Zn doped catalyst.

3.2.2 BET Surface areas and Analysis of amount of zinc present.

The BET surface areas of the undoped and Zn doped catalysts are shown in Table 3.1. Also analysed was the Zn content present in the catalysts. This was performed by Atomic Absorption spectroscopy and the data is also presented in Table 3.1.

Sample	Surface area (m^2g^{-1})	Zn (wt%)
1% Zn/CuMnOx	140	1.2
2% Zn/CuMnOx	156	2.4
5% Zn/CuMnOx	116	4.7
10% Zn/CuMnOx	99	10.8
25% Zn/CuMnOx	109	25.6
CuMnOx	110	0

Table 3.1 BET surface areas and AAS data – Zn doped CuMnOx catalysts aged for 0h

The surface areas of the 0h aged catalysts show no obvious trend between the amounts of zinc added and surface area. The addition of zinc as a dopant shows increased activity with the exception of the 10% Zn doped catalyst. The atomic absorption data, Table 3.1, shows that the calculated amounts of zinc dopant, present in the CuMnOx catalyst, is consistent with the actual amount present in the samples tested for CO oxidation. The amount of Zn present is shown as a weight percentage. The catalytic activities of the 0h catalysts were normalised to take into account differences in surface areas (Figure 3.2). The possibility of experimental error has been taken into consideration. The catalytic results shown in this chapter are repeated results. Catalysts were tested several times and the error in the percentage conversions

is ca. ± 2%. The surface areas were analysed several times and the error in the measurements were ca. ± 5 m²g⁻¹.
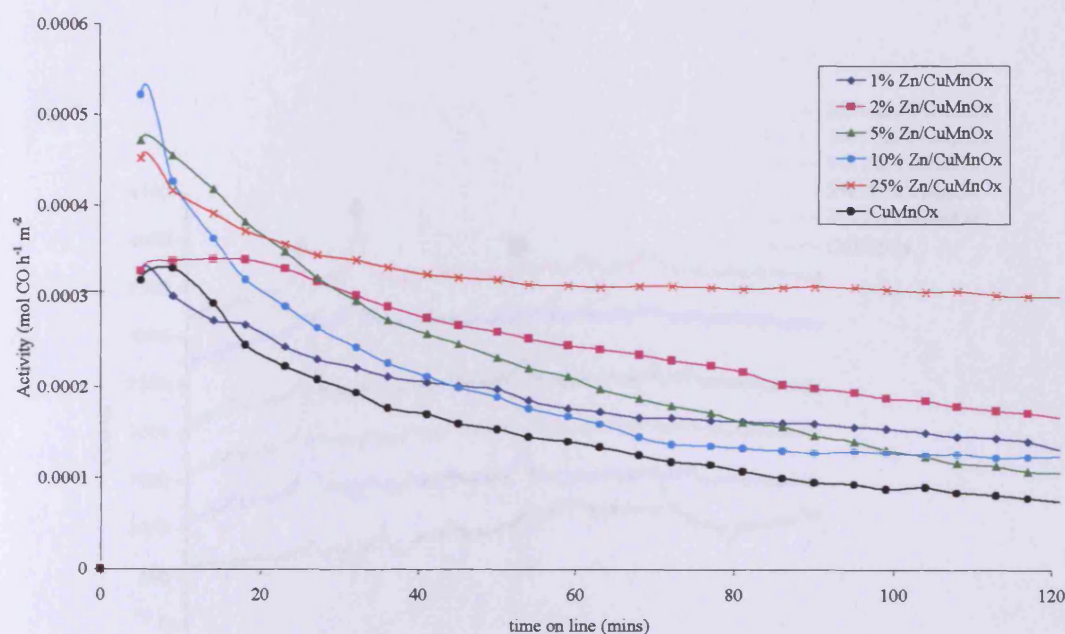
Figure 3.2 Surface area normalized activity – Zn doped CuMnOx catalysts aged for 0h

The activities, taking into account surface areas, show slightly different profiles compared to data shown in Figure 3.1. The 5%, 10% and 25% Zn doped catalysts have similarly high start up conversion rates, little difference compared to the CO conversion data. The 1% and 2% Zn doped catalysts show similar start-up conversion to the undoped CuMnOx. The normalized data shows a significant decrease in activity of the 2% Zn doped catalyst. The 25 % Zn doped catalyst demonstrates a clear improvement of activity after the effect of surface area is accounted for.

3.2.3 Powder X-ray Diffraction

The powder XRD data of the undoped and Zn doped catalysts (Figure 3.3) show slight differences between the amounts of zinc present.
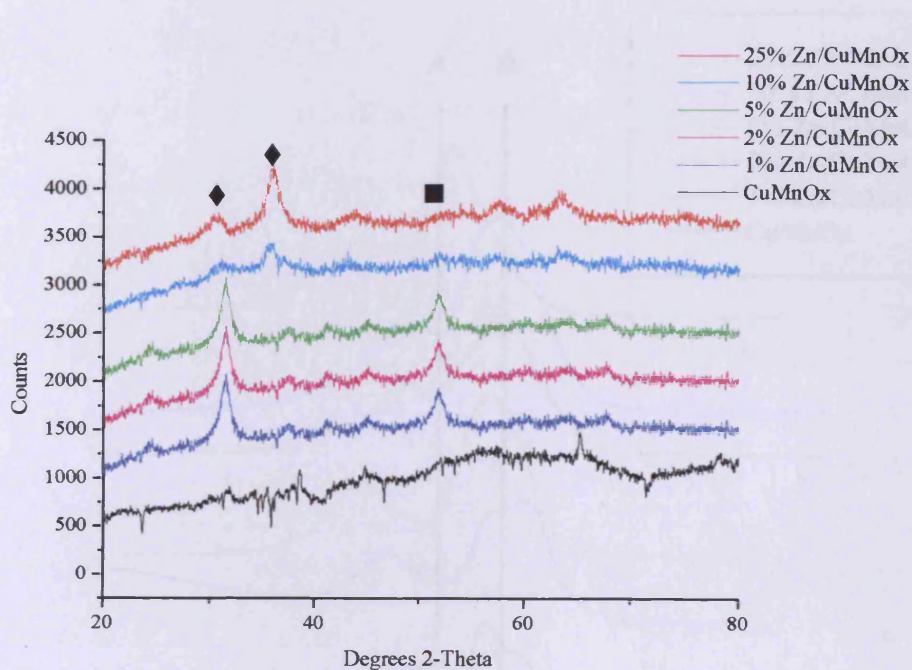
Figure 3.3 Powder XRD – Zn doped CuMnOx catalysts aged for 0h.
($\blacklozenge$) Mn_2O_3, ($\blacksquare$) $Cu_{1.5}Mn_{1.5}O_4$

The undoped catalyst was clearly amorphous to X-rays, whilst increasing the amount of Zn into the catalyst resulted in the observation of slightly crystalline phases. The peaks are broad and of low intensity and therefore difficult to analyze phases that may be present. However, the detectable phases present are Mn_2O_3 and $Cu_{1.5}Mn_{1.5}O_4$. No zinc oxide was detected in the diffraction patterns. It must be noted that there is a shift in diffraction peaks towards higher 2θ angles for the 25% Zn doped sample. This effect will be discussed later in the chapter.

3.2.4 Temperature Programmed Reduction

In order to further investigate the effect of Zn present in the CuMnOx catalyst, temperature programmed reduction studies were performed using dilute hydrogen.
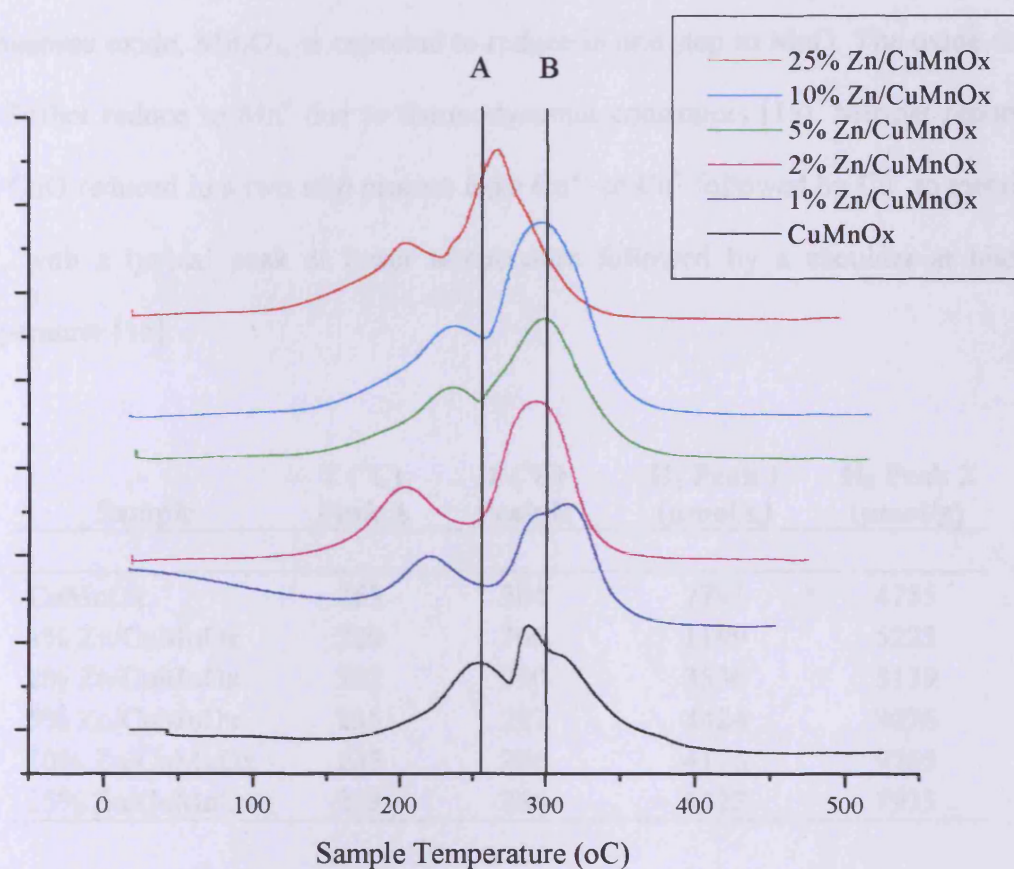
Figure 3.3 TPR Profiles – Zn doped CuMnOx catalysts aged for 0h

15 mg sample, Temperature programmed regime from ambient temperature to 500°C at 10°C min^{-1}. Reducing gas was 10% H_2 in Ar with a flow rate of 20ml min^{-1}.

The profiles (Figure 3.3) show that, for each catalyst, two distinct reduction peaks could be observed with a shoulder on the higher temperature peak. TPR profiles of Hopcalite catalysts have often been reported as difficult to interpret, due to the large number of possibilities of mixed copper manganese oxidation states, resulting from the multi-valency of each element [13]. However, it is expected that the lower

80

temperature peak (Peak A) corresponds to the reduction of Cu^{2+} as copper is reported to have a higher reducibility than manganese in mixed compounds [14]. This is due to more negative free energy of formation of the manganese oxides compared to the copper oxide.

Manganese oxide, Mn_2O_3, is expected to reduce in one step to MnO. The oxide does not further reduce to Mn^0 due to thermodynamic constraints [15]. Mirzaei reported that CuO reduced in a two step process from Cu^{2+} to Cu^+ followed by Cu^+ to metallic Cu^0, with a typical peak at lower temperature followed by a shoulder at higher temperature [16].

Sample	T ($^{\circ}$C) Peak A	T ($^{\circ}$C) Peak B	H_2 Peak 1 (μmol/g)	H_2 Peak 2 (μmol/g)
CuMnOx	253	304	2791	4755
1% Zn/CuMnOx	220	306	1199	5223
2% Zn/CuMnOx	202	290	3536	8139
5% Zn/CuMnOx	235	297	3424	8076
10% Zn/CuMnOx	235	296	4176	9765
25% Zn/CuMnOx	203	266	3422	7935

Table 3.2 TPR results of catalysts aged for 0h

The TPR results, Table 3.2, show a general shift in peak position to lower temperatures, indicating that the presence of the zinc dopant has caused the oxide species to become reduced more easily. The reduction profile for the undoped catalyst shows two peaks at 253°C and 304°C, represented as Peak A and Peak B respectively. Also, increasing the amount of dopant has generally increased the area under the peaks leading to increased hydrogen consumption. The 25% Zn doped catalyst showed peaks at 203°C (Peak A) and 266°C (Peak B). Comparing the undoped and 25% Zn doped catalyst, the lowering of the reduction temperature for

Peak A is greater than that for Peak B. The Zn doped catalysts appear to have similar oxide species present but the 25% Zn doped catalyst may have species that are more readily available for the oxidation reaction. The results from the reduction profiles indicate that the addition of zinc to the CuMnOx catalyst has a greater influence on the redox properties of copper species more than manganese species.

3.3 Zn doped CuMnOx aged for 0.5h

A series of zinc doped CuMnOx catalysts were prepared by a co-precipitation method. In each case, an ageing time of 0.5h was used on the catalyst precursor.

3.3.1 Catalyst activity

The undoped and Zn doped catalysts aged for 0.5h, Figure 3.4, were tested for CO oxidation and the addition of zinc as a dopant caused differences in activity. The profiles of the activities showed similar trends in that there was a high starting activity followed by gradual deactivation. The significant difference of the 0.5h aged catalysts (Figure 3.4) and the 0h catalysts (Figure 3.1) is the undoped CuMnOx. The 0.5h undoped catalyst now has a high initial activity (ca. 90% conversion) whereas the undoped 0h aged catalyst showed ca. 60% conversion. However, the 0.5h aged undoped catalyst shows a high rate of deactivation compared to the Zn doped catalysts aged for 0.5h.
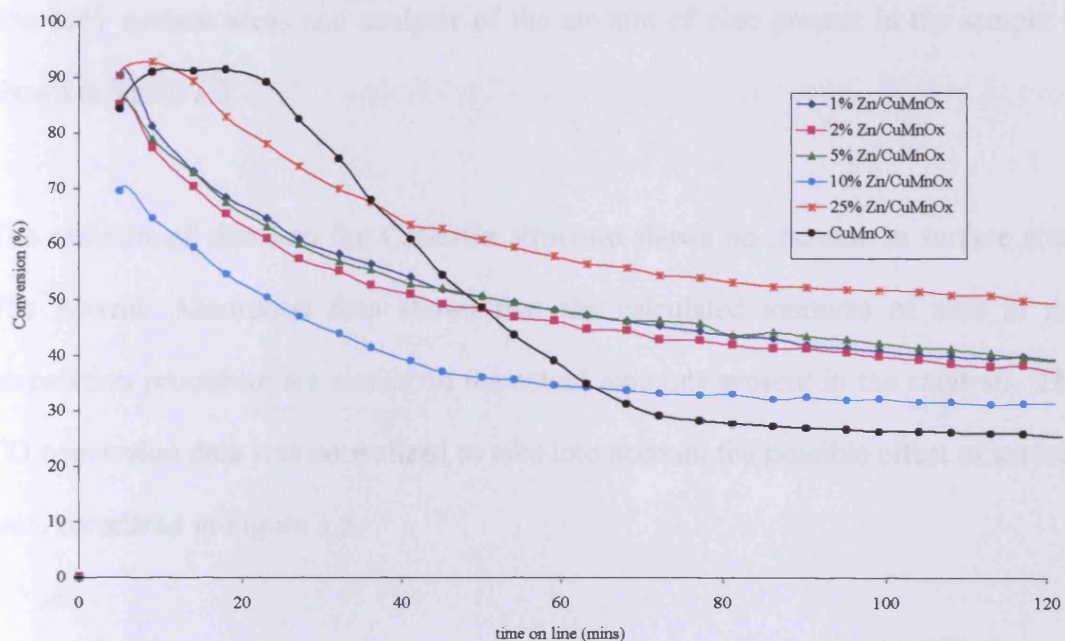
Figure 3.4 CO oxidation – Zn doped CuMnOx catalysts aged for 0.5h

The 1%, 2% and 5% doped catalysts have similar initial activities followed by similar deactivation, to give activities of ca. 40% conversion after 2h of time on line testing. The 25% Zn doped catalyst has the highest overall catalytic activity, with steady state conversion of ca. 55% compared to the undoped catalyst, which shows CO conversion of ca. 30%. The data presented so far shows that with the addition of zinc to the CuMnOx catalyst, the 25% Zn doped catalyst has the highest activity.

3.3.2 BET Surface areas and Analysis of amount of zinc present.

Sample	Surface area (m^2g^{-1})	Zn (wt%)
1% Zn/CuMnOx	108	0.98
2% Zn/CuMnOx	105	2.3
5% Zn/CuMnOx	105	5.3
10% Zn/CuMnOx	141	11
25% Zn/CuMnOx	116	25.4
CuMnOx	130	0

Table 3.3 BET surface areas and AAS data – Zn doped CuMnOx catalysts
aged for 0.5h

The BET surface areas and analysis of the amount of zinc present in the sample is shown in Table 3.3.

The addition of zinc into the CuMnOx structure shows no increase in surface area. The Atomic Absorption data shows that the calculated amounts of zinc in the preparation procedure are similar to the actual amounts present in the catalysts. The CO conversion data was normalized to take into account the possible effect of surface area, correlated in Figure 3.5.
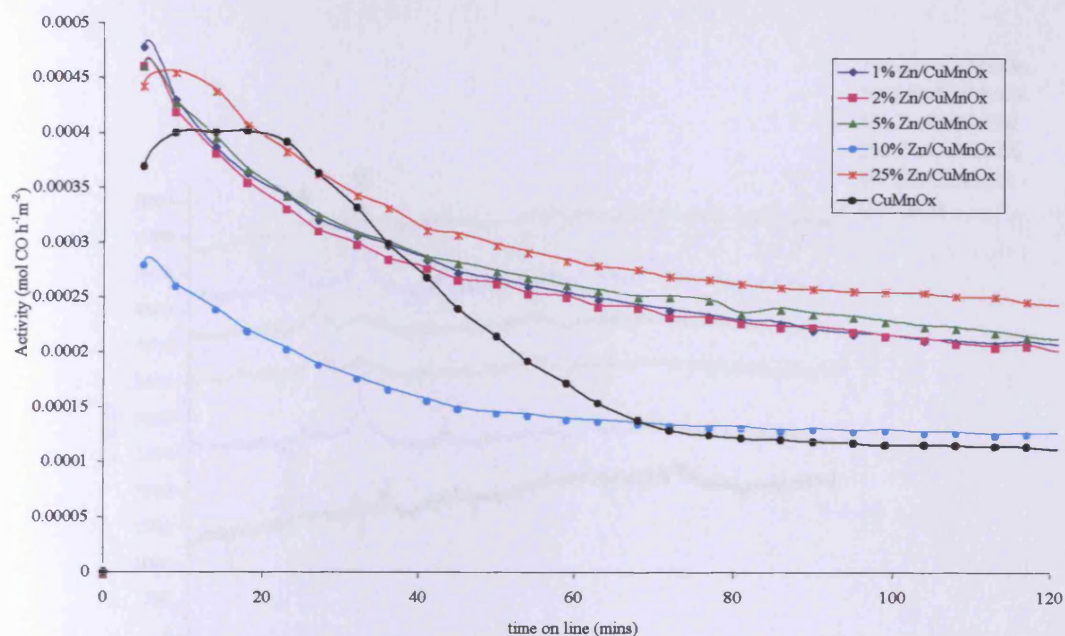
Figure 3.5 Surface area normalized activity – Zn doped CuMnOx catalysts aged for 0.5h

The normalized activities of the 0.5h aged catalysts (Figure 3.5) show that the catalytic performances show slightly different profiles. Comparing with the catalytic activities in Figure 3.4, the 10% Zn doped catalyst has the lowest initial conversion rate ca. 3×10^{-3} mol CO h^{-1} m^{-2}. The 1%, 2%, 5% and 25% Zn doped catalysts have higher conversion rates (ca. 4.5×10^{-3} mol CO h^{-1} m^{-2}) compared to the undoped catalyst (ca. 4×10^{-3} mol CO h^{-1} m^{-2}).

The rate of deactivation, with exception of the 10% Zn doped sample, is less significant with the doped catalysts compared to the undoped catalyst. The addition of 10 wt% of zinc to the catalyst aged for 0.5h appears to have had a negative effect on activity for CO oxidation.

3.3.3 Powder X-ray Diffraction

The powder x-ray diffraction patterns (Figure 3.6) show that there are slight differences in the morphologies of the catalysts.
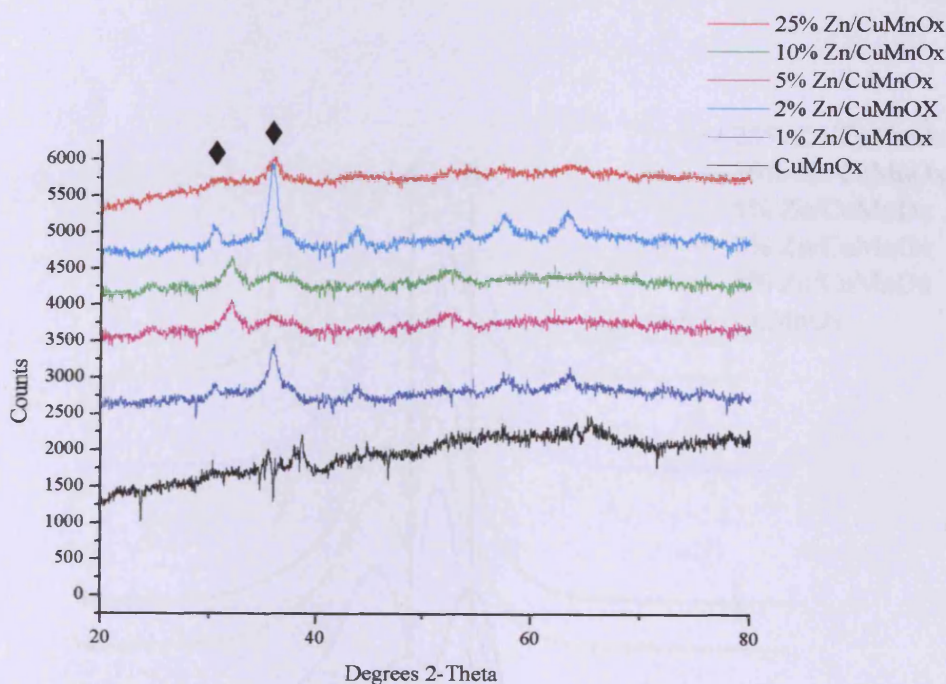
Figure 3.6 Powder XRD – Zn doped CuMnOx aged for 0.5h
(♦) Mn_2O_3

The peaks shown on the patterns are broad and difficult to identify whether there are different phases present, which may relate to catalytic activity. However, the 10% Zn doped catalyst has a peak at 2θ at ca. $36°$ which more distinguishable than the other

patterns shown in Figure 3.6. These detectable peaks correspond to the Mn_2O_3 phase. This could relate to the low activity of the 10% Zn doped catalyst compared the remaining amounts for zinc dopant. The 25% Zn doped catalyst is highly amorphous and shows no detectable peaks in the diffraction pattern. Similarly, there is evidence that the diffraction peaks are shifting as the amount of dopant is varied.

3.3.4 Temperature Programmed Reduction

The temperature programmed reduction analysis of the 0.5h aged catalysts was performed and shown in Figure 3.7.
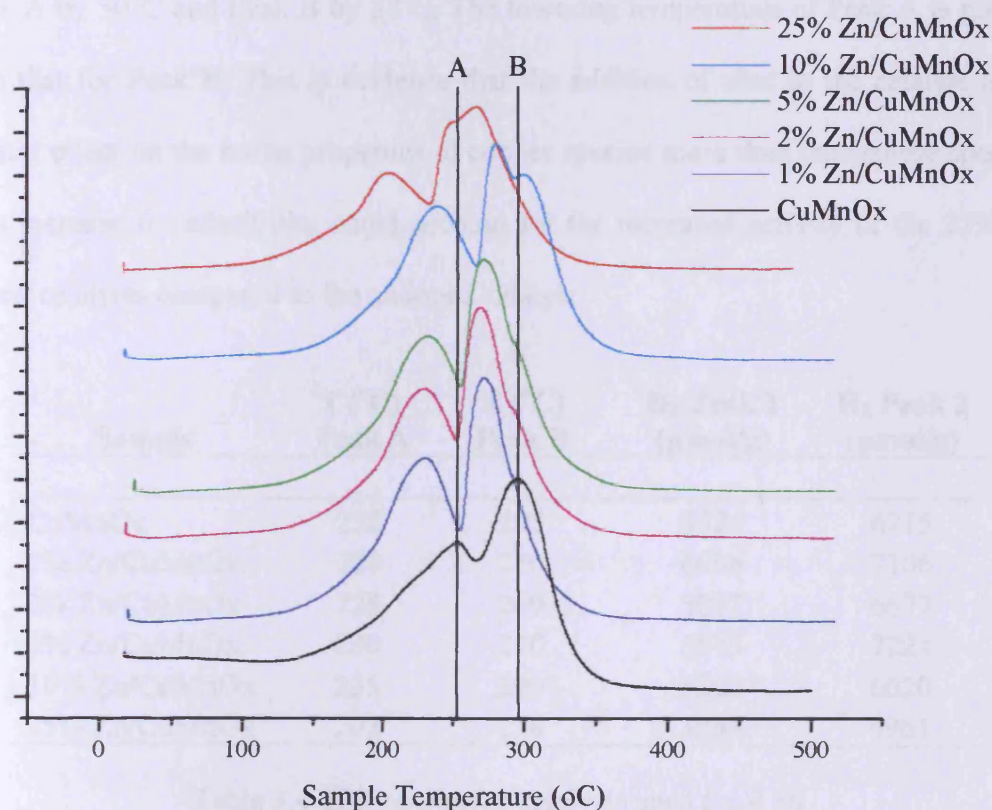
Figure 3.7 TPR profiles – Zn doped CuMnOx catalysts aged for 0.5h

The TPR patterns show that the presence of Zn in the CuMnOx catalyst has caused a general shift of the reduction peaks to lower temperatures. The undoped catalyst showed reduction peaks centred at 252°C (Peak A) and 295°C (Peak B). The 25% Zn doped catalysts, which has the highest activity, has reduction peaks centred at 202°C (Peak A) and 252°C (Peak B). This shift to a lower temperature corresponds to the reduction of species which could be linked to the observation that doped samples possess higher activity towards CO oxidation. This could be due to the lower activation energies of the doped samples for CO oxidation compared to the undoped sample. There is little change for the 10% Zn doped catalyst compared to the undoped catalyst. The 25% Zn doped catalyst shows a lowering of reduction temperature of Peak A by 50°C and Peak B by 37°C. The lowering temperature of Peak A is greater than that for Peak B. This is evidence that the addition of zinc to the catalyst has a greater effect on the redox properties of copper species more than manganese species. This increase in reducibility could account for the increased activity of the 25% Zn doped catalysts compared to the undoped catalyst.

Sample	T (°C) Peak A	T (°C) Peak B	H_2 Peak 1 (μmol/g)	H_2 Peak 2 (μmol/g)
CuMnOx	252	295	3524	6215
1% Zn/CuMnOx	229	270	6096	7106
2% Zn/CuMnOx	228	269	5037	6677
5% Zn/CuMnOx	230	270	5573	7224
10% Zn/CuMnOx	235	290	5292	6620
25% Zn/CuMnOx	202	258	3885	6961

Table 3.4 TPR results for catalysts aged for 0.5h

The results shown in Table 3.4 summarise the TPR data for 0.5h aged catalysts. It can be seen that is no general trend with the amount of zinc present and the amount of H_2 consumed in the analysis.

3.4 Zn doped CuMnOx catalysts aged for 1h

A series of zinc doped CuMnOx catalysts were prepared by a co-precipitation method. In each case, an ageing time of 1h was used on the catalyst precursor.

3.4.1 Catalyst Activity

The catalytic activities of the Zn doped CuMnOx catalysts aged for 1h (Figure 3.7) show differences of activities, compared to the catalysts aged for 0.5h (Figure 3.4).
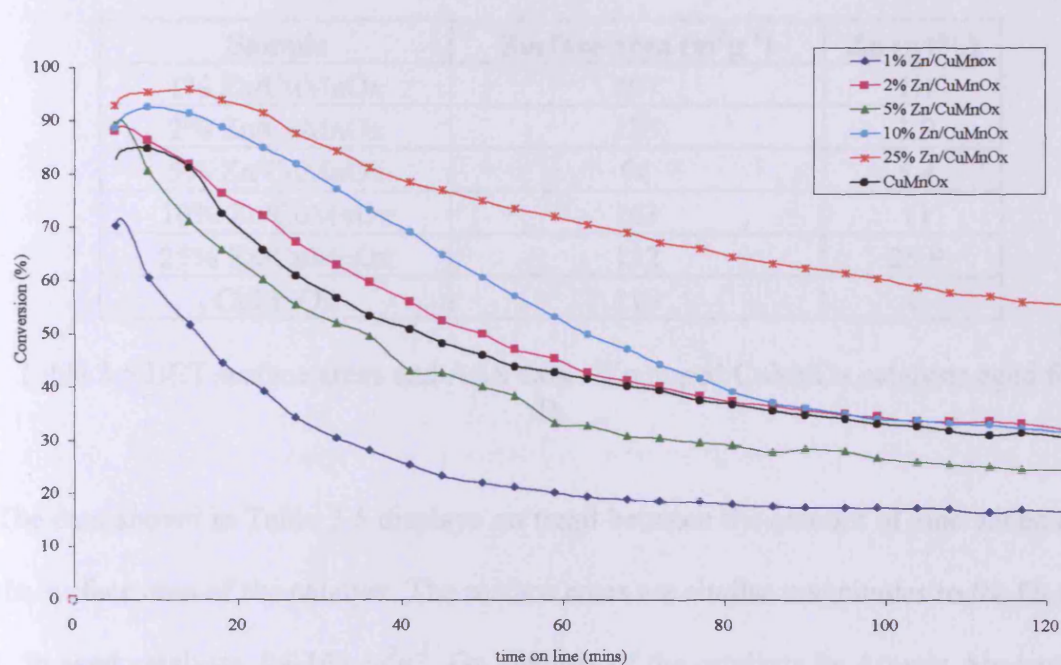
Figure 3.7 CO oxidation Zn doped CuMnOx catalysts aged for 1h

The initial activities of the 1h aged catalysts are similar; with the exception of the 1% Zn doped catalyst. The start up activities of the undoped and doped catalysts range from ca. 85-95% conversion. The 25% Zn doped catalyst displays the highest initial activity, the rate of deactivation is considerably lower than the remaining doped catalysts, reaching steady state activity of ca. 70% conversion. The undoped CuMnOx catalyst aged for 1h shows less deactivation compared to the undoped

88

catalyst aged for 0.5h. After 2h of catalyst testing, there are little differences in conversions between the 2% and 10% Zn doped catalysts with the undoped catalyst (ca. 40 % conversion). The addition of 1wt% Zn to the CuMnOx aged for 1h has decreased activity compared to the undoped CuMnOx catalyst.

3.4.2 BET Surface areas and Analysis of amount of zinc present.

The BET surface areas and analysis of the amount of zinc present in the sample is shown in Table 3.5.

Sample	Surface area (m^2g^{-1})	Zn (wt%)
1% Zn/CuMnOx	107	1.1
2% Zn/CuMnOx	125	1.9
5% Zn/CuMnOx	94	5.4
10% Zn/CuMnOx	163	11
25% Zn/CuMnOx	132	25.9
CuMnOx	119	0

Table 3.5 BET surface areas and AAS data – Zn doped CuMnOx catalysts aged for 1h.

The data shown in Table 3.5 displays no trend between the amount of zinc added and the surface area of the catalyst. The surface areas are similar magnitudes to the 0h and 0.5h aged catalysts, 94-163 m^2g^{-1}. On analysis of the catalysts by Atomic Absorption spectroscopy, the amount of zinc present in the catalysts were similar to the calculated amount in the synthesis procedure (Table 3.5). The activities were normalised to take into effect the differences in surface areas and are correlated in Figure 3.8.
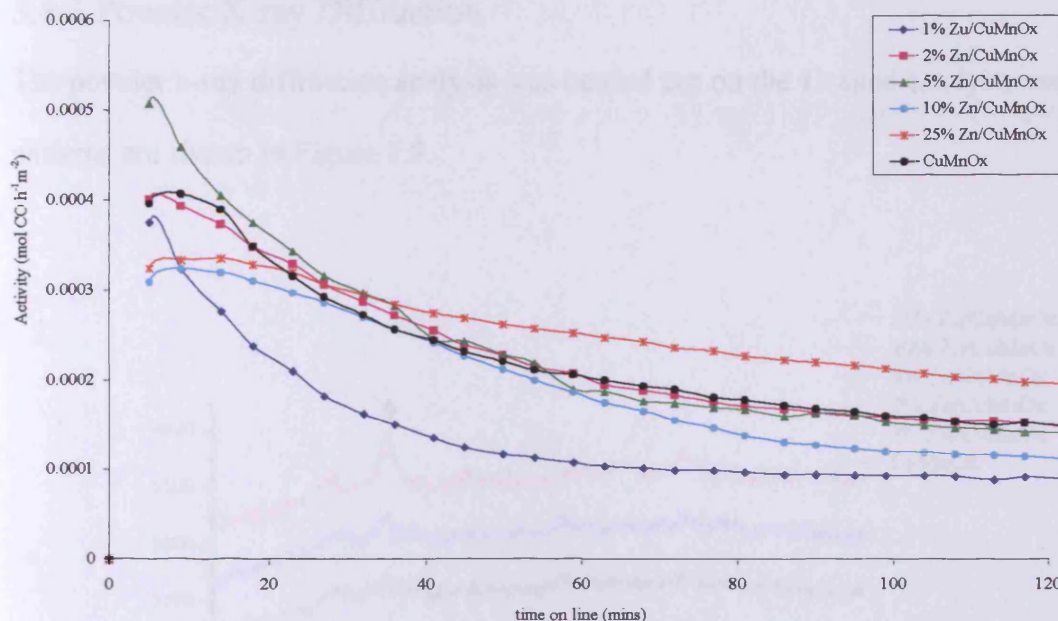
Figure 3.8 Surface area normalized activity – Zn doped CuMnOx catalysts aged for 1h

On taking into account the differences in surface areas, it was possible to demonstrate that several catalysts, aged for 1h, have similar CO conversion per unit surface area per hour. The 5 % Zn doped catalyst showed the highest initial rate of CO conversion per unit surface area per hour (ca. 5×10^{-3} mol CO h^{-1} m^{-2}). After 2h of catalyst testing, the 25% Zn doped catalyst had the highest rate of conversion of CO. This result is similar to the activities of the 25% Zn doped catalyst aged for 0h and 0.5h. The 1% Zn doped catalyst showed no change in profile when considering surface area effects. It has the lowest conversion and lowest rate of conversion per unit surface area per hour.

3.4.3 Powder X-ray Diffraction

The powder x-ray diffraction analysis was carried out on the 1h aged catalysts and the patterns are shown in Figure 3.9.
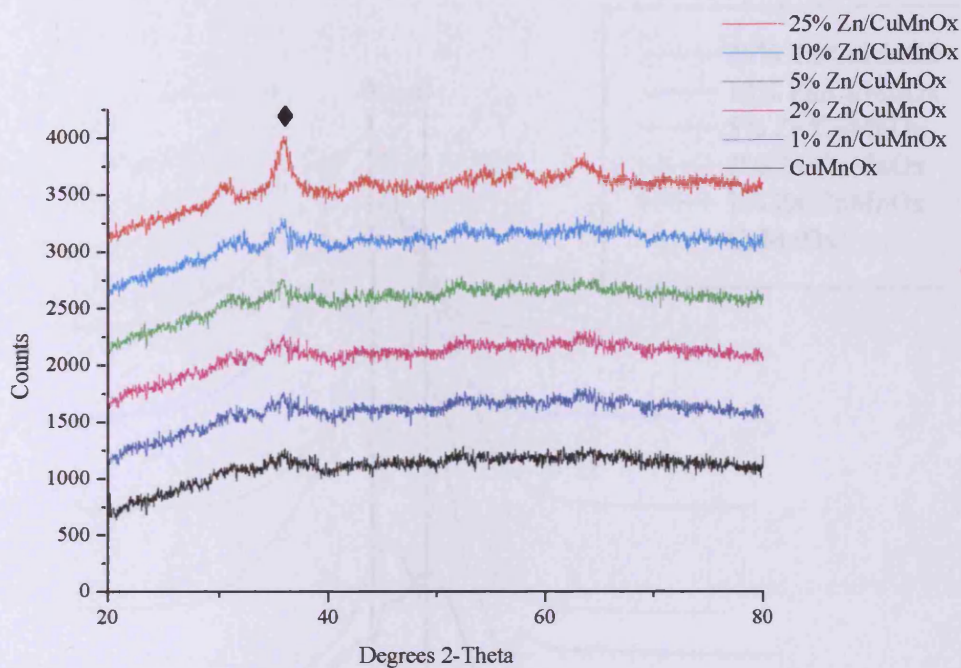
Figure 3.9 Powder XRD patterns – Zn doped CuMnOx aged for 1h.
(♦) Mn$_2$O$_3$

On XRD analysis, it was not possible to differentiate between the undoped and the Zn doped catalysts. The similarities in the catalysts are that they were all poorly crystalline and there was little difference in patterns regardless of their zinc content. The 25% Zn doped catalyst shows a peak at 2θ ca. 37° but this peak is so broad that it was impossible to identify what this peak corresponded to. Comparing to the 0h and 0.5h samples, this peak could be identified as the Mn$_2$O$_3$ phase.

3.4.4 Temperature Programmed Reduction

Temperature programmed reduction analysis was carried out on the undoped and Zn doped catalyst aged for 1h (Figure 3.10).
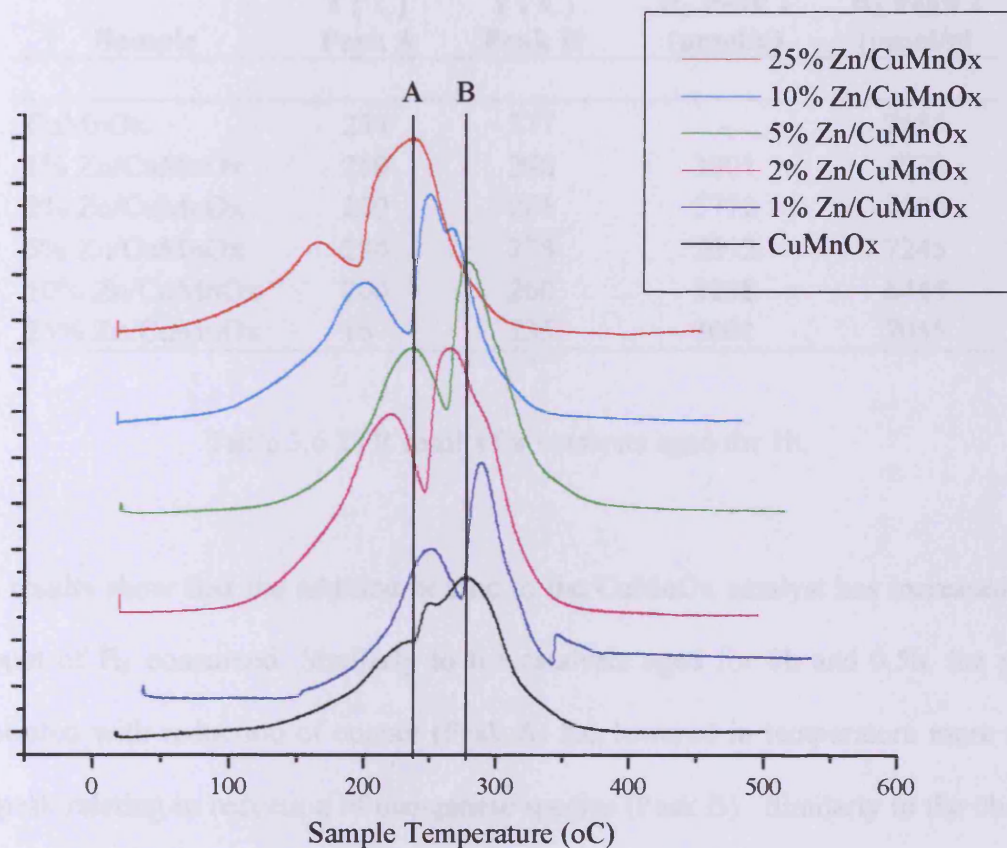
Figure 3.10 TPR profiles – Zn doped CuMnOx catalysts aged for 1h

There was a general decrease in reduction temperature of the most reducible species in the catalysts, with the addition of zinc as a dopant. A decrease in reduction temperature indicates that the presence of zinc has increased the ability of the oxides species present to react more readily during the CO oxidation reaction. The increase of H_2 consumption for the Zn doped catalysts indicates an increase in active oxide species compared to the undoped catalyst. The results for the TPR analysis are summarised in Table 3.6. The undoped CuMnOx catalyst, Peak A, which

corresponding to reduction of copper oxide was not able to be integrated. The area

under Peak B, for the undoped catalyst, corresponds to the total area under the profile

ca. 7685 μmol/g.

Sample	T (°C) Peak A	T (°C) Peak B	H$_2$ Peak 1 (μmol/g)	H$_2$ Peak 2 (μmol/g)
CuMnOx	234	277	-	7685
1% Zn/CuMnOx	250	290	3901	4773
2% Zn/CuMnOx	220	265	5772	7094
5% Zn/CuMnOx	234	278	5692	7245
10% Zn/CuMnOx	200	260	5238	6445
25% Zn/CuMnOx	167	235	3001	7055

Table 3.6 TPR results for catalysts aged for 1h.

The results show that the addition of zinc to the CuMnOx catalyst has increased the

amount of H$_2$ consumed. Similarly to the catalysts aged for 0h and 0.5h, the peak

associated with reduction of copper (Peak A) has lowered in temperature more than

the peak relating to reduction of manganese species (Peak B). Similarly to the 0h and

0.5h aged catalysts, the presence of zinc has a greater influence on the redox

properties of the copper species than manganese species.

3.5 Zn doped CuMnOx aged for 6h

A series of zinc doped CuMnOx catalysts were prepared by a co-precipitation method.

In each case, an ageing time of 6h was used on the catalyst precursor.

3.5.1 Catalyst activity

The profiles of the catalysts aged for a longer period (i.e. 6h) show a greater difference compared to the shorter ageing times.
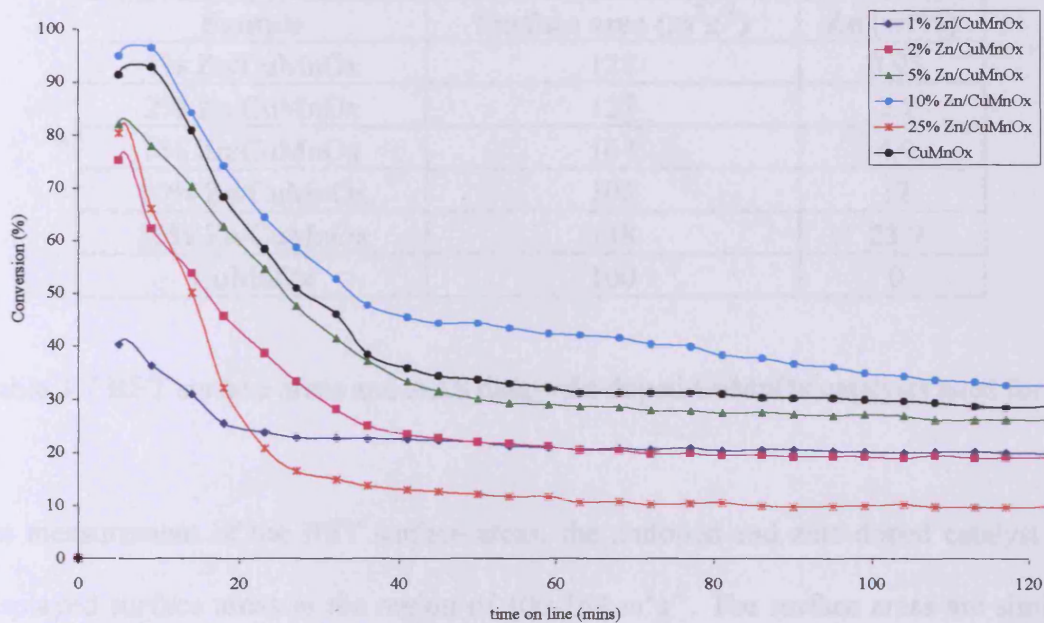
Figure 3.11 CO oxidation – Zn doped CuMnOx catalysts aged for 6h

The 6h aged catalysts show high start up activities, followed by high rates of deactivation. Steady state activity appears to occur from 40 minutes onwards during catalyst testing. The 10 % Zn doped catalyst shows the only improvement in catalytic activity compared to the undoped CuMnOx catalyst. The 10% Zn doped catalyst has an initial activity of ca. 95% conversion followed by deactivation, leading to steady activity of ca. 41% conversion. The 25% Zn doped catalyst, which had the highest steady state activity for the lower ageing times, now has the lowest activity of the doped catalysts. There is a significant difference between the 1h aged doped catalyst and the 6h aged catalyst. The 1% Zn doped catalyst has a low initial activity (ca. 40% conversion) but shows very steady activity for a sustained period of time.

94

3.5.2 BET Surface areas and Analysis of amount of zinc present.

The BET surface areas and analysis of the amount of zinc present in the sample is shown in Table 3.7.

Sample	Surface area (m^2g^{-1})	Zn (wt%)
1% Zn/CuMnOx	128	0.95
2% Zn/CuMnOx	127	2.1
5% Zn/CuMnOx	164	4.9
10% Zn/CuMnOx	102	12
25% Zn/CuMnOx	138	23.9
CuMnOx	100	0

Table 3.7 BET surface areas and AAS data – Zn doped CuMnOx catalysts aged for 6h

On measurement of the BET surface areas, the undoped and zinc doped catalyst all displayed surface areas in the region of 100-164 m^2g^{-1}. The surface areas are similar to the lower ageing times of 0h – 1h. The AAS analysis confirmed the presence of zinc in the doped CuMnOx catalysts. The experimental values were similar to the calculated amounts in the experimental procedure. The differences in surface areas of the 6h aged catalysts were correlated with catalytic activities. The surface area normalised activities are shown in Figure 3.12.

The effect of surface area shows very little difference for the conversion profiles compared to the activities shown in Figure 3.11. The 25% Zn doped, which had the lowest overall conversion after 2h testing, has the lowest rate of CO conversion per unit surface area per hour (ca. 5 x 10^{-4} mol CO h^{-1} m^{-2}). The undoped CuMnOx catalyst aged for 6h shows a high rate of deactivation. The 10% Zn doped catalyst has the highest overall rate of conversion of CO (ca. 2.5 x 10^{-3}). The 6h aged catalysts

show much higher rates of deactivation but do show steady activities after 2h that show no indication of further deactivation.
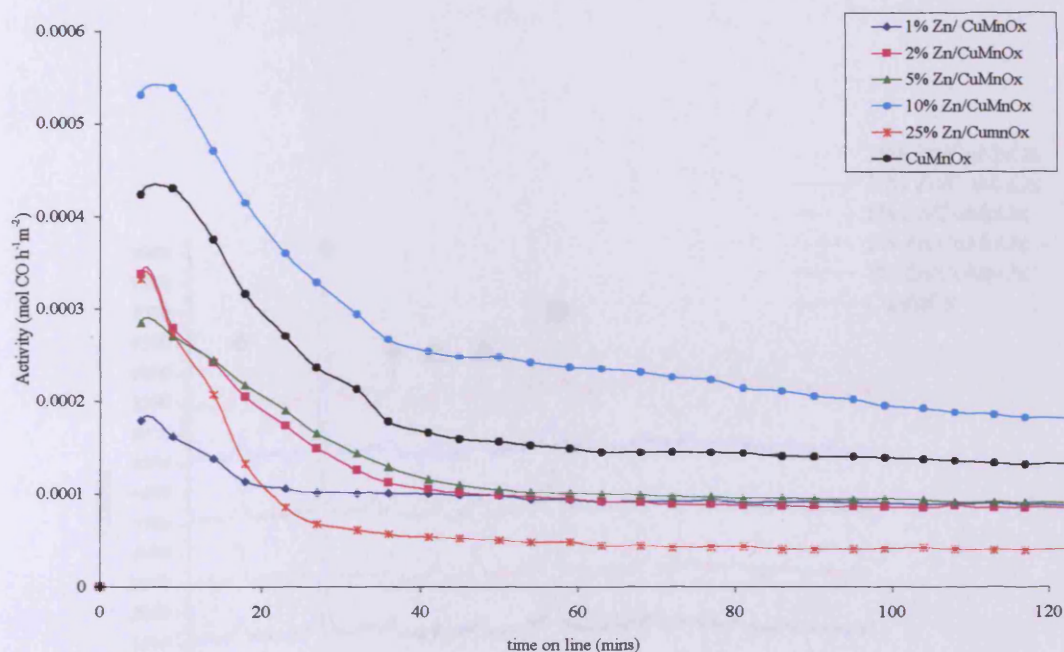
Figure 3.12 Surface area normalized activity – Zn doped CuMnOx catalysts aged for 6h.

3.5.3 Powder X-ray Diffraction

The powder XRD patterns of the catalysts aged for 6h are shown in Figure 3.13.

The patterns of the 6h aged catalysts show that there is little difference between the amount of zinc added and the structure of the samples. The catalysts aged for 6h are poorly crystalline. However, the difference of the patterns for the 6h aged catalysts compared to the 0h-1h aged patterns is that they are micro-crystalline. There is a peak 2θ at ca. 32° which is predominately present in the longer aged catalyst; this corresponds to a Mn_2O_3 phase. The increase in crystallinity could be the cause of the high deactivation caused for the 6h aged catalysts. The diffraction pattern shows that a mixed oxide phase, $Cu_{1.5}Mn_{1.5}O_4$, is present. The difference in the XRD patterns of

96

the 12h aged samples, compared to the shorter aged samples, is that two peaks 2θ at ca. $42°$ and $45°$ are present. These peaks correspond to CuO. Increasing the ageing time has increased crystallinity and the formation of new phases.
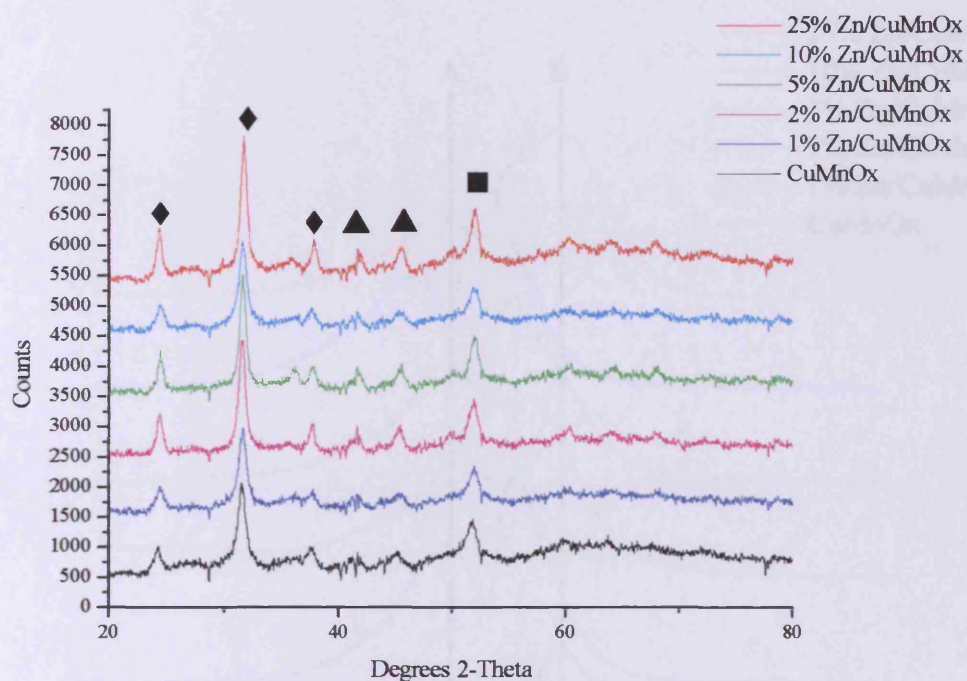
Figure 3.13 Powder XRD – Zn doped CuMnOx aged for 6h
($\blacklozenge$) Mn_2O_3, ($\blacksquare$) $Cu_{1.5}Mn_{1.5}O_4$, ($\blacktriangle$) CuO

3.5.4 Temperature Programmed Reduction

In order to investigate further the effect of Zn present in the CuMnOx, temperature programmed reduction studies were performed using dilute hydrogen. The reduction profiles of the undoped and Zn doped CuMnOx catalysts aged for 6h are shown in Figure 3.14.

The TPR profiles of the 6h aged catalysts show that the addition of zinc to the CuMnOx catalysts has lowered the reduction temperature. The 10% Zn doped catalyst, which has the highest activity towards CO oxidation, has reduction peaks centered at 206°C (Peak A) and 252°C (Peak B).
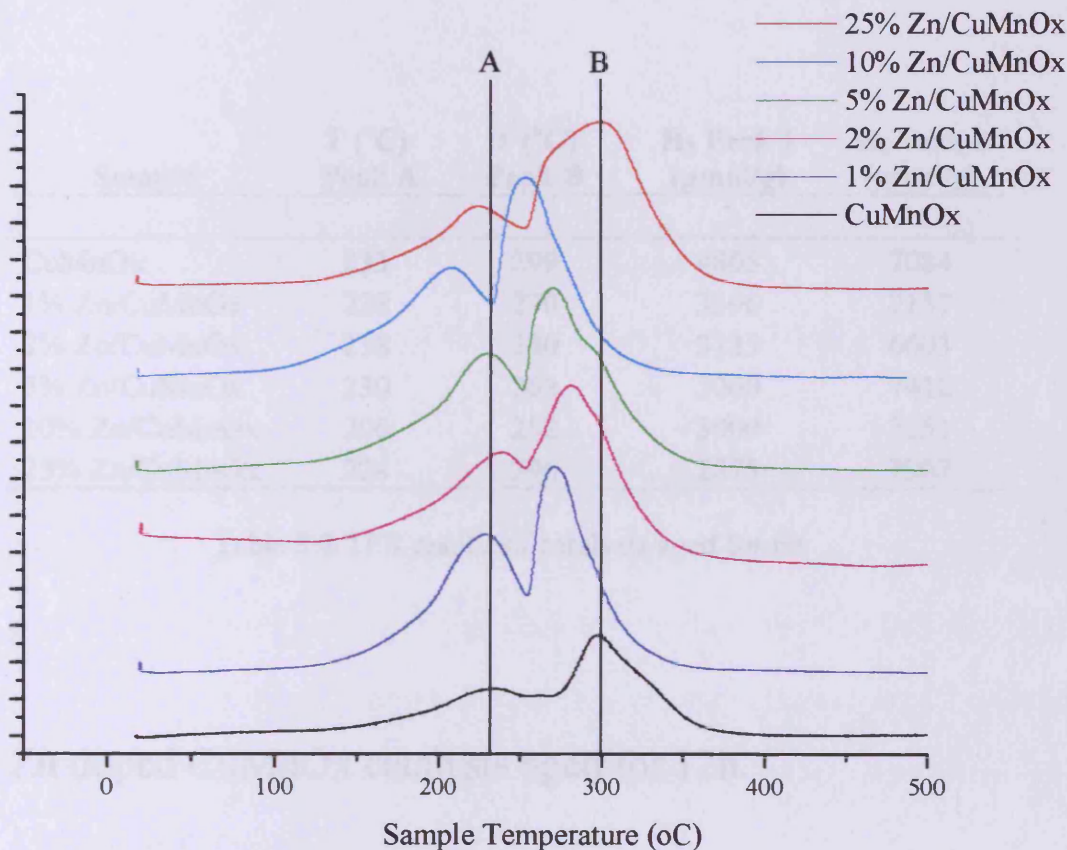
Figure 3.14 TPR profiles – Zn doped CuMnOx catalysts aged for 6h

Generally, the lowering of Peak B for the doped catalysts is greater than of Peak A. This result is different to the doped catalysts aged for 0h, 0.5h and 1h. This could be due to the ageing time of the catalyst precursor which has an affect on the species present in the catalyst. The powder X-ray diffraction patterns show that the catalysts aged for 6h are more crystalline than the shorter aged catalyst. The nature of the species present could lead to the addition of zinc having a greater influence on the redox properties of the manganese species present This increase in reducibility means

that the 10% Zn doped catalysts could have oxide species that are energetically more favorable to react during the CO oxidation reaction. The area under the peaks, corresponding to H_2 consumption, shows no trend for the addition of zinc with H_2 consumption. However, the results have shown that the ageing time during catalyst preparation is important in preparing an active catalyst.

Sample	T (°C) Peak A	T (°C) Peak B	H_2 Peak 1 ($\mu mol/g$)	H_2 Peak 2 ($\mu mol/g$)
CuMnOx	233	299	4805	7084
1% Zn/CuMnOx	228	270	3396	7157
2% Zn/CuMnOx	238	280	3125	6603
5% Zn/CuMnOx	230	268	5060	7412
10% Zn/CuMnOx	206	252	3000	7251
25% Zn/CuMnOx	224	296	2875	7907

Table 3.8 TPR results of catalysts aged for 6h

3.6 Zn doped CuMnOx catalysts aged for 12h.

A series of zinc doped CuMnOx catalysts were prepared by a co-precipitation method using an extended ageing time. In each case, an ageing time of 12h was used on the catalyst precursor.

3.6.1 Catalytic Activity

The 12h aged catalysts were tested for activity towards CO oxidation and compared with the results reported for shorter aged catalysts. A similar trend is shown to the 6h aged catalyst in that a fast rate of deactivation is shown followed by steady state activity over the 2h testing period.
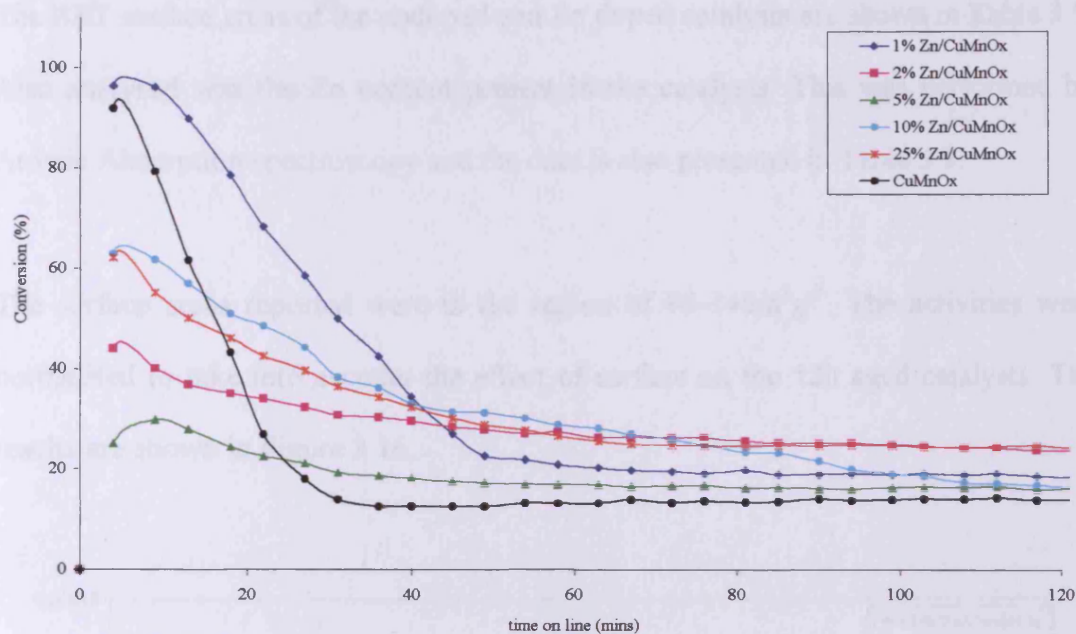
Figure 3.15 CO oxidation – Zn doped CuMnOx catalysts aged for 12h

However, the initial activities of the 2%, 5%, 10% and 25% Zn doped catalysts are much lower than the 6h aged catalysts. The 1% Zn doped and undoped CuMnOx catalysts show high start up activities (ca. 90% conversion) followed by rapid deactivation over a 30 minute period. The addition of zinc to the 12h aged CuMnOx catalyst shows slight improvement but the activities are much lower than the conversions reported for the 0h-1h aged catalysts.

3.6.2 BET Surface areas and Analysis of amount of zinc present.

Sample	Surface area (m^2g^{-1})	Zn (wt%)
1% Zn/CuMnOx	141	1.3
2% Zn/CuMnOx	148	2.4
5% Zn/CuMnOx	140	5.3
10% Zn/CuMnOx	140	9.6
25% Zn/CuMnOx	95	24.1
CuMnOx	135	0

Table 3.9 BET surface areas and AAS data – Zn doped CuMnOx catalysts aged for12h

The BET surface areas of the undoped and Zn doped catalysts are shown in Table 3.9. Also analysed was the Zn content present in the catalysts. This was performed by Atomic Absorption spectroscopy and the data is also presented in Table 3.9.

The surface areas reported were in the region of 95-148m^2g^{-1}. The activities were normalised to take into account the effect of surface on the 12h aged catalysts. The results are shown in Figure 3.16.
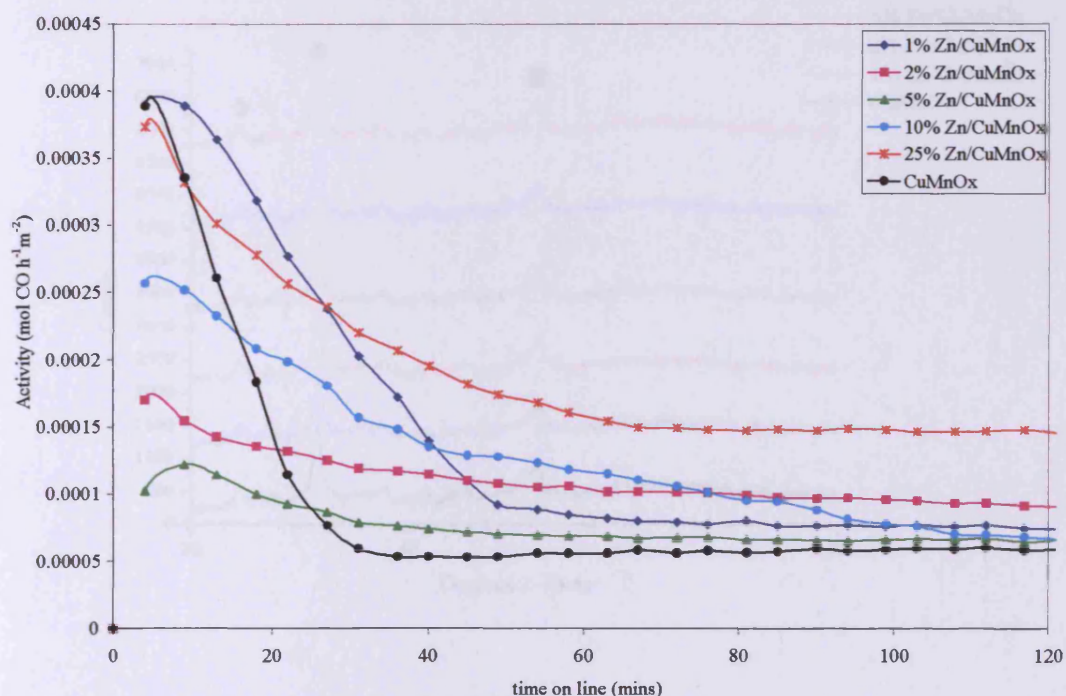
Figure 3.16 Surface area normalized activity – Zn doped CuMnOx catalysts aged for 12h

The major difference of the catalytic activity profiles of the surface area normalized activity was with the 25% Zn doped catalyst. The rate of conversion of CO was much higher than that of the other 12h aged catalysts. The rate of conversion of the 25% doped catalysts was ca. 2×10^{-3} mol CO h^{-1} m^{-2} whereas the undoped CuMnOx catalyst had a conversion rate of ca. 7.5×10^{-4} mol CO h^{-1} m^{-2}. The 25% doped

101

catalyst had the highest rate of conversion of the doped catalyst for the ageing times of 0h, 0.5h, 1h and 12h. The exception being the catalysts aged for 6h.

3.6.3 Powder X-ray Diffraction

The Powder XRD patterns for the undoped and Zn doped CuMnOx catalysts are shown in Figure 3.17.
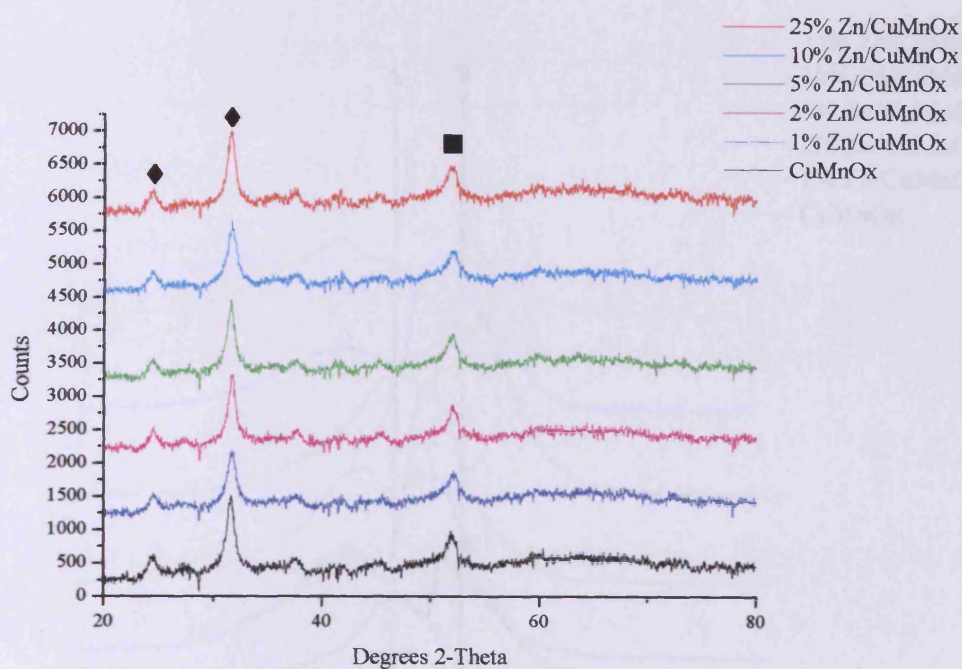
Figure 3.17 Powder XRD – Zn doped CuMnOx aged for 12h

(●) Mn_2O_3, (■) $Cu_{1.5}Mn_{1.5}O_4$

The XRD patterns of the 12h aged catalysts show that they are micro-crystalline and not as amorphous as the shorter aged samples. The XRD results showed the $Cu_{1.5}Mn_{1.5}O_4$ and Mn_2O_3 phases were present. There are little differences between patterns of the 12h aged catalysts and there is no shift in peaks compared to the shorter aged samples. However, the increase in crystallinity, compared to the shorter

ageing times, could be evidence of the decrease in catalytic activity. The patterns for

the 12h catalysts are slightly less crystalline than the than the 6h aged catalysts.

3.6.4 Temperature Programmed Reduction

The TPR profiles of the undoped and Zn doped CuMnOx catalysts are shown in
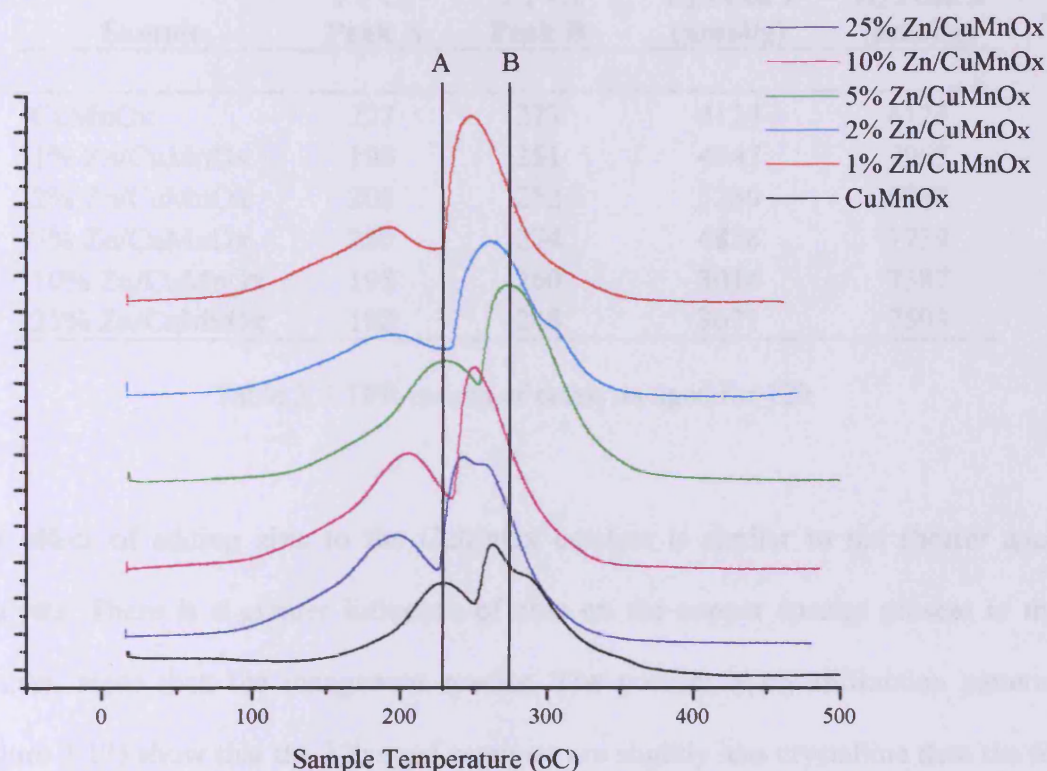
Figure 3.18.

Figure 3.18 TPR profiles – Zn doped CuMnOx catalysts aged for 12h

The TPR profiles show a general shift of reduction peaks to lower temperatures with

the addition of zinc to the CuMnOx catalyst. The reduction peaks for the undoped

CuMnOx catalyst are centered at 227°C (Peak A) and 273°C (Peak). The peaks for

the 25% Zn doped catalyst show a lowering of reduction Peak A by 35°C and

reduction Peak B by 25°C. This increased reducibility shows evidence of a smaller

amount of energy required to liberate the oxide component present during CO oxidation. Also, the addition of the zinc dopant increases the area under the reduction peaks shown in Figure 3.18. This increase in area is related to increase H_2 absorbed and therefore an increase in the amount of active species present.

The results for the TPR analysis for catalysts aged for 12h are summarised in Table 3.9.

Sample	T (°C) Peak A	T (°C) Peak B	H_2 Peak 1 (μmol/g)	H_2 Peak 2 (μmol/g)
CuMnOx	227	273	4124	6124
1% Zn/CuMnOx	198	251	4947	7955
2% Zn/CuMnOx	205	252	5280	6732
5% Zn/CuMnOx	230	274	4858	7739
10% Zn/CuMnOx	195	260	3014	7387
25% Zn/CuMnOx	192	248	3671	7593

Table 3.9 TPR results of catalysts aged for 12h

The effect of adding zinc to the CuMnOx catalyst is similar to the shorter aged catalysts. There is a greater influence of zinc on the copper species present in the catalyst; more than the manganese species. The powder X-ray diffraction patterns (Figure 3.17) show that the 12h aged catalysts are slightly less crystalline than the 6h aged catalyst (Figure 3.13). This could be further evidence that ageing time of the catalyst precursor is a vital step in influencing the structure and morphology of the precursors and catalysts.

3.7 Discussion

A series of catalysts were prepared with varying amounts of zinc present, with a range of ageing times for the precipitate (0-12h). The ageing of a precipitate is a process that can have a controlling effect on the catalytic activity of the resulting material [1, 17,18]. It is apparent to see that varying the ageing time of the catalyst has an effect on the activity of the catalyst. The steady state CO conversions for the undoped and zinc doped catalysts are summarized in Figure 3.19.
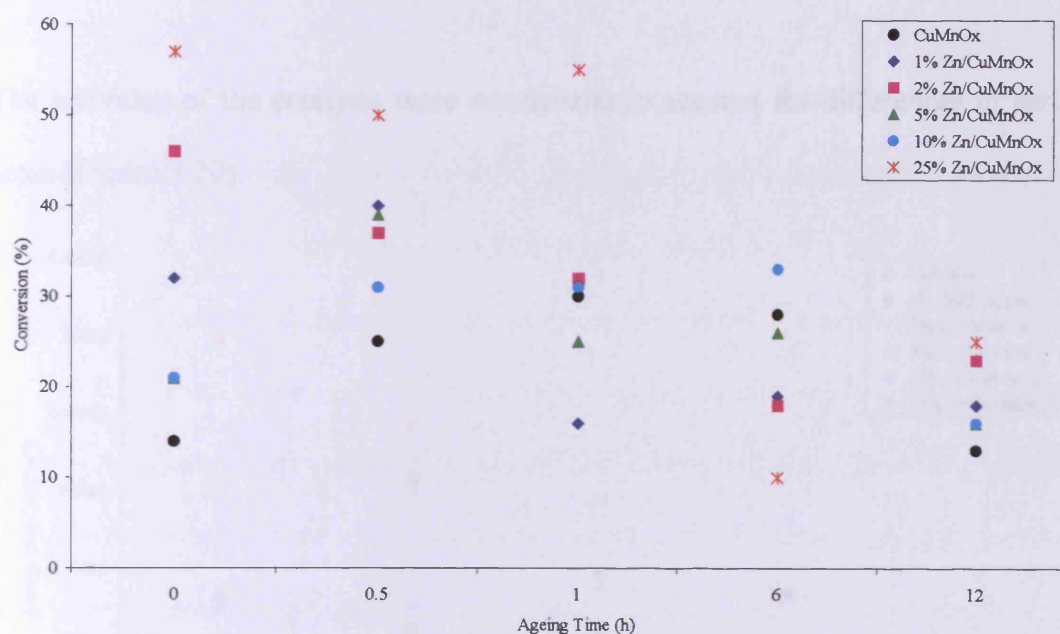
Figure 3.19 Variation of CO conversions after 2h on line as a function of ageing time and % zinc dopant

Each data point on the graph (Figure 3.19) represents the result of each catalyst prepared three times, with each catalyst being tested three times. In summary, each data point represents nine individual data points. This emphasises the reproducibility of the catalyst preparation.

Taking the 25% Zn doped CuMnOx as an example, it can be seen for the shorter ageing times (0-1h) of the catalyst precipitate, there is improvement in activity compared to the undoped CuMnOx catalyst. Ageing the catalyst precursor for longer periods (6-12h) showed a decrease in catalytic activity. The 0h and 0.5h ageing times showed improvement of catalytic activity of the Zn doped catalysts compared to the undoped catalyst. The 10% Zn doped catalyst is consistently more active than the undoped CuMnOx catalyst for all the ageing times shown in Figure 3.19. The 25% Zn doped catalyst follows a similar pattern except for the 6h aged catalyst, which has significantly decreased in activity.

The activities of the catalysts were normalized to account for differences in surface areas (Figure 3.20).
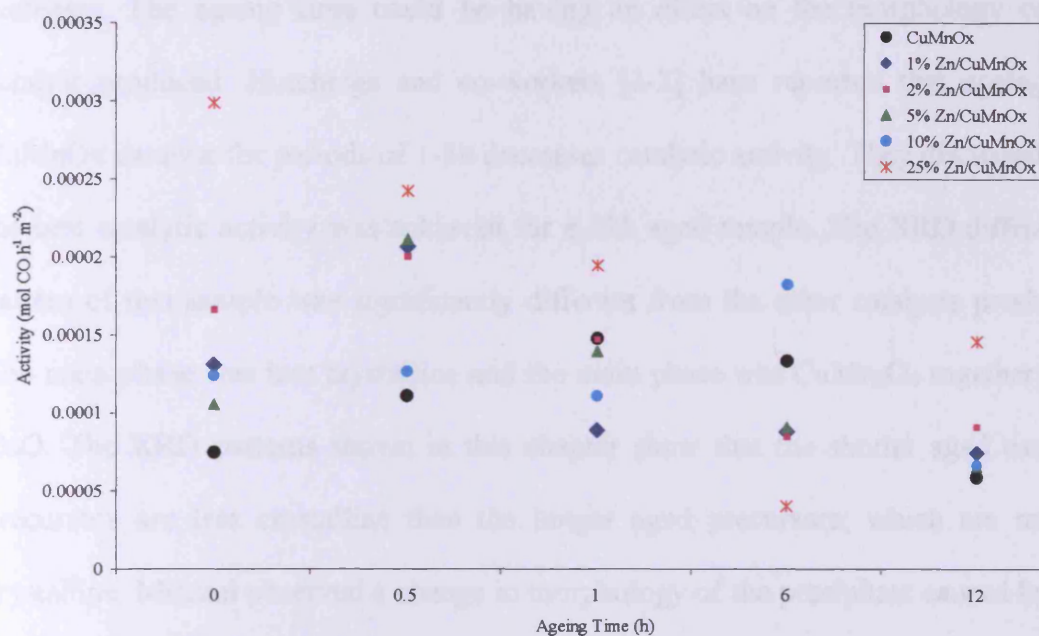

Figure 3.20 Surface Area normalized activity of CO conversion after 2h on line as a function of ageing time and % zinc dopant

Similar results are shown here in that the 25% Zn doped catalyst aged for 0h has the highest rate of CO conversion over the other catalysts shown (ca. 3×10^{-3} h^{-1} m^{-2}). This conversion decreases as the ageing time increases. The ageing times of 0 to 0.5h produce Zn doped catalysts that show increased conversion of CO compared to the undoped catalyst. Generally, increasing the ageing times of the catalyst precipitate showed that the catalytic activity of the doped catalysts decreased.

The morphology of the 12h aged catalysts was slightly less crystalline than the 6h aged catalysts. The presence of crystalline phases could be due to the extended ageing time for up to 6h. Increasing the ageing time to 12h, could lead to crystalline phases re-dissolving in the precipitate medium leading to poorly defined crystallites. The activity of the 25% Zn doped catalyst significantly decreased as the ageing time increases. The ageing time could be having an effect on the morphology of the catalyst produced. Hutchings and co-workers [1-2] have reported that ageing the CuMnOx catalyst for periods of 1-5h decreases catalytic activity. They discussed that the best catalytic activity was achieved for a 12h aged sample. The XRD diffraction pattern of this sample was significantly different from the other catalysts produced. The main phase was less crystalline and the main phase was $CuMn_2O_4$ together with CuO. The XRD patterns shown in this chapter show that the shorter aged catalyst precursors are less crystalline than the longer aged precursors; which are micro-crystalline. Mirzaei observed a change in morphology of the precipitate caused by the agglomeration of particles during the ageing process [16]. The effect on morphology of the catalyst could be determined by Scanning Electron Microscopy (SEM).

The crystallinity of the samples prepared has an affect on catalytic activity. The shorter aged samples are highly amorphous whereas the longer aged samples are

micro-crystalline. The catalytic activities for the 6h aged samples, which are micro-crystalline, showed that only the 10% Zn doped catalyst had improved activity. This could be due to the morphology of the catalyst; the structure must be amorphous to incorporate the dopant metal. The XRD patterns shown in this chapter have shown that varying the amount of zinc dopant in the structure can cause diffracted peaks to shift. In most cases, there was a shift of the diffraction peaks of samples towards higher 2θ angles. Cu^{2+} and Zn^{2+} have small ionic radius than Mn^{2+} (0.73, 0.74 and 0.83Å respectively, in octahedral co-ordination) [19]. The shift in diffracted peaks could be due to the inclusion of the dopant (Zn) into the host lattice causing deformations of the respective lattice. These 'deformations' are evident in the shorter aged samples. This gives rise to the idea that the shorter ageing times are causing successful defects in the lattice which leads to increased activity towards CO oxidation. However, from these results, it is difficult to distinguish where the dopant metal may be located.

Yoon and Cocke [20] have discussed that there are larger amount of catalytic sites found on amorphous materials than on crystalline materials particularly when sites involve defect structures. The smaller number of catalytic sites on crystalline materials has two effects. The catalytic activity decreases on crystallization and the catalyst becomes more susceptible to poisoning [21]. Based on magnetic susceptibility data, X-ray diffraction, FT-IR spectra and catalyst tests, Spassova and co-workers [22] reported that an interaction between CuO and MnOx with formation of highly disordered mixed oxide of spinel like structure was the cause of high catalytic activity of CuO-MnOx samples.

The amount of zinc added to the CuMnOx catalyst and its affect on the total amount of hydrogen consumed, during TPR analysis, is shown in Figure 3.21. The TPR data shows that, for the shorter aged catalysts, the addition of zinc has generally increased H_2 consumption. The presence of zinc as a dopant has increased the number of oxide species present. The 12h aged catalysts show similar results in that the undoped catalyst has the lowest overall amount of H_2 consumption. The 6h aged catalyst shows a difference in the trend, the undoped CuMnOx catalyst has the second highest consumption of hydrogen (ca. 12,000 µmol/g). The TPR data shows that the ageing time does not influence the amount of oxide species present within the prepared catalysts. However, the addition of zinc to the CuMnOx catalyst increases reducibility.
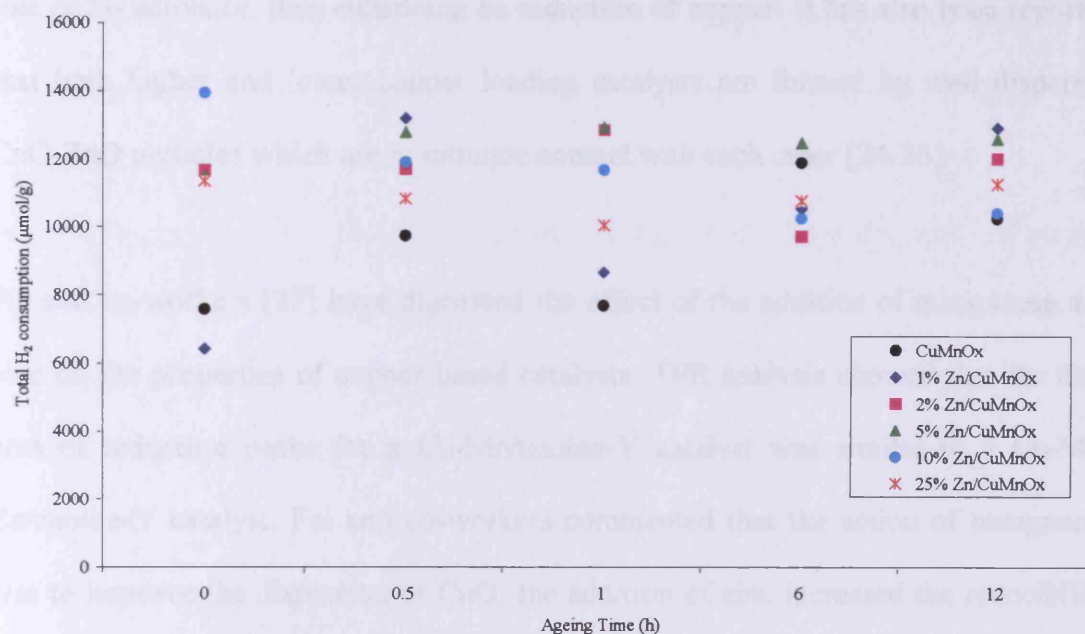

Figure 3.21 TPR data – H_2 consumption (µmol/g) of CuMnOx and Zn doped catalysts at varying ageing times

The 0h, 0.5h, 1h and 12h aged catalysts have less crystalline structures compared to the 6h aged catalysts. The TPR profiles showed a general decrease in reduction temperatures of the most readily reduced peaks with the addition of zinc as a dopant. The reduction profiles for the 0h, 0.5h, 1h and 12h show that the peaks associated with reduction of copper species, are lowered in temperature more than the manganese reduction peak. This suggests that the addition of zinc has a greater influence on the redox properties of copper species.

Fierro and co-workers [23] have reported the effect of ZnO promoting the reducibility of copper. They discovered that the activation energy for the reduction of pure CuO was higher than that found for the reduction of a CuO-ZnO catalyst. Fierro and co-workers discussed that ZnO, besides being a dispersive agent, was likely to play the role of H_2 activator, thus enhancing he reduction of copper. It has also been reported that both higher and lower copper loading catalysts are formed by well dispersed CuO-ZnO particles which are in intimate contact with each other [24-26].

Fei and co-workers [27] have discussed the effect of the addition of manganese and zinc on the properties of copper based catalysts. TPR analysis showed that the total area of reduction peaks for a Cu-Mn/zeolite-Y catalyst was similar to a Cu-Mn-Zn/zeolite-Y catalyst. Fei and co-workers commented that the action of manganese was to improve the dispersion of CuO; the addition of zinc increased the reducibility and dispersion of CuO. They also postulated that the co-addition of manganese and zinc not only promoted CuO toward good dispersion, but also increased the reducibility of CuO, via the synergistic effects of the metallic components. They concluded that a Cu-Mn-Zn/zeolite-Y catalyst promoted a high conversion of CO (ca. 53 mol %).

Further work by Fierro and co-workers [5], they reported that copper strongly enhances the reproducibility of Cu/ZnMnOx spinels with respect to pure $ZnMn_2O_4$. In another publication by Fierro and co-workers [28] they investigate the effect of Cu, Co, Fe metal ions on the redox properties of zinc manganite spinels. They reported that the spinel reducibility is affected by doping with transition metal which, depending on their nature, plays a different role. The reduction was inhibited by iron in some extent, almost unchanged by cobalt and markedly enhanced by copper.

The addition of zinc as a dopant to the CuMnOx has, for the shorter ageing times, has reduced the rate of deactivation compared to the undoped catalyst. The relative stable activity with time on line of the zinc doped catalysts dispels the perceived standard decrease of activity with time, which has been observed with many Hopcalite catalysts [29]. It has generally been accepted that copper has a promoting effect on the reduction of manganese ions in the spinel catalyst. The presence of zinc in the CuMnOx catalyst, could be promoting the copper species reducibility. There could a possible synergy effect that that manganese improves the dispersion of copper species, whilst the addition of zinc improves the reducibility of the copper. This is not a defining explanation, due to the number of possible oxide species present, but does indicate the possibilities of introducing dopants to improve catalytic activity.

The internal redox equilibrium $Cu^{2+} + Mn^{3+} \leftrightarrow Cu^{1+} + Mn^{4+}$, existing in the $CuMn_2O_4$ spinel [21] could be operative also in the zinc doped catalysts and play a role in enhancing its catalytic activity.

3.8 Conclusions

The zinc doping experiments have shown that the catalytic activity of the CuMnOx Hopcalite catalyst can be improved by the addition of a metal dopant. It is shown that the ageing time is important in controlling the catalytic activity. Also, the amount of dopant added at a particular ageing time controls activity. The most active catalyst was a 25% Zn doped CuMnOx aged for 0h. Correcting the catalyst activity for the effect of surface area demonstrated that doped catalysts aged $\leq$ 1h had the greatest oxidation rates compared to undoped catalysts. The powder X-ray diffraction showed little difference in morphologies of the shorter aged catalysts. Increased ageing time did produce increase crystallinity which caused a decrease in activity.

The role of the zinc in the Hopcalite catalyst has not been clearly defined; it is possible to draw some possible conclusions. The increased reducibility of the catalyst with zinc present shows an indication that the dopant present is playing part during the oxidation process.

3.9   Chapter 3 References

[1]   G.J. Hutchings, A.A. Mirzaei, R.W. Joyner, M.R.H. Siddiqui, S.H. Taylor, Catal. Lett. 42 (1996) 21.

[2]   G. J. Hutchings, A.A. Mirzaei, R. W. Joyner, S H. Taylor, Appl. Catal. A: Gen. 166 (1998) 143.

[3]   C.D. Jones, PhD Thesis, The Ambient Temperature of Carbon Monoxide by Copper Manganese oxide based Catalysts, Cardiff University (2005).

[4]   J.D. Hem, C.E. Roberson, C. J. Lind, Geochima et Cosmochimica Acta Vol. 51, pp. 1539-1547.

[5]   G. Fierro, S. Morpurgo, M. Lo Jacono, M. Inversi, I. Pettit, Appl. Catal A. Gen 166 (1998) 407.

[6]   K. Kier, Adv. Catal. 31 (1982) 243.

[7]   G.C. Chinchen, P.J. Denny, J.R. Jennings, M.S. Spencer, K.C. Waugh, Appl. Catal. A 36 (1998) 1.

[8]   C. Rhodes, G.J. Hutchings, A.M. Ward, Catal. Today 23 (1995) 43.

[9]   D. Waller, D. Stirling, F.S. Stone, M.S. Spencer, Faraday Discuss. Chem. Soc. 87 (1987) 107.

[10]   S. H. Taylor, G.J. Hutchings, A.A. Mirzaei, Catal. Today, 84 (2003) 113.

[11]   R.W. Joyner, F. King, M.A. Thomas, G. Roberts, Catal. Today 10 (1991) 417.

[12]   S.Fujita, A.M. Satriyo, G.C. Shen, N. Takezawa, Catal. Lett. 34 (1995) 85.

[13]   G. Fierro, M. Lojacono, M. Inversi, G. Moretti, P. Porta, P. Lavecchia, Proceedings of the 10th International Congress on Catalysis, Budapest, 1992.

[14]   H.R Oswald., W. Feitknect, M.J Wampetich., *Nature* (London) 207 (1965) 72.

[15]   L.R. Leith and M.G. Howden, Appl. Catal. 37 (1988) 75.

[16]   A.A. Mirzaei, PhD Thesis, Low Temperature Carbon Monoxide Oxidation

Catalysis, University of Liverpool (1998).

[17]   G. J. Hutchings, M.R.H. Siddiqui, A. Burrows, C.J. Kiely and R. Whyman, J.

Chem Soc. Faraday Trans. 93 (1997) 187.

[18]   M.S. Spencer, Catal. Lett. 66 (2000) 255.

[19]   R.D. Shannon, Acta Cryst., 32 (1976) 751.

[20]   C. Yoon, D.L. Cocke, J. Non-Cryst. Solids 79 (1986) 217.

[21]   S. Veprek, D.L. Cocke, S. Kehl, H.R. Oswald J. Catal. 100 (1986) 250.

[22]   I. Spassova, M. Kristova, D. Panayotov, D. Mehandjiev, J. Catal. 185 (1999)

43.

[23]   G. Fierro, M. Lo Jacono, M. Inversi, P. Porta, F. Cioci and R. Lavecchia,

Appl. Catal. A: Gen. 137 (1996) 327.

[24]   P. Porta, R. Dragone, M. Lo Jacono, G. Minelli and G. Moretti, Solid State

Ionics, 32/33 (1989) 1019.

[25]   G. Moretti, G. Fierro, M. Lo Jacono and P. Porta, Surf. Interf. Anal. 14 (1989)

325.

[26]   G. Moretti, S. De Rossi and G. Farraris, Appl. Surf. Sci. 45 (1990) 341.

[27]   J.-H Fei, M.-X Yang, Z.-Y Hou, X.-M Zheng, Energy and Fuels 18 (2004)

1584.

[28]   G. Fierro, G. Ferraris, R. Dragone, M. Lo Jacono, M. Faticanti, Catal. Today

116 (2006) 38.

[29]   J. Jansson, M. Skoglundh, E. Fridell, P. Thormahlen, Topics in Catalysis. 16-

17 (2001) 385.

Gold supported copper manganese mixed oxides

4

In this chapter, the effect of the addition of a dopant by a method different to the discussed co-precipitation method has been investigated. Hopcalite and Au-based catalysts play an important role in ambient temperature CO oxidation. There have been very little studies investigating the addition of Au to Hopcalite catalysts. Only recently has Au doped Hopcalite for low temperature CO oxidation been reported [1]. Au doped catalysts were prepared by a co-precipitation method. Haurta and co-workers have reported that Au, dispersed on a variety of metal oxides, is highly active at sub-ambient temperatures for the oxidation of CO [2].

Platinum and Palladium are known as oxidation catalysts and have been incorporated into three way car exhaust catalysts. However, the economics of Pt/Pd is considerably more expensive than Au. Gold has shown to be a metal capable of excellent catalytic activity when present as nano-crystals on a support [2-3].

The purpose of this chapter was to apply a method of depositing gold particles onto a support – in this case, the Hopcalite catalyst would act as a support. This method of preparation used for Au particles supported on a Hopcalite based catalyst has yet to be reported.

4.1 Gold supported Hopcalite catalyst

The Hopcalite catalyst was first produced by a co-precipitation method, with ageing times ranging from 0h to 6h. Gold was added to the Hopcalite catalyst by a deposition-precipitation method. The preparation method is outlined in Chapter 2.

The difference of this procedure to the reported co-precipitation method was that a lower amount of gold was used. The co-precipitation method for Au supported CuMnOx catalysts used Au loadings ranging from 1 to 6 wt % [1]. The deposition precipitation method investigated here used Au loadings of 0.5, 1 and 2wt% respectively. A CuMnOx catalyst was also subjected to the same preparation conditions as deposition precipitation but without the addition of Au.

4.1.1 Au supported Hopcalite catalyst with ageing time of 0h

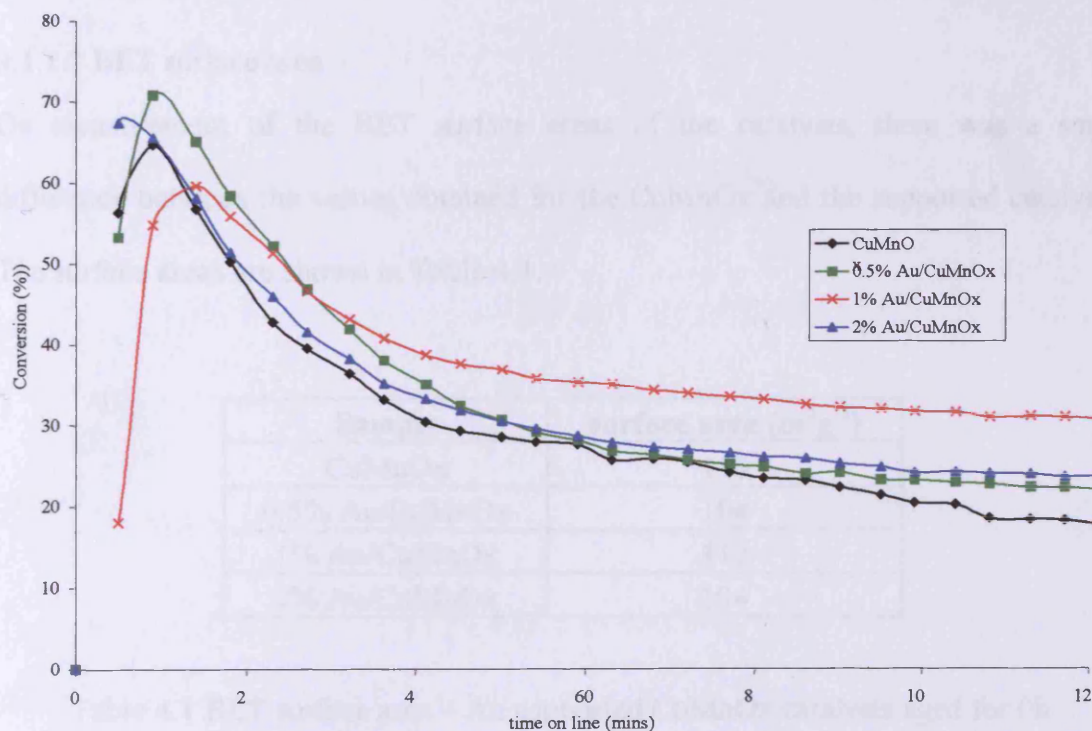#### 4.1.1.1 Catalyst Activity

Figure 4.1 CO oxidation – Au supported CuMnOx catalysts aged for 0h

The activities, shown in Figure 4.1, demonstrate similar trends in terms of high initial activity resulting in gradual deactivation as time on line increases. The data presented in Figure 4.1 shows the result of catalysts prepared three times and tested three times. The data presented falls within a 2-3% error range.

The initial activities range from 60 to 70% with the 0.5% Au/CuMnOx displaying the highest activity. As the catalysts show steady state activities, the 1% supported catalyst exhibits the highest activity at ca. 35% conversion. It can be observed that the activities of the unsupported CuMnOx, 0.5% Au and 2% Au catalysts are clustered together. The 1% Au catalyst shows an improvement of ca. 10% conversion compared to the Hopcalite catalyst. The addition of Au has shown to promote CO conversion relative to the CuMnOx catalyst. Also, the steady state activities (Figure 4.1) show that no further deactivation occurred.

4.1.1.2 BET surface area

On measurement of the BET surface areas of the catalysts, there was a small difference between the values obtained for the CuMnOx and the supported catalysts. The surface areas are shown in Table 4.1.

Sample	surface area (m^2g^{-1})
CuMnOx	110
0.5% Au/CuMnOx	104
1% Au/CuMnOx	112
2% Au/CuMnOx	104

Table 4.1 BET surface area – Au supported CuMnOx catalysts aged for 0h

The activities were adjusted to account for surface area differences between catalysts.

The activities normalised for surface area, shown in Figure 4.2, show little deviation from the original activity data in Figure 4.1. There is very little relationship between catalytic activity and surface area. However, the 1% Au supported catalyst has the highest overall activity and produces the highest surface area. The 1% Au supported catalyst has the lowest initial activity of all the catalyst aged for 0h.
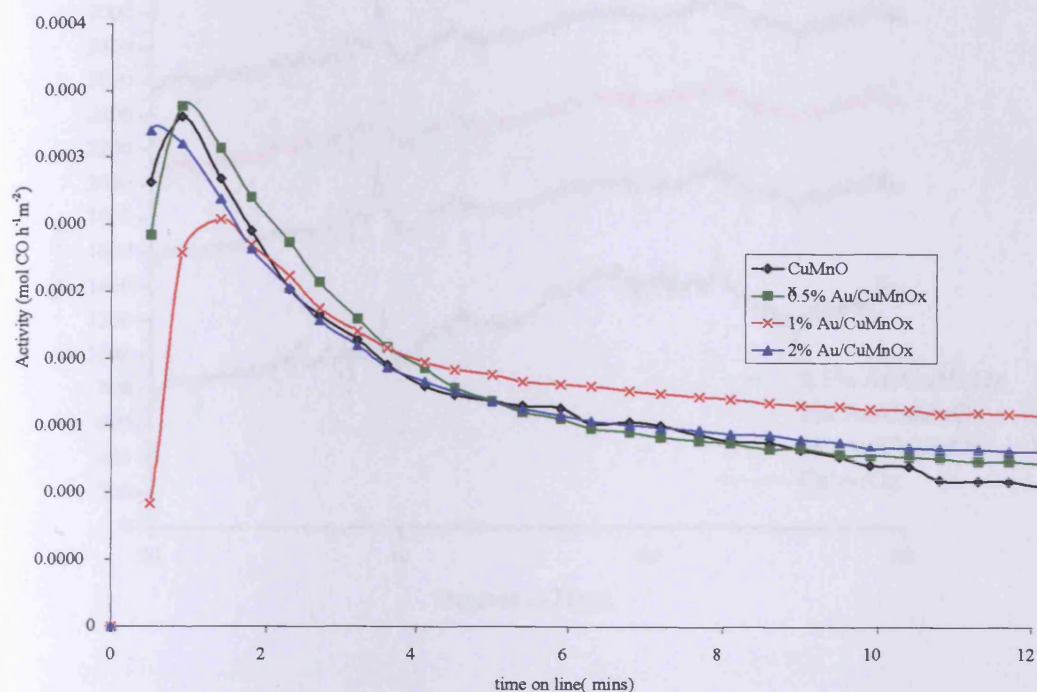
Figure 4.2 Surface area normalised activity – Au supported CuMnOx catalysts aged for 0h.

4.1.1.3 Powder X-ray diffraction

The powder XRD patterns of the CuMnOx and Au supported CuMnOx samples aged for 0h are shown in Figure 4.3. It was not possible to differentiate between the four samples. The calcined catalysts are highly amorphous and no crystalline phase could be clearly identified. However, the XRD patterns of the uncalcined material (not shown) confirmed the presence of CuO and $MnCO_3$ phases. However it is not possible

to propose that copper and manganese components of the catalyst were present in separate species as opposed to a mixed oxide. It cannot be clearly defined whether metallic Au is present, a peak at 2θ ca. $38.5°$ is detected but very broad and of low intensity. Several catalysts with gold present show this characteristic reflection corresponding to metallic Au [4].
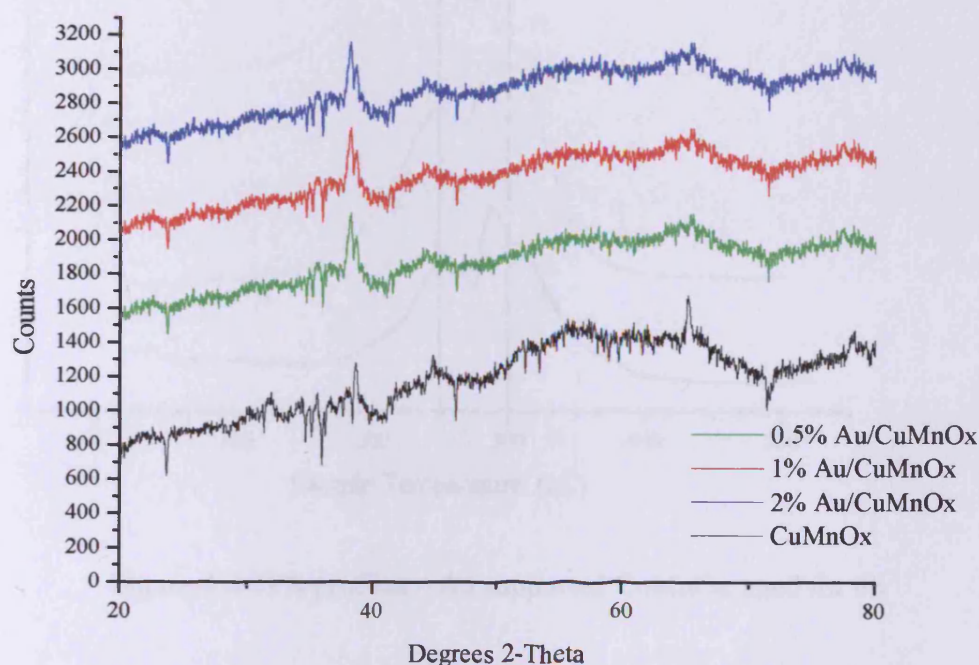
Figure 4.3 Powder XRD – Au supported CuMnOx catalysts aged for 0h

It may be considered that only very small Au particles (2-5nm) may be present in these catalysts, which is close to the detection limit for XRD. The phases present in the catalyst are related to the ageing time of the catalyst precursor [5]. CuMnOx are highly active in the amorphous state. Alternative characterisation techniques are used to differentiate between samples with different ageing times and different amounts of Au added. This would be beneficial to identify if gold particles are present.

4.1.1.4 Temperature Programmed Reduction
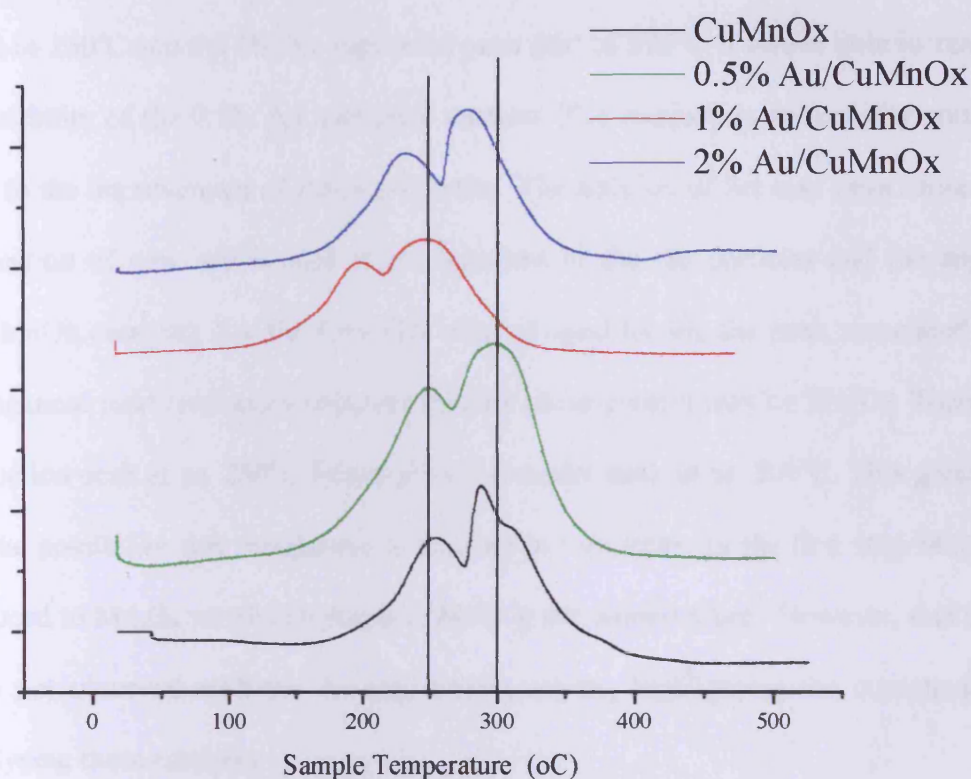
Figure 4.4 TPR profiles – Au supported CuMnOx aged for 0h

The TPR profile of mixed compounds can be difficult to interpret, due to the large number of possible combinations of different oxidation states of copper and manganese and the range of mixed phases that can be present. The TPR patterns show two peaks for reduction taking place indicating two possible phases that may be present, CuO and Mn_2O_3, though it is hard to define a clear boundary between the two regions. The lower temperature peaks are more likely to correspond to the reduction of Cu^{2+} as copper is reported to have a higher reducibility than manganese in mixed compounds [6]. The TPR profiles of the Au supported CuMnOx catalysts aged for 0h (Figure 4.4) show the effect of adding gold as a dopant to the reducibility of a catalyst. The higher temperature peak associated with the reduction of manganese

oxides centres at 300°C for the CuMnOx catalyst. The reduction peaks of the 1% Au and 2% Au supported catalysts move to lower temperatures, 1% Au supported peak shift to 250°C and the 2% Au supported peak shift to 275°C. There is little increase in reducibility of the 0.5% Au supported catalyst. The increase in reducibility could be due to the improvement of redox properties. The addition of Au may have caused the formation of new active sites at the interface of the Au particles and the support (CuMnOx catalyst). For the CuMnOx catalyst aged for 0h, the peak associated with manganese oxide reduction indicates that the phase present may be Mn_2O_3. There is a reduction peak at ca. 280°C followed by a shoulder peak at ca. 300°C. This gives rise to the possibility that manganese is reduced in two steps. In the first step Mn_2O_3 is reduced to Mn_3O_4 which is reduced to MnO in the second stage. However, this effect was not observed with the Au supported catalysts, highlighting the complexity of analysing these catalysts.

4.1.1.5 Scanning Electron Microscopy image

The SEM image shown in Figure 4.5 displays the microstructure of the CuMnOx catalyst aged for 0h. The powder particles exhibit a spherical morphology. The particles are randomly dispersed and range from 2.6 μm to 5.6 μm size. The spheres consist of agglomerates composed of copper and manganese phases. The shape of the particles makes the occurrence of thermodynamically unrelaxed crystallographic orientations possible, so that very reactive sites towards CO and O_2 are formed [7].
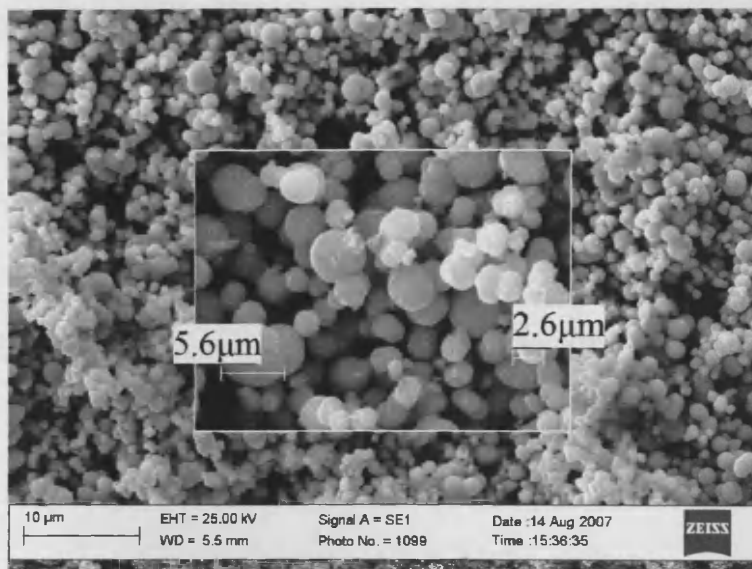
Figure 4.5 SEM image of CuMnOx catalyst aged for 0h
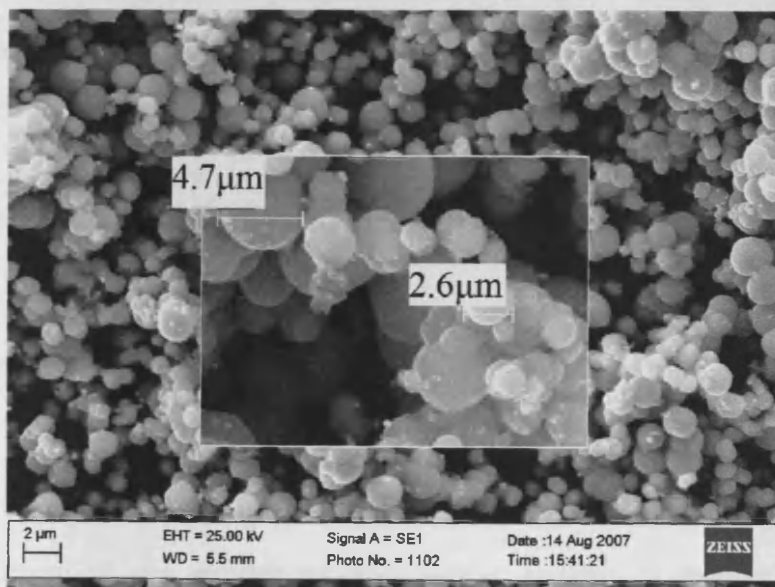
Figure 4.6 SEM image of 1% Au supported CuMnOx catalyst aged for 0h

Figure 4.6 shows the SEM image of the 1% Au supported CuMnOx catalyst aged for

0h. The morphology of the gold supported catalyst is similar to the morphology of the

CuMnOx catalyst. Particle sizes range from 2 μm to 4.7 μm. The treatment of the

catalyst through the deposition precipitation method has not altered particle size or caused further agglomeration.

4.1.1.6 Energy Dispersive X-ray Spectroscopy

The EDX a spectrum shown in Figure 4.7 confirms that only present are copper and manganese and oxygen, with carbon as a ubiquitous impurity. Sodium peaks were not detected. Catalytic activity is heavily dependant upon the surface concentration of sodium that remains as a residue on the copper manganese oxide following the precipitation procedure [8].
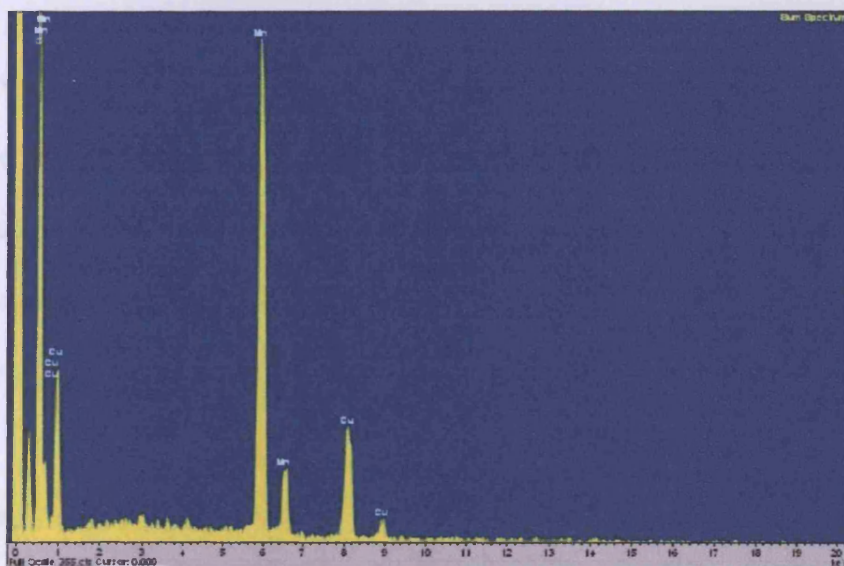
Figure 4.7– EDX spectra of CuMnOx catalyst aged for 0h

The composition of the manganese and copper present in sample is 1 to 1.9 respectively. The starting ratio for the catalyst precursor is 1:2 Cu:Mn. This type of characterisation is used to clarify whether that Au particles have been deposited onto the surface of the catalyst and the addition of a dopant is related to the increase in activity.
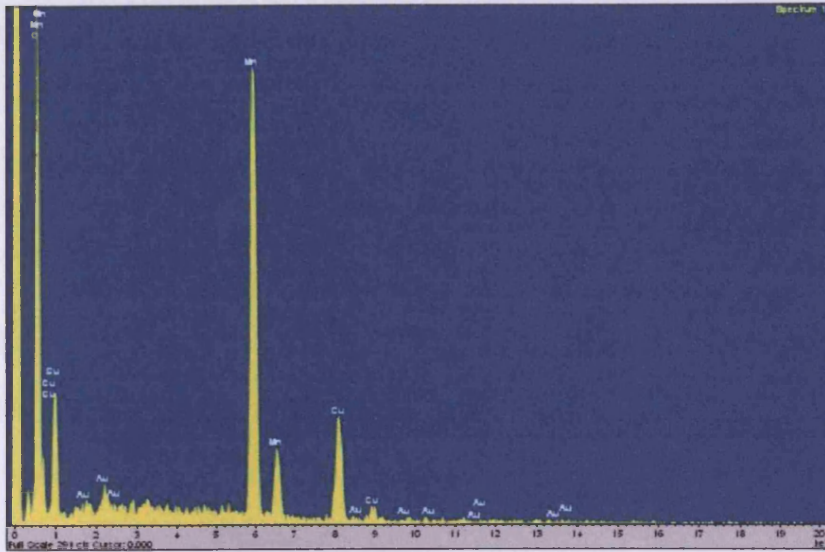
Figure 4.8 EDX spectra of 1% Au supported CuMnOx catalyst aged for 0h

The EDX spectra, shown in Figure 4.8, confirms that Au particles are present in the Hopcalite catalyst. The ratio of elements present is shown in Table 4.2. The results show that Au is present as 1.5 wt% compared to the calculated value of 1 wt% during the preparation procedure. The improvement of activity of the CuMnOx catalyst for CO oxidation can be related to the presence of Au particles on the catalyst.

CuMnOx 0h aged		Element	O	Mn	Cu	Au
		Weight (%)	29	46.3	24.68	0
1% Au supported CuMnOx 0h aged		Element	O	Mn	Cu	Au
		Weight (%)	29	46.2	23.28	1.5

Table 4.2 Percentage weight – CuMnOx aged for 0h

1% Au supported CuMnOx catalyst aged for 0h

4.1.2 Au supported Hopcalite catalyst with ageing time of 0.5h

A series of CuMnOx and Au supported CuMnOx catalysts aged for 0.5h were prepared. The Au supported catalysts were prepared by a deposition precipitation method.

4.1.2.1 Catalyst Activity

The CuMnOx and Au supported CuMnOx catalysts aged for 0.5h were tested for CO oxidation activity as shown in Figure 4.9.
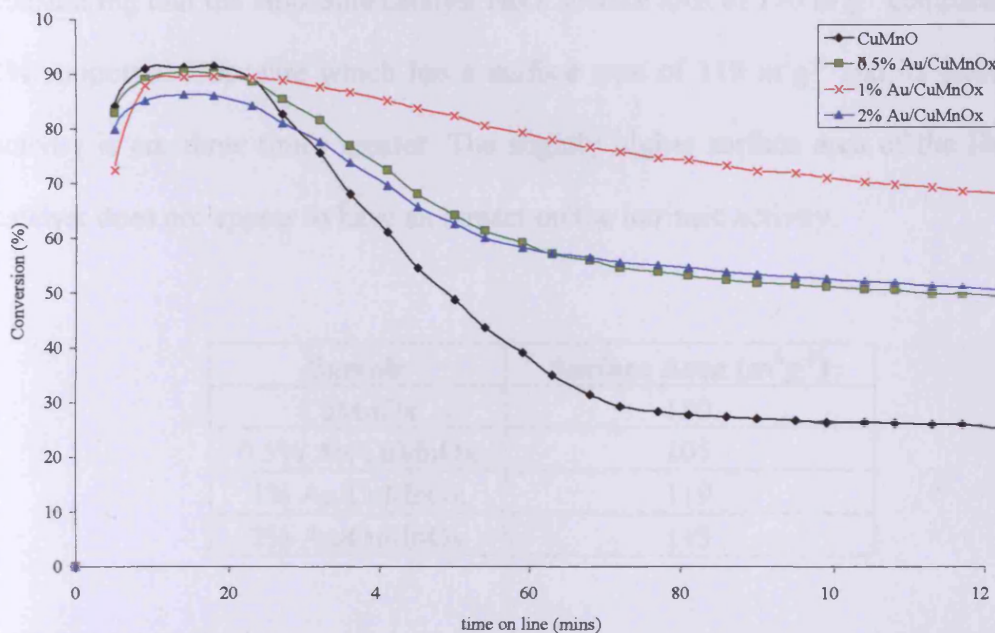
Figure 4.9 CO oxidation – Au supported CuMnOx catalysts aged for 0.5h

The catalysts aged for 0.5h show a similar trend with the 0h aged, in that the 1% Au has the highest steady state activity and CuMnO$_x$ has the lowest. The 1% Au deposited catalyst shows significant improvement, almost three times the activity after 120mins of time on line. The CuMnOx and Au supported Hopcalite catalysts all exhibit similar initial activities (*ca.* 90% conversion). The Au supported catalysts experience less deactivation compared to the CuMnOx catalyst. The 0.5% and 2% Au catalysts show similar trends. The addition of Au to the CuMnOx catalyst has

improved activity. Also, the activities of the 0.5h aged catalysts are higher than that of the 0h aged catalyst. This could be due to the ageing time used for the catalyst precursor, varying the precipitate ageing time dramatically affects catalytic activity [9].

4.1.2.2 BET surface area

The BET surface areas shown in Table 4.4 show that the catalysts aged for 0.5h are relatively similar. There is no real relationship between activity and surface area, considering that the Hopcalite catalyst has a surface area of 130 m^2g^{-1} compared to the 1% supported Hopcalite which has a surface area of 119 m^2g^{-1} and its steady state activity is *ca.* three times greater. The slightly higher surface area of the Hopcalite catalyst does not appear to have an impact on the intrinsic activity.

Sample	Surface Area (m^2g^{-1})
CuMnOx	130
0.5% Au/CuMnOx	105
1% Au/CuMnOx	119
2% Au/CuMnOx	115

Table 4.4 BET surface area – Au supported Hopcalite catalyst aged for 0.5h aged

The catalytic activities were adjusted to take in account surface area affects. The adjusted activities were calculated and are shown in Figure 4.10.

Normalising the activities to take into account surface area, show that the catalytic performance shows a similar profile to Figure 4.9. The only difference is the initial conversion, the 1% Au and 2% Au catalyst show similar activities ca 4 x 10^{-4} mol CO_2

h^{-1} m^2 whereas the 0.5% Au supported catalyst displays an activity of 5 x 10^{-4} mol CO_2 h^{-1} m^2.
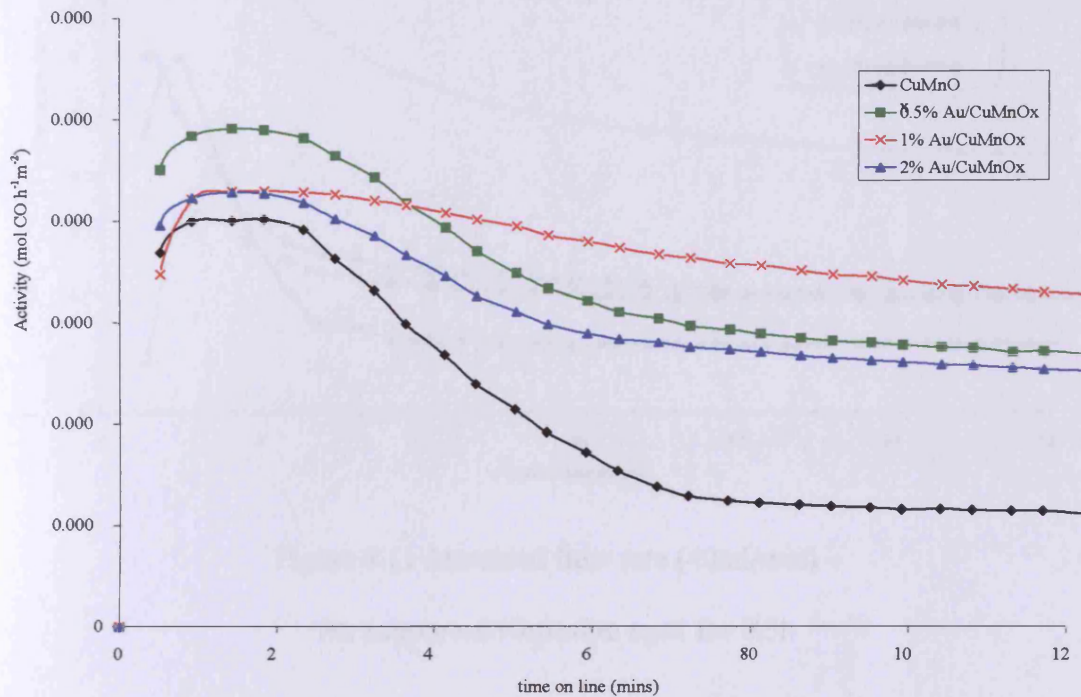
Figure 4.10 Surface area normalised activity –

Au supported CuMnOx catalysts 0.5h aged

4.1.2.3 Increased Flow Rate

The initial activities of the CuMnOx and Au supported catalysts, shown in Figure 4.9, are very similar. It was investigated if this was the actual activity of the gas phase reactants with the catalyst bed. An experiment was performed to analyse if whether this was the case. The flow rate of the CO oxidation reactor was doubled to 40 ml/min; this would decrease the contact time of the reactant gas with the catalyst bed. The resulting activity is shown in Figure 4.11.
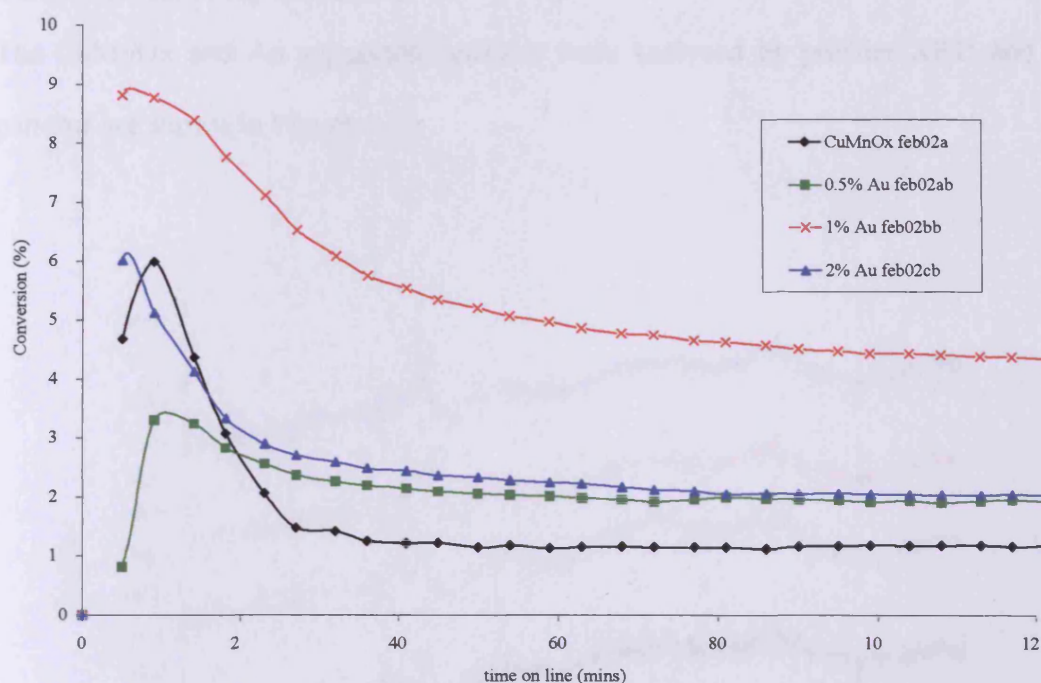
Figure 4.11 Increased flow rate (40ml/min) –

Au supported Hopcalite aged for 0.5h

The decrease in contact time of the gas with the catalyst has shown clear differences in the light off activity. The profiles of the activities are similar to the standard flow rate of 21.3ml/min CO conversions. They show the same order of activity with the amount of Au added. It is interesting to see that the light off conversion of the 0.5% supported catalyst (ca. 30%) is half that of the CuMnOx catalyst. As time on line increases, the activity of the catalysts follow similar trends, the 0.5% and 2% Au supported catalysts have similar steady state activities.

4.1.2.4 Powder X-ray Diffraction

The CuMnOx and Au supported catalysts were analysed by powder XRD and the patterns are shown in Figure 4.12.
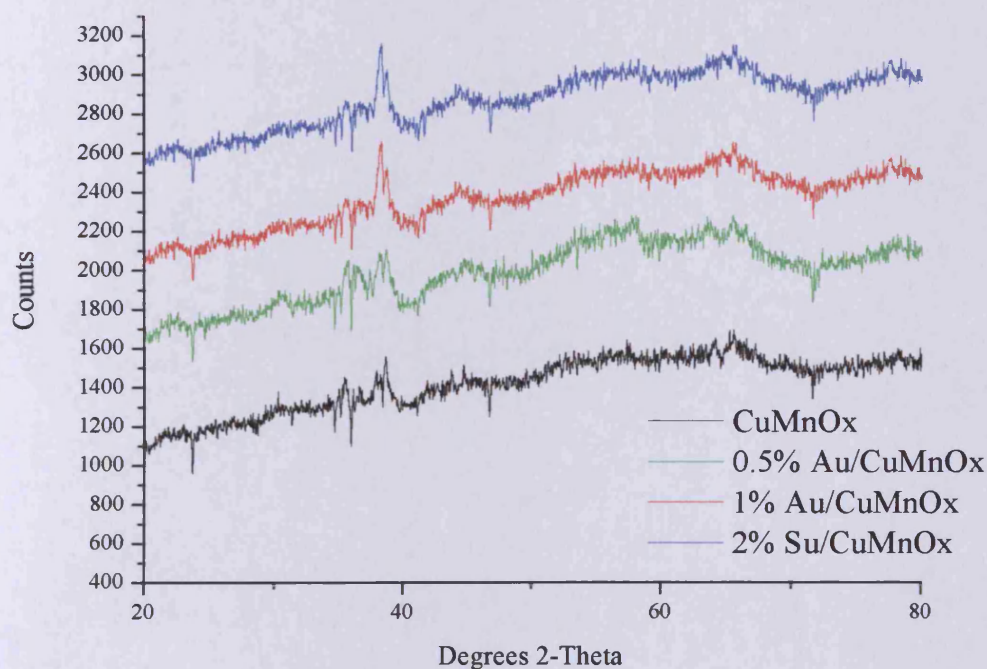
Figure 4.12 Powder XRD – Au supported CuMnOx aged for 0.5h

The XRD analysis of the catalyst showed little information of the phases present in the catalyst bulk structure due to the amorphous nature of the samples. Line spacings were broad and difficult to assign changes between catalysts. The phases that may be present in the catalyst are below the detection of the x-ray diffractometer.

4.1.2.5 Temperature Programmed Reduction
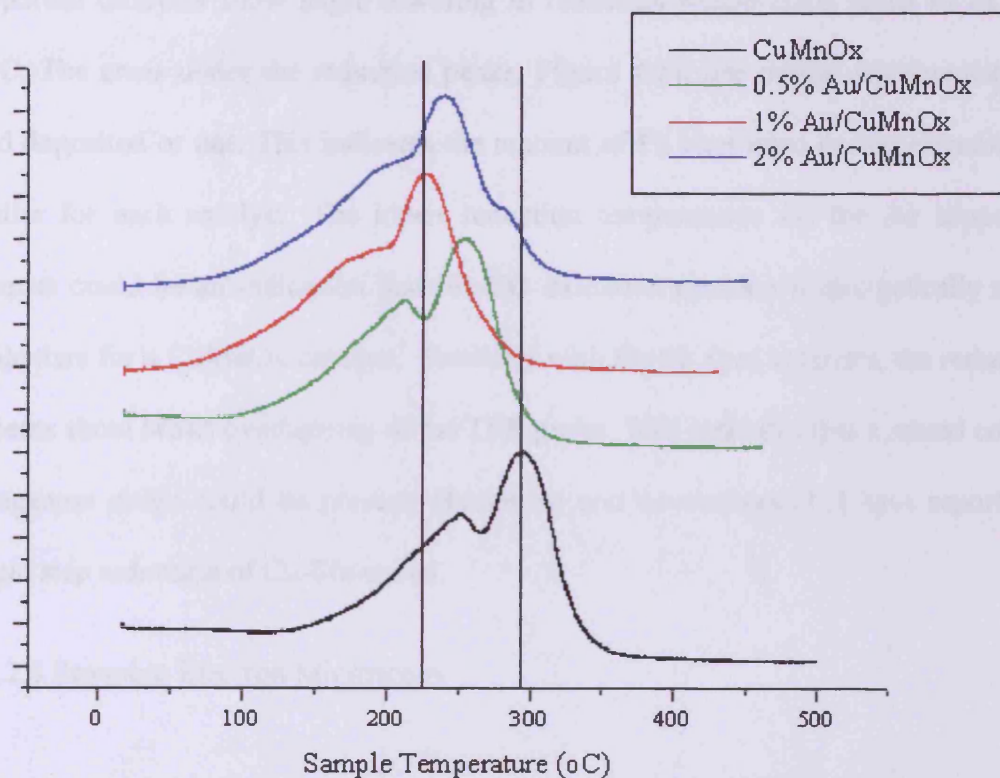
Figure 4.13 TPR profiles – Au supported CuMnOx catalysts aged for 0.5h

The TPR profile of the Au supported CuMnOx catalysts aged for 0.5h show that the addition of Au has shifted the reduction peaks to lower temperatures. The high temperature peak, attributed to a reduction of manganese, for the CuMnOx catalyst is centred at ca. $330^{\circ}C$. The peak associated with the reduction of copper is centred at ca. $250^{\circ}C$. There is the possibility that two phases are present, CuO and Mn_2O_3, since there are two reduction peaks present and not one. It is clear to see that the addition of gold has caused a shift of the reduction peaks to lower temperatures. Au was likely to be present in all the samples mainly as Au° since the calcination temperature at $400^{\circ}C$ leads to the reduction of gold [10]. The significant shift in peaks is the 1% Au supported catalyst. The higher temperature peak has shifted from $300^{\circ}C$ to $225^{\circ}C$. It can be correlated with the catalytic activity of the 1% Au supported catalyst; it has the

highest overall activity and the lowest reduction temperatures. The 0.5% and 2% Au supported catalysts show slight lowering in reduction temperature, shifts of ca. 25-30°C. The areas under the reduction peaks, Figure 4.13, are similar whether there is gold deposited or not. This indicates the amount of H_2 consumed during reduction is similar for each catalyst. The lower reduction temperatures for the Au supported samples could be an indication that the CO oxidation reaction is energetically more facile than for a CuMnOx catalyst. Similarly with the 0h aged catalysts, the reduction patterns show broad overlapping of the TPR peaks. This indicates that a mixed copper manganese oxide could be present. Buciuman and co-workers [11] have reported a single step reduction of Cu-Mn spinel.

4.1.2.6 Scanning Electron Microscopy
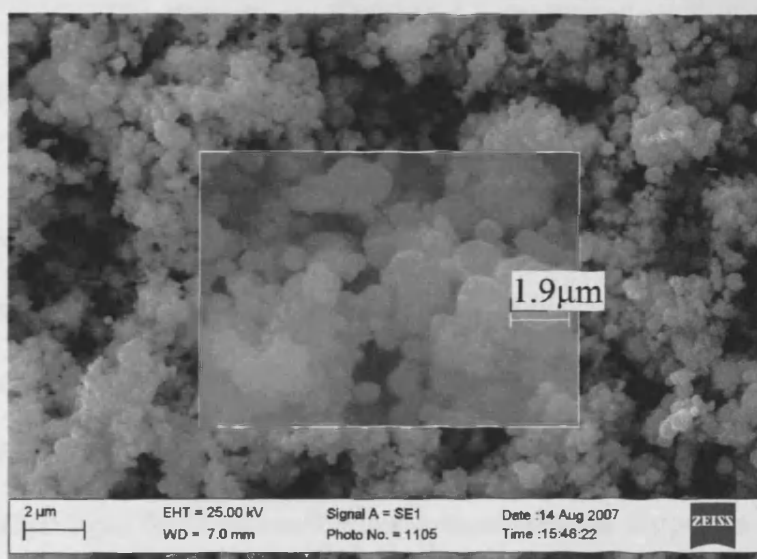
Figure 4.14 SEM image of CuMnOx catalyst aged for 0.5h

The image shown in Figure 4.14 illustrates the microstructure of the CuMnOx catalyst aged for 0.5h. The CuMnOx aged for 0h displayed powder particles with spherical morphology. The CuMnOx aged for 0.5h shows less spherical structure and are

increasingly clustered particles. The particle sizes in Figure 4.14 are *ca.* 1.9 μm, which are smaller than the CuMnOx catalyst aged for 0h. It appears that the spheres have fragmented to smaller particles. This fragmentation could attribute to increased active sites at the surface and increasing activity of the CuMnOx catalyst aged for 0.5h.
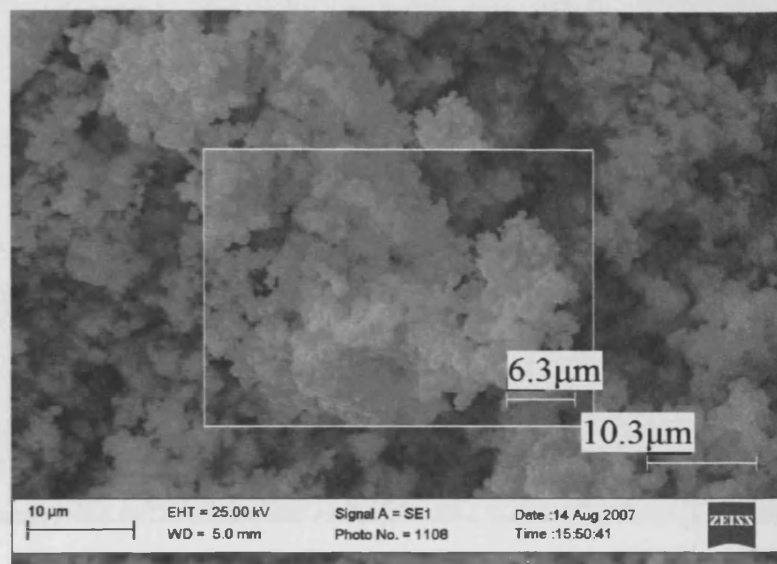
Figure 4.15 1% Au supported CuMnOx catalyst aged for 0.5h

The SEM image of the 1% Au supported CuMnOx catalyst, Figure 4.15, shows the spherical particles are smaller than the catalysts aged for 0h. The average particle size is *ca.* 1.3 μm. The morphology of the 0.5h aged catalysts could promote the interaction of deposits of Au particles and the catalyst surface. The morphology of the CuMnOx catalyst aged for 0.5h could mean a more suitable support is present with a high distribution of active sites for CO oxidation. The 1% Au dopant appears to be the optimum amount required to achieve the maximum amount of improvement in activity.

4.1.2.7 Energy Dispersive X-ray spectroscopy

The EDX spectra shown in Figure 4.16 confirms that only present are copper and manganese and oxygen, with carbon as a ubiquitous impurity.
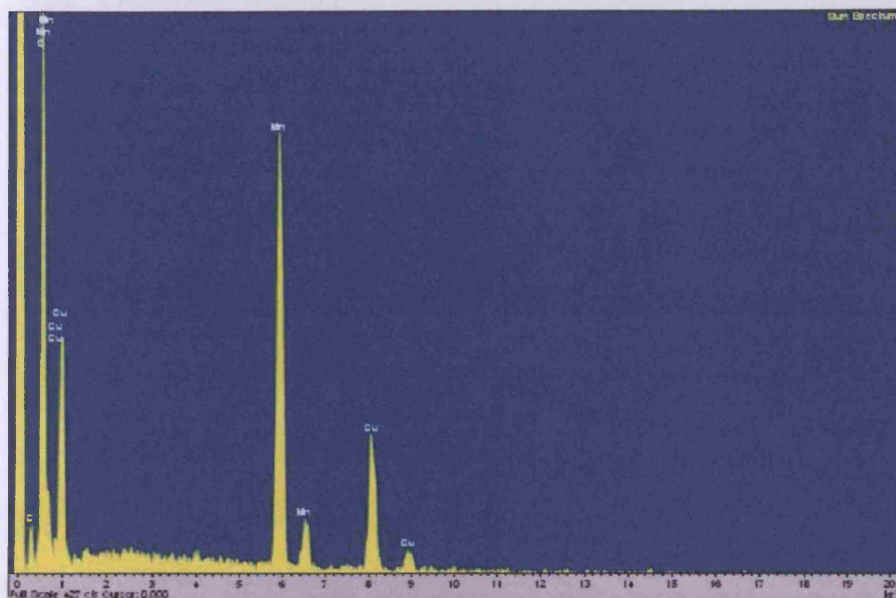
Figure 4.16 EDX spectra of CuMnOx catalyst aged for 0.5h

The ratio of manganese to copper present in the sample is ca. 1.4:1 respectively. There are no sodium peaks detected, which can poison the catalyst and affect the activity towards CO oxidation [8].

The EDX spectra shown in Figure 4.17 confirms the presence of Au particles on the surface of the Hopcalite catalyst. The ratio of elements present is shown in Table 4.6. The results show that Au is present as 1.8 wt% compared to the calculated value of 1 wt% during the preparation procedure. This is an indication that the addition of 1 wt% Au to the CuMnOx catalyst is the optimum amount of dopant required for a significant improvement in activity towards CO oxidation.
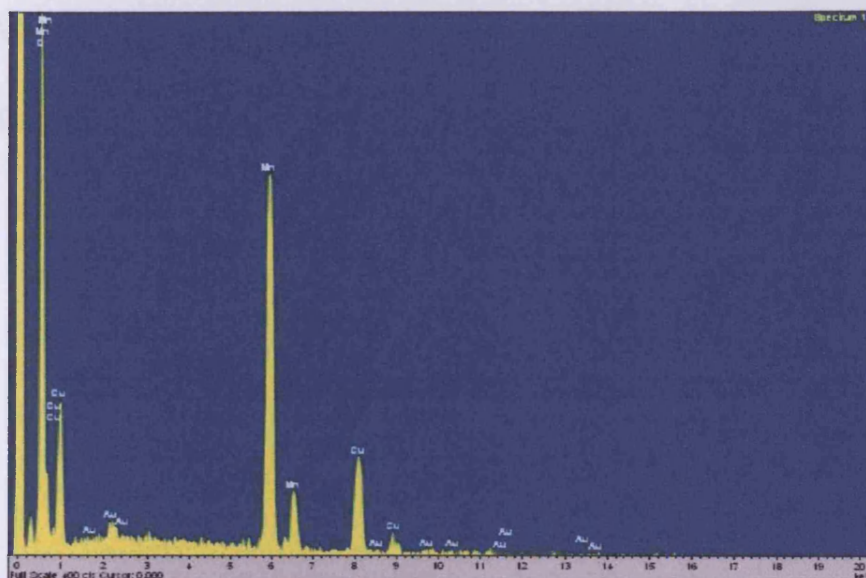
Figure 4.17 EDX spectra of 1% supported CuMnOx catalyst aged for 0.5h

The quantification of the elements present are summarised in Table 4.4. This is only an indication if the deposition precipitation has been successful and not a quantification of the ratio of copper to manganese species present.

CuMnOx 0.5h aged		Element	O	Mn	Cu	Au
		Weight (%)	30.16	40.8	29.04	0
1% Au supported CuMnOx 0.5h aged		Element	O	Mn	Cu	Au
		Weight (%)	31.46	41.93	24.80	1.8

Table 4.4 Percentage weight – CuMnOx aged for 0.5h

1% Au supported CuMnOx catalyst aged for 0.5h.

4.1.3 Au supported Hopcalite catalyst with ageing time of 1h

4.1.3.1 Catalyst Activity
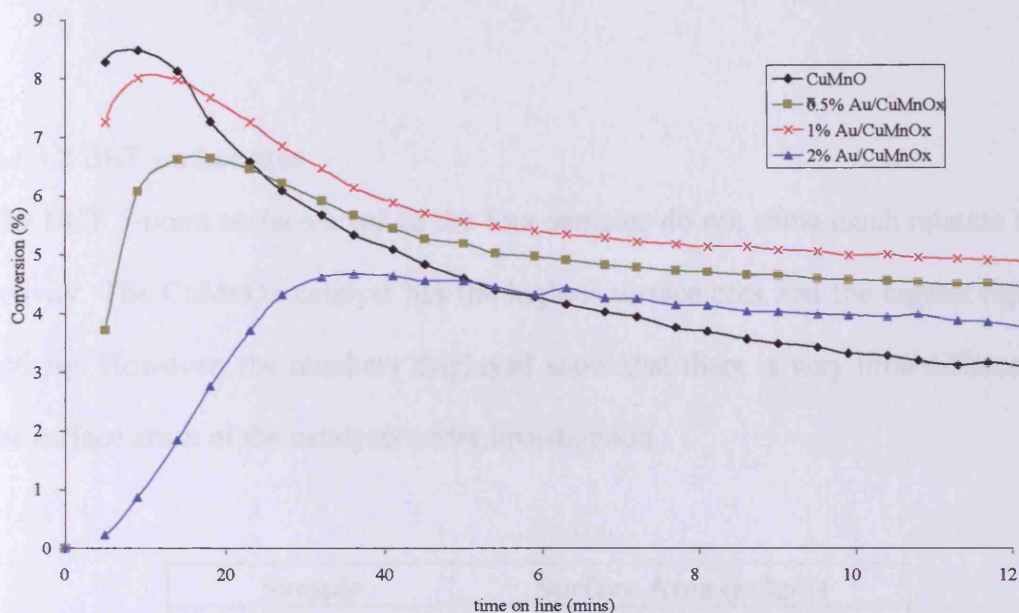
Figure 4.18 CO oxidation – Au supported Hopcalite catalyst aged for 1h

The CuMnOx catalyst displayed the highest initial actvity for the 1h aged catalysts with a maximum conversion of *ca.* 85%. The maximum activity was followed by a sharp decrease in activity compared to the supported catalysts, displaying the highest rate of deactivation after 2h time on line to *ca.* 38% conversion. The 0.5% and 1% Au supported catalysts experienced similar patterns in activity, both showing much slower rates of deactivation. The 1% Au supported catalyst having the overall highest steady state activity after 2h of time on line. A trend is shown in the ageing times shown so far, the 1% Au supported catalyst does not initially have the highest light off activity but in terms of steady state then the 1% Au supported displays the highest activity overall. The 2% Au supported catalyst does not follow the activity trends shown by the other catalysts plotted in Figure 4.18. The 2% Au supported catalyst showed a gradual increase in activity in the first 30 minutes of testing, reaching an

135

activity of *ca.* 45 % conversion. The activity remains steady as the time on line increases and remains at *ca.* 40% conversion, which is 10% more active than the CuMnOx catalyst.

4.1.3.2 BET surface area

The BET 5-point surface areas of the four samples do not show much relation to the activity. The CuMnOx catalyst has the highest surface area and the highest light off activity. However, the numbers displayed show that there is very little difference in the surface areas of the catalysts under investigation.

Sample	Surface Area (m2g-1)
CuMnOx	119
0.5% Au/CuMnOx	110
1% Au/CuMnOx	116
2% Au/CuMnOx	114

Table 4.5 BET surface area – Au supported Hopcalite catalyst aged for 1h

The activities of the catalysts aged for 1h were adjusted to incorporate the affect of surface area and shown in Figure 4.19. Observing the graph, there is only slight differences in the catalytic profiles. The CuMnOx and 1% Au supported CuMnOx have similar initial activities in the region of 4×10^{-4} mol CO_2 h^{-1} m^{-2}. The order of activities for the catalysts do not change, the 1% supported catalyst having the highest overall activity and the CuMnOx catalyst displaying the highest rate of deactivation.
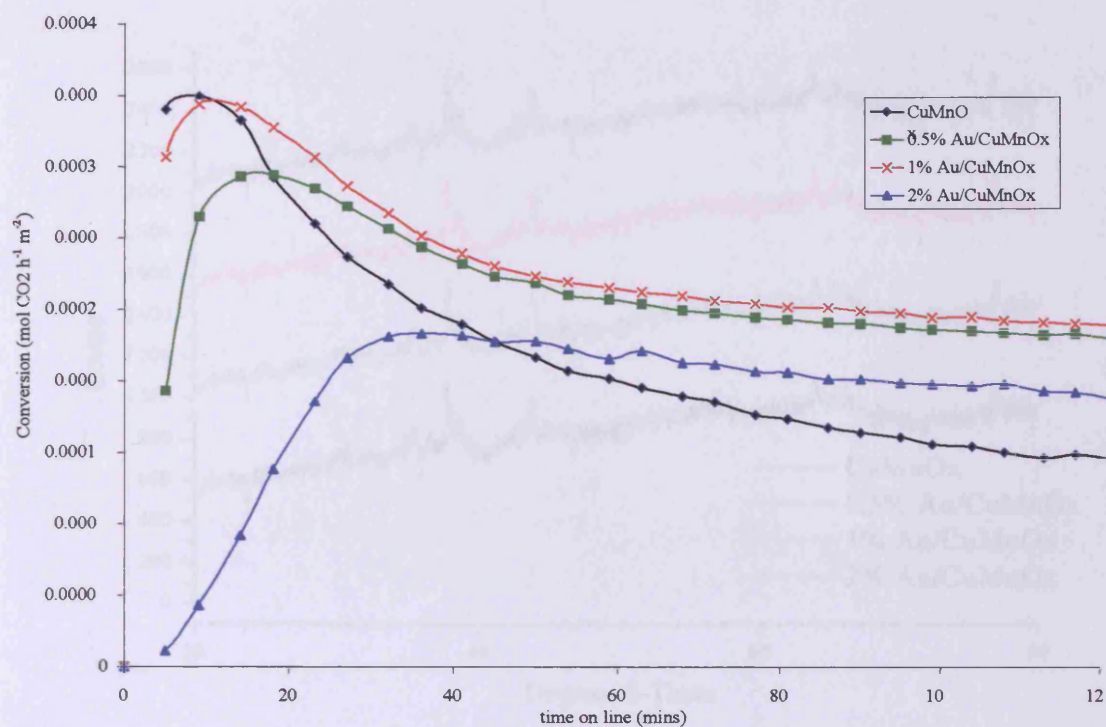
Figure 4.19 Surface area adjusted activity – Au supported CuMnOx catalysts

aged for 1h

4.1.3.3 Powder X-ray diffraction

The powder x-ray diffraction analysis was performed on the CuMnOx and Au supported CuMnOx catalysts aged for 1h.

The powder XRD patterns for the samples aged for 1h show little difference in terms phases present or whether Au metal is present. It is difficult to identify if metallic Au is present from the XRD patterns. The patterns are similar to the CuMnOx catalysts aged for 0.5h in that the material is highly amorphous. However, there is no evidence if Au particles are present.
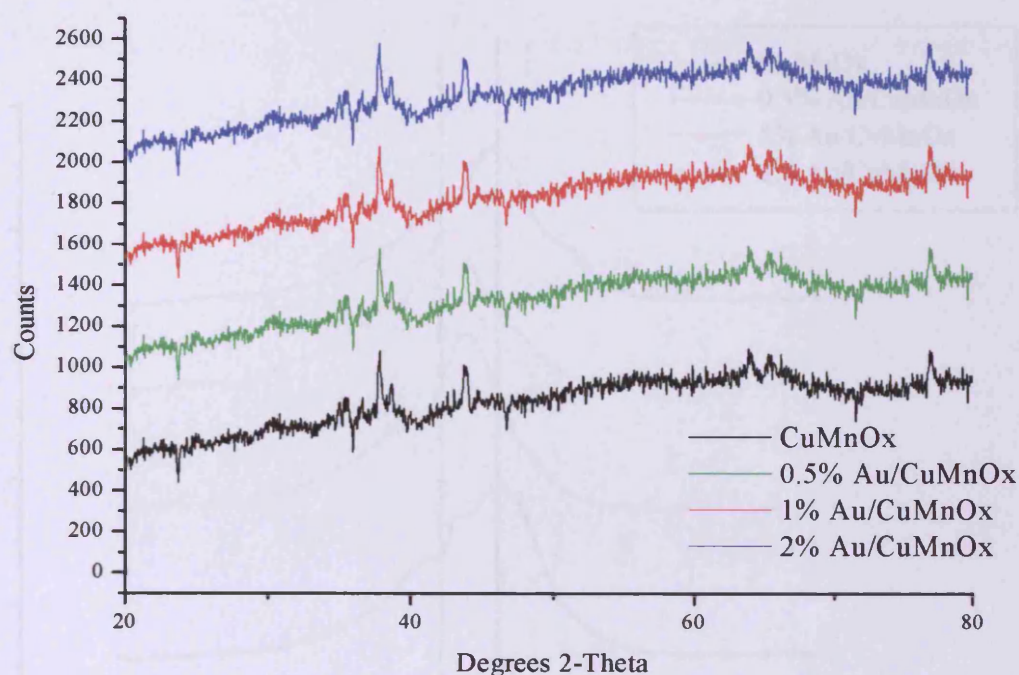
Figure 4.20 Powder XRD – Au supported CuMnOx catalysts aged for 1h

4.1.3.4 Temperature Programmed Reduction

Temperature programmed reduction analysis was performed to account for differences in reducibility of the 1h aged catalysts.

The TPR profiles (Figure 4.21) show a similar effect of the addition of Au to the CuMnOx catalyst as the 0.5h aged catalysts. The presence of Au on the CuMnOx catalyst has caused a shift of reduction peaks to lower temperatures. The 1% Au supported catalyst displays the greatest shift from the CuMnOx catalyst, 300°C → 225°C for the peak associated with the reduction of manganese oxide.
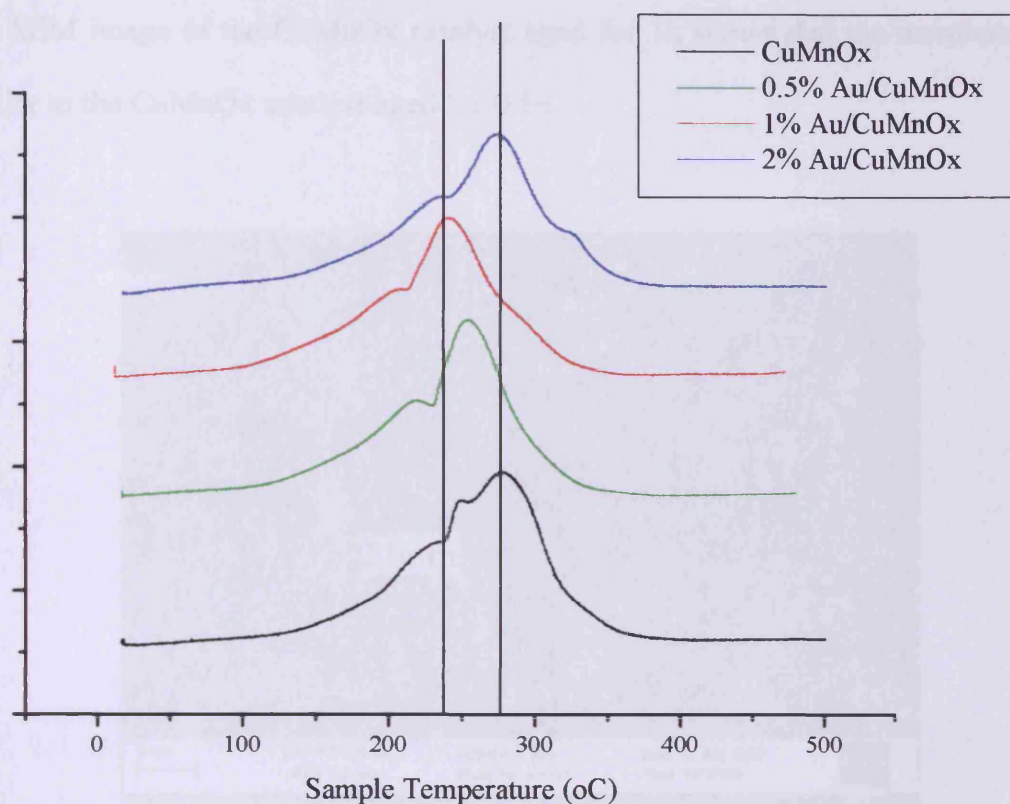
Figure 4.21 TPR profiles – Au supported CuMnOx catalysts aged for 1h

There is an association with the activity towards CO oxidation as the 1% Au supported catalyst shows the greatest improvement in catalytic activity. The 0.5% supported catalyst show increased reducibility compared to the CuMnOx. There are probably many active components comprising copper and manganese in an oxide matrix. However, the presence of 0.5% and 1% Au has increased the reducibility of the supported catalyst. Similarly, the TPR profiles show overlapping of the copper and manganese oxides rather than separate reduction peaks. This leads to an indication that mixed copper manganese oxide species may be present in the catalyst.

4.1.3.5 Scanning Electron Microscopy

The SEM image of the CuMnOx catalyst aged for 1h shows that the morphology is similar to the CuMnOx catalyst aged for 0.5h.
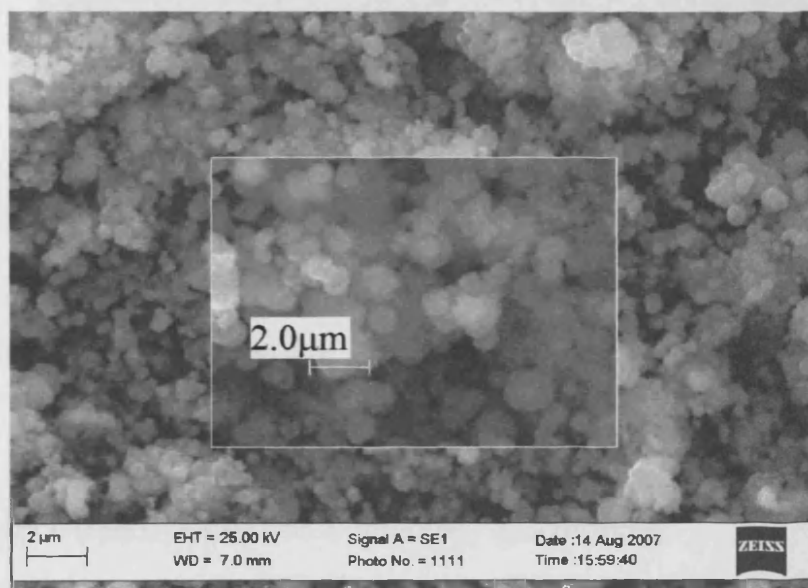
Figure 4.21 SEM image of CuMnOx age for 1h

The particles have fragmented to smaller spheres with an average size of *ca*. 1.5 μm. This type of morphology, highly dispersed smaller particles, could lead to a structure that is suitable to be used as a support for Au particles. The activities for the 1h aged catalysts are generally higher than the 0h aged catalysts; the 0h aged catalysts having larger spherical particles. Figure 4.22 also shows that individual particles have fragmented to form an area consisting of these particles. The deposition precipitation method has not altered the morphology of the catalyst and the particles are of similar size to the CuMnOx catalyst (ca. 1.5 μm). There could be a possible correlation developing between ageing time of the catalyst and average particle size.
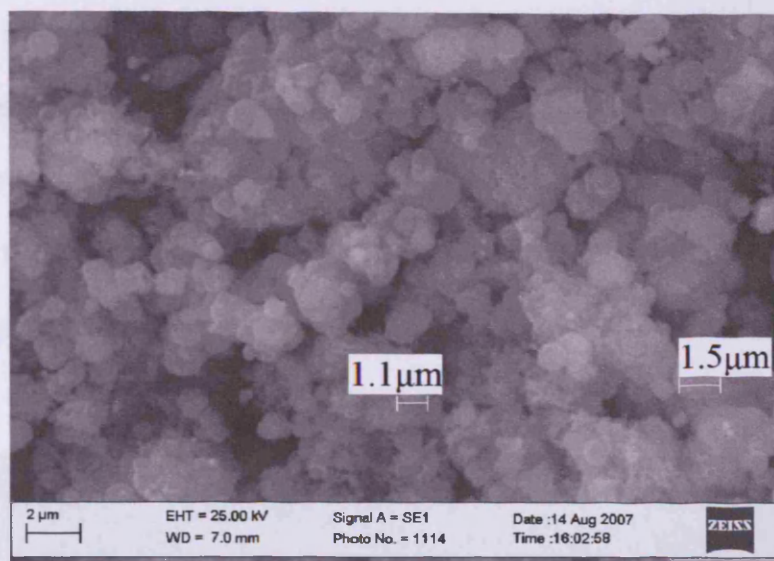
Figure 4.22 SEM image of 1% Au supported CuMnOx aged for 1h

4.1.3.6 Energy Dispersive Electron Microscopy spectroscopy

The EDX spectra (Figure 4.23) shows the composition of the CuMnOx catalyst aged

for 1h. The ratio of Mn to Cu is ca. 1.5:1 respectively.
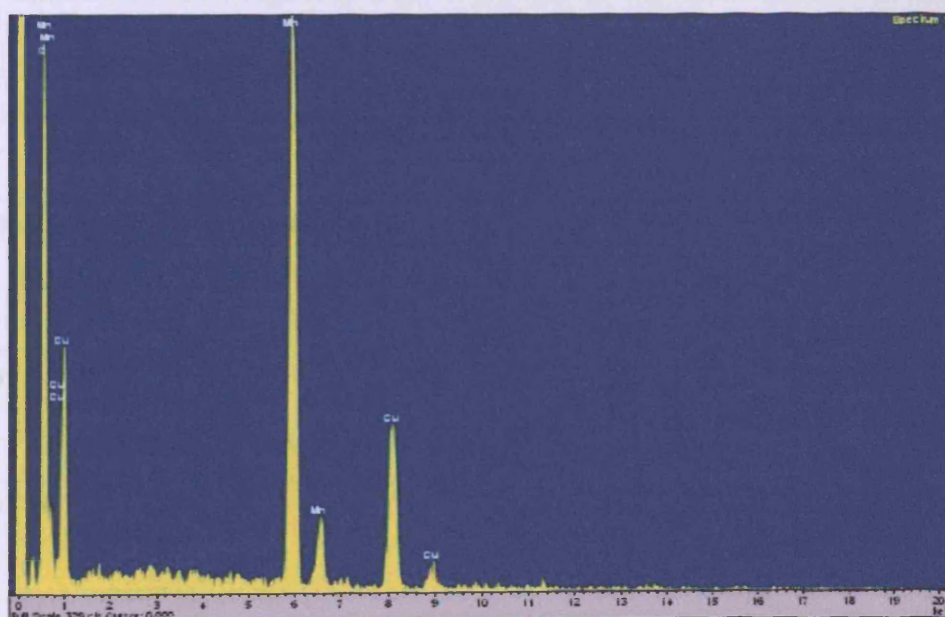
Figure 4.23 EDX spectra of CuMnOx aged for 1h

The spectra shown in Figure 4.24 provides evidence that there is Au deposited particles present on the surface of the supported catalyst. The quantitative analysis gives a result that is *ca.* 1.7% Au present (Table 4.6) in the catalyst. It is an indication that the improvement in activity towards CO oxidation can be related to the addition of the Au dopant.
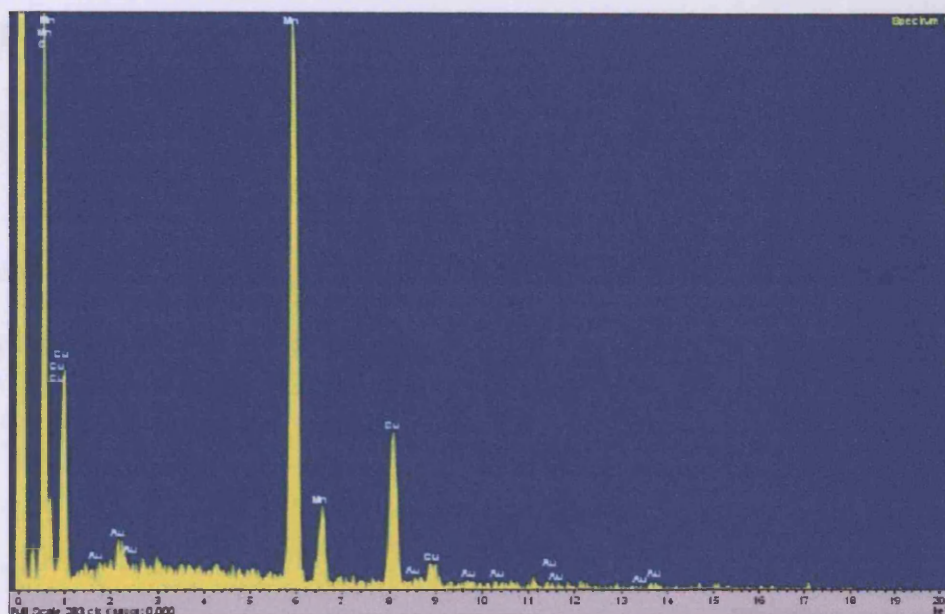
Figure 4.24 EDX spectra of 1% Au supported CuMnOx aged for 1h.

The percentage weight of elements present is summarised in Table 4.2

CuMnOx 1h aged		Element	O	Mn	Cu	Au
		Weight (%)	25.87	44.12	30.01	0
1% Au supported CuMnOx 1h aged		Element	O	Mn	Cu	Au
		Weight (%)	26.66	43.58	28.06	1.7

Table 4.6 Percentage weight – CuMnOx aged for 1h

1% Au supported CuMnOx catalyst aged for 1h

4.1.4 Au supported Hopcalite catalyst with ageing time of 6h

The final ageing time investigated was for 6h to compare the effect it would have on

the catalyst produced and hence the ability of the Au supported particles to promote

catalytic activity. The effect of ageing the catalyst precursor has been discussed

previously. As the ageing time is increased, the formation of mixed CuMnOx oxides

becomes more predominant, in particular the amount of Mn incorporation into the

mixed phase is enhanced [7].

4.1.4.1 Catalyst Activity

The CuMnOx and Au supported catalysts aged for 6h were tested for CO oxidation

activity and the data is shown in Figure 4.25.
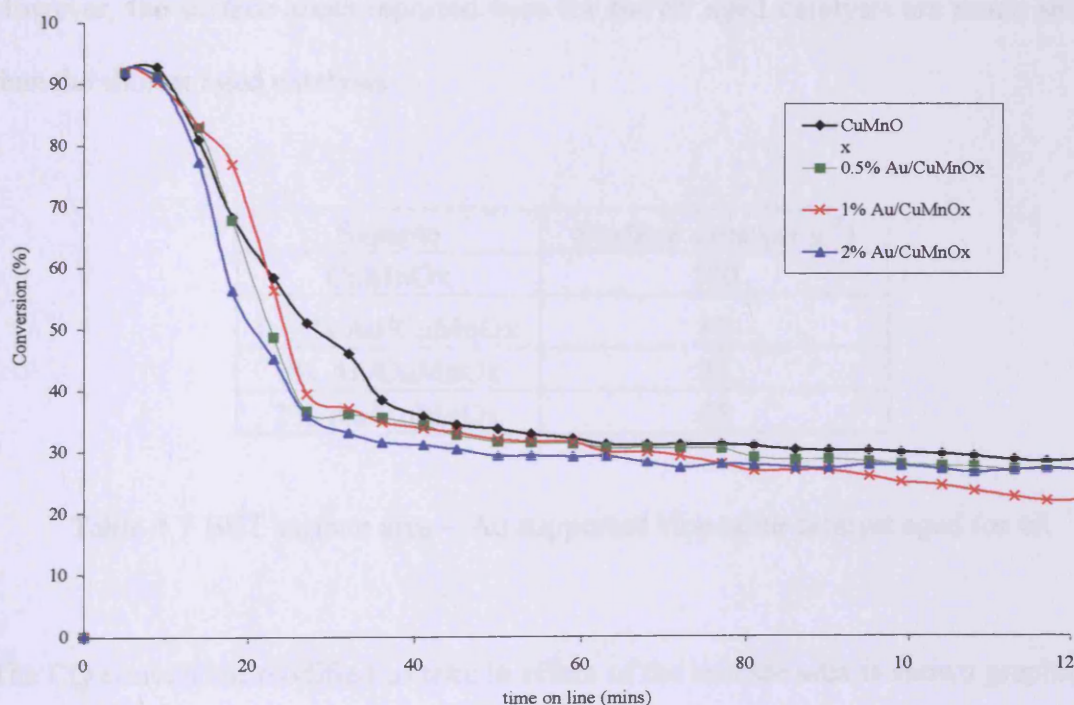
Figure 4.25 CO oxidation – Au supported Hopcalite catalyst aged for 6h

The CuMnOx catalyst and Au supported CuMnOx catalysts aged for 6h show very little variation in activity over 2h of catalyst testing. The CuMnOx and Au supported catalysts exhibit the familiar initial high activity (*ca.* 90% conversion) associated with the Hopcalite catalyst. The major difference with the longer aged catalyst to the shorter ageing times is that the rate of deactivation is more rapid. After 30 minutes of testing, the CuMnOx and Au supported CuMnOx catalysts have deactivated by at least 50%. However, both catalysts do show long term steady state activity; there is no further deactivation. The addition of 0.5%, 1% or 2% Au has not shown any improvement in activity towards CO oxidation.

4.1.4.2 BET Surface Area

The BET surface areas for both the CuMnOx and Au supported catalysts are similar (considering the amount of error associated with the use of the BET machine). However, the surface areas reported here for the 6h aged catalysts are much smaller than the shorter aged catalysts

Sample	Surface area (m^2g^{-1})
CuMnOx	100
0.5 % Au/CuMnOx	82
1% Au/CuMnOx	84
2% Au/CuMnOx	85

Table 4.7 BET surface area – Au supported Hopcalite catalyst aged for 6h

The CO conversion modified to take in effect of the surface area is shown graphically in Figure 4.26. The similarity in surfaces areas has shown no significant difference in the activities of the longer aged catalysts. The only alteration is the initial activity of the CuMnOx has slightly lowered.
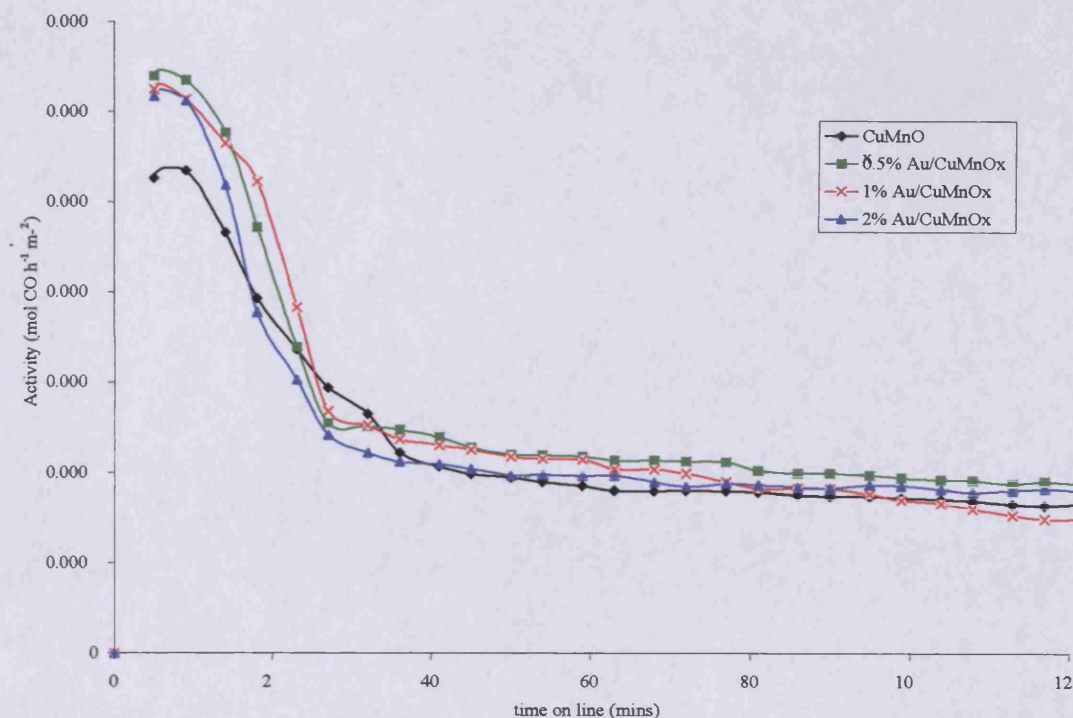
Figure 4.26 Surface area adjusted activity – Au supported CuMnOx catalysts

aged for 6h

4.1.4.3 Powder X-ray Diffraction

The powder X-ray diffraction studies were performed on the 6h aged catalysts. On XRD analysis it was not possible to fully differentiate between the four samples. The catalysts were poorly crystalline. It was difficult to fully distinguish the actual phases present in the 6h aged catalysts. Mn_2O_3 phases were the only detectable at peaks at 2θ ca. $32°$ and $36°$. However, the presence of metallic Au cannot be ruled out since a peak at 2θ ca. $38.2°$ was detected. There is indication that gold is present as the intensity of the peak at $38.2°$ increases as the calculated Au weight percentage is increased. The peaks are close to the baseline of the spectra that it is very difficult to distinguish what copper and manganese phases are present in Figure 4.27. However, the patterns are slightly more crystalline than the shorter aged catalysts. The extended

ageing time may have caused crystal growth which may have produced a combination of phases that has lower catalytic activity compared to a more amorphous material.
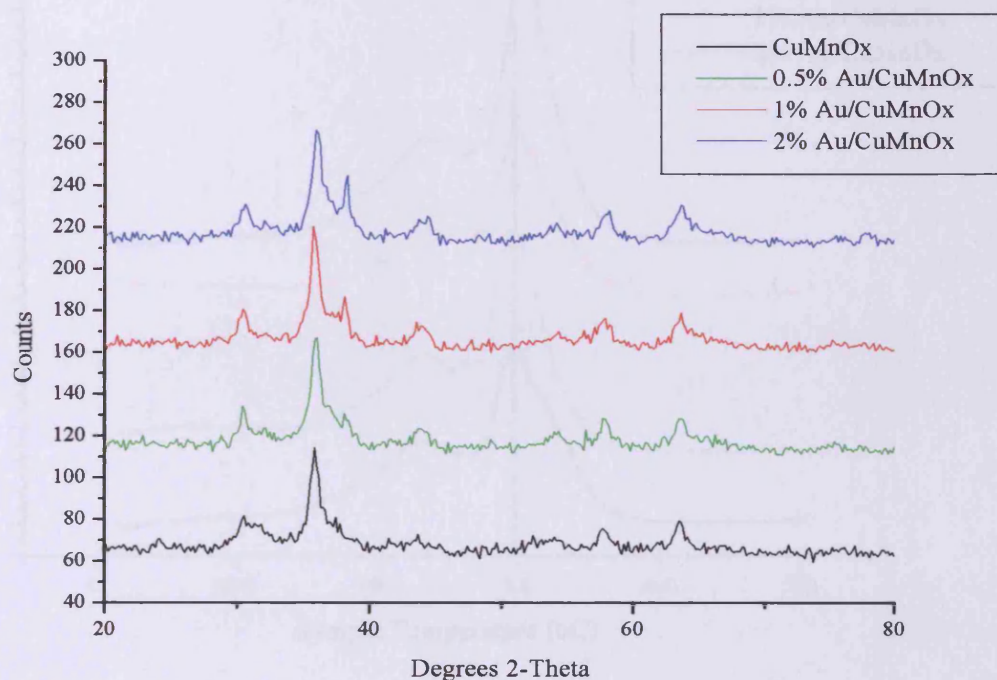
Figure 4.27 Powder XRD – Au supported CuMnOx aged for 6h

4.1.4.4 Temperature Programmed Analysis

The TPR profiles of the Au supported CuMnOx (Figure 4.28) show very little difference in reduction temperatures. The peak associated with reduction of CuO (T = 225°C) shows no alteration with the possible addition of Au particles. The same is shown with the manganese oxide reduction peak (T= 300°C), no shift to a lower temperature. This effect is shown in the catalytic data for the catalysts aged for 6h. The possible addition of Au has shown no increased reducibility of the catalyst. This could be due to the CuMnOx support produced not interacting with Au particles or whether there are no Au particles present in the catalyst.
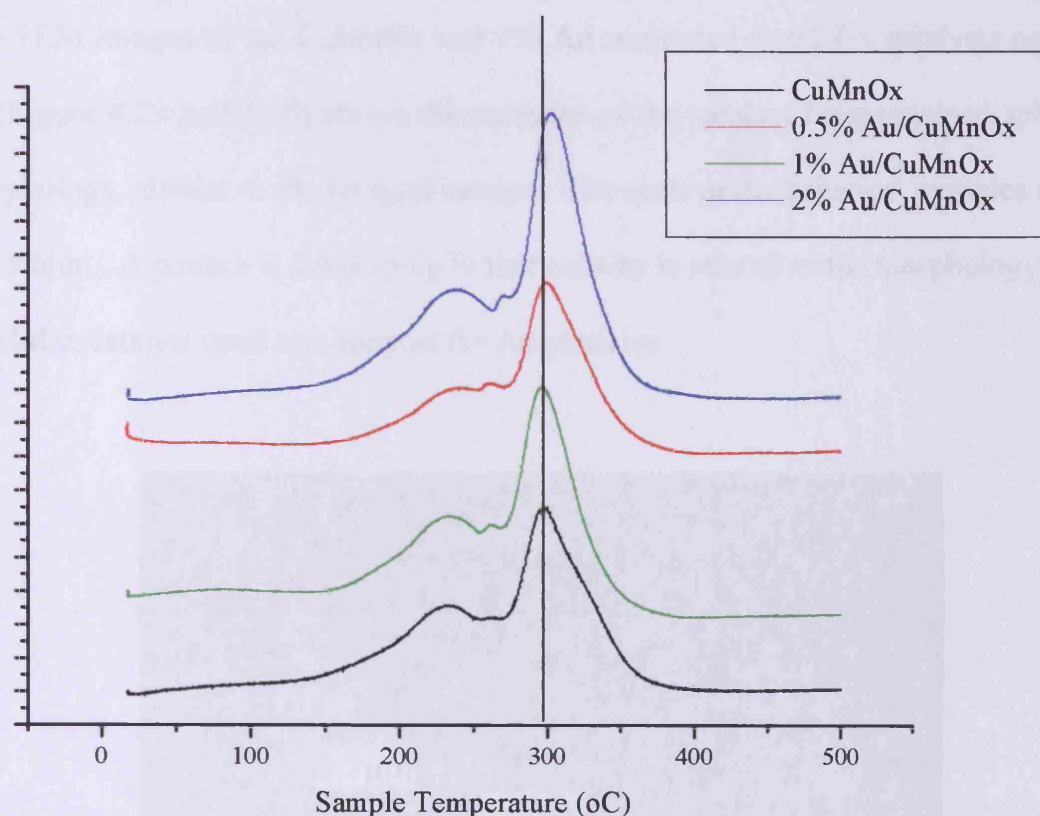
Figure 4.28 TPR profile – Au supported CuMnOx aged for 6h

The increased ageing time has lead to two distinguishable reduction peaks. Also the peaks are further apart than for the shorter ageing times. In the case for the 6h aged samples, the peak associated with manganese reduction appears to be more predominant. This gives rise to the possibility that separate phases are present in the sample. The X-ray diffraction patterns, for the 6h aged samples, show evidence that a Mn_2O_3 phase is present. These separate phases, rather a mixed phase, could be the cause of the low activity of the catalysts.

4.1.4.5 Scanning Electron Microscopy

The SEM images of the CuMnOx and 1% Au supported CuMnOx catalysts aged for 6h (Figure 4.29 and 4.30) shows the particles of the catalyst have regained spherical morphology, similar to the 0h aged catalyst. The sizes of the spherical particles are *ca.* 3.7-5.6μm. A pattern is developing in that activity is related to the morphology of the CuMnOx catalyst used as a support for Au particles.
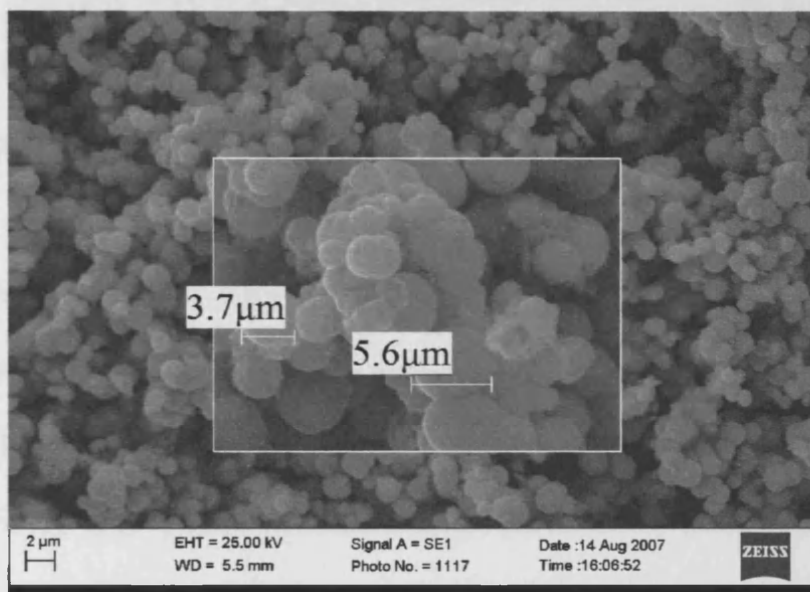
Figure 4.29 SEM image of CuMnOx catalyst aged for 6h

The smaller less spherical particles, associated with 0.5h and 1h ageing times, produce an active catalyst that also acts as a suitable support for the addition of Au particles. The larger spherical particles (0h aged and 6h aged catalysts) show lower activity and the addition of Au to the CuMnOx shows very little improvement towards CO oxidation. In addition to morphology, the amount of Au deposited onto the CuMnOx catalyst shows some trend with activity towards CO oxidation. The 1% Au supported catalysts show the overall highest activity for each ageing time.

148
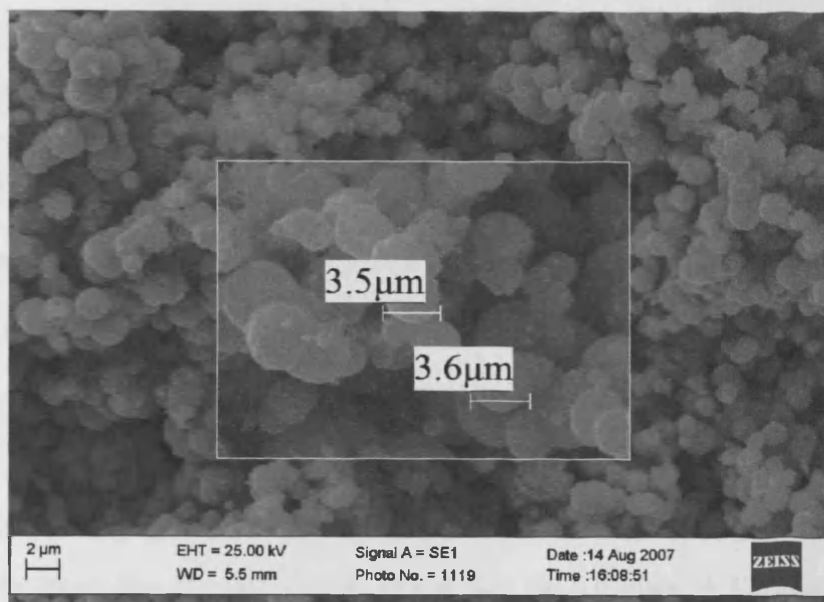
Figure 4.30 SEM image of 1% Au supported CuMnOx aged for 6h

The morphology of the Au supported CuMnOx catalyst has not been altered by the deposition precipitation method. The particle sizes of the Au supported CuMnOx catalyst aged for 6h are larger than for the 0.5h and 1h supported catalysts. A comparison of the ageing time with the average particle size is summarised in Figure 4.31.
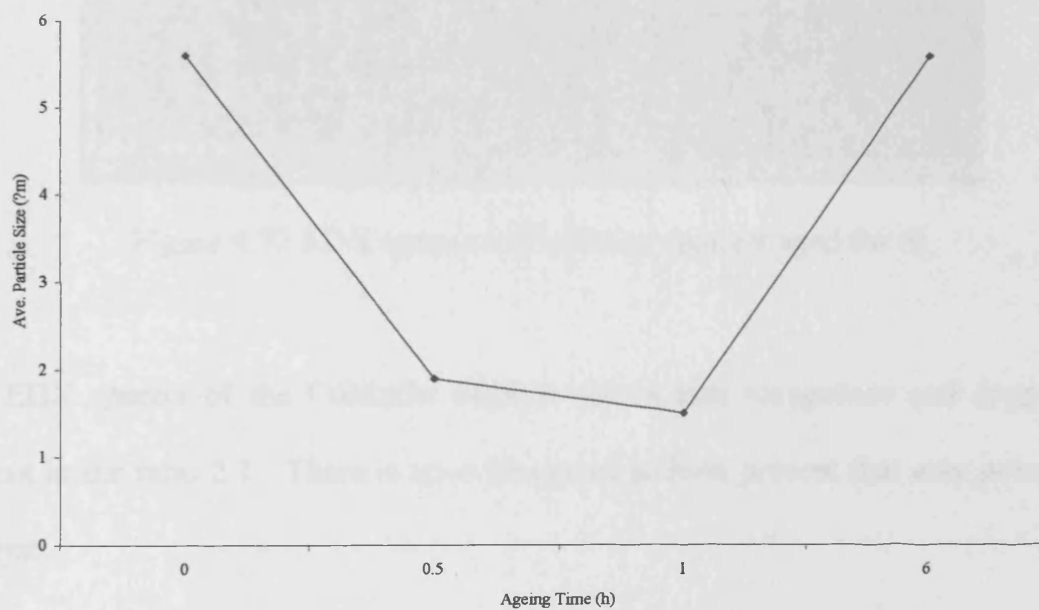
Figure 4.31 Average particle size of CuMnOx catalyst as a function of ageing time

The data shown in Figure 4.31 shows how that ageing time of the catalyst used affects the size of the particles produced. The 0.5h and 1h ageing times produces materials which an average particle size of ca. 2 μm. The 0h and 6h aged catalysts have larger particle sizes of ca. 5.5 μm. The difference in particle sizes of the CuMnOx support could control the catalytic activity for CO oxidation.

4.1.4.6 Energy Dispersive X-ray spectroscopy

The EDX spectras for the CuMnOx aged for 6h (Figure 4.32) and the 1% Au supported CuMnOx (Figure 4.33) show the composition of elements present in the catalysts.
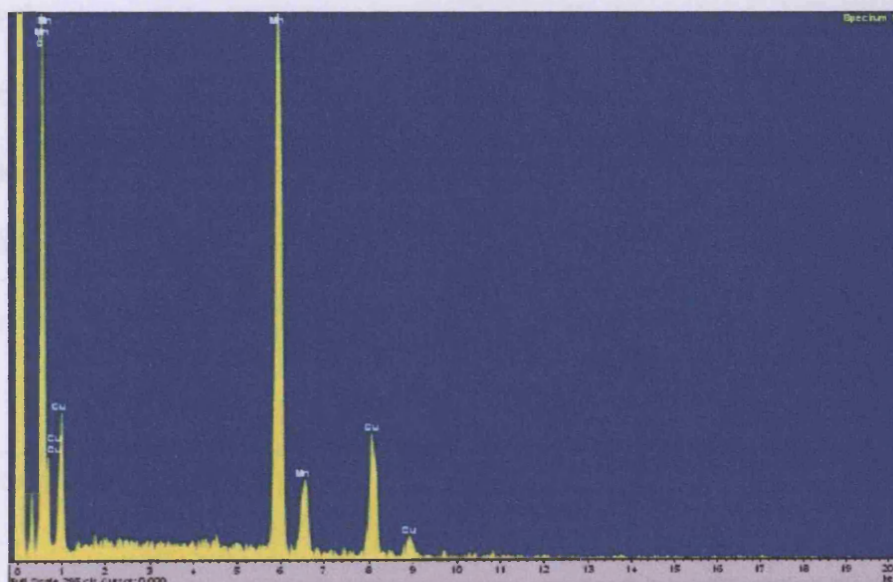
Figure 4.32 EDX spectra of CuMnOx catalyst aged for 6h

The EDX spectra of the CuMnOx catalyst shows that manganese and copper are present in the ratio 2:1. There is no evidence of sodium present that may poison the catalyst.
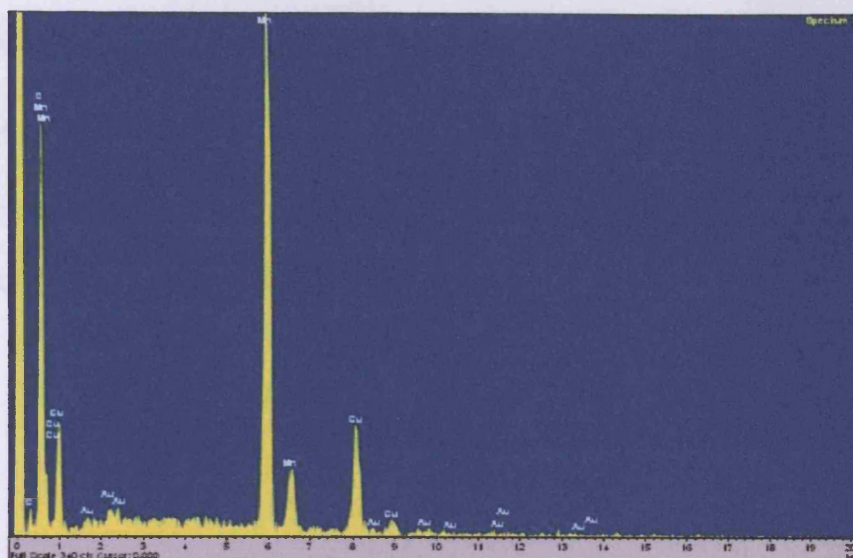
Figure 4.33 EDX spectra of 1% Au supported CuMnOx aged for 6h

The quantification of the EDX spectrum of the 1% Au supported CuMnOx catalyst aged for 6h is shown in Table 4.8. The data supports evidence that the deposition precipitation method has been successful in depositing gold particles onto the surface of the CuMnOx catalyst. This clarifies the uncertainty that Au particles may not have been present since there were no differences in the TPR data shown in Figure 4.28.

CuMnOx 6h aged		Element	O	Mn	Cu	Au
		Weight (%)	26.51	49.33	24.15	0
1% Au supported CuMnOx 6h aged						
		Element	O	Mn	Cu	Au
		Weight (%)	26.36	49.04	23.5	1.1

Table 4.8 Percentage weight – CuMnOx aged for 6h

1% Au CuMnOx catalyst aged for 6h.

4.2 Discussion

The steady state activity of the Au supported catalysts is summarised in Figure 4.34. The general trend from this graph is that improvement in activity is shown with the addition of gold, with the exception with the 6h aged catalysts.
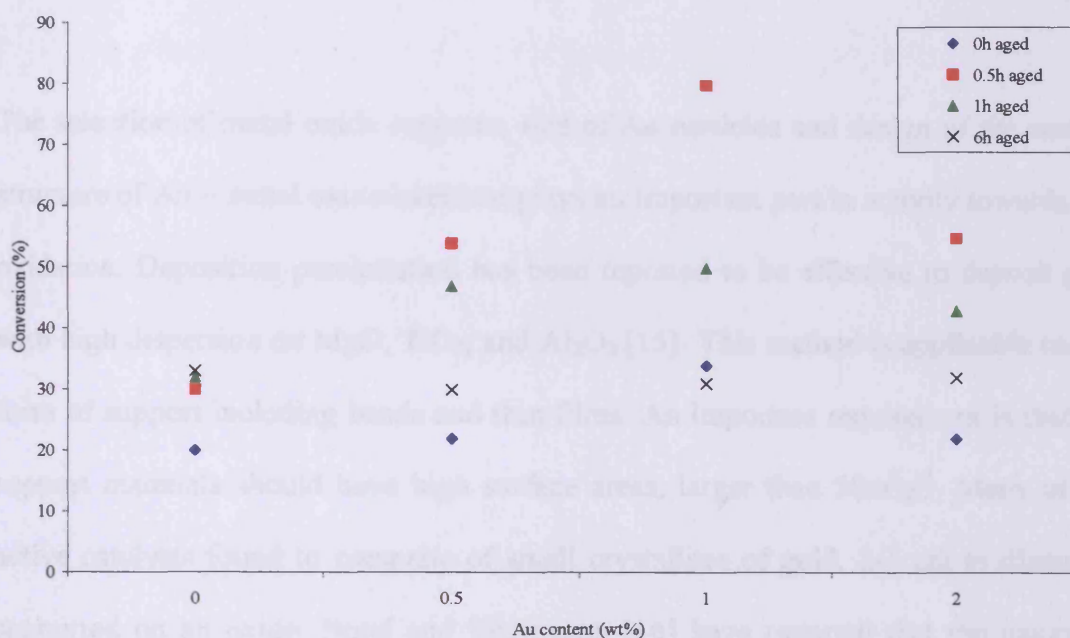
Figure 4.34 Summary of the influence of Au loading on

CO oxidation activity after 2h time on-line

This trend in activity could be due to a combination of the morphology of the CuMnOx interacting with Au particles on the catalyst surface. The dispersion of Au may also be different depending on the detailed morphology and composition of the CuMnOx support. The catalytic performance of Au supported CuMnOx is related to the gold loading. Generally, the overall activity in CO oxidation increased as the gold content was increased from 0.5 to 1 wt% and then decreased with the further increase in gold loading to 2 wt%. Wu and co-workers have reported that the CO conversion on Au/SnO_2 increased as the gold loading was increased from 0.36 to 2.86%, and then decreased as the gold loading was further increased to 5 wt% [13]. Zhu and co-

workers [14] also found that increasing gold content from 0.6 to 2.5 wt% increased CO oxidation, followed by a decrease in activity with a further increase of gold loading to 4.3 wt%. This could be consistent with Haruta's assertions that the total surface area of exposed Au metal increases initially with Au content, but may decline when the gold loading increases further due to the coagulation of the Au particles [2].

The selection of metal oxide supports, size of Au particles and design of the contact structure of Au – metal oxide interface plays an important part in activity towards CO oxidation. Deposition precipitation has been reported to be effective to deposit gold with high dispersion on MgO, TiO_2, and Al_2O_3 [15]. This method is applicable to any form of support including beads and thin films. An important requirement is that the support materials should have high surface areas, larger than $50m^2g^{-1}$. Many of the active catalysts found to comprise of small crystallites of gold, 2-4 nm in diameter, supported on an oxide. Bond and Thompson [16] have reported that the nature of these active sites for CO oxidation is due to an interaction at the interface between the Au particle and the oxide. Baker [17] has noted that the role of the support should not be neglected and that activity should not be solely based on the size of the Au particles present.

In relation to the Hopcalite catalyst, the preparation conditions used are an important factor in controlling catalytic activity [9]. The catalytic activity of the CuMnOx for CO oxidation was affected by the varying of the precipitate ageing time. The 1% Au supported catalyst aged for 0.5h showed the greatest increase in activity of all the catalysts tested. There could possible be an interaction between the Au particles present and the CuMnOx support present.

The X-ray diffraction patterns for the shorter ageing times (0 to 1h) showed that the CuMnOx was amorphous whereas he 6h aged CuMnOx catalyst was quite crystalline in character. The X-ray diffraction patterns, for 6h aged catalysts, showed that Mn_2O_3 was predominately present. The morphology of the catalyst can be related to activity towards CO oxidation and this could relate to the low activity of the 6h aged catalyst [18]. The effect of morphology of the CuMnOx catalyst was discussed in chapter 3. The increased ageing time may have a caused micro-crystalline morphology to form. This increase in crystallinity could lead to lower catalytic activity.

SEM images showed that varying the ageing time had an affect on the structure of the CuMnOx. Powder particles exhibited spherical morphology (5.6 μm) for the 0h aged catalyst but fragmented into small particles (1.9 μm) as the ageing time was increased to 1h. The longer 6h ageing time displayed larger spherical particles (ca. 5 μm) similar to the 0h aged catalyst. The 0.5 and 1h aged catalysts showed the greater improvement towards CO oxidation with the addition of Au particles. This could lead to the generation of more active sites for catalytic oxidation of CO or possibly greater distribution of Au particles on the surface. There could possibly be a stronger interaction between the Au particles and the support.

Several authors have investigated the influence of the support used for CO oxidation. In particular, the activities of Au/Al_2O_3, Au/TiO_2 and Au/Co_3O_4 have been reported in terms of the support used [19-20]. Park and co workers have suggested that TiO_2 forms an interface with gold more easily than Al_2O_3. However, strong support interactions reported for noble metal/TiO_2 catalysts only develop after reduction at ca. 500°C, which in the case of gold leads to less active catalysts. Schubert and co-workers [7] discussed the observed differences in catalytic activities of Au/Al_2O_3,

Au/TiO_2 and Au/Co_3O_4 in terms of the reaction mechanism. Active supports like TiO_2 and Co_3O_4 act as oxygen suppliers, in the case of inactive supports like Al_2O_3 the oxygen has to be adsorbed on the gold surface. Hutchings and co-workers [24] have reported TiO_2 prepared using a supercritical CO_2 anti-solvent precipitation method. The Au supported sc-TiO_2 demonstrated higher activity (100 % conversion for CO) compared to conventional preparation methods. Reducible supports are described as advantageous because they often contain oxygen vacancies that can serve as Au anchor sites [21-23]. For Au/TiO_2 catalyst, the Au support interaction becomes more attractive with increasing oxygen vacancy density; the number of low co-ordinated atoms can be expected to increase with increasing oxygen vacancy density in the support, which affects the catalytic activity of the catalyst [21].

The activities of the Au supported CuMnOx by deposition precipitation are different to the reported activities for the co-precipitated Au supported CuMnOx. Taylor and co-workers [1] reported catalytic improvement of the CuMnOx with the addition of gold. A 3 wt% Au doped CuMnOx improved the steady state activity by ca. 50%. Further investigation would be needed to fully compare the deposition precipitation method with the co-precipitation. However, Khoudiakov and co-workers [24] have reported a Au/Fe_2O_3 catalyst produced by co-precipitation and by a deposition precipitation method. The catalytic activities overall reported that the deposition precipitation method produced a more active catalyst because it allowed complete precipitation of gold from solution. Khoudiakov and co-workers discuss that the deposition precipitation method has a potential advantage over co-precipitation in that the entire active component remains on the surface of the support and none is buried within it.

The surface areas of the Au supported catalysts show little difference when gold is added to the support. However, the 0.5h and 1h aged catalysts show slightly larger surface areas (ca. 120 m^2g^{-1}) compared to the 6h aged catalyst (ca. $90m^2g^{-1}$). This could a possible reason for the higher activities for the 0.5h and 1h aged catalysts. Slightly higher surface areas would promote better distribution of gold particles.

The improvement of activity for CO oxidation is related to the presence of gold. The EDX spectras are indications that Au particles are present in the catalyst but determining the size of these particles by X-ray diffraction is impossible.

The TPR profiles show that in most cases, a shift of the reduction peaks to lower temperatures occurred when gold was added to the CuMnOx support. The 1% Au supported catalysts aged for 0, 0.5h and 1h show increased reducibility compared to the CuMnOx catalysts. The lower temperature reduction peaks indicated a more energetically favourable oxidation process, where oxygen from the catalyst bulk or surface was easily available to react with the CO reagent in the production of CO_2. The area of the peaks, which corresponds to H_2 consumption, did not differ with the varying Au loading. This indicates that the addition of gold does not increase the amount of oxygen species present in the catalyst but let the oxide species present to become more energetically favourable for reaction with CO. Pillai and Deevi [26] reported, using TPR analysis, that the addition of gold can weaken surface oxygen on ceria-zirconia and improve the reducibility of the catalyst. This phenomenon was also report by S.P. Wang and co-workers [27]. Y.M. Kang and B.Z Wan [28] also commented that the presence of gold in a iron/ zeolite-Y catalyst improved reducibility. They reported that the bonding between gold-oxygen was so weak that oxygen was easily dissociated from gold oxides. The TPR profiles for aged catalysts

show a few differences. As the catalysts were aged from 0h to 1h, the overlapping of

reduction peaks became more predominate. As the ageing time was increased to 6h,

the peaks associated with copper and manganese reduction were separated. This

indicates that, for the shorter ageing times, mixed oxide species were present.

Increasing the ageing time of the precipitate, lead to separate phases to form. This

means that the active phase of the catalyst is the mixed copper manganese oxide.

There has been much discussion concerning the nature of the active site for these

catalysts. It remains unclear whether Au^{3+} or Au is the active form of gold [16]. The

presence of hydroxy groups [12] and gold particle size [16] are also thought to

influence CO oxidation.

It should be noted that the Au supported catalysts take a longer time to reach its

maximum activity, rather than starting at high activity and deactivating. This may be

due to gold particles sat on the active sites on the Hopcalite support. The TPR data

shows that the Au supported catalysts are more reducible. There could be a synergy

between the possible active gold site and lattice oxygen from the Hopcalite support.

However, this is not a full explanation as the Au supported catalysts have higher

steady state activity. This effect will be discussed in the following chapter along with

the effect of moisture.

4.3 Conclusion

A series of Au supported CuMnOx catalysts have been prepared by a deposition

precipitation method. The addition of gold particles to CuMnOx catalyst generally

improved activity for CO oxidation. The most active catalyst was a 1% Au supported

CuMnOx catalyst aged for 0.5h. The Au supported catalysts showed less deactivation after 2h of catalyst testing compared to the CuMnOx catalysts. The activities of the catalysts prepared are controlled by the ageing time of the CuMnOx precursor and the amount of gold added. Varying the ageing time influenced the particle size of the support. The amount of gold loading was a controlling factor of activity, 1 wt% Au being the optimum quantity. The Au supported catalysts have shown greater resistance to deactivation than the CuMnOx catalyst.

4.4   Chapter 4 References

[1]   B. Solsona, G.J. Hutchings, T. Garcia, S.H. Taylor, New. J. Chem. 28 (2004) 708.

[2]   M. Haruta, N. Yamada, T. Kobayashi, S. Iijima , J. Catal. 115 (1989) 301.

[3]   G.J. Hutchings, J.Catal. 96 (1985) 292.

[4]   B.E. Solsona, T. Garcia, C. Jones, S.H. Taylor, A.F. Carley, G.J. Hutchings, App. Catal. A: Gen. 312 (2006) 67.

[5]   A.A. Mirzaei, H.R. Shaterian, M. Habibi, G.J, Hutchings, S.H. Taylor, Appl. Catal. A: Gen. 253 (2003) 499.

[6]   H.R. Oswald, W. Feitknect, M.J. Wampetich, Nature (London) 207 (1965) 72

[7]   G. Fortunato, H.R. Oswald, A. Reller, J. Mater. Chem.,11 (2001) 905.

[8]   A.A. Mirzaei, H.R. Shaterian, R.W. Joyner, M. Stockenhuber, S.H. Taylor, G.J. Hutchings, Cat. Comm. 4 (2003) 17.

[9]   G.J. Hutchings, A.A. Mirzaei, R.W. Joyner, M.R.H. Siddiqui, S.H. Taylor, Catal. Lett. 42 (1996) 21.

[10]   N.A. Hodge, C.J. Kiely, R. Whyman, M.R.H Siddiqui, G.J. Hutchings, Q.A. Pankhurst, F.E. Wagner, R.R. Rajaram, S.E. Golunski, Catal. Today 72 (2002) 133.

[11]   F.C Buciuman, F. Patcas, T. Hahn, Chem. Eng. Process. 38 (1999) 563.

[12]   M. Date and M. Haruta, J. Catal. 201 (2001), 21.

[13]   S.R.Wang, J. Huang, Y.Q. Zhao, S.P.Wang, X.Y.Wang, T.Y. Zhang, S.H. Wu, S.M. Zhang, W.P. Huang, J. Mol. Catal. A., 259 (2006) 245.

[14]   H. Zhu, Z. Ma, J.C. Clark, Z. Pan, S.H. Overbury, S. Dai, App. Catal. A: Gen. 326 (2007) 89-99.

[15] S. Tsubota, D.A.H. Cunningham, Y. Bando, M. Haruta, Preparation of Catalysis VI, G. Poncelet et al. Eds., Elsvier, Amsterdam, 1995 pp.227-235.

[16] G.C. Bond, D.T. Thompson, Gold Bull. 33 (2000) 41.

[17] H. Baker, Science Perspectives, vol. 301, 15 August 2003.

[18] S.B. Kanungo, J. Catal. 58 (1979) 419.

[19] M.M. Scubert, S, Hackenberg, A.C. van Veen, M. Muhler, V. Plzak, R.J. Behm , J. Catal. 197 (2001)113.

[20] E.D. Park, J.S. Lee, J. Catal. 186 (1999) 1.

[21] N. Lopez, J.K. Nørskov, T.V.W. Janssens, A. Carlsson, A. Puig-Molina,B.S.Clausen, J.-D. Grunwaldt, J. Catal. 225 (2004) 86.

[22] Z. Yan, S. Chinta, A.A. Mohamed, J.P. Fackler Jr., D.W. Goodman, J. Am. Chem. Soc. 127 (2005) 1604.

[23] N. Lopez, J.K. Nørskov, Surf. Sci. 515 (2002) 175.

[24] M. Khoudiakov, M.C. Gupta, S. Deevi, App. Catal. A: General 291 (2005) 151.

[25] Z. Tang, J.K. Bartley, G.J. Hutchings, S.H. Taylor, Stud. Surf. Sci. Catal. 162 (2006) Pages 219.

[26] U.R. Pillai, S. Deevi, Appl. Catal. A 299 (2006) 266.

[27] S.P Wang, T.Y. Zhang, X.Y. Wang, S.M. Zhang, S.R. Wang, W.P Huang, S.H. Wu, J. Mol. Catal. A: Chem. 272 (2007) 45.

[28] Y.-M. Kang, B.-Z Wan. Catal. Today 26 (1995) 59.

Moisture Removal Effect on CuMnOx Catalyst

5

The catalysts tested in Chapter 4 have been performed in ambient conditions using a gas chromatograph. The gas cylinder connected to the testing system is not moisture free and so trace amounts of moisture are present in the reactor system. It has been reported that the hopcalite catalyst deactivates considerably in the presence of moisture [1]. This is a disadvantage of this type of catalyst compared to gold supported catalysts; where deactivation is much less [2]. The investigation of the Au supported CuMnOx catalyst has shown that the addition of gold particles increases the activity of the catalyst in ambient conditions / presence of moisture. Haurta and co-workers have reported that supported Au catalysts show significant activity at low temperature CO oxidation and in the presence of moisture [2-3]. They reported that moisture enhances the catalytic activity for several types of Au supported metal oxides. CuMnOx catalysts have been reported to deactivate in the presence of moisture. A series of experiments were performed to see if removing moisture from the reactor system would have a significant effect on the CuMnOx catalyst and the Au supported CuMnOx catalyst.

The reaction conditions discussed in this chapter are split into ambient conditions and moisture removed conditions. This is summarised as follows:

Ambient conditions – 5000ppm CO/synthetic air, flow rate of 21.3 ml min^{-1}

Moisture removed conditions- 5000ppm CO/synthetic air, flow rate of 21.3 ml min^{-1},

Cold trap or molecular sieve present.

5.1 Initial Moisture Test with molecular sieve

CuMnOx catalysts aged for 0h, 0.5h and 1h were re-tested in ambient conditions for CO oxidation. The results are shown in Figure 5.1.
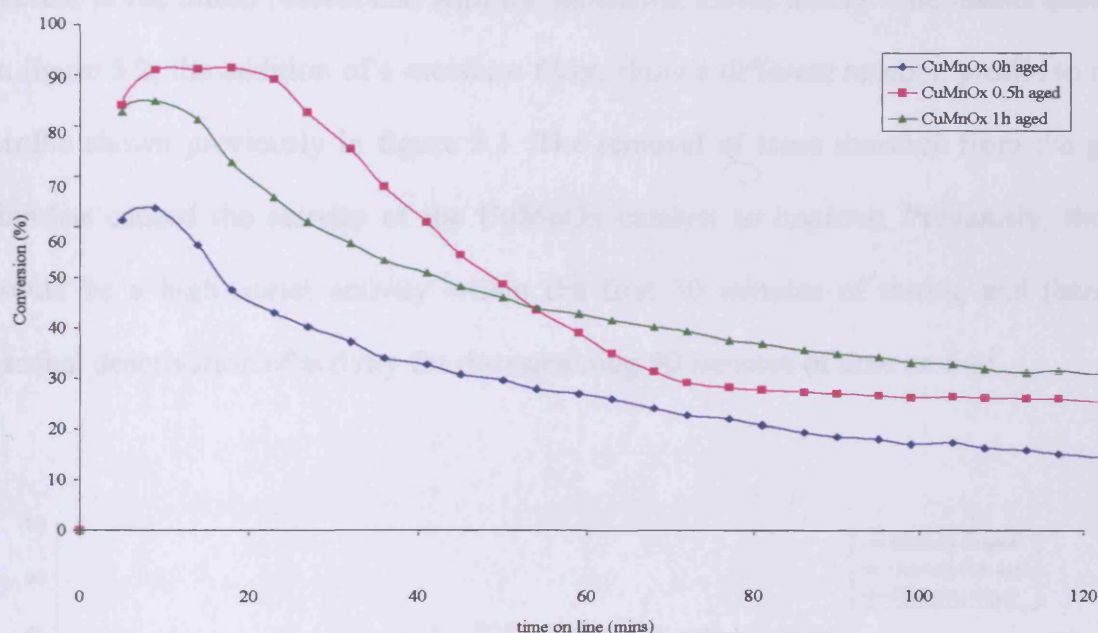
Figure 5.1 CuMnOx catalyst tested in moisture presence / no molecular sieves
21.3 ml min^{-1} of 5000ppm CO/air at 25°C

The catalytic results are identical to the data discussed in this chapter 4. The three catalysts tested show the similar trend of initially high activity followed by a gradual decrease in activity as time on line increases. The 0.5h aged catalyst has a much higher initial activity followed by a higher rate of deactivation. Initially, the idea of the molecular sieves would be to remove traces of moisture in the gas line that may lead to deactivation of the CuMnOx catalyst. If the presence of moisture was removed

162

then there might be a smaller amount of deactivation of activity. A blank run was conducted with only the molecular sieves present in the sample tube. No activity towards CO oxidation was reported.

A test procedure was setup with a few pellets of molecular sieve placed in the micro reactor before the gas reaches the catalyst bed. The molecular sieves and catalyst sample were not in contact with each other and were separated by a small amount of glass wool. CuMnOx aged for 0h, 0.5h and 1h were tested with the molecular sieves present in the micro reactor and with the molecular sieves absent. The results shown in figure 5.2, the addition of a moisture filter, show a different reaction profile to the profile shown previously in figure 5.1. The removal of trace moisture from the gas line has caused the activity of the CuMnOx catalyst to improve. Previously, there would be a high initial activity within the first 30 minutes of testing and then a gradual deactivation of activity for the remaining 90 minutes of time on line.
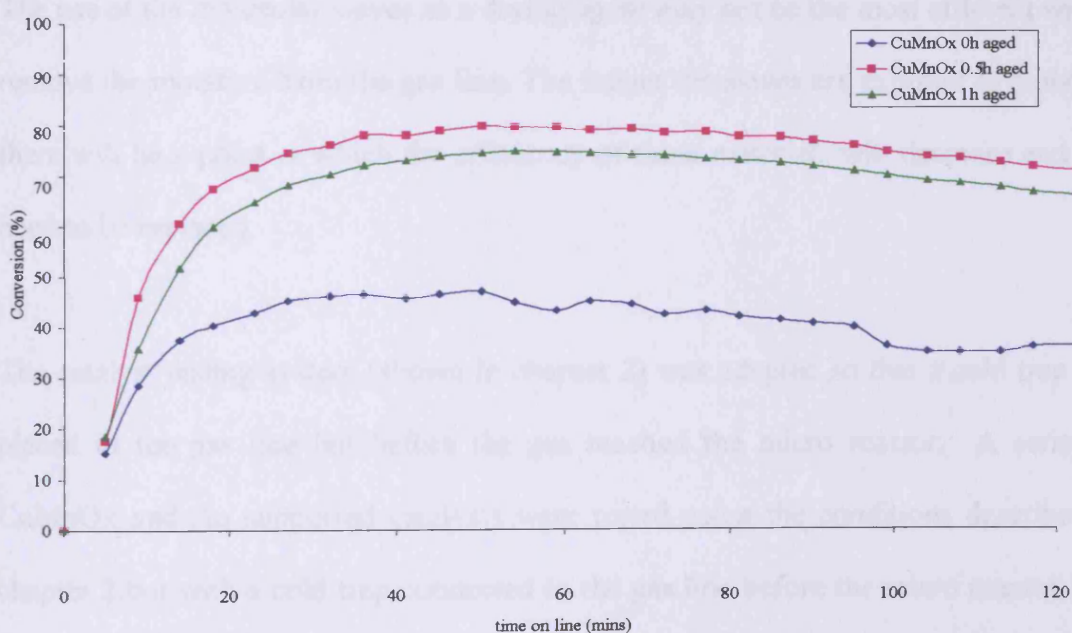
Figure 5.2 CuMnOx catalyst tested in moisture absence / molecular sieves present.

The catalysts shown in figure 5.2 show a much lower initial activity during the first 30 minutes of testing. However, there is very little deactivation of the catalysts as the time on line increases. The removal of moisture has lowered the initial high activity of the CuMnOx catalyst but has managed to retain its activity for a longer period of time. The opposite effect happens in normal ambient conditions; there is a high initial activity but a significant deactivation of the catalyst as the time on line increases. This result leads to a theory that the presence of hydroxyl species may play an important part in the CO oxidation reaction. During the initial 30 minutes of catalyst testing, the hydroxyl species that may be present interact with the catalyst surface and cause an effect that will promote CO oxidation. As catalyst testing increases, the hydroxyl groups present may be accumulating at the surface and consequently blocking active sites that now cannot interact with the CO and lead to the deactivation that we see in figure 5.1. These are some of the assumptions that could be taking place.

The use of the molecular sieves as a drying agent may not be the most efficient way to remove the moisture from the gas line. The longer the sieves are exposed to moisture, there will be a point at which the efficiency of these materials will decrease and will need to be replaced.

The catalyst testing system (shown in chapter 2) was adapted so that a cold trap was placed in the gas line but before the gas reached the micro reactor. A series of CuMnOx and Au supported catalysts were tested using the conditions described in chapter 2 but with a cold trap connected to the gas line before the micro reactor. The cold trap consisted of a mixture of liquid nitrogen and isopropanol, the temperature of the mixture was *ca.* -70°C and was maintained for the whole of the testing time.

5.2 CuMnOx 0h aged – Moisture removed with cold trap

The data shown in figure 5.3 consists of a CuMnOx catalyst and a series of Au supported CuMnOx catalysts aged for 0h and tested in the presence of a cold trap.

Figure 5.3 CO oxidation – Au supported CuMnOx and CuMnOx catalyst aged for 0h in the absence of moisture. CuMnOx catalyst tested in ambient conditions.

Also shown is a CuMnOx catalyst aged for 0h aged but tested in ambient conditions (cold trap removed).

The results shown in figure 5.3 shows a similar trend to the catalysts tested in the presence of molecular sieves. The Au supported catalysts tested with the cold trap in the gas line show similar reaction profiles. They all show a steady increase of activity in the initial stages of catalyst testing then a gradual depreciation of catalytic activity. The Au supported CuMnOx catalysts show steady state activity, there is very little to differentiate between activities. The steady state activities of the Au supported catalysts are similar to the CuMnOx catalyst, with moisture removed.

165

The interesting result to look at is the difference in activities between CuMnOx catalyst in the absence of moisture and the CuMnOx catalyst in ambient conditions. The CuMnOx in ambient conditions (presence of moisture) shows a high initial activity followed by a deactivation of activity after 2h of testing (*ca.* 20% conversion).

The CuMnOx in the absence of moisture displays a low initial conversion followed by steady activity and little deactivation (*ca.* 40% conversion). The method of using a cold trap to remove moisture from the gas line has caused a 50% increase in the activity of the CuMnOx catalyst.

The assumption of the presence of hydroxyl species needed during the early stages of catalyst testing to promote initial activity is shown here. There may be other reasons taking place but there is an indication that removing moisture affects the activity of the catalyst during the first 30 minutes of the reaction.

5.3 CuMnOx 0.5h aged – moisture removed with cold trap

Figure 5.4 shows data for a CuMnOx catalyst and a series of Au supported CuMnOx catalysts aged for 0.5h and tested in the presence of a cold trap. Also shown is a CuMnOx catalyst aged for 0.5h aged but tested in normal conditions (cold trap removed).

Figure 5.4 CO oxidation – Au supported CuMnOx and CuMnOx catalyst aged for

0.5h in the absence of moisture. CuMnOx catalyst tested in ambient conditions.

The data shown in figure 5.4 are similar to the information shown for catalyst aged for

0h. The removal of moisture has significantly improved the activity of the CuMnOx

and the Au supported CuMnOx catalysts. The 0.5h aged catalysts, in the absence of

moisture, shows low initial conversion compared to the CuMnOx catalyst in ambient

conditions. There is a gradual increase in activity for the 30 minutes followed by

steady state activity. There is very little deactivation shown by the catalysts with

moisture removed. The 1% Au supported catalyst has the highest overall activity *ca.*

90% conversion compared to the CuMnOx catalyst (moisture removed) which as a

conversion of *ca.* 70%. The 0.5%, 1% and 2% Au supported catalysts show small

improvement of activity when moisture is removed.

A similar result is shown with the CuMnOx catalyst 0.5h aged and the CuMnOx

catalyst aged for 0h. The removal of moisture has greatly improved the activity of the

catalyst, in terms of testing for 2h. The CuMnOx catalyst in normal conditions has a high initial activity of *ca.* 90% but conversion heavily decreases as time on line continues. The CuMnOx catalyst, with moisture removed, shows a steady increase in activity to *ca.* 75% conversion and maintains this for the remainder of the reaction. It can be shown that the activity of the 0.5h aged CuMnOx catalyst has improved compared to the 0h aged CuMnOx catalyst. As discussed previously in chapter 4, the ageing time of the catalyst has also had an effect on activity. It could be the combination of ideas that the 0.5h ageing process produces a more active catalyst. The smaller sized particles of the CuMnOx catalyst leading to increased active sites of the support for CO oxidation.

In the absence of moisture, there is very little difference in the 0.5% supported, 2% Au supported and the CuMnOx catalyst. The 1% Au supported catalyst does show improvement in activity from the other catalysts. This could be due to the 1% Au doping is an optimum amount to produce the highest amount of improvement from the catalyst. The differences in activity for different ageing times, gold loadings were discussed in chapter 4.

5.4 CuMnOx 1 h aged – moisture removed with cold trap.
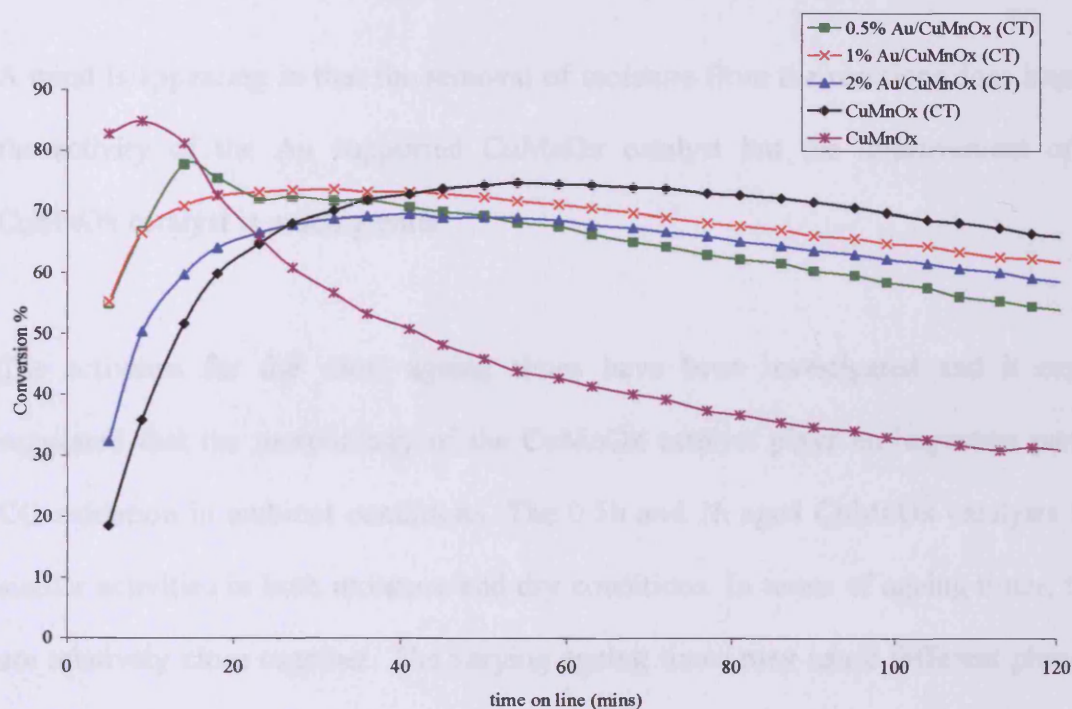
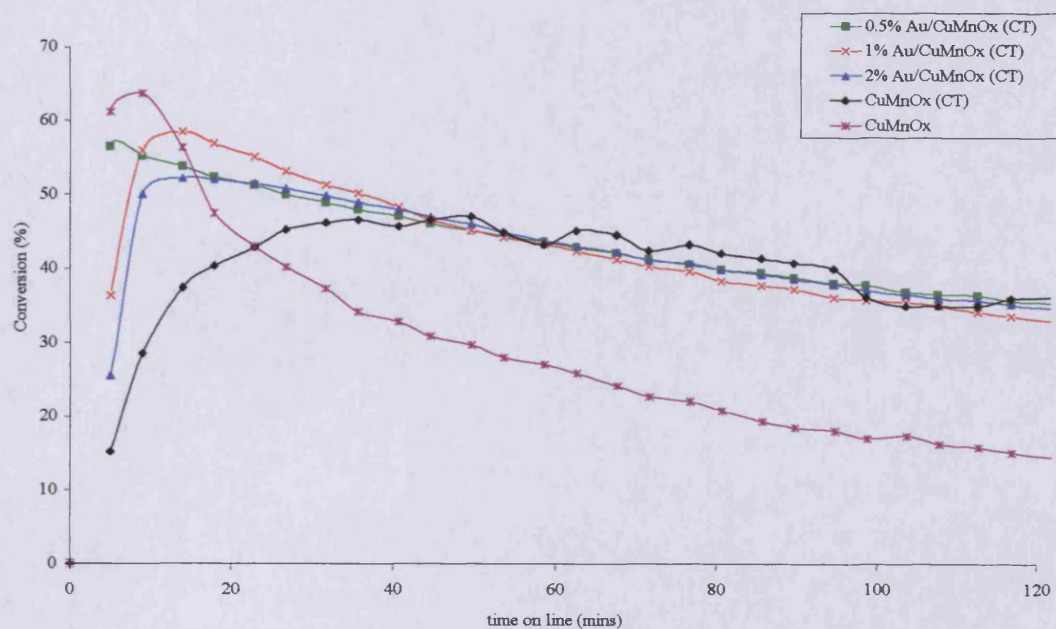Figure 5.5 CO oxidation – Au supported CuMnOx and CuMnOx catalyst aged for 1h in absence of moisture. CuMnOx catalyst tested in ambient conditions.

Figure 5.5 consists of a CuMnOx catalyst and Au supported CuMnOx catalysts aged for 1h and tested in the absence of moisture (cold trap present). Also shown is a CuMnOx catalyst aged for 1h aged but tested in ambient conditions.

The removal of moisture from the reaction system for catalyst aged for 1h has shown similar results to the shorter ageing times. In the absence of moisture, the initial activity of the catalysts is low compared to the catalyst tested in ambient conditions. The significant difference here is that, in the absence of moisture, the CuMnOx catalyst has the highest overall steady state activity (*ca.* 70% conversion). The

addition of Au to the CuMnOx catalyst has not improved the activity towards CO oxidation in the absence of moisture compared to the CuMnOx catalyst.

A trend is appearing in that the removal of moisture from the reactions does improve the activity of the Au supported CuMnOx catalyst but the improvement of the CuMnOx catalyst is much greater.

The activities for the short ageing times have been investigated and it can be suggested that the morphology of the CuMnOx catalyst plays an important part for CO oxidation in ambient conditions. The 0.5h and 1h aged CuMnOx catalysts have similar activities in both moisture and dry conditions. In terms of ageing times, these are relatively close together. The varying ageing times may cause different phases to be present in the final catalyst. The X-ray diffraction patterns, shown in Chapter 4, showed that different phases were present as the ageing time was increased.

A longer ageing time was investigated to see if there was a significant difference in catalytic activities. The other reason for considering a longer ageing time, in terms of industrial applicability, is that a shorter ageing would be commercially beneficial because of the faster through put of catalyst manufacture.

5.5 CuMnOx 6 h aged – moisture removed with cold trap

The longest ageing time chosen to produce a CuMnOx catalyst for depositing Au particles was 6h.

Figure 5.6 shows a CuMnOx catalyst aged for 6h and a range of Au supported CuMnOx catalysts aged for 6h in the presence of a cold trap (labelled CT). Also shown is a CuMnOx catalyst aged for 6h in the presence of moisture.
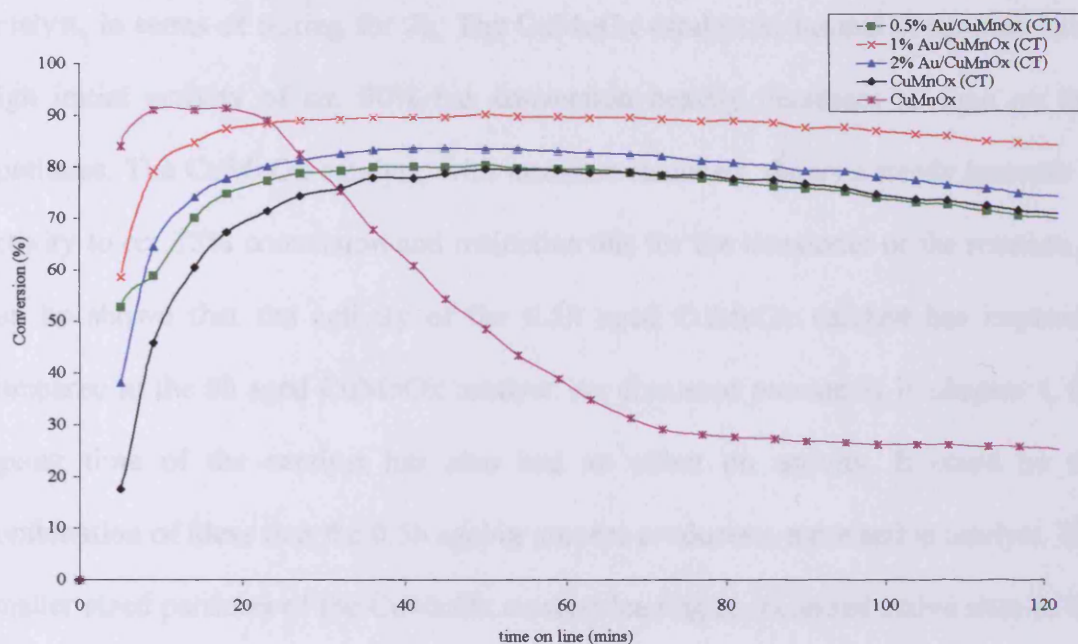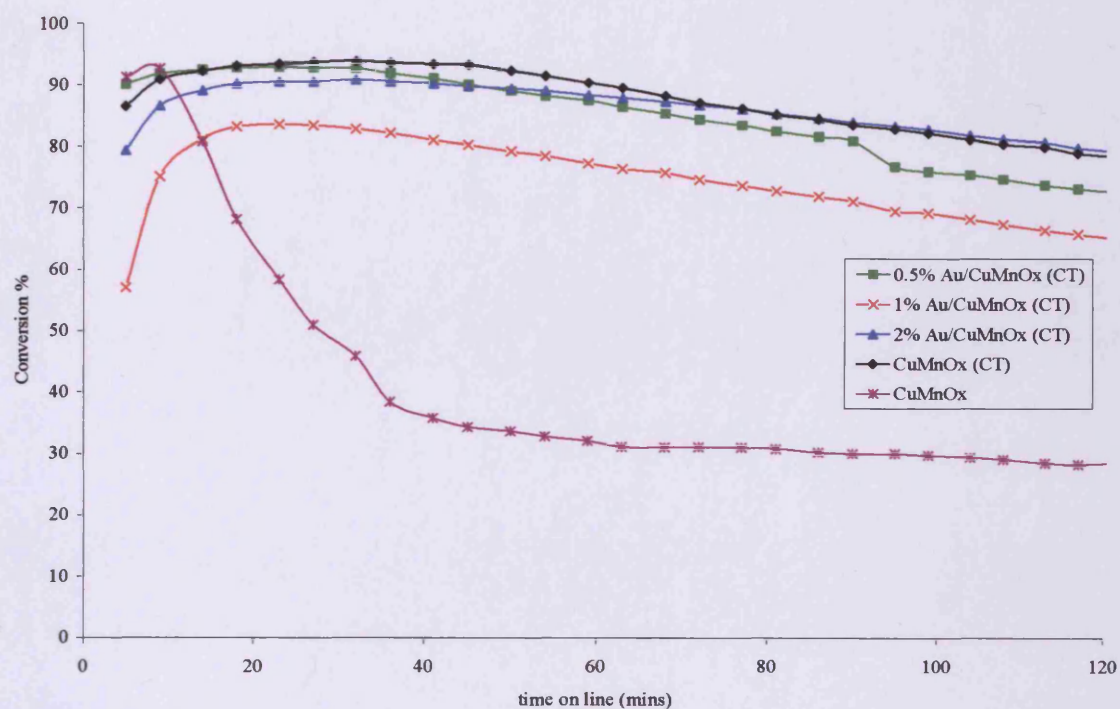

Figure 5.6 CO oxidation – Au supported CuMnOx and CuMnOx catalyst aged for 6h in the absence of moisture. CuMnOx catalyst tested in ambient conditions.

As shown previously, the CuMnOx and Au supported CuMnOx catalysts displayed little difference in catalytic activity in the presence of moisture (*ca.* 85% conversion). The addition of a cold trap and removal of moisture has shown noteworthy improvement not only steady state activity but also initial activity. This is the first ageing time discussed that shows high light off activities in the absence of moisture. The catalytic data shown in chapter 4 (figure 4.25) demonstrates that the addition of Au particles does not improve activity after 6h of ageing. However, it must be noted

that the activities of the CuMnOx and Au supported catalysts, in the presence of moisture, were relatively similar. An assumption is that the 6h ageing time has produced a CuMnOx catalyst that is not suitable for incorporating Au particles.

However, the 6h ageing time for the CuMnOx catalyst has shown improvement in activity in the absence of moisture. The longer ageing time produces a catalyst that has a morphology that is not suitable for the addition of a noble metal. As discussed in chapter 4, a highly active oxide would be more beneficial as a support for Au particles. However, this does not rule out the addition of a metal into the bulk structure of the catalyst.

The Au supported CuMnOx catalyst have shown that a method other than the co-precipitation method can improve the activity of the hopcalite catalyst towards CO oxidation. The deposition-precipitation method has shown that Au particles can be deposited onto the surface and have a significant effect. The suggestion would be whether this method used for depositing Au particles onto a CuMnOx catalyst could be used on a commercially available catalyst. The catalyst used was Moleculite^{TM} - manganese based mixed oxide.

5.6 Au supported on Moleculite^{TM}

The deposition-precipitation method described in chapter 2 was used to deposit Au particles onto the Moleculite^{TM} surface. Moleculite^{TM} is a commercially available catalyst that has similar properties to hopcalite. The preparation method was similar to the Au supported CuMnOx catalysts except the Au/Moleculite^{TM} was dried at 110°C for 16h and not calcined.

The Moleculite^{TM} catalyst was doped with 0.5 wt% and 1 wt% Au. The reason for these amounts of dopants was that to make the addition of gold particles to the catalyst commercially viable. If the catalytic activity of a catalyst could be improved by the addition of 1% or less dopant, the deposition precipitation method would be commercially attractive.
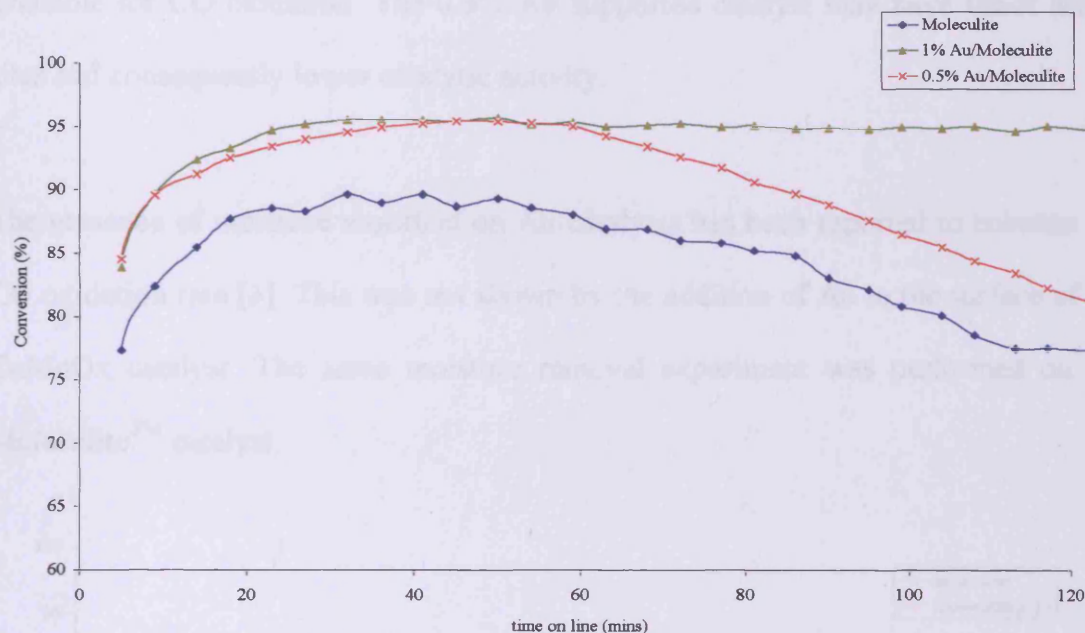
Figure 5.7 CO oxidation – Au supported Moleculite^{TM} in ambient conditions

Figure 5.7 shows the result of CO oxidation of a Moleculite^{TM} catalyst, 0.5 % and 1% Au supported Moleculite^{TM} catalyst. The catalytic data presented show that Au deposited particles onto the surface of the catalyst has improved activity. The reaction profile shown in figure 5.7 is typical for a Moleculite^{TM} catalyst. There is a high initial activity followed a slow deactivation process as time on line increases whereas the hopcalite catalyst has a high initial activity followed by a higher rate of deactivation. The 0.5% and 1% Au supported Moleculite^{TM} catalysts exhibit similar promotion effects for the first hour of catalyst testing.

The 1% Au supported catalyst maintains steady state activity whereas the 0.5% Au shows a gradual decrease in activity. This could be due to the Au particles deposited having a promotion effect but the difference in sustaining activity depends on amount of gold present. The difference in activity could be due to the dispersion of Au – 1% Au supported catalyst has highly dispersed particles leading more active sites available for CO oxidation. The 0.5% Au supported catalyst may have fewer active sites and consequently lower catalytic activity.

The presence of moisture absorbed on Au catalysts has been reported to enhance the CO oxidation rate [3]. This was not shown by the addition of Au to the surface of the CuMnOx catalyst. The same moisture removal experiment was performed on the Moleculite^TM catalyst.
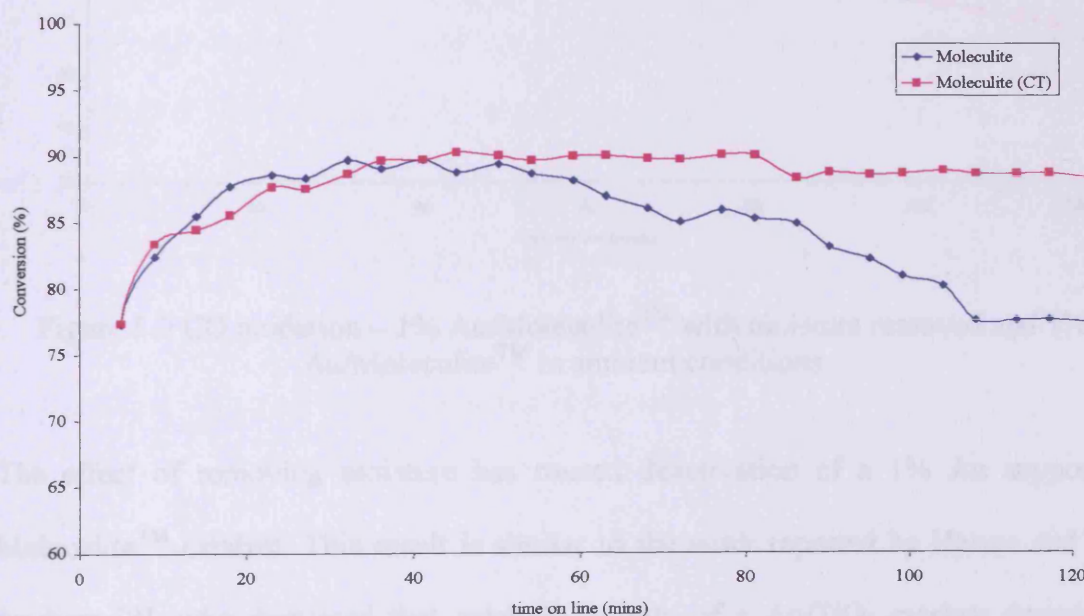
Figure 5.8 CO oxidation – Moleculite^TM in the absence of moisture and in ambient conditions

Figure 5.8 shows the Moleculite^TM catalyst tested in the presence and absence of a cold trap/moisture removal. The catalytic data shows that in a dry environment, the

Moleculite[TM] catalyst shows very little sign of deactivation. This result is similar to the CuMnOx catalysts tested in the absence of moisture.

Figure 5.9 exhibits an opposite effect of the 1% Au supported catalyst with the Moleculite[TM] catalyst in the absence of moisture. The removal of moisture from the gas line has caused the 1% Au supported Moleculite[TM] catalyst to deactivate compared to the same catalyst in ambient conditions.
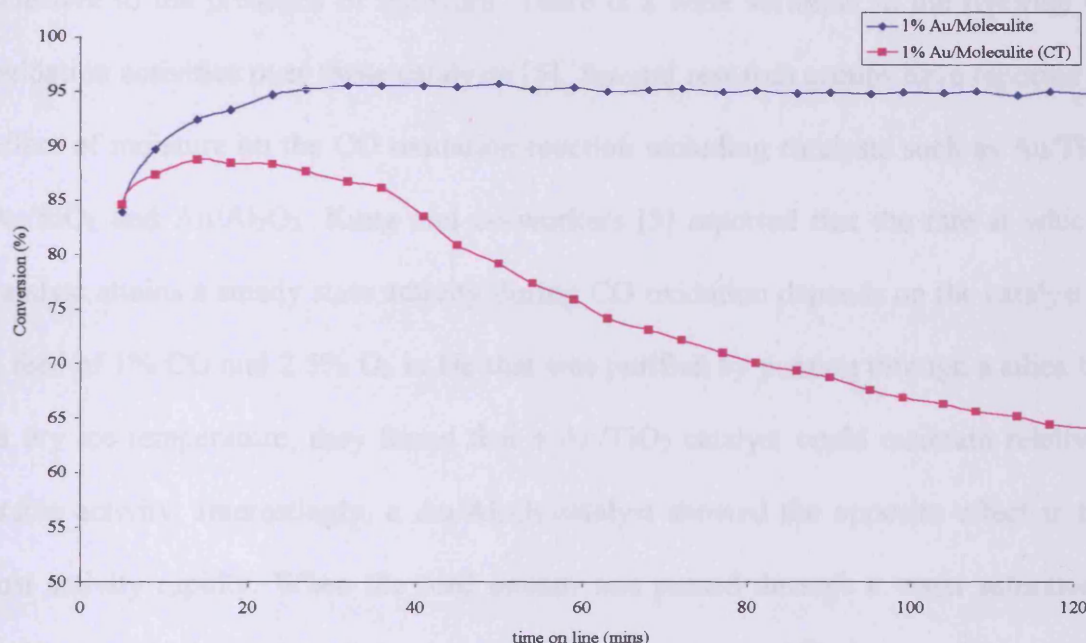
Figure 5.9 CO oxidation – 1% Au/Moleculite[TM] with moisture removed and 1% Au/Moleculite[TM] in ambient conditions.

The effect of removing moisture has caused deactivation of a 1% Au supported Moleculite[TM] catalyst. This result is similar to the work reported by Haruta and co-workers [2], who discussed that catalytic activity of a Au/TiO_2 catalyst decreased when the levels of moisture were removed from the gas stream. This result for Au supported on Moleculite highlights that moisture present has a positive effect on CO oxidation. The role of the water derived species, such as –OH, on the catalyst surface

should be considered. The presence of moisture may activate O_2 molecules or modify

the electronic state of the gold particles exposed at the surface.

5.7 Discussion

A feature of the CO oxidation reaction over Au supported catalysts is that it is

sensitive to the presence of moisture. There is a wide variation in the reported CO

oxidation activities over these catalysts [5]. Several research groups have reported the

effect of moisture on the CO oxidation reaction including catalysts such as Au/TiO_2,

Au/SiO_2 and Au/Al_2O_3. Kung and co-workers [5] reported that the rate at which a

catalyst attains a steady state activity during CO oxidation depends on the catalyst. In

a feed of 1% CO and 2.5% O_2 in He that was purified by passing through a silica trap

at dry ice temperature, they found that a Au/TiO_2 catalyst could maintain relatively

stable activity. Interestingly, a Au/Al_2O_3 catalyst showed the opposite effect in that

lost activity rapidly. When the feed stream was passed through a water saturator at

25°C, the initial activity of the Au/Al_2O_3 was maintained [6]. Kung and co-workers

did exercise caution in comparing CO oxidation activities between different research

groups due to the sensitivity to water partial pressure.

Haruta and co-workers studied the effect of moisture in the reactant gas on CO

oxidation over Au/TiO_2, Au/SiO_2 and Au/Al_2O_3 catalysts with a wide range of

concentrations from 0.1 ppm to 6000 ppm [2]. The effect of moisture became

considerable above 200 ppm H_2O for Au/Al_2O_3, while the activity for Au/SiO_2

diminishes noticeably with a decrease in moisture to about 0.3 ppm. The activity of

Au/TiO_2 at about 3000 ppm H_2O was so high that it reached 100% conversion of CO.

Haruta and co-workers discussed that the degree of rate enhancement depends on the type of support used: high for insulating Al_2O_3 and SiO_2; moderate for semi-conducting TiO_2. It is reported that the concentration of the residual moisture in a commercial gas cylinder is ca. 3ppm [7]. Baiker and co-workers have observed similar effects of moisture over Au/TiO_2 [8] and proposed that the inhibition effect of water at high moisture content is due to adsorption of water on the active site or due to pore filling. Haruta and Baiker have reported using a cooling trap in the feed gas line to control the moisture content, but this practice has not been commonly employed in many other studies. This may be a source of differences in the CO oxidation activities between various research groups.

The results of the Au supported CuMnOx catalysts in the absence of residual moisture are different to the catalysts report by Haurta and co-workers and by Kung and co-workers. The decrease in moisture content of the gas feed to the micro reactor improved, not only activity of the Au supported CuMnOx catalysts, but also the CuMnOx catalyst. The catalytic activities of the Au supported catalysts tested in ambient conditions (chapter 4), show that the presence of gold makes the hopcalite catalyst more moisture tolerant than a catalyst without Au. In the absence of moisture, the Au supported CuMnOx catalysts show similar activities to the CuMnOx catalysts. This means that the choice of support for Au supported catalysts for CO oxidation is very important. As discussed before, the water durability of a hopcalite catalyst is poor at ambient conditions [1]. This leads to a discussion of the mechanism taking place and what species may be present that may promote or inhibit activity. It would be possible to propose that with Au particles in contact with the CuMnOx, there are two active phases. Activity from the lattice oxygen of the CuMnOx 'support' in addition, gold deposited particles are providing active sites. The improvement of

catalytic activity could be a synergy between active sites on the support and sites associated with gold particles.

The mechanism of CO oxidation by Bond and Thompson [9] and Kung [10-11] and co-workers are similar. The model is that CO is adsorbed on the Au cation and is inserted into the hydroxyl group to form a hydroxycarbonyl. Oxidation of the hydroxycarbonyl will result in the formation of the bicarbonate which is decarboxylated to CO_2, and the active site Au-OH is regenerated.

Knell and co-workers [12] proposed a similar reaction sequence for CO oxidation over Au/ZrO_2. They also ascribed the deactivation of Au/ZrO_2 to the high concentration of surface formate which is very stable in the presence of excess oxygen and consequently blocks active sites.

Boccuzzi and co-workers [13] have suggested that multiple reaction pathways are operative during CO oxidation over supported Au catalysts. Different catalyst preparations lead to different reaction pathways. This could be possible since different research groups have detected different surface species. Quantum chemical calculations have offered insight into the reaction mechanism. The support may play an active role. It provides a metal-support interface where adsorption of oxygen becomes favorable [14], and it may stabilize a O-O-CO intermediate [15]. The oxidation reaction occurs on Au steps in two steps: $CO + O_2 \rightarrow CO_2 + O$, and $CO + O \rightarrow CO_2$ [14].

Y.-M Yang and B.-Z. Wan [16] have reported the presence of moisture of CO oxidation over gold/iron/zeolite-Y catalyst. They suggest that water vapour is

probably strongly absorbed and suppresses the ability of the catalyst to chemisorb oxygen. The presence of water has been shown to inhibit the adsorption of oxygen on metal oxide surfaces. Takita and co-workers [17] have discussed that as the quantity of water was increased over a Co_3O_4 surface, the quantity of oxygen available to populate the surface decreased. Co_3O_4 has similar properties to $CuMn_2O_4$, in that they are both spinel structures. Desiccants in combination with hopcalite catalysts have been used as protectors to the catalysts from the effects of moisture [18].

The possible reaction pathways taking place during CO oxidation could be due to a few factors. The accumulation of carbonate species at the surface of the catalyst that blocks active sites resulting in deactivation. In ambient conditions (presence of moisture) the Au supported CuMnOx catalysts show significant improvement in catalytic activity. The role of the Au particles play an important part in the presence of trace amounts of moisture. The decomposition of the carbonate species accumulated during the reaction at the perimeter interface between the Au particles and the oxide support. The carbonate species block active sites, its removal results in enhancement of the steady state activity. The CuMnOx catalyst shows lower steady state activity due to the moisture present that may be blocking active sites that prevent the decomposition of the carbonate species. Also, the presence of moisture could inhibit the adsorption of oxygen onto the support required for conversion of CO.

In the absence of moisture (presence of cold trap) the Au supported CuMnOx catalyst shows no significant improvement in activity compared to the CuMnOx. There could be possible causes for this result. The removal of moisture from the gas feed may have caused the active sites present, in CuMnOx, to become uninhibited and available for oxygen adsorption. The lowering of the amount of moisture could lead to one

active site becoming more predominant than another. The active sites that may be present involve the interface of Au particles with the oxide support. In the absence of moisture, the active sites of the CuMnOx catalyst could be more predominant than the Au particles – support interface. The small improvement of the Au supported catalysts, in the absence of moisture, could be that actually not all of the moisture has been removed or residual moisture from the catalyst could be present. Zou [19] and co-workers have reported that thermal treatment of a Au/Al$_2$O$_3$ catalyst contributed to the lowering of its catalytic activity for CO oxidation.

Janssens and co-workers [20] reported that it is possible to obtain different contributions to the overall activity via multiple reaction pathways occurring simultaneously. Remediakia and co-workers proposed two different reaction pathways for CO oxidation on Au nanoparticles: a 'gold only' pathway and a 'metalloxide boundary' pathway. In both pathways, the function of the low co-coordinated Au atoms is to bind the CO molecules [21-22]. The difference between these pathways lies in how the oxygen is adsorbed on the Au nanoparticle; there is no significant interaction between the oxygen and the support. In the metalloxide boundary pathway, the adsorbed oxygen interacts with the support, thus a mechanism is feasible only at the Au-support interface. The majority of Au supported catalysts involve a support, which alone is inactive towards CO oxidation. The advance of using CuMnOx as a support is that alone it is highly active for CO oxidation. This suggests there are three possible reactions pathway for CO oxidation. This proposed mechanism for a Au supported CuMnOx catalyst is illustrated in Figure 5.10. This highlights three possible reactions taking place during CO oxidation; gold only route, a 'metalloxide boundary' route and a support route. The red arrow represents lattice oxygen bulk diffusion.
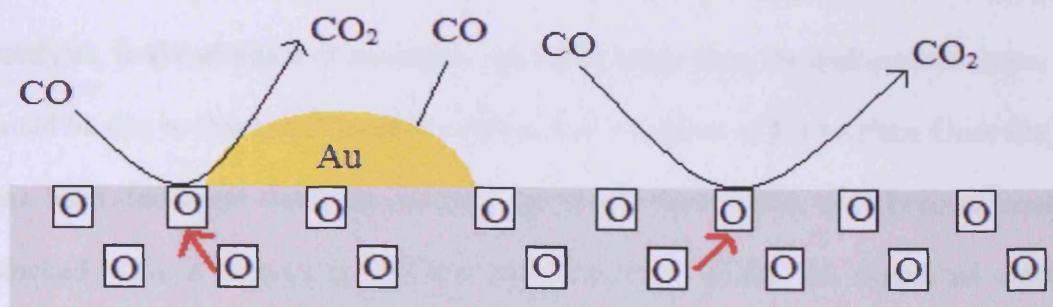
Figure 5.10 Reaction mechanism for CO oxidation with Au supported CuMnOx

Figure 5.11 shows the mechanism taking place with a CuMnOx catalyst that contains no Au particles. This mechanism can also be related to the zinc doped CuMnOx catalysts discussed in Chapter 3.
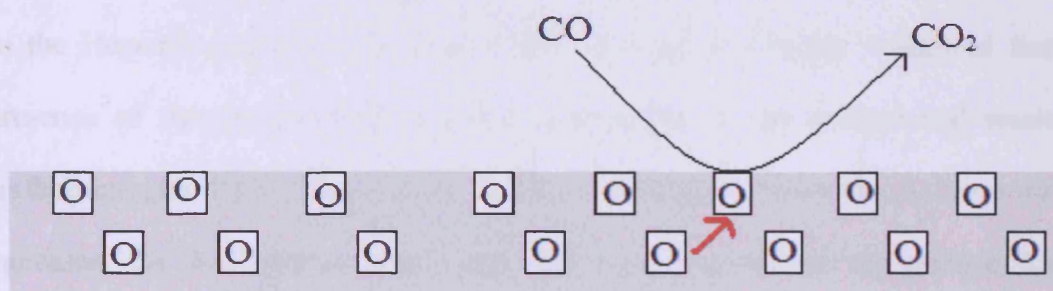
Figure 5.11 Reaction mechanism for CO oxidation with CuMnOx

The overall 'ideal' reaction conditions for CuMnOx based catalysts could be a combination of factors. The low amount of hydroxyl groups may be required for efficiency of the Au supported CuMnOx for catalytic activity. A dry environment would significantly improve the activity of the CuMnOx catalyst, but this would cause problems in terms of storage and handling. Different catalysts require different reaction conditions to have maximum efficiency.

The catalytic data in this chapter shows that the initial activities of Au supported catalysts, in the absence of moisture, are much lower than the undoped catalysts. This could be due to that the Hopcalite catalyst has a number of active sites. Once the gold has been deposited onto the catalyst, some of these active sites become cover or blocked. This is shown by the low initial activity of the Au supported catalysts. However, the undoped Hopcalite catalyst, in the absence of moisture, also has low initial activity.

The Au supported catalysts have low initial conversion; this could be due to active sites of the support being covered by gold particles. However CO conversion increases with time on line. This could be due to a number of factors. The Au particles are acting as active sites themselves but not significantly improving activity compared to the Hopcalite catalyst. Also, the TPR analysis in Chapter 4 showed that the presence of Au particles increased the reducibility of the catalyst and weakened surface oxygen. This oxygen reacts at the gold-support interface. As time on line increases, the Au particles continually use oxygen atoms on the surface. Lattice oxygen is being transporting to the surface to replace the surface oxygen. It must be noted that the moisture in the gas feed may have not been totally removed, there may be low amounts of moisture present. The role of low amounts of –OH could be involved with Au particles present and carbonate species forming at the surface. The involvement of OH groups in the reaction intermediate in the form of hydroxyl carbonyl (CO-Au-OH) could be a possibility. In some cases, the Hopcalite has higher conversion of CO than Au supported catalysts in the absence of moisture. Overall, to produce a highly active catalyst there is relationship between the active phase of the support and the amount of Au particles deposited. It would have been interesting to

have tested these catalysts for a longer period to see how long it would take to obtain complete deactivation.

The main active sites are due to the support but the Au particles play an important role in increasing the amount of lattice oxygen available for CO conversion. Enhancing the removal of carbonate species, that appears to block active sites on the Hopcalite support. It would be of interest to investigate the source of oxygen in the reaction. Using labeled oxygen would enable to determine whether lattice oxygen is playing an important part in CO oxidation. Temperature programmed desorption experiments would be useful to determine what species are being removed from the catalyst surface, for example carbonyl species or labeled oxygen.

The amount of moisture present in the gas feed after using the cold trap was not determined. It would be beneficial to set up apparatus that would monitor the levels of moisture to determine at what moisture level the catalysts become highly active.

5.8 Conclusion

A series of CuMnOx and Au supported CuMnOx catalysts have been produced and tested in ambient and moisture free conditions. Moisture may play a role by the activation of oxygen and the decomposition of carbonate species accumulated during the reaction for Au supported CuMnOx. The experiments have shown that the deposition precipitation method for depositing gold particles onto a catalyst surface has proven to be successful. There is a possibility that several possible reactions are taking place during the CO oxidation reaction. This leads on to the possibility of

studying the actual mechanism taking place during CO oxidation and the choice of support required to achieve promotion of catalytic activities.

5.9 Chapter 5 References

[1]   M. I. Brittan, H. Bliss, C.A. Walker, AIChE J. 16 (1970) 305.

[2]   M. Date, M. Okumura, S. Tsubota, M. Haruta, Angew. Chem. Int. ed. 43 (2004) 2129

[3]   M. Date and M. Haruta, J. Catal. 201 (2001) 21.

[4]   C.K. Costello, J.H. Yang, H.Y. Law, Y. Wang, J.-N. Lin, L.D. Marks, M.C.Kung, H.H. Kung, Appl. Catal. A: Gen. 243 (2003) 15.

[5]   H. H. Kung, M. C. Kung, C. K. Costello, J. Catal. 216 (2003) 425.

[6]   C. K. Costello, J. H. Yang, H. Y. Law, Y. Wang, J.-N. Lin, L. D. Marks, M. C. Kung, H. H. Kung, Applied Catal. A: Gen. 232 (2002) 159.

[7]   M. Haruta, Catal. Surv. Jpn. 1 (1997) 61.

[8]   J.-D. Grunwald, C. Keener, C. Wogerbauer, A. Baiker, J. Catal. 181 (1999) 223.

[9]   G. C. Bond, D. T. Thompson, Gold Bull. 33 (2000) 41.

[10]   H.-S. Oh, C. K. Costello, C. Cheung, H. H. Kung, M. C. Kung, Stud. Surf. Sci.and Catal. 139 (2001) 375.

[11]   H.-S. Oh, C. K. Costello, C. Cheung, H. H. Kung, M. C. Kung, in Proceedings of the papers presented at the Pacific Chem. Conference, December 2000 and at the North American Catalysis Society Meeting, June 2001.

[12]   A. Knell, P. Barnickel, A. Baiker, A. Wokaun, J. Catal. 137 (1992) 306-321.

[13]   F. Boccuzzi, A. Chiorinio, A. Tsubota, H. Haruta, J. Phys. Chem. 100 (1996) 3625.

[14]   Z.-P. Liu, P. Hu, and A. Alavi, J. Amer. Chem . Soc. 124 (2002) 14770.

[15]   L. M. Molina and B. Hammer, Phys. Rev. Lett. 90 (2003) 206102.

[16]   Y.-M. Kang, B.-Z., Catal. Today, 26 (1995) 59-69.

[17]   Y. Takita, T. Tashiro, Y. Saito, F. Hori, J. Catal. 97 (1986) 25.

[18]   N. Harwood, J. Wojtasik, US Patent 4,925,631, 15th May 1990.

[19]   X.-H. Zou, S.-X. Qi, Z. H. Suo, L.-D An, F. Li, Cat. Comm. 8 (2007) 784-788.

[20]   T.V.W. Janssens, A. Carlsson, A. Puig-Molina, B.S. Clausen, J. Catal. 240 (2006) 108-113.

[21]   I.N. Remediakis, N. Lopez, J.K. Nørskov, Angew. Chem. Int. Ed. 44 (2005) 1824.

[22]   I.N. Remediakis, N. Lopez, J.K. Nørskov, Appl. Catal. A 291 (2005) 13.

Applications of CuMnOx based catalysts for oxidation reactions

6

6.1 Introduction

Copper manganese mixed oxide catalysts have been extensively researched for ambient temperature CO oxidation. The previous chapters have demonstrated that the activity of the CuMnOx catalyst can be improved by the addition of dopants. In recent times, there has been increased interest in a range of oxidation reactions. The literature review in Chapter 1 highlighted alternative reactions where this type of catalyst may be applied. The catalytic data presented so far has dealt with oxidation reactions at ambient temperature. The aim of this chapter is to investigate the possibility of CuMnOx catalysts for higher temperature oxidation reactions. The reactions investigated were:

- Ethylene oxide oxidation

- Preferential oxidation of carbon monoxide

6.2 Volatile Organic Compounds – Ethylene oxide

Volatile organic compounds (VOCs), emitted from industrial processes and automobile exhaust emissions, are recognised as major contributors to air pollution because of their toxic properties and their involvement in the formation of photochemical smog. The emissions of VOCs are subject to strict legislation [1]. In air pollution control, catalytic combustion is used to oxidise VOCs to CO_2 and H_2O. As the catalytic combustion is mainly applied at low VOC concentration [2], heat recovery by downstream heat exchangers or by catalyst coated heat exchangers have been reported [3].

Supported precious metals, such as platinum and palladium, are most commonly used for catalytic combustion. However, single and mixed metal oxides are also used in reactions [4-6]. Among these non-noble metal oxide catalysts investigated; manganese oxides have exhibited high activity for VOC removal. Lahousse and co-workers [7] compared performances of Pt/TiO_2 and γ-Mn_2O_3 catalysts for VOC removal and stated that the latter one was more active than the noble metal based catalyst. The catalytic properties of MnOx based catalysts are attributed to the ability of manganese to form oxides with different oxidation states and their high oxygen storage capacity [8]. Chang and McCarthy stated that a MnOx catalyst has higher oxygen storage capacity, faster oxygen adsorption and oxide reduction rates than the present commercial ceria-stabilised alumina support [9].

A mixture of the oxides of manganese and copper produce an oxidative catalyst which was first used to convert carbon monoxide to carbon dioxide [10-12].The catalyst also has oxidative activity towards hydrogen, numerous alkanes, alkynes, aromatics, and

nitrogen containing organic compounds generally resulting in complete oxidative decomposition to carbon dioxide and water [13-16].

Ethylene oxide is the simplest cyclic ether. It is a colourless gas or liquid. Ethylene oxide is very reactive because its highly strained ring can be easily opened, and is thus one of the most versatile chemical intermediates. Ethylene oxide is used as an intermediate for many organic syntheses. Derivatives of ethylene oxide, especially ethylene glycol, are commonly used in the plastics industry for manufacturing bottles and to produce polyester fibres for clothing and furniture [17]. Significant quantities of ethylene oxide are released into the atmosphere from sterilisation processes of healthcare materials and other heat sensitive products in medical facilities.

An effect of ethylene oxide on human health consists of inducing a wide range of tumours and interactions with genetic material. Generally, it is considered that exposure of ethylene oxide at any level is harmful to health. Ethylene oxide emissions can be treated by different technologies; these are wet-scrubbers, thermal oxidisers, catalytic oxidisers and reactors or columns loaded with solid sorbents. Thermal oxidisers operate by oxidising or burning ethylene oxide to form products of CO_2, water vapour and heat. Thermal oxidisers generally require additional fuel whereas catalytic oxidisers operate with the same end result but at lower temperatures [18].

Copper manganese mixed oxide catalysts for ambient temperature CO oxidation has been extensively researched. These catalysts, prepared by a co-precipitation method described in chapter 2, have shown good activity towards CO oxidation. The addition of gold particles to the CuMnOx catalyst has improved activity. However, there is little in the literature investigating these types of catalysts for ethylene oxide

oxidation. The aim for this part of the chapter was to study these catalysts for VOC destruction and compare them with the activity of a commercially available catalyst. The catalysts used for the study of ethylene oxide oxidation were the same catalysts investigated in chapters 4 and 5, CuMnOx and Au supported CuMnOx catalysts. The same variables were investigated; the ageing time of the precursor and the amount of Au dopant present.

6.2.1 CuMnOx and Au supported CuMnOx catalysts aged for 0h
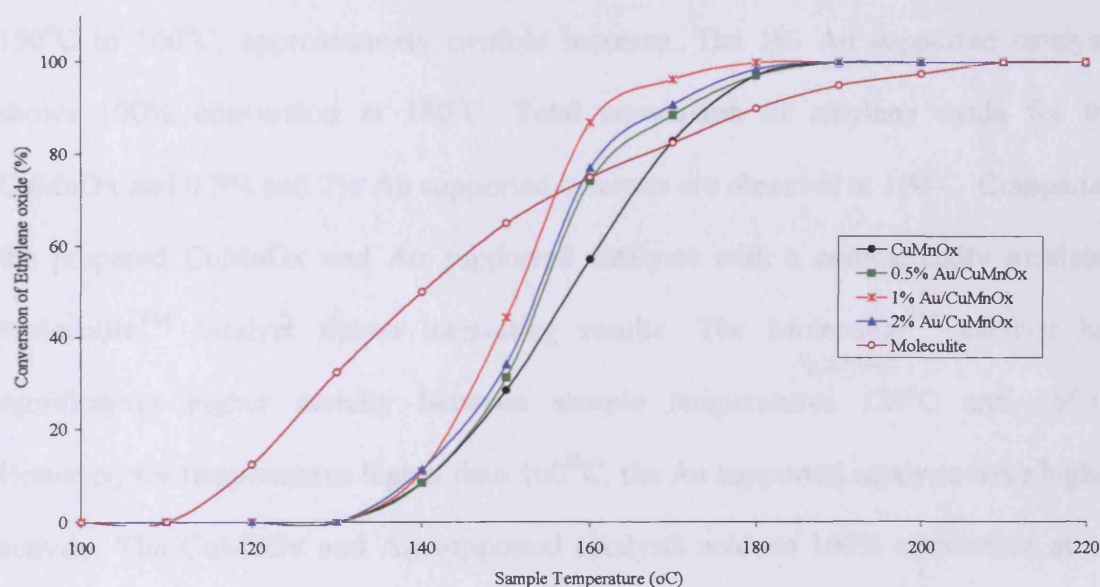
Figure 6.1 Ethylene oxide conversions for CuMnOx, Au supported CuMnOx catalysts aged for 0h and Moleculite^{TM}. A mixture of ethylene oxide (3000ppm EtO in balance N$_2$, 18ml/min) and O$_2$ (3ml/min) were fed to the reactor.

CuMnOx and Au supported CuMnOx catalysts aged for 0h were investigated for the oxidation of ethylene oxide. The conditions and experimental procedures are summarised in chapter 2. The catalyst was held in a straight wall reactor tube and the temperature of the catalyst bed was increased to 220°C, in intervals of 10°C. The

initial temperature of the catalyst testing was 30°C, however, no conversion was observed below 100°C. The concentrations of reactant and product gases were calibrated and carbon mass balances were checked.

The catalytic activities of ethylene oxide oxidation were measured as a function of reaction temperature on a series of catalysts aged for 0h. The addition of Au particles has improved activity compared to the CuMnOx catalyst. The 1% Au supported catalyst has the overall highest activity of the catalysts under investigation. Figure 6.1 shows considerable increase in conversions for the catalysts, from sample temperature 150°C to 160°C, approximately twofold increase. The 1% Au supported catalysts shows 100% conversion at 180°C. Total conversion of ethylene oxide for the CuMnOx and 0.5% and 2% Au supported catalysts are observed at 190°C. Comparing the prepared CuMnOx and Au supported catalysts with a commercially available Moleculite™ catalyst shows interesting results. The Moleculite™ catalyst has significantly higher activity between sample temperatures 120°C and 160°C. However, for temperatures higher than 160°C, the Au supported catalysts have higher activity. The CuMnOx and Au supported catalysts achieve 100% conversion at ca. 190°C, whereas the commercial catalyst reaches total conversion at 210°C. The possible reasons for improvement in activity for the Au supported catalysts are collectively discussed in Section 6.2.5.

6.2.2 CuMnOx and Au supported CuMnOx catalysts aged for 0.5h

The catalytic activities of the catalysts aged for 0.5h were similar to the 0h catalysts. The 0h aged catalysts (Figure 6.1), initial conversion occurred at 140°C whereas the 0.5h aged catalysts (Figure 6.2) show activity at 120°C. In figure 6.2, it is shown that

During catalyst testing, the temperature of the sample was increased in $10^{\circ}C$ increments to a desired temperature and then decreased in a similar stepwise manner. The results for this procedure of increasing and decreasing sample temperatures are shown in Figure 6.3.
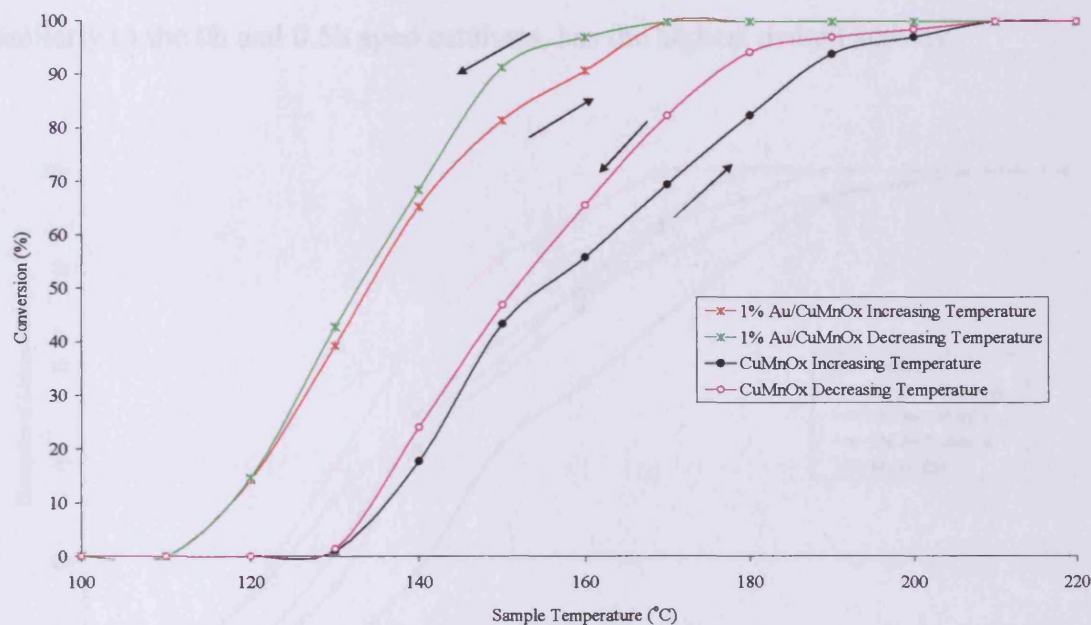
Figure 6.3 Effect of increasing then decreasing sample temperature on EtO conversion.

The activity curves of decreasing the sample temperature lies above that for increasing the temperature, indicating that the activity of the catalyst does increase with reaction time. There is evidence from Figure 6.3 that a temperature hysteresis is occurring when adjusting sample temperature to a lower value. Hysteresis is explained as when the measured temperature of the catalyst decreases below the ignition temperature. As a result, local overheating sites appear, and their temperature is essentially higher than the average temperature of the catalyst [19]. However, the

descending branch overlaps on the ascending branch with increasing sample temperature at higher ethylene oxide conversion.

6.2.3 CuMnOx and Au supported CuMnOx catalysts aged for 1h

The catalysts aged for 1h show significant differences in activity between the CuMnOx and Au supported samples (Figure 6.4). The 1% Au supported sample, similarly to the 0h and 0.5h aged catalysts, has the highest overall activity.
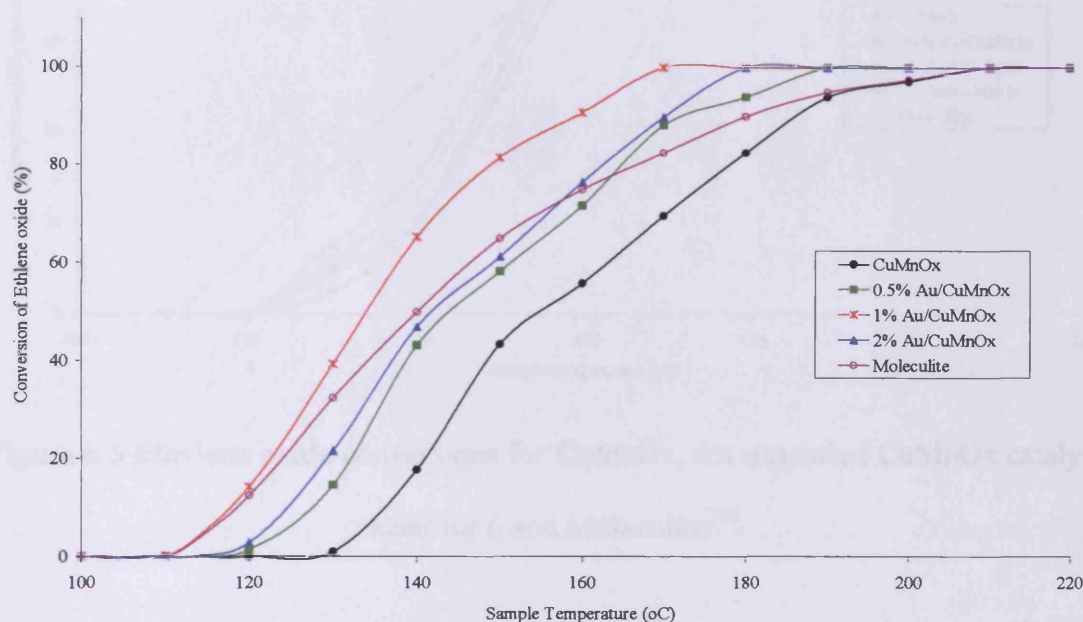
Figure 6.4 Ethylene oxide conversions for CuMnOx, Au supported CuMnOx catalysts aged for 1h and Moleculite^{TM}.

The 1% Au supported catalyst shows the highest initial activity at 120°C (ca.15% conversion) and total conversion of ethylene oxide at 170°C. The order of activity for the catalysts is 1% Au > 2% Au > 0.5% Au > CuMnOx. The interesting result is for the 1% Au supported CuMnOx catalyst. The supported catalyst exhibits higher catalytic activity, between 120°C and 210°C, than Moleculite^{TM}. The addition of Au to CuMnOx produces a catalyst that has higher activity than the commercial catalyst at temperatures above 160°C.

6.2.4 CuMnOx and Au supported CuMnOx catalysts aged for 6 h

The catalytic data for the samples aged for 6h (Figure 6.5) shows that the addition of Au particles has improved activity towards ethylene oxide conversion.
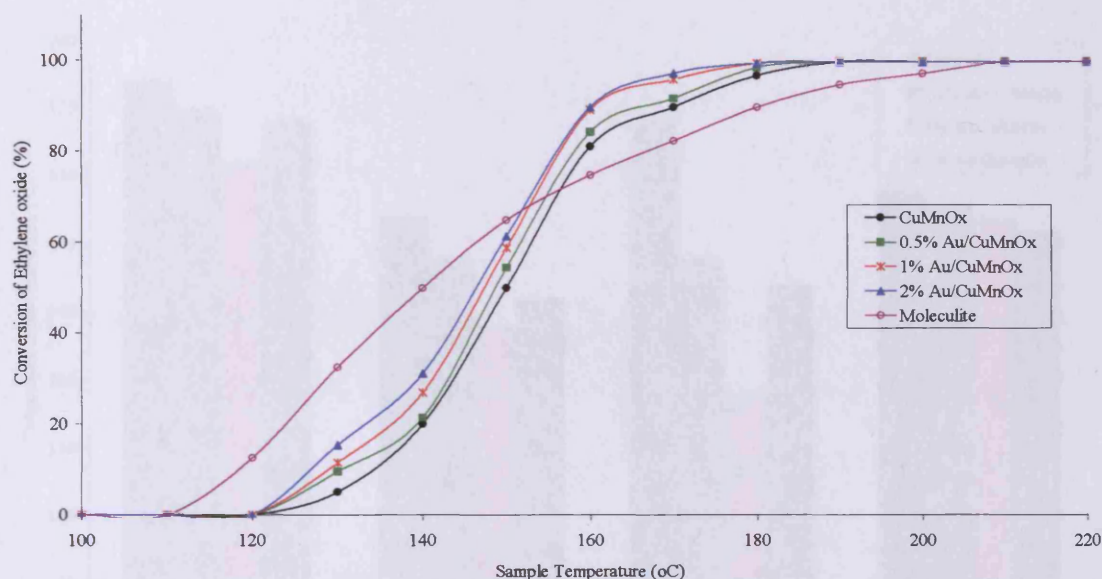
Figure 6.5 Ethylene oxide conversions for CuMnOx, Au supported CuMnOx catalysts aged for 6 and Moleculite^{TM}.

The addition of 2wt% Au to the CuMnOx catalyst has improved conversion by 10% compared to the CuMnOx catalyst. 100% conversion is observed for the 1% and 2% Au supported samples at 180°C, the 0.5% supported sample and CuMnOx catalyst shows total conversion at 190°C. The 6h aged catalysts show lower activity for ethylene oxide conversion compared to the Moleculite^{TM} catalyst, at temperatures between 120°C and 150°C. As the sample temperatures are increased from 150°C to 200°C, the Moleculite^{TM} catalyst becomes the least active.

6.2.5 Discussion of ethylene oxide conversion

Transition metal oxide supported gold catalysts exhibit high activity towards different kinds of reactions, especially CO oxidation at relatively low temperatures [20].
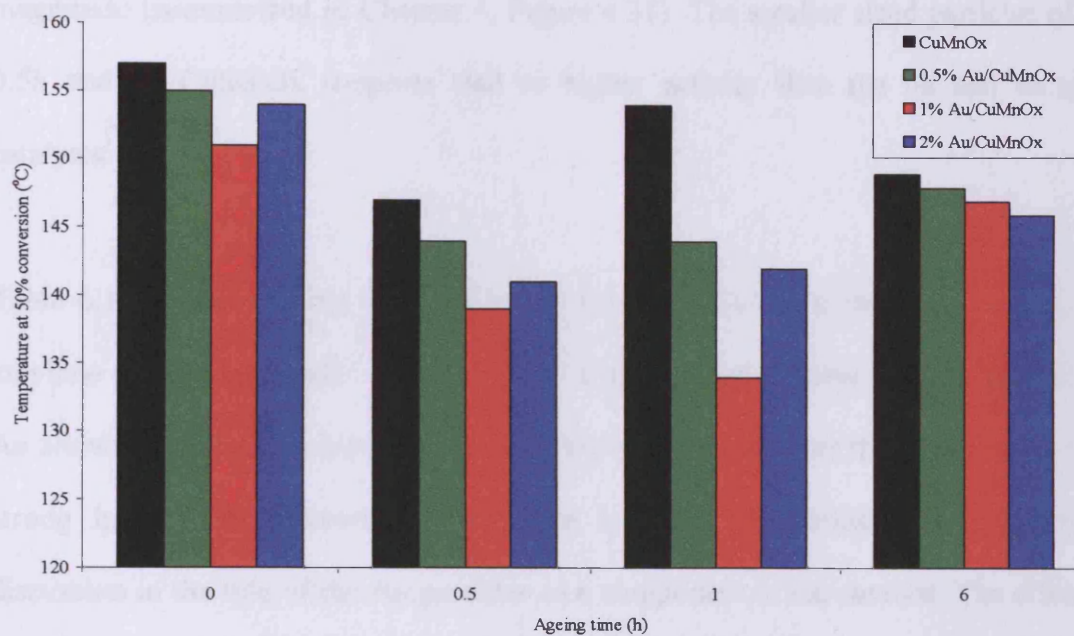
Figure 6.6 Dependence of the temperature of 50% conversion of ethylene oxide on Au supported CuMnOx contents for samples aged at 0h, 0.5h, 1h and 6h, respectively.

The ageing times for the CuMnOx catalyst have an effect on not only the conversion of CO at ambient temperature but also for ethylene oxide conversion. The data presented in Figure 6.6 shows that there is an order of ageing times for catalytic activity: 1h aged > 0.5h aged > 6h aged > 0h aged. It is interesting to note that this is in a similar order of activity observed for CO oxidation. The 0.5h and 1h aged catalysts having higher activities than the 0h and 6h aged samples. The similarity of the order of catalytic activity for the aged catalysts supports that idea that the preparation conditions of the CuMnOx support is paramount. The SEM images of the

differently aged catalysts were discussed in Chapter 4. The images showed that varying the ageing time, different morphologies and particle sizes were produced. The 0h and 6h aged samples showed large spherical particles ca. 5μm in size. The 0.5h and 1h aged catalysts displayed much smaller particle sizes which were ca. 2μm in magnitude (summarised in Chapter 4, Figure 4.31). The smaller sized particles of the 0.5h and 1h CuMnOx supports lead to higher activity than the 0h and 6h aged catalysts.

Table 6.1 summarises that the addition of Au to the CuMnOx improves activity for ethylene oxide conversion. The 0.5h and 1h aged samples show that the addition of Au shows considerable improvement in activity. This indicates that there could be a strong interaction between gold and the support. This brings about a similar discussion in the role of the Au particles as a component of the catalyst. The effect of Au on the catalytic activity of Au supported CuMnOx catalysts can be explained by TPR analysis. The peaks associated with copper reduction (Peak A) and manganese reduction (Peak B) along with the temperatures for ethylene oxide conversion of 50% is shown in Table 6.1. The TPR data shows a general trend that the addition of Au to the CuMnOx catalyst shows an increase of reducibility. For example, comparing the CuMnOx and 1% Au supported catalysts aged for 1h, the peak associated with copper reduction shifts from 233°C to 206°C with the addition of Au particles. This could be due to the addition of gold weakening surface oxygen on the CuMnOx catalyst. It must be noted that the redox properties for catalytic oxidation and reducibility obtained by TPR analysis are related, but they are not equivalent. The oxidation part of the redox cycle is missing and H_2 gas was not employed in catalytic tests. However, the increase in reducibility when gold is present is likely to be related to the

improvement of the redox properties. This may be due to the introduction of defects around the interface of the gold particles on the surface of the CuMnOx support.

Ageing	Catalyst	TPR Peaks Peak A (°C)	Peak B (°C)	EtO Conv. T_{50} (°C)
0h aged	CuMnOx	254	300	157
	0.5% Au/CuMnOx	251	298	155
	1% Au/CuMnOx	198	248	151
	2% Au/CuMnOx	231	276	154
0.5h aged	CuMnOx	252	295	147
	0.5% Au/CuMnOx	213	254	144
	1% Au/CuMnOx	176	226	139
	2% Au/CuMnOx	198	239	141
1h aged	CuMnOx	233	278	142
	0.5% Au/CuMnOx	218	253	144
	1% Au/CuMnOx	206	241	134
	2% Au/CuMnOx	234	274	142
6h aged	CuMnOx	233	297	149
	0.5% Au/CuMnOx	234	296	148
	1% Au/CuMnOx	242	298	147
	2% Au/CuMnOx	239	302	146

Table 6.1 Catalytic behaviour of CuMnOx and Au supported catalysts for ethylene oxide conversion, showing reaction temperature T_{50} for 50% EtO conversion and TPR data.

It has been widely reported that several combustion reactions take place through a Mars van Krevelen redox mechanism [21-23]. Ethylene oxide oxidation has been described by several kinetic mechanisms; the Langmuir-Hinshelwood mechanism where surface reaction proceeds between weakly adsorbed species; the Eley-Rideal mechanism where the surface oxygen reacts with EtO from a gas phase. Arsenijević and co-workers have discussed that deeper insight into the reaction mechanism and

further comprehensive investigations are required [18]. Following from discussions of the possible mechanisms for CO oxidation using CuMnOx and Au supported catalysts, the redox properties are more complicated. The CuMnOx catalysts show reasonable activity for ethylene oxide conversion. This would imply that there are three possible types of active sites. The presence of gold could cause possible surface defects on sites of the oxide support, the surface of gold particles could possess active sites and sites at the interface between the Au particles and the support. These active sites have been reported in low temperature oxidation of CO on oxide supported Au catalysts [24]. Solsona and co-workers [25] reported the promotional effect of Au supported on transition metal oxides for propane conversion. They discussed that the metal oxide supports were active for alkane oxidation in the absence of gold.

A comparison of the activities of the CuMnOx and Au supported CuMnOx catalysts for ambient temperature CO oxidation and ethylene oxide oxidation are summarised in Figures 6.7 and 6.8. It can be seen from Figure 6.7 and 6.8 that the addition of Au to CuMnOx has an effect on the activities towards EtO oxidation and CO oxidation. The catalysts aged for 0h, 0.5 and 1h show improvement in activity, for both reactions, with the addition of 1% Au. The 1% Au supported CuMnOx catalysts show the highest activities towards ambient temperature CO oxidation and higher temperature EtO oxidation. This suggests that Au supported CuMnOx catalysts possess similar active sites for ethylene oxide conversion with ambient temperature CO oxidation.
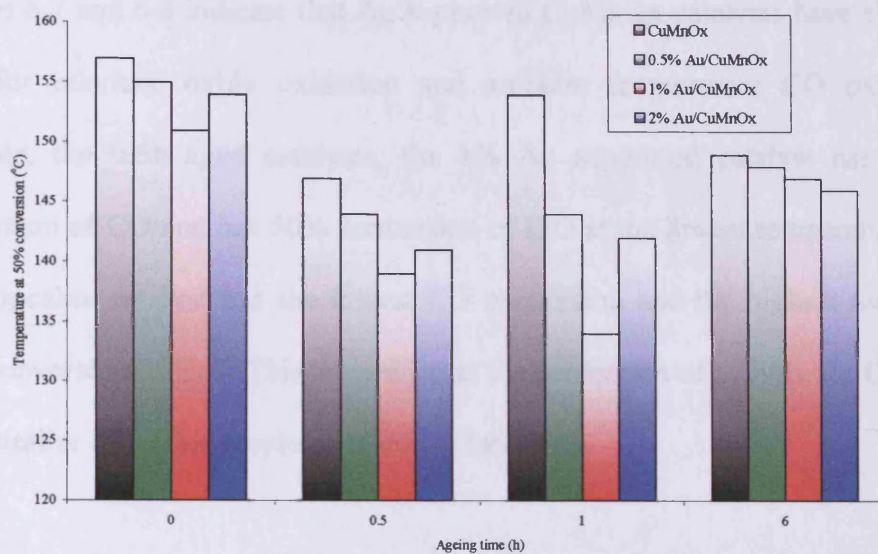
Figure 6.7 Comparison of temperatures using CuMnOx and
Au supported CuMnOx catalysts at 50% EtO conversion.
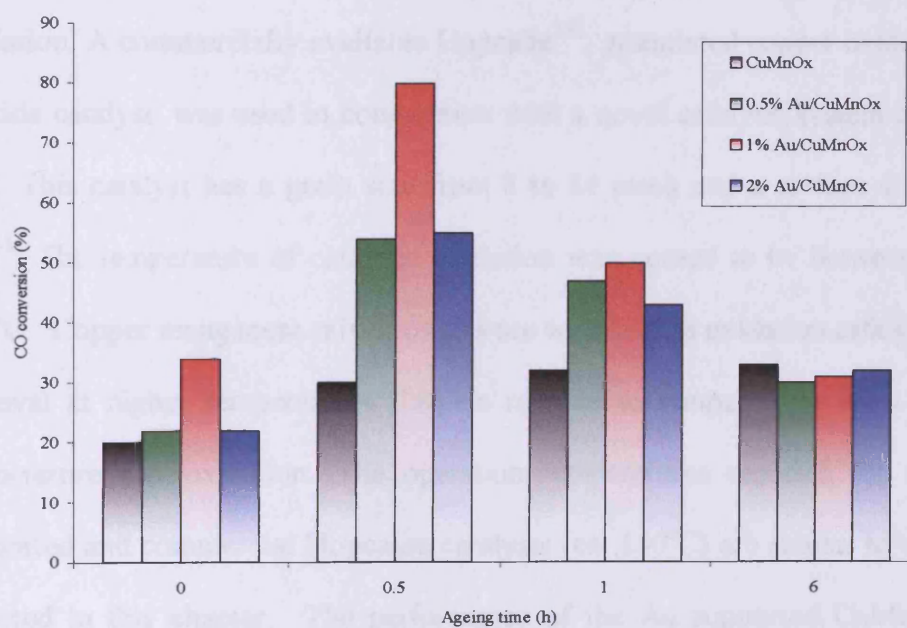
Figure 6.8 Comparison of CO oxidation using CuMnOx and
Au supported CuMnOx catalysts

Figures 6.7 and 6.8 indicate that Au supported CuMnOx catalysts have similar active sites for ethylene oxide oxidation and ambient temperature CO oxidation. For example, the 0.5h aged catalysts, the 1% Au supported catalyst has the highest conversion of CO and has 50% conversion of EtO at the lowest temperature. Whereas the Hopcalite catalyst has the lowest CO conversion and the highest temperature at 50% conversion of EtO. This suggests that the promotion of activity for CO oxidation has a similar effect for ethylene oxide oxidation.

Arsenijević and co-workers [26] have investigated the catalytic incineration of ethylene oxide over a Pt/Al_2O_3 catalyst. Although a direct comparison cannot be made, Arsenijević and co-workers stated that in the reaction section, initial heating to the temperature of 200°C was sufficient to start up self-sustained deep ethylene oxide oxidation. A commercially available Hopcalte^{TM}, granulated copper oxide-manganese dioxide catalyst, was used in conjunction with a novel catalytic system configuration [27]. This catalyst has a grain size from 8 to 14 mesh and a surface area of ca.200 m^2g^{-1}. The temperature of catalytic oxidation was quoted to be between 148°C and 205°C. Copper manganese mixed oxides are well known oxidation catalysts for VOC removal at higher temperatures [28], in relation to temperatures used for ambient temperature CO oxidation. The operation temperatures reported for noble metal supported and commercial Hopcalite catalysts (ca. 160°C) are similar to temperatures reported in this chapter. The performance of the Au supported CuMnOx catalyst indicates that the addition of a dopant could improve activity towards ethylene oxide oxidation.

6.3 Preferential oxidation (PROX) of carbon monoxide

Fuels cells have been considered to be promising tools for energy conversion. The proton electron membrane (PEM) fuel cell has attracted much attention in improving fuel efficiency and cleanliness of automobiles [27]. Pure hydrogen is the fuel used for the fuel cell system since it simplifies system integration, maximises efficiency, and provides zero emissions. However, since no effective and potentially safe means of storing adequate amounts of hydrogen in a vehicle exists, onboard hydrogen generation by steam reforming of methanol or partial oxidation of liquid hydrocarbons followed by water gas shift reaction, are alternative ways of giving a fuel cell powered vehicle adequate range. The gas mixture produced from these processes contains 0.5-2 vol.% CO [29,30], which degrades the performance of the fuel cell. The electrodes of fuel cells are typically made of platinum, which is sensitive to CO poisoning [31,32]. The catalytic preferential CO oxidation (PROX) is the simplest and most cost effective method for removing CO from H_2 rich fuels [29]. An effective PROX catalyst must fulfil three important requirements: (i) high oxidation rate, (ii) high selectivity with respect to the undesired H_2 oxidation side reaction and (iii) stability with reaction time [33].

Several catalytic systems have been discussed in the literature for the preferential CO oxidation reaction [34-37]. The majority of the reports are related to Pt group metal based catalysts. The negative aspect to these systems is that they cannot avoid significant losses of H_2 due to oxidation. However, highly dispersed Au nano-particles supported on selected reducible metal oxides such as Fe_2O_3, MnOx, TiO_2 and CeO_2 [37-45], were found to be superior than Pt group catalysts, since they are able to remove CO from reformed fuels with an extraordinarily high oxidation rate and a

better selectivity at much lower temperatures, ca. < 100°C. However, the presence of both CO_2 and H_2O lowers the CO conversion, especially in the low temperature region [37,38,41,43]. From an economical point of view, substitution of the noble metal based catalysts by less expensive catalysts is essential.

Copper manganese mixed oxides for ambient temperature CO oxidation has been extensively researched for the past century. However, there is little reported on the activity of these catalysts, prepared by the co-precipitation method, at high temperatures and especially for preferential oxidation of CO. The purpose of this investigation was to test the Au supported CuMnOx catalysts previously prepared and compare activities with a catalyst that has reported high activity for this reaction (Au/TiO_2).

6.3.1 CuMnOx and 1% Au supported CuMnOx aged for 0h

Preferential CO oxidation experiments were conducted over CuMnOx and 1% Au supported CuMnOx aged for 0h. The results presented in Figure 6.8 show conversion of CO and oxygen selectivity. Oxygen selectivity is defined as the percentage of the oxygen fed that is consumed in the oxidation of CO, and for commercial operation a selectivity of 50% is acceptable, since at this selectivity minimal H_2 is oxidised to water [46].

Figure 6.8 PROX CO oxidation for CuMnOx and 1% Au supported CuMnOx aged

for 0h. Reaction conditions: 80°C, 1% CO/24% CO_2/20% N_2/55% H_2 (18ml/min) and

Air (1ml/min), 100 mg of catalyst, GHSV = 12000 h^{-1}.

The catalytic data (Figure 6.8) shows that for preferential CO oxidation, the addition

of gold has improved activity. The CuMnOx catalyst shows high initial activity (ca.

100% conversion) after 0.5h time on line. This is followed by gradual deactivation of

the catalyst, CO conversion after 5h of testing was ca. 5%. The 1% Au supported

catalyst displayed ca, 70% conversion followed by deactivation. Conversion after 5h

of testing was ca. 20%. The aim of the investigation was also to study competitive

oxidation of H_2, which must be minimised. Using the CuMnOx catalyst, the

selectivity of O_2 to oxidise CO was ca. 3%, whereas the using the 1% Au supported

CuMnOx catalyst, the selectivity of O_2 for CO was ca. 10%. The assumption is that

the remainder of the O_2 in gas feed was used to oxidise H_2.

6.3.2 CuMnOx and 1% Au supported CuMnOx aged for 0.5h

The preferential CO oxidation studies were continued with catalysts aged for 0.5h. Similarly, the CuMnOx and 1% Au supported CuMnOx catalysts were tested. The catalytic data displayed in Figure 6.9, shows that for the CuMnOx and Au supported catalysts, high activity is followed by a gradual decrease in CO conversion as time on line increases. After 5h of testing, for the CuMnOx catalyst, CO conversion was ca. 20% and O_2 selectivity was ca. 10%. For the 1% Au supported sample, conversion after 5h time on line was ca. 30% and selectivity was ca. 10%. The presence of gold has improved activity towards preferential CO oxidation; also the catalytic data for the 0.5h aged catalysts differs from the 0h aged catalysts. There are slight improvements for activity and selectivity for the 0.5h aged catalysts.
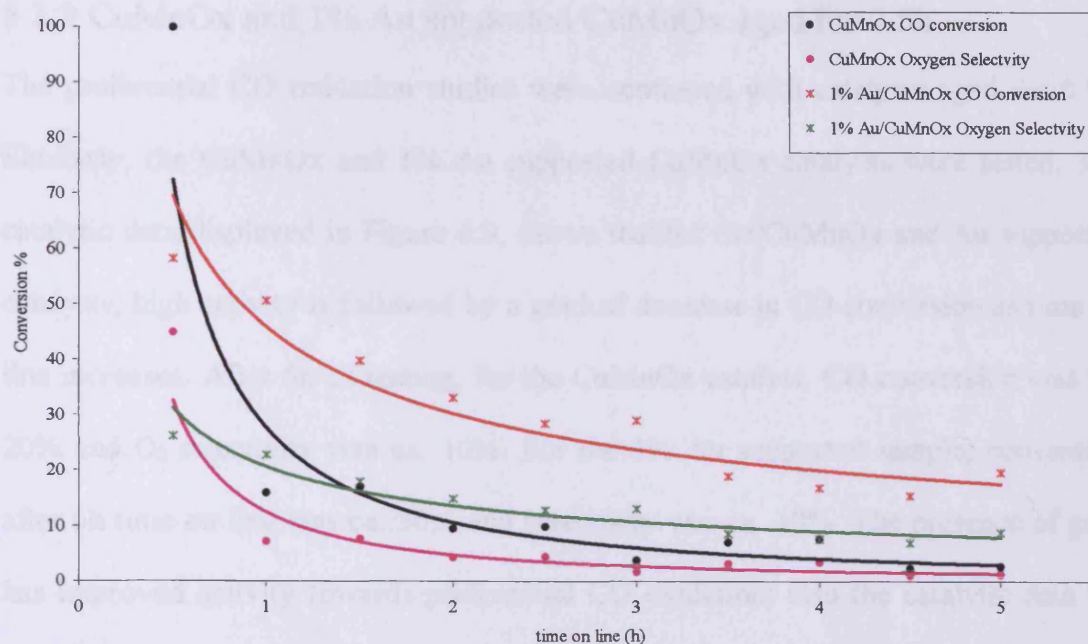

Figure 6.9 PROX CO oxidation for CuMnOx and 1% Au supported CuMnOx aged for 0.5h. Reaction conditions: 80°C, 1% CO/24% CO_2/20% N_2/55% H_2 (18ml/min) and Air (1ml/min), 100 mg of catalyst, GHSV = 12000 h^{-1}.

6.3.3 CuMnOx and 1% Au supported CuMnOx aged for 1h

The catalytic data for preferential CO oxidation over CuMnOx and 1% Au supported CuMnOx catalysts aged for 1h are shown in Figure6.10. The CuMnOx catalyst aged for 1h shows similar results to the CuMnOx catalyst, CO conversion after 5h testing was ca. 20% and selectivity was ca. 10%. The 1% Au supported catalyst shows significant improvement in activity; 100% conversion is observed after 0.5h testing. Deactivation was observed but conversion after 5h time on line was ca. 45%. The selectivity of oxygen to oxidise CO was ca. 20%.

Figure 6.10 PROX CO oxidation for CuMnOx and 1% Au supported CuMnOx aged for 1h. Reaction conditions: 80°C, 1% CO/24% CO_2/20% N_2/55% H_2 (18ml/min) and Air (1ml/min), 100 mg of catalyst, GHSV = 12000 h^{-1}.

The results from Figure 6.10 show that the presence of Au has a positive effect on the activity of catalysts for preferential CO oxidation. The 1% Au supported catalyst

shows higher activity than for the supported catalysts aged for 0h and 0.5h respectively. This indicates that the ageing time of the CuMnOx support plays an important part in producing an appropriate support for Au particles. The 1h supported catalyst shows high activity for ambient temperature CO oxidation and ethylene oxide conversion.

6.3.4 CuMnOx and 1% Au supported CuMnOx aged for 6h

Preferential CO oxidation data over CuMnOx and 1% Au/CuMnOx catalysts aged for 6h is shown in Figure 6.11.
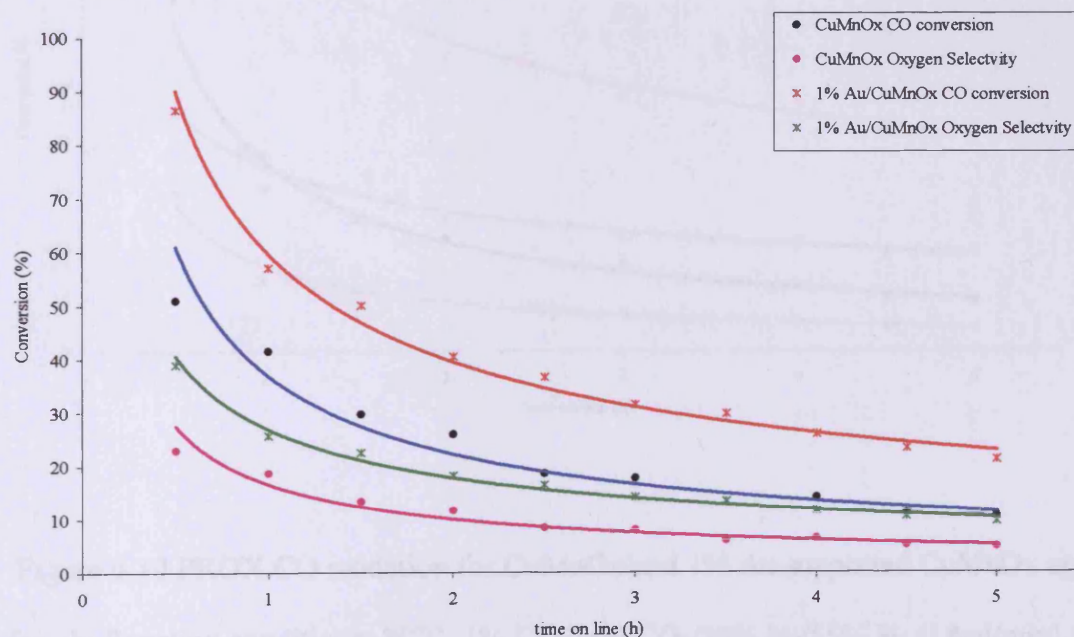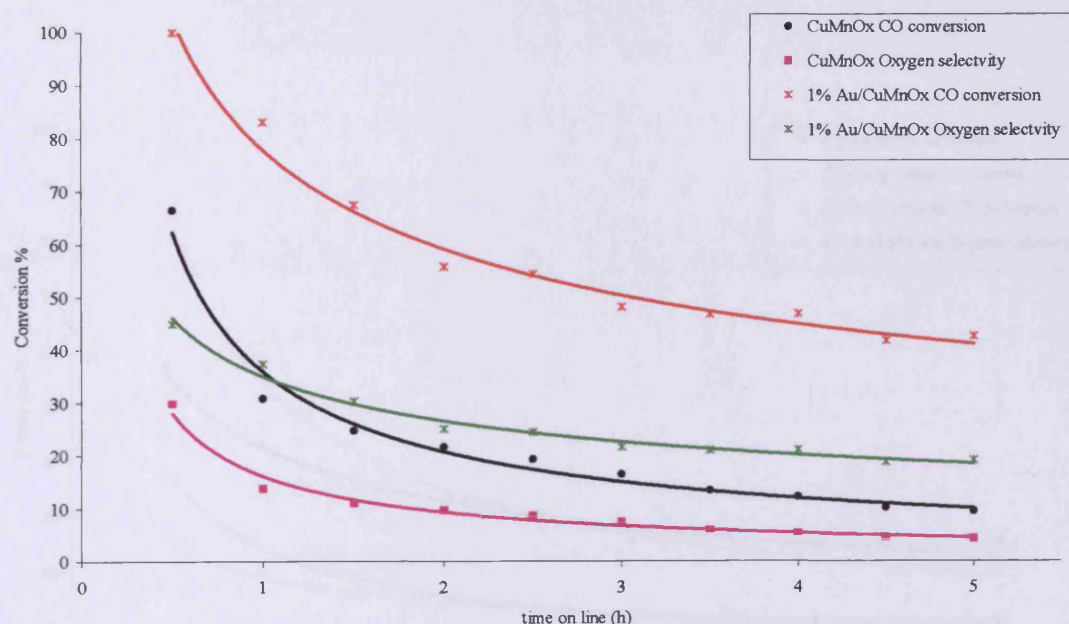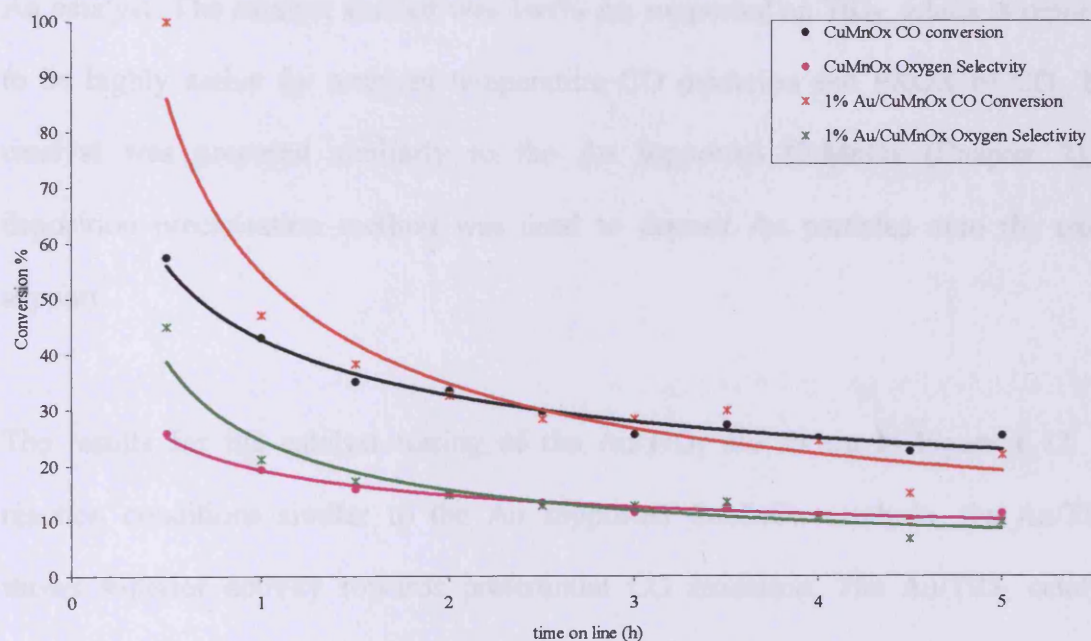

Figure 6.11 PROX CO oxidation for CuMnOx and 1% Au supported CuMnOx aged for 6h. Reaction conditions: 80 °C, 1% CO/24% CO$_2$/20% N$_2$/55% H$_2$ (18ml/min) and Air (1ml/min), 100 mg of catalyst, GHSV = 12000 h^{-1}.

The catalytic data (Figure 6.11) shows little difference between the CuMnOx and Au supported CuMnOx catalysts aged for 6h. The 1% Au supported catalyst shows high activity after 0.5h of testing (ca. 100% conversion) but the steady state activities are similar to the CuMnOx catalyst. After 5h of catalyst testing, both samples show CO conversions of ca. 25% and selectivity towards CO oxidation of ca. 15%.

6.3.5 Comparison with Au/TiO$_2$

The PROX of CO using CuMnOx and Au supported CuMnOx shows that the addition of gold to CuMnOx improves conversion. Activities are also shown to be dependant on the nature of the support used, i.e. the ageing of the CuMnOx precursor. The activities of Au supported CuMnOx catalysts were compared with another supported Au catalyst. The catalyst studied was 1wt% Au supported on TiO$_2$, which is reported to be highly active for ambient temperature CO oxidation and PROX of CO. The catalyst was prepared similarly to the Au supported CuMnOx (Chapter 2), a deposition precipitation method was used to deposit Au particles onto the oxide support.

The results for the catalyst testing of the Au/TiO$_2$ are shown in Figure 6.12. At reaction conditions similar to the Au supported CuMnOx catalysts, the Au/TiO$_2$ shows superior activity towards preferential CO oxidation. The Au/TiO$_2$ catalyst shows 100% conversion of CO in the presence of H$_2$ and CO$_2$. The selectivity of oxygen species to oxidise CO in the presence of H$_2$ was ca. 45%. The Au/TiO$_2$ showed no sign of deactivation for the 5h testing period. The catalyst data for the Au/TiO$_2$ catalyst (100% CO conversion, 45% selectivity) is reasonable for the type of testing conditions used. Şimşek and co-workers [47] have reported 1% Pt-0.25% SnO$_x$

on activated carbon, in the presence of CO_2, with 100% CO conversion with selectivity of ca. 50%.

Figure 6.12 PROX CO oxidation for Au/TiO$_2$. Reaction conditions: 80°C, 1% CO/24% CO$_2$/20% N$_2$/55% H$_2$ (18ml/min) and Air (1ml/min), 100 mg of catalyst, GHSV = 12000 h^{-1}.

The catalytic results show the reason that TiO_2 is one of the most commonly used supports for Au particles in CO oxidation [48]. The Au/TiO$_2$ catalyst has shown to be resistive to CO_2, which is contained in the feed stream. The magnitude of the inhibiting effect provoked by CO_2 strongly depends on the nature of the catalyst [33]. The presence of CO_2 and H_2 in the gas feed could lead to a deactivation of the CuMnOx and Au supported CuMnOx catalysts. The effect of hydrogen can be ascribed to the formation of water during the reaction. Water has reported to have a positive effect for Au/TiO$_2$ in CO oxidation [49] and Au/MnO$_x$/Al$_2$O$_3$ in preferential CO oxidation [40], and explained by the action of OH groups on the support on electronic state of Ti ions [49].

on activated carbon, in the presence of CO_2, with 100% CO conversion with selectivity of ca. 50%.

Figure 6.12 PROX CO oxidation for Au/TiO$_2$. Reaction conditions: 80°C, 1% CO/24% CO$_2$/20% N$_2$/55% H$_2$ (18ml/min) and Air (1ml/min), 100 mg of catalyst, GHSV = 12000 h^{-1}.

The catalytic results show the reason that TiO$_2$ is one of the most commonly used supports for Au particles in CO oxidation [48]. The Au/TiO$_2$ catalyst has shown to be resistive to CO$_2$, which is contained in the feed stream. The magnitude of the inhibiting effect provoked by CO$_2$ strongly depends on the nature of the catalyst [33]. The presence of CO$_2$ and H$_2$ in the gas feed could lead to a deactivation of the CuMnOx and Au supported CuMnOx catalysts. The effect of hydrogen can be ascribed to the formation of water during the reaction. Water has reported to have a positive effect for Au/TiO$_2$ in CO oxidation [49] and Au/MnO$_x$/Al$_2$O$_3$ in preferential CO oxidation [40], and explained by the action of OH groups on the support on electronic state of Ti ions [49].

6.3.6 Discussion of PROX of CO

The preferential CO oxidation reaction over CuMnOx and 1% Au supported CuMnOx catalysts has shown similar findings to the reactions for ambient temperature CO oxidation and ethylene oxide conversion. The varying ageing times have produced catalysts with different activities. The catalysts aged for 1h appear to have the overall highest activity for ambient temperature CO oxidation, ethylene oxide conversion and PROX of CO. The reason for the high activity, compared to the CuMnOx catalyst, could be due to the nature of the support present. The 1h ageing time producing a catalyst has a morphology suitable to act as support for Au particles. The 1h aged support having smaller sized particles compared to the 0h and 6h aged catalysts. The phases that are present in the catalyst play an important part in catalytic activity. The X-ray diffraction patterns along with the TPR data (shown in Chapter 4) shows that for the shorter ageing times, mixed oxide species are responsible for increased catalytic activity. Increasing the ageing time, leads to separate oxide phases such as Mn_2O_3 and CuO, this leads to a decrease in catalytic activity.

In the case for preferential CO oxidation, the catalysts exhibit high activities in the early stages of catalyst testing. However, this is followed by appreciable deactivation compared to Au/TiO_2. This could be due to the nature of the catalyst support used and the conditions of the PROX reaction. The selectivity of the CuMnOx and Au supported CuMnOx catalysts are less than 30%. This implies that the remainder of the oxygen in the reaction would be oxidising hydrogen to produce water. Comparing the CuMnOx catalysts with the Au/TiO_2, the results show the limitations of the Hopcalite catalyst in that it is not ideal for preferential CO oxidation. The conversions and selectivity's of the Hopcalite are significantly lower than a Au supported TiO_2 catalyst. As discussed in previous chapters, the presence of water has a negative

effect on CuMnOx and Au supported catalysts. For other supports, such as TiO_2, water can have a positive effect on the CO oxidation reaction [50]. It was demonstrated that the amount of moisture adsorbed on the catalyst mainly determines the activity. In the investigation, the concentration of water was lower than those of the reactants, CO and O_2. Haruta and co-workers commented that the moisture effect did not originate from the direct reaction with H_2O, in the vapour phase producing CO_2. Although the water gas shift reaction does proceed over Au/TiO_2 [51,52], this was reported at much higher reaction temperatures (ca. 300°C). Also, the concentration of water required by stoichiometry for the reaction with CO should be ca. 10000ppm.

Avgouropoulos and co-workers [37] have investigated the influence of CO_2 and H_2O on catalyst activity for the preferential oxidation of CO over a $Au/\alpha\text{-}Fe_2O_3$ catalyst. They reported that the presence of H_2O and CO_2 further reduced CO conversion, but increased CO selectivity. However, Hutchings and co-workers [46] have reported a Au/Fe_2O_3 catalyst, in the presence of CO_2 and water that has activity of 99.5% conversion and selectivity of ca. 50%. Hutchings and co-workers stated that the preparation procedure was of crucial importance; especially the calcination temperature used to prepare supported Au nano-crystals.

In the literature, deactivation of Au-metal oxide catalysts for the CO oxidation reaction is mostly attributed to the accumulation of carbonate species, which can block active sites [41]. However, the presence of moisture, from the oxidation of H_2, may enhance the rate of decomposition of carbonate species by reactive conversion to bicarbonate species, which are thermally less stable. The accumulation of carbonate species and the low selectivity could be the reasons why the CuMnOx based catalysts

suffer high deactivation. The addition of Au does show improvement of activity for CO oxidation but not in the same magnitude as Au/TiO_2 or Au/Fe_2O_3. However, this study has shown that the choices of support and preparation conditions are vital to produce a catalyst that will preferentially oxidise CO in the presence of H_2 and CO_2.

6.4 Conclusion

The oxidation reactions of ethylene oxide oxidation and preferential CO oxidation have shown the possibility of copper manganese based mixed oxides as alternative catalysts. The addition of Au particles to CuMnOx showed improvement of ethylene oxide conversion compared to an industrially available catalyst. Similar results were observed for preferential CO oxidation. However, the established Au/TiO_2 was far superior in activity compared to the CuMnOx based catalysts. The investigation has highlighted possible alternative oxidation reactions that could be further studied. It also showed the limitations of the CuMnOx catalyst, in terms of selectivity to oxidise CO in the presence of H_2. However, this chapter has shown that CuMnOx catalysts are not limited to just ambient temperature CO oxidation reactions.

6.5 Chapter 6 References

[1]   http://ec.europa.eu/environment/air/stationary.html,   Directive   1999/13/EC,

        (1999).

[2]   M. Kosusko, C. Nunez, J. Air Waste Manag. Assoc. 40 (1990) 254.

[3]   Y. Matros, Noskov, Chem. Eng. Proc. 32 (1993) 89.

[4]   S. Shelley, Chem. Eng. (1997) 57.

[5]   J.J. Spivey, Ind. Eng. Chem Res. 26 (1987) 2165.

[6]   T. Lawton, Hydrocarbon Eng. (1997) 79.

[7]   C. Lahousse, A. Bernier, P. Grange, B. Delmon, P. Papaefthimiou, T.

        Ionnides, X. Verykios, J. Catal. 178 (1998) 214.

[8]   R. Craciun, B. Nentwick, K. Hadjiivanov, H. Knozinger, Appl. Catal. A 243

        (2003) 67.

[9]   Y.-F. Chang, J.G. McCarthy, Catal. Today 30 (1996) 163.

[10]   A.B. Lamb, W.C. Bray, J.C.W. Frazer, J. Ind. Eng. Chem. 12 (1920) 213.

[11]   T.H. Rogers, C.S. Piggot, W.H. Buhlke, J.M. Jennings, J. Am. Chem. Soc. 43

        (1921) 1973.

[12]   D.R. Merrill, C.C. Scalione, J. Am. Chem. Soc. 43 (1921) 1982.

[13]   J.G. Christian, J.E. Johnson, Int. J. Air Water Poll. 9 (1965) 1.

[14]   J.K. Musick, F.W. Williams, Ind. Eng. Chem. Prod. Res. Dev. 13 (1974) 175.

[15]   J.K. Musick, F.W. Williams, Am. Soc. Mech. Eng. ASME Tech. Report 75-

        ENAs-17.

[16]   J.K. Musick, F.S. Thomas, J.E. Johnson, Ind. Eng. Chem. Prod. Res. Dev. 11

        (1972) 350.

[17]   O. Rentz, Emissions of Volatile Organic Compunds (VOC) from Stationary Sources and Possibilities of their Control, ECE VOC Task Force Report (91-010), Karlsruhe, 1990.

[18]   Z.Lj. Arsenijević, B.V. Grbić. N.D. Radić, Ž.B. Grbavčić, Chem. Eng. J. 116 (2006) 173.

[19]   A.N. Subbotin, B.S. Gudkov, Z.L. Dykh, V.I. Yakerson, React. Kinet. Catal. Lett. 66 (1999) 97.

[19]   P. Bera, M.S. Hegde, Catal. Letters, 79 (2002) 75.

[20]   T.V. Choudhary, S. Banerjee, V.R. Choudhary, Appl. Catal. A: Gen. 234 (2002) 1.

[21]   S.K. Gangwal, M.E. Mullins, J.J. Spivey, P.R. Caffrey, B.A. Tichenor, Appl. Catal. 36 (1988) 231.

[22]   S. Ordonez, L. Bello, H. Sastre, R. Rosal, F.V. Diez, Appl. Catal. B: Environ. 38 (2002) 139.

[23]   G.C. Bond, D.T. Thompson, Gold Bull. 33 (2000) 41.

[24]   B.E. Solsona, T. Garcia, C.Jones, S.H. Taylor, A.F. Carley, G.J. Hutchings, Appl. Catal. A: Gen. 312 (2006) 67.

[25]   Z.Lj. Arsenijevic, B.V. Grbic, Z.B. Grbavcic, N.D. Radic, A.V. Terlecki-Baricevic, Chem. Eng. Sci. 54 (1999) 1519.

[26]   D. Meo III, United States Patent 5229071 (1993).

[27]   S. Gottesfeld, J. Pafford, J. Electrochem. Soc. 135 (1988) 2651.

[28]   N. Singh, K.S. Pisarcyzk, US Patent 5260248 (1993).

[29]   G. Avgouropoulos, T. Ioannides, Appl. Catal. A: Gen. 244 (2003) 155.

[30]   D.L. Trimm, Z.I. Onsan, Catal. Rev. Sci. Eng. 43 (2001) 31.

[31]   M. Götz, H. Wendt, Electrochimica Acta 43 (1998) 3637.

[32]   B. Rohland, V. Plzak, J. Power Sources 84 (1999) 183.

[33]   G. Avouropoulos, J. Papavasilou, T. Tabakova, V. Idakiev, T. Ioannides, Chem. Eng. J. 124 (2006) 41.

[34]   S.H. Oh, R.M. Sinkevitch, J. Catal. 142 (1993) 254.

[35]   H. Igarashi, H. Ushida, M. Suzuki, Y. Sasaki, M. Watanabe, Appl. Catal. A: Gen. 159 (1997) 159.

[36]   P. Syntnikov, V. Sobyanin, V. Belyaev, P. Tsyrulnikov, N. Shitova, D. Shlyapin, Appl. Catal. A: Gen. 239 (2003) 149.

[37]   G. Avgouropoulos, T. ioannides, Ch. Papadopoulou, J. Batista, S. Hocevar, H. Matralis, Catal. Today 75 (2002) 157.

[38]   G. Panzera, V. Modafferi, S. Candamano, A. Donato, F. Frusteri, P.L. Antonucci, J. Power Sources 135 (2004) 177.

[39]   M.J. Kahlich, H.A. Gasteiger, R.J. Behm, J. Catal. 182 (1999) 430.

[40]   R.J.H. Grisel, B.E. Nieuwenhuys, J. Catal.199 (2001) 48.

[41]   M.M. Schubert, A. Venugopal, M.J. Kahlich, V. Plzak, R.J. Behm, J. Catal. 222 (2004) 32.

[42]   W. Deng, J. De Jesus, H. Saltsburg, M. Flytzani-Stephanopoulos, Appl. Catal. A: Gen. 291 (2005) 126.

[43]   A. Luengnaruemitchai, S. Osuwan, E. Gulari, Int. J. Hydrogen Energy 29 (2004) 429.

[44]   A. Luengnaruemitchai, D.T. Kim Thoa, S. Osuwan, E. Gulari, Int. J. Hydrogen Energy 30 (2005) 981.

[45]   R.M. Torres Sanchez, A. Ueda, K. Tanaka, M. Haruta, J. Catal. 168 (1997) 125.

[46]   P. Landon, J. Ferguson, B.E. Solsona, T. Garcia, A.F. Carley, A.A. Herzing, C.J Kiely, S.E. Golunskic, Graham J. Hutchings, Chem. Comm. (2005) 3385.

[47]   E. Şimşek, Ş Özkara, A.E. Aksoylu, Z.I. Önsan, Appl. Catal. A: Gen. 316

        (2007) 169.

[48]   M. Ruszel, B. Grzybowska, M. Laniecki, M. Wójtowski, Catal. Comm. 8

        (2007) 1284

[49]   L.M. Liu, B. McAllister, H.Q. Ye, P. Hu, J. Am. Chem. Soc. 128 (2006) 4017.

[50]   M. Date, M. Okumura, S. Tsubota, M. Haruta, Angew. Chem. Int. Ed. 43

        (2004) 2129.

[51]   H. Sakurai, A. Ueda, T. Kobayashi, M. Haruta, Chem. Comm. (1997) 271.

[52]   F. Boccuzzi, A. Chiorino, M. Mazzoli, D. Andreeva, T. Tabakova, J. Catal.

        188 (1999) 176.

Conclusions and Future Work

7

7.1 Conclusions

7.1.1 Zinc doped copper manganese oxide

The addition of a dopant to copper manganese mixed oxides has shown improvement in activity for CO oxidation at ambient temperatures. Varying the ageing time of the catalyst precursor appears to control the activity of the catalysts produced. CuMnOx doped with zinc shows an improvement in activity towards CO oxidation. Power X-ray diffraction studies showed that for the shorter ageing times, a highly amorphous structure was present. The 25% Zn doped CuMnOx catalyst aged for 0h was the most active catalyst for CO oxidation. Temperature programmed reduction (TPR) studies showed that, it most cases, the addition of zinc increased reducibility of the catalyst. The addition of zinc had a greater effect on the redox properties of copper species compared to manganese species. This synergy between copper and zinc was shown to be in an agreement with the literature.

7.1.2 Gold supported copper manganese mixed oxides

CO oxidation, especially at low temperatures, is an important matter in industrial, environmental and domestic sectors of society. Copper manganese based mixed

oxides are not water tolerant for CO oxidation at ambient temperatures. However, supported gold catalysts have been reported as highly active for CO oxidation in the presence of moisture. The investigations in Chapters 4 and 5 highlighted the possibility of CuMnOx catalysts as supports for gold particles. Studies showed that the ageing time had an affect on the morphology of the support used. Ageing times of 0.5h and 1h, produced materials which were highly amorphous and had smaller particles compared to other ageing times. The highest activity reported for CO oxidation was the 1% Au supported CuMnOx aged for 0.5h. This investigation relates to the literature, in that the type of support used is paramount in producing a highly active catalyst. The preparation method used to deposit gold particles onto a metal oxide, could also be applied to an industrially available copper manganese oxide catalyst. The addition of gold improved the stability of the catalyst. However, removal of moisture from the CO gas feed showed how CuMnOx catalysts are affected by the presence of moisture. The oxidation of CO, using a Au supported CuMnOx catalyst, could take place through a 'three-phase' mechanism. This proposal would have to be determined experimentally.

7.1.3 Alternative Reactions

Copper manganese based mixed oxides were tested for higher temperature oxidation reactions. Ethylene oxide oxidation reactions showed that Au supported CuMnOx catalysts have similar activities to commercially available catalysts. In the reaction for the preferential oxidation of CO, the addition of gold improved activity. However, the activities and selectivities reported were not as high as standard catalysts used for this reaction. The CuMnOx based catalyst was found to be highly selective for H_2 oxidation, which would cause deactivation of the catalyst.

This thesis has shown that even though copper manganese mixed oxides have been reported for almost a century, they are sill important catalysts for CO oxidation. The catalyst is versatile in that, on its own, it is a highly active catalyst. Also, it can act as support for the addition of gold particles. This gives the possibility that the catalyst can be adapted to improve CO oxidation conversions. Also, comparing low temperature oxidation reactions with higher temperature reactions, similar conclusions scan can be drawn. The variables in the preparation procedure, for example the ageing time of the precipitate, control the activities of the catalyst produced. The Au supported CuMnOx catalyst may have similar active sites for ambient temperature CO oxidation as well as higher temperature ethylene oxide oxidation.

The thesis has highlighted the importance to probe the mechanism taking place during CO oxidation. The experiments used in this investigation have given some idea of what might be happening during the oxidation. However, experimental evidence is required to confirm this theory.

7.2 Future Work

This thesis has highlighted the beneficial aspects of adding a dopant to copper manganese mixed oxides for CO oxidation. However, due to the complexity of the catalyst, there are several investigations that could further clarify the improvement in activity.

Temporal analysis of products (TAP) could be used to probe mechanisms of oxidation, reduction and deactivation using zinc doped catalysts and gold supported CuMnOx catalysts. TAP experiments allow sub millisecond resolution for heterogeneous catalytic transient experiments. TAP can perform experiments such as

determination of the lifetime of reactive surface intermediates. It would be beneficial to study the mechanism of CO oxidation taking place using these types of catalysts and the role of the dopant. The origin of where the oxidation processes are taking place, e.g. possible lattice oxygen that may be involved in the CO oxidation reaction.

Transmission electron microscopy would be beneficial in explaining how the catalyst structures differ with changing ageing time. Powder X-ray diffraction has offered limited evidence of the species present and their part in catalytic activity. However, in-situ XRD may explain the amorphous to crystalline phase transition that appears to form the boundary between active and inactive CuMnOx catalysts. It may help provide the appropriate level of crystallinity by identifying the heat treatment required for active phases to form.

Fourier transform infrared spectroscopy could be used to explore the oxide species present in Hopcalite catalyst. Fourier transform infrared (FTIR) spectroscopy is a measurement technique for collecting infrared spectra. Instead of recording the amount of energy absorbed when the frequency of the infra-red light is varied (monochromator), the IR light is guided through an interferometer. The majority of the X-ray diffraction patterns shown in this thesis have revealed how amorphous the catalyst is and its difficulty in characterising possible oxide species. FT-IR would be useful to identify IR bands that correspond to pure oxides or a particular bond of a copper manganese mixed oxide phase. FT-IR or Raman spectroscopy may provide sources to explain the reason for catalyst deactivation. These techniques may be able to probe surface adsorbed species that may be present, e.g. hydroxyl or carbonyl species.

As discussed in previous chapters concerning Au supported CuMnOx catalysts, X-ray photoelectron spectroscopy (XPS) should be used to identify the nature of the gold species present. The oxidation states of the copper and manganese in the Hopcalite catalysts could be determined by XPS surface analysis. The surface atomic ratios could be calculated and compared with bulk ratios. XPS would hopefully determined whether Mn^{3+}, Mn^{4+}, Cu^{2+} and Cu^{1+} species are simultaneously present in the catalyst. Electron paramagnetic resonance (EPR) would be another useful method in determining the oxidation states of the metals present. EPR is a technique for studying chemical species that have one or more unpaired electrons.

The particle size and dispersion of the gold particles could be determined by Transmission electron microscopy. The advantage of using TEM would be that one would be able to image objects to the order of a few angstroms (10^{-10} m). This would give a clear idea of the dispersion of the gold particles.

Further moisture experiments could be investigated using the Au supported CuMnOx catalysts, hydroxyl species that affect the activity of catalyst. Experiments could include saturating the CO gas stream, with known amounts of moisture, to determine the tolerance level of the Hopcalite catalyst towards moisture. Ideally to produce a catalyst that is water tolerant and rivals a commercially available catalyst. Scaling-up experiments could be possible; to produce samples that could be tested for industrial applications. Further work could look into the preparation procedure to produce Au supported CuMnOx catalysts. For example, looking at precursor ageing times between 0h and 1h, to produce the optimum support for gold particles.

APPENDIX 1

Gas Chromatograph conditions for Chapter 2

CO oxidation – ambient temperature

GC Settings

Column

Column Type	1.5 m packed Carbosieve
Column Oven Temperature	195°C

TCD

TCD Temperature	180°C
Range	0.05
Filament Temperature	200°C

Injector

Injector Temperature	165°C

Gas Sample Conditions

Injection Time (mins)	Gas Sample Valve
Initial	-
0.01	+

Ethylene oxide oxidation

GC Settings

Column

Type   Poropak Q (PQ, 2m x 2mm i.d)
                                  Molecular Sieve 13X (MS13X, 2m i.d)

Column Oven Temperature

Step	Temp (°C)	Rate (°C/min)	Hold (mins)	Total (mins)
Initial	100	-	2	2
1	140	20	0	4
2	180	30	0	5.33
3	220	60	2	8

TCD

TCD Temperature   200°C
Range   0.05
Filament Temperature   250°C

FID

FID Temperature   200°C
Range   10

Injector

Injector Temperature   150°C

Gas Sample Programme

Injection Time (mins)	Gas Sample Valve	Series Bypass
Initial	-	-
0.02	+	-
1.27	+	+
3.86	+	-
6	+	+

Preferential CO oxidation (PROX)

GC Settings

Column

Type   Molecular Sieve 5A
                              Porapak

Column Oven Temperature

Step	Temp (°C)	Rate (°C/min)	Hold (mins)	Total (mins)
Initial	85	-	19	19
1	125	40	5.9	25.58

TCD

TCD Temperature   185°C
Range   0.05
Filament Temperature   220°C

Injector

Injector Temperature   150°C

Gas Sample Programme

Injection Time (mins)	Gas Sample Valve	Series Bypass
Initial	-	-
0.01	+	-
2.25	+	+
13	+	-